

**Evaluation of the Leakage Current Performance of
RTV Silicone Rubber-Coated Glass Samples,
energized under AC, DC+, and DC- in a Controlled
Local Laboratory**

by

Siyabonga Silinga

**A thesis submitted in fulfilment of the requirements
for the degree**

Master of Engineering: Electrical Engineering

in
**the Faculty of Engineering
at the Cape Peninsula University of Technology**

Supervisor: Dr Panos Lazanas

Bellville Campus

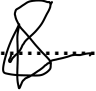
February 2022

CPUT Copyright Information

This thesis may not be published either in part (in scholarly, scientific, or technical journals), or as a whole (as a monograph), unless permission has been obtained from the University.

DECLARATION

I, Siyabonga Silinga, declare that the contents of this thesis represent my own unaided work, and that this thesis has not previously been submitted for academic examination towards any qualification. Furthermore, it represents my own opinions, not necessarily those of the Cape Peninsula University of Technology.

Signed:  Date: 2022-02-27

ABSTRACT

Insulators are of the most important components of electrical transmission and distribution networks. Therefore, it is necessary to find ways to improve insulator performance and save maintenance costs. Various materials have been used in the manufacture of power line insulators. Originally, porcelain and glass were used in the industry. Later materials such as epoxy and silicone rubber have been used. Silicone rubber possesses the property of hydrophobicity i.e. it is water repellent. Silicone rubber is also used as a coating on conventional insulators.

This research project evaluates the performance of RTV-SR coated borosilicate glass and HTV-SR extruded onto glass fibre, rod test samples, and compared them with each other under HVAC, HVDC+, and HVDC-, in a controlled laboratory using the Rotating Wheel Dip Test (RWDT) method. The study was conducted in an existing Rotating Wheel Dip Test (RWDT) facility located in the Eskom Stikland substation in Cape Town. Six (6) × RTV-SR and six (6) HTV-SR test samples were used to provide a measured creepage distance of 275 mm. The tests were carried out using a modified version of the test methods described in the IEC 62730:2012 standard.

The IEC / TR 62730:2012 standard for wheel test specifies the total test duration of 30 000 cycles. In the current study, 2 700 cycles were used for each of the three tests (AC, DC+, and DC-), for a total of 8 100 cycles. This means that instead of 30 000 cycles for each test, only 2 700 cycles were completed. Each subtest was conducted over six days or 144 hours. Thus, the total hours for the entire test (AC, DC+, and DC-) were 432 hours or 18 days.

Further, the study used the Jarrar *et al.* (2014) hydrophobicity classification method to determine whether each insulator at the end of the test cycle retained its hydrophobicity and, therefore, its insulating properties. Visual inspection was also used to determine the ageing, cracking, erosion, discolouration, pollution build-up etc. on the surface of the test samples.

The following results were obtained:

Under AC conditions, the cumulative electric charge values for the HTV-SR samples were slightly lower than that of the RTV-SR. But this result is not conclusive, further testing is required over longer periods to determine which of the two performs better.

The hydrophobicity test indicated that the RTV-SR performed better, and the ageing test also indicated that the RTV-SR performed better.

Under DC+ conditions, the RTV-SR performed better than the HTV-SR in all four categories (leakage current, cumulative electric charge, hydrophobicity, and insulator ageing).

Under DC- conditions, the HTV-SR samples performed slightly better than the RTV-SR samples, in the categories of (leakage current, cumulative electric charge, and hydrophobicity). The RTV-SR performed better in the insulator-ageing category.

Due to the short duration of the tests and other limitations, further testing is recommended, particularly in an outdoor environment for a longer duration.

ACKNOWLEDGEMENTS

I would like to express my heartfelt thanks to:

- My supervisor, Dr Panos Lazanas, for the continuous support, weekly meetings, and commitment to completing my dissertation.
- My co-supervisor, Dr Wallace Vosloo, for providing technical advice during this research and support over the past three years.
- Mr Thembinkosi Mtonjeni, for his valuable contributions in terms of document review and technical editing.
- Mr Frans Jooste, Mr David Mvayo, Mr Rob Watson and Mr Richardo Davey for technical guidance and support during the long days of testing and observation at the Eskom Stikland substation.
- EPPEI Renewable Energy Program Manager, Ms Carmen Lewis, for her support and assistance in purchasing RTV-SR test samples through the CPUT channels offered by Senior Lecturer Dr P. Lazanas.
- My parents, Agrinette N. Silinga and Augustus S. Silinga, for their many sacrifices.
- God, my Father, the Highest and Almighty one, that he let me walk this path of life. I feel your guidance every day at every stage of this work. You are the one who did a great job on this thesis. Thank you, Lord, for your endless blessings showered upon me; I will always be grateful to you.

For those who believe, everything is possible. (Mark 9:23)

Siyabonga Silinga

DEDICATION

This thesis is dedicated to my parents, Mr Augustus Silinga and Ms Agrinette Silinga. Thank you for your support and dedication throughout my studies and for making my dream of starting my career in electrical engineering come true. You see the fruit of your love and support in this work.

TABLE OF CONTENTS

Chapter 1.0 INTRODUCTION AND BACKGROUND	1
1.1 Introduction.....	1
1.2 Background.....	3
1.3 Motivation for the Study.....	6
1.4 Problem Statement.....	7
1.5 Research Objectives.....	7
1.6 Research Questions.....	7
1.7 Importance of the Study.....	8
1.8 Scope and Limitations of the Study.....	9
1.9 Structure of the Thesis.....	9
Chapter 2.0 Literature Review	10
2.1 Progression of the Design of High-Voltage Insulators.....	10
2.1.1 Outdoor Insulators.....	12
2.1.2 Insulator Material.....	14
2.2 Comparing Glass and Polymeric Insulators.....	15
2.3 Literature relating to the Research Question.....	18
2.3.1 Leakage current on glass insulators.....	18
2.3.2 Leakage current on polymeric insulators.....	19
2.4 Literature relating to the Coatings.....	23
2.4.1 High-temperature vulcanising (HTV) silicone rubber (SR).....	23
2.4.2 Room temperature vulcanised (RTV) silicone rubber (SR).....	26
2.5 Literature on Methods used for Evaluating Leakage Current.....	31
2.5.1 Non-artificial test methods to evaluate leakage current performance on RTV-SR coating.....	31
2.5.2 Artificial test methods to evaluate leakage current performance on RTV-SR coating.....	33
2.6 RTV and HTV Silicone Rubber Test Results according to IEC / TR 62730.....	40
2.7 Highlights of the Literature Review Chapter.....	42
2.8 Chapter Summary.....	49
Chapter 3.0 TEST SAMPLES, METHODOLOGY, AND PROCEDURE	50
3.1 Form factor.....	51
3.2 Properties of HTV-SR and RTV-SR Test Samples.....	52
3.3 Testing Methodology.....	53
3.4 Test Conditions.....	54
3.5 Preliminary Tests.....	55
3.6 During the Test.....	56
3.7 Measurement of Leakage Current on Insulator Test Sample.....	57
3.8 cumulative Electric Charge.....	58
3.9 Hydrophobicity Classification.....	58
3.10 Justification of the Duration of the Test.....	61
3.11 Chapter Summary.....	62
Chapter 4.0 TEST DESIGN AND IDENTIFICATION OF APPARATUS	64
4.1 Location of Testing Facility.....	64
4.2 Identification of Testing Devices.....	65
4.2.1 Single-phase transformer and DC rectifier.....	65
4.2.2 Diode rectifier.....	66
4.3 Voltage Ripple Calculation.....	68
4.4 Basic Design of Sodium Chloride (NaCl) Water Resistor for Load Test.....	69
4.4.1 Calculation of the test voltage.....	69
4.4.2 Calculation of the resistance.....	70
4.4.3 Calculation of the electric power.....	70
4.5 Construction of Sodium Chloride (NaCl) Water Resistor.....	70

4.5.1 Material	71
4.5.2 Dimensions	71
4.5.3 Area, volume, and mass	72
4.5.4 Resistance of the water.....	72
4.5.5 A rise in the temperature of the water.....	73
4.6 Load Test Setup.....	74
4.7 Identification of Data Logging and Measuring Devices.....	76
4.7.1 Data logger device: Online Leakage Current Analyser (OLCA)	76
4.7.2 Data measuring device: Leakage Current Sensor.....	77
4.7.3 Calibration of the Hall effect current sensor.....	79
4.7.4 Rotating wheel dip test (RWDT)	81
4.7.5 Glassy carbon electrode	84
4.7.6 Conductivity meter GMH 3410.....	85
4.7.7 Citizen scale CG 4102	86
4.7.8 Hikvision IR network camera	87
4.8 Chapter summary.....	88
Chapter 5.0 TEST RESULTS AND INTERPRETATION	89
5.1 Overview of Leakage Current Tests.....	89
5.2 Failure Indicators in Test Samples.....	92
5.3 Wettability / Hydrophobicity Classification	93
5.4 Rotating Wheel Dip Test (Rwdt) Under AC Excitation (Ch1 – Ch4)	94
5.4.1 Leakage current performance for HTV-SR test sample 1 in channel 1	94
5.4.2 Leakage current performance for RTV-SR test sample 2 in channel 2	100
5.4.3 Visual observation of ageing on RTV-SR test sample 2 in channel 2	101
5.4.4 Leakage current performance for HTV-SR test sample 3 in channel 3.....	104
5.4.5 Leakage current performance for RTV-SR test sample 4 in channel 4	108
5.5 Rotating Wheel Dip Test (RWDT) under dc+ Excitation (Ch1 – Ch4)	113
5.5.1 Leakage current performance for HTV-SR test sample 5 in channel 1	113
5.5.2 Leakage current performance for RTV-SR test sample 6 in channel 2.....	118
5.5.3 Leakage current performance for HTV-SR test sample 7 in channel 3.....	122
5.5.4 Leakage current performance for RTV-SR test sample 8 in channel 4.....	127
5.6 Rotating Wheel Dip Test (RWDT) Under DC- Excitation (Ch1 – Ch4)	133
5.6.1 Leakage current performance for HTV-SR test sample 9 in channel 1	133
5.6.2 Leakage current performance for RTV-SR test sample 10 in channel 2.....	137
5.6.3 Leakage current performance for HTV-SR test sample 11 in channel 3.....	141
5.6.4 Leakage current performance for RTV-SR test sample 12 in channel 4.....	145
5.7 Overall Summary of test Results.....	151
5.8 Chapter Summary	156
Chapter 6.0 CONCLUSION and RECOMMENDATIONS	157
6.1 Conclusion.....	157
6.1.1 Concluding remarks on the leakage current test results for AC, DC+, and DC-	160
6.1.2 Concluding remarks on the cumulative electric charge test results for AC, DC+, and DC-	161
6.1.3 Concluding remarks on the hydrophobicity and hydrophilicity observations for AC, DC+, and DC- ..	161
6.1.4 Concluding remarks on the insulator ageing observations for AC, DC+, and DC-.....	162
6.1.5 Overall conclusion.....	162
6.1.6 Limitations of the study	163
6.2 Recommendations	164

LIST OF FIGURES

Figure 1-1: Ceramic and non-ceramic insulators	4
Figure 2-1: Porcelain insulators for aerial lines (1820-1877)	10
Figure 2-2: High-voltage insulators (a) porcelain (b) glass (c) polymeric	13
Figure 2-3: HTV silicone rubber insulator.....	24
Figure 2-4: Polydialkylsiloxanes (Colas, 2005)	25
Figure 2-5: Spray painting of high-voltage insulator with RTV-SR coating.....	28
Figure 2-6: Chemical structure of PDMS (Ghosh & Khastgir, 2018; Jia et al. 2006)	28
Figure 3-1: HTV-SR extruded onto glass fibre test samples (6x)	50
Figure 3-2: RTV-SR coated borosilicate glass test samples (6x)	50
Figure 3-3: Graphical representation of the form factor equation	51
Figure 3-4: Schematic diagram of the RWDT (IEC / TR 6273:2012; Krzma, 2020)	54
Figure 3-5: 230 V/30 kV transformer and DC rectifier circuit diagram	57
Figure 3-6: A: hydrophobic surface; B: a less hydrophobic surface	59
Figure 3-7: Hydrophobicity classes with percentages - HC1 to HC6.....	60
Figure 4-1: Stikland substation (RWDT test facility)	64
Figure 4-2: Overview of the test apparatus inside insulated shipping container: (a) control panels (b) 30 kV transformer and DC rectifier (c) RWDT and (d) HV earth stick	65
Figure 4-3: 230 V / 30 kV transformer and DC rectifier.....	66
Figure 4-4: Diode rectifier.....	67
Figure 4-5: Capacitor bank.....	67
Figure 4-6: Basic design drawing of a sodium chloride (NaCl) water resistor	73
Figure 4-7: Fully constructed sodium chloride (NaCl) water resistor	74
Figure 4-8: Load test schematic diagram.....	74
Figure 4-9: Front view of the OLCA used as a leakage current data logging device	76
Figure 4-10: Current sensor with Hall probe	78
Figure 4-11: Photo of the Hall sensor	79
Figure 4-12: Calibration of the Hall effect current sensors (AC and DC).....	80
Figure 4-13: AC waveform	80
Figure 4-14: DC waveform	80
Figure 4-15: Overview of RWDT	81
Figure 4-16: Wheel hub.....	82
Figure 4-17: Worm-gear drive motor.....	82
Figure 4-18: Measurement output points	83
Figure 4-19: High-voltage electrode.....	83
Figure 4-20: Aluminium water tank	84
Figure 4-21: Overview of the glassy carbon electrode.....	84
Figure 4-22: Conductivity meter GMH 3410	85
Figure 4-23: Citizen scale CG 4102 for weighing of salt content.....	86
Figure 4-24: Hikvision IR network camera	87
Figure 5-1: Maximum or highest leakage current captured by OLCA.....	90
Figure 5-2: Dots representing positive maximum or highest leakage current.....	90
Figure 5-3: Dots representing negative maximum or highest leakage current	90
Figure 5-4: Schematic diagram of the RWDT (IEC / TR 62730:2012).....	91
Figure 5-5: Test sample material ageing modes.....	93
Figure 5-6: Overview of visual observations made (on RTV-SR and HTV-SR test samples) under AC, DC+, and DC- excitation voltages after the 6-day testing period.....	93
Figure 5-7: Criteria for evaluating the hydrophobicity classification (HC)	94
Figure 5-8: AC positive/negative 1-minute peak current.....	96
Figure 5-9: Peak leakage current over the 54-day period for the HTV-SR (Limbo, 2009)	96

Figure 5-10: Material erosion, crazing, dry band activities, and unstable arc discharges observed on the HTV-SR test sample	98
Figure 5-11: Hydrophobicity of the HTV-SR sample 1	99
Figure 5-12: Cumulative positive/negative charge	100
Figure 5-13: AC positive/negative 1-minute peak current	101
Figure 5-14: Peak current for the RTV SR coated porcelain insulator (channel 6) for HVAC excitation (Limbo, 2009)	101
Figure 5-15: Dark pollution build-up and discolouration on RTV-SR test sample	102
Figure 5-16: Hydrophobicity of the RTV-SR sample 2	103
Figure 5-17: Positive/negative cumulative electric charge graph	104
Figure 5-18: AC positive/negative 1-minute peak current	105
Figure 5-19: Peak leakage current over 54 days period for the HTV-SR (Limbo, 2009)	105
Figure 5-20: Traces of dry band activities, crazing and material erosion on HTV-SR test sample	106
Figure 5-21: Hydrophobicity of the HTV-SR sample 3	107
Figure 5-22: Cumulated positive/negative charge	108
Figure 5-23: AC positive/negative 1-minute peak current	109
Figure 5-24: Peak current for the RTV-SR coated porcelain insulator (channel 6) for HVAC excitation (Limbo, 2009)	109
Figure 5-25: Tracking and erosion, discolouration, and pollution on RTV-SR test sample	110
Figure 5-26: Hydrophobicity of the RTV-SR sample 4	111
Figure 5-27: Cumulative positive/negative charge	111
Figure 5-28: Overall cumulative positive/negative electrical charge between HTV-SR and RTV-SR	112
Figure 5-29: Accumulative coulomb-ampere for all the HTV-SR insulators installed on the AC excitation voltage (Elombo, 2012)	113
Figure 5-30: DC+ 1-minute peak current	114
Figure 5-31: The time-of-day maximum absolute peak leakage current profile recorded for all the HTV-SR 29 insulators (Elombo, 2012)	114
Figure 5-32: Crazing, pollution build-up, and burn marks over a glassy carbon electrode on the HTV-SR test sample	115
Figure 5-33: Hydrophilicity of the HTV-SR sample 5	117
Figure 5-34: Cumulative positive charge	118
Figure 5-35: DC+ 1-minute peak current	119
Figure 5-36: Peak current for the RTV-SR coated porcelain insulator (channel 6) for positive polarity HVDC excitation (Limbo, 2009)	119
Figure 5-37: Black marks, burn marks on glassy carbon electrode, discolouration, and pollution on RTV-SR test sample	120
Figure 5-38: Hydrophobicity of the RTV-SR sample 6	121
Figure 5-39: Cumulative positive charge	121
Figure 5-40: DC+ positive 1-minute peak current	122
Figure 5-41: The time-of-day maximum absolute peak leakage current profile recorded for all the HTV-SR 29 insulators (Elombo, 2012)	123
Figure 5-42: Discoloration, tracking, and light erosion and burn marks on a glassy carbon electrode tip observed on HTV-SR test sample	124
Figure 5-43: Hydrophobicity of the HTV-SR sample 7	126
Figure 5-44: Cumulative positive charge	127
Figure 5-45: DC+ 1-minute peak current	128
Figure 5-46: Peak leakage currents for the glass and RTV-SR coated glass rods with a creepage distance of 346 mm (Elombo, 2012)	128
Figure 5-47: Material erosion, pollution, and discolouration on RTV-SR test sample	129
Figure 5-48: Hydrophilicity of the RTV-SR sample 8	130
Figure 5-49: Cumulative positive charge	131
Figure 5-50: Overall cumulative positive electrical charge between HTV-SR and RTV-SR	132
Figure 5-51: Accumulative coulomb-ampere for all the HTV-SR insulators installed on the DC+ excitation voltage (Elombo, 2012)	132

Figure 5-52: DC- 1-minute peak current	134
Figure 5-53: Peak leakage currents for the EPDM insulator (Channel 1) and HTV-SR insulator (Channel 2) for negative HVDC negative excitation (Limbo, 2009)	134
Figure 5-54: Discoloration, material erosion, crazing and dark pollution/contamination build-up on the HTV-SR test sample	135
Figure 5-55: Hydrophobicity of the HTV-SR sample 9.....	136
Figure 5-56: Cumulative negative charge	137
Figure 5-57: DC- 1-minute peak current	138
Figure 5-58: Peak leakage currents for the porcelain insulator (Channel 5) and the RTV-SR.....	138
Figure 5-59: Pollution build-up and tracking on RTV-SR test sample	139
Figure 5-60: Hydrophobicity of the RTV-SR sample 10.....	140
Figure 5-61: Cumulative negative charge	141
Figure 5-62: DC- 1-minute peak current	142
Figure 5-63: Peak leakage currents for the EPDM insulator (Channel 1) and HTV-SR insulator (Channel 2) for negative HVDC negative excitation (Limbo, 2009)	142
Figure 5-64: Dry band activity on HTV-SR test sample	143
Figure 5-65: Hydrophilicity of the HTV-SR sample 11	144
Figure 5-66: Cumulative negative charge	145
Figure 5-67: DC- negative 1-minute peak current.....	146
Figure 5-68: Peak leakage currents for the porcelain insulator (Channel 5) and the RTV-SR (Limbo, 2009)	146
Figure 5-69: Discolouration, burn marks and pollution observed on an RTV-SR test sample	147
Figure 5-70: Hydrophilicity of the HTV-SR sample 12	148
Figure 5-71: Cumulative negative charge	148
Figure 5-72: Overall cumulative negative electrical charge between HTV-SR and RTV-SR	150
Figure 5-73: Accumulative coulomb-ampere for all the HTV-SR insulators installed on the DC-excitation voltage (Elombo, 2012).....	150

LIST OF TABLES

Table 2-1: Comparison of glass and polymeric insulators (Mackevich & Shah, 1997; Gubanski et al. 2007)	16
Table 2-2: Comparison of silicone rubber in high-voltage insulation applications	26
Table 2-3: Mechanical properties of ceramic insulators	29
Table 2-4: Summary of properties of insulator dielectrics (Looms, 1988)	29
Table 2-5: Chemical composition of ceramics (Kitouni & Harabi, 2011)	30
Table 2-6: General overview of the high-voltage insulators plus the coating of insulators	45
Table 3-1: HTV-SR and RTV-SR test sample dimensions and parameters	51
Table 3-2: Typical properties of HTV-SR and RTV-SR test samples	52
Table 3-3: Borosilicate glass properties	53
Table 3-4: Insulation resistance test on RTV-SR and HTV-SR test samples	55
Table 3-5: Rotating wheel dip tests according to IEC / TR 62730:2012	61
Table 4-1: Semikron SK1/16 rectifier diode technical specification	67
Table 4-2: Electronicon capacitor technical specification	68
Table 4-3: Sodium chloride (NaCl) water resistor load test results	75
Table 4-4: Technical specification of an integrated sensor with closed-loop	79
Table 4-5: Typical values for the glassy carbon electrode used on HTV-SR and RTV-SR test samples as end tips	85
Table 4-6: Conductivity meter GMH 3410 technical data	86
Table 4-7: Technical specifications of Citizen scale CG 4102	87
Table 4-8: Technical specification of Hikvision camera	88
Table 5-1: Leakage current test results summary for AC, DC+, and DC-	151
Table 5-2: Hydrophobicity and hydrophilicity observation summary	152
Table 5-3: Cumulative electric charge test results summary	153
Table 5-4: Insulator ageing observation summary	154
Table 6-1: Overall test results and observations for each excitation (AC, DC+, and DC-) for HTV-SR and RTV-SR	159

APPENDICES

None.

ABBREVIATIONS

Abbreviation	Definition
AC	Alternating Current
ANSI	American National Standard Institute
ATH	Alumina Tri-hydrate
CMOS	Complementary Metal Oxide Semiconductor
DC	Direct Current
EG	Epoxy Glass
EHV	Extra High Voltage
EPDM	Ethylene Propylene Diene Monomer
EMI	Electromagnetic Induction
EPR	Ethylene Propylene Rubber
EVA	Ethylene Vinyl Acetate
FRP	Fibreglass Reinforced Polymer
HC	Hydrophobicity Class
HCR	High Consistency Rubber
HTV	High Temperature Vulcanised
HV	High Voltage
IEC	International Electrotechnical Commission
IPT	Inclined Plane Test
ISO	International Organisation for Standard
KIPTS	Koeberg Insulator Pollution Test Station
LC	Leakage Current
LTV	Low Temperature Vulcanizable
LSR	Liquid Silicone Rubber
MV	Medium Voltage
NCI	Non-Ceramic Insulator
OLCA	Online Leakage Current Analyser
PD	Partial Discharge
PDMS	Polydimethylsiloxanes
PUR	Polyurethane
PTFE	Polytetrafluoroethylene
RTD	Research Testing and Development
RTV	Room Temperature Vulcanised
RWDT	Rotating Wheel Dip Tester
RWT	Rotating Wheel Tracking

ABBREVIATIONS

Abbreviation	Definition
SANAS	South African National Accreditation System
SCC	Stress Corrosion Cracking
SCD	Specified Creepage Distance
SFT	Salt Fog Test
SR	Silicone Rubber
TWT	Tracking Wheel Tester
UV	Ultraviolet

GLOSSARY

Term	Definition
Leakage current	A current that flows over the surface of a polluted insulator.
Insulator	A material that does not conduct electricity.
Room-temperature vulcanised silicone rubber (RTV-SR)	A type of silicone rubber that cures at room temperature.
Cumulative electric charge	The sum of the products of the leakage current value and the time interval.

CHAPTER 1.0

INTRODUCTION AND BACKGROUND

This chapter introduces the study in which the leakage current performance of RTV-SR-coated glass test samples energised under AC, DC+, and DC- is evaluated in a locally controlled laboratory. The chapter presents the background, the problem statement, research questions and the significance of the study. It also describes the structure of the study document.

1.1 INTRODUCTION

Insulators are made from various materials. For the work presented here, the leakage current performance of glass RTV-SR coated and fiber glass HTV-SR coated insulators are evaluated. As outdoor insulators are exposed to contaminants in the air, they gradually become coated with salts and inert materials. This coat is mostly formed by industrial emissions and salt blown from the sea. Amongst the factors that affect insulator pollution are, wind, electrostatic forces, the aerodynamic properties of insulators, pollutant particle size and composition, and moisture. The contaminated surface of insulators can become wet due to adverse weather conditions (such as rain, dew, or fog). Salts dissolved by humidity increase the conductivity of the surface and therefore increase leakage current. This energy dissipated by this current produces heat, which tends to evaporate parts of the moisture coating. The evaporation rate is faster in areas with high leakage current density, resulting in dry bands. Almost all the working voltage is held across these dry bands, causing strong electrical stresses (from the buildup of an electrostatic field) which ionize the air around the insulator and can lead to arcing. The localized arcing may lead to, flash-over and insulator failure.

This research project evaluates the performance of HTV-SR and RTV-SR coated test samples for leakage current, cumulative electric charge, hydrophobicity, and insulator ageing under AC, DC+, and DC- conditions in a controlled local laboratory environment. Under normal operating conditions, leakage currents are undesirable but inevitable due to surface pollution of insulators, so they must be controlled. Several studies have shown that the leakage current of insulators is a critical indicator of the insulator's condition and the severity of its surface contamination. Insulator leakage current is the current flowing over the surface of the insulator from the conductor to the ground. High-voltage insulators are prone to leakage current in transmission and

distribution lines when they are exposed to pollution from the environment in which they are placed. Pollutants include dust, ash, smoke, clay powder and chemicals from nearby industries or salt-spray on seashore areas. The particles on the surface of the insulator can mix with water droplets in a wet atmosphere and form a conductive path to ground. When wet atmospheric conditions prevail, particles on the insulator surface dissolve with water droplets and provide a leakage current path from the high-voltage conductor to the grounded steel structure. In other words, night dew and light rain can increase the conductivity of the polluted layer. The leakage current can sometimes escalate to arcing, resulting in a flash-over. This happens when the air around the insulator ionises and becomes conductive, leading to the destruction of the whole insulator and subsequent power line outages.

Measuring leakage current is key to minimising system outages attributable to pollution since transmission lines are exposed to severe and varying pollution conditions (Ramirez *et al.* 2012). Researchers such as Huang *et al.* (2018) and Karady *et al.* (2007) who regard electric insulation as a vital part of an electrical power system state that insulation faults can lead to permanent device damage and long-term failures and outages.

An insulator is a device made of non-conductive material used to mechanically support electrical conductors and insulate them from contact with the via the metal support structures (Al-Gheilani *et al.* 2017; Bojovschi *et al.* 2019; Han *et al.* 2009). Insulators are exposed to various hazardous environmental conditions (Karady *et al.* 2007). Since insulators are one of the important components in the electric distribution or energy transmission network system (Amin *et al.* 2007; Samimi *et al.* 2013), the choice of their composition (whether glass or polymer) can improve the performance of a power line (Izadi *et al.* 2017). Depending on the line voltage, environmental conditions, construction materials and manufacturer, high-voltage insulators come in various sizes and designs (Nzenwa & Adebayo, 2019).

In addition to being mounted on suitable cross-arms, insulators must provide the necessary clearances between the line conductors, the line conductors and the ground, and between the line conductors and the pole or tower (Han *et al.* 2009). The insulators' non-conductive material forms a dielectric barrier between two electrodes with different electrical potentials (Bojovschi *et al.* 2019). For better reliability, insulators should be tested to verify their compliance with specifications (Samimi *et al.* 2013). Research indicates that the insulators commonly used in the industry are glass,

porcelain and polymeric (Bojovschi *et al.* 2019; Rezaei *et al.* 2013; Samimi *et al.* 2013). Glass and porcelain insulators were once dominant in the market, but polymeric insulators have since surpassed them due to their appealing features. This is due to their ability to withstand adverse climatic conditions, high voltage, and ultraviolet conditions (Belhouchet *et al.* 2019; Goswami, 2017; Gubanski, 2005). Polymeric insulators are also lighter.

However, there is insufficient knowledge regarding the long-term performance of the polymeric materials used and an absence of reliable methods for assessing materials and products (Gubanski, 2005). The most successful method to determine the ideal insulator out of insulators made of different materials and shapes is to verify their performance by conducting long-term field measurements in the same environment (Wijayatilake, 2014). Effective methods for monitoring and minimising power outages and leakage current, reducing maintenance costs, and enhancing insulator durability are constantly under investigation. Essentially, insulators with silicone rubber are considered a viable solution (Ansoerge *et al.* 2012; Chakraborty & Reddy, 2017; Cherney, 1995; Fang *et al.* 2014; Jamaludin *et al.* 2017; Schmidt *et al.* 2010; Wang *et al.* 2017). From the above, an evaluation of the leakage current performance of room temperature vulcanised (RTV) silicone rubber (SR) coated-glass, and high temperature vulcanised (HTV) silicone rubber (SR) extruded onto glass fibre, energised under HVAC, HVDC+, and HVDC- excitation in a controlled laboratory using the Rotating Wheel Dip Test (RWDT) method was deemed necessary.

1.2 BACKGROUND

Energy generation and distribution are key pillars of social, economic, and human development in modern society (Gubanski, 2005; Taalo *et al.* 2015). According to Bergasse *et al.* (2013), energy is an essential commodity for most human activities: it is accessed directly as fuel or indirectly to provide power, light, and mobility. To meet the country's development needs, South Africa will need an additional 29 000 MW of electricity by 2030. This means that new power plants with a capacity of 40 000 MW must be built to increase the existing capacity of 10 900 MW (National Development Plan, 2030). The additional power generation suggests the construction of further infrastructure and an increase in voltage distribution, which would require an investment in efficient and long-lasting insulators.

In most cases, electric power networks (from generating sites to load centres) rely on high-voltage insulators, which must be bolted to masts or towers to prevent current from flowing to the ground. According to Wijayatilake (2014), overhead power lines are subjected to changes in climatic and environmental conditions (rain, wind, sunlight, fog, humidity) and pollution conditions (marine, chemical, industrial), which subsequently negatively affect the performance and lifespan of insulators.

Glass and polymeric insulators are commonly used in the industry. Glass insulators first appeared in the power transmission industry in the United States of America in 1865. They were used on the telegraph network that Edison used to provide electrical power to New York City in 1882. It should be noted that the insulators introduced in 1880 were also made of wood. Wooden insulators performed well in dry conditions but caused leakage current when wet. To overcome this leakage current, porcelain insulators were manufactured in 1880, which paved the way for the high-voltage ceramic insulator industry. Porcelain insulators were used for a century until the polymeric insulators were produced in the 1960s (Anjum, 2014; Bojovschi *et al.* 2019; Gubanski, 2005; Han *et al.* 2009).

Because polymeric insulators can work efficiently in varied climatic conditions, they have gained popularity as high-voltage transmission insulators (Darwison *et al.* 2019). The superior material used in manufacturing polymeric insulators allows for easy handling during installation and maintenance by washing (Izadi *et al.* 2017). Figure 1-1 shows the different types of insulators (i.e. ceramic and non-ceramic).



Figure 1-1: Ceramic and non-ceramic insulators

Belhouchet *et al.* (2019) believe that glass and porcelain insulators have an extremely low thermal expansion, low thermal conductivity, and high mechanical strength. Such

properties give an excellent thermal shock resistance. Nonetheless, according to Goswami (2017), the poor quality of porcelain insulators (glazed) paved the way for composite insulators with epoxy-glass (EG) core and silicone rubber (SR) sheds. Polymeric or composite insulators now represent a large share of the insulator market, as they offer numerous advantages over porcelain and glass insulators. Their acceptance is growing among traditionally reluctant utilities. These insulators possess the following properties: they are lightweight, have an improved mechanical strength-to-weight ratio, perform better under heavy contamination and wet conditions, and are resistant to vandalism (Anjum, 2014).

Polymeric insulators have shown excellent performance under heavily polluted conditions compared to glass types (Izadi *et al.* 2017). These insulators offer several advantages, such as being lightweight, resistant to vandalism and relatively low cost (Khan, 2010; Jamaludin *et al.* 2017). Using silicone rubber insulators (non-ceramic) enabled Eskom (local energy company) in South Africa to increase the reliability of their transmission lines despite being highly polluted. Previously, glass insulators were mostly used in these areas, which led to many contamination flash-overs. Silicone rubber and other composite types of insulators, such as EPDM, are mainly used in areas of high pollution and vandalism (Garrard, 2008). Silicone rubber is widely used as a housing material for manufacturing polymer insulators. Silicone is a polymer that bonds silicon, carbon, hydrogen, and oxygen. Silicone polymer rubber is stable, non-reactive and resistant to extreme environments and temperatures. Higher leakage current (LC) levels on insulators may indicate inferior contamination performance of an insulator, leading to faults, such as flash-over. This is especially relevant along coastal areas. Compared to glass insulators, the benefits of composite insulators are improved contamination performance, the hydrophobicity of their surfaces, and lighter weight.

When an insulator test sample gets wet, it forms a thin film of water on the sample's surface, causing a small leakage current to flow. As this film of water evaporates due to an increase in ambient temperature, a dry band forms on/around the surface of the insulator test sample. When this dry band is formed, the current flow is interrupted, and a voltage gradient appears across the dry band. This voltage gradient exerts electrostatic stress across the surface of the insulator test sample and causes further evaporation and an increase in the width of the dry band. This increase in width of the band causes a higher voltage gradient, which causes minor arcing that can lead to flash over.

A variety of studies have been conducted on commonly used insulator materials under various conditions (Elombo, 2012; Mouton, 2012; Limbo, 2009) both in laboratories and in the field to better understand their performance in application. Most of these studies involved alternating current (AC) voltages, the most commonly encountered scenario in high-voltage applications. Although high-voltage direct current (HVDC) lines are a relatively recent development, they are growing in popularity (Bahrman, 2008). The test procedure for multi-stress ageing with DC application is also examined (Verma & Reddy, 2018).

Various methods of detecting faults in live line insulators have been successfully applied, such as electric field measurement, corona detection, infrared thermography, hydrophobicity analysis, airborne noise detection and visual detection (Ferreira *et al.* 2010; Roman *et al.* 2014). Various tracking and erosion tests (such as the salt fog test, the rotating wheel dip test and the inclined plane test) have been performed on non-ceramic insulators. These tests will be discussed in detail in Chapter 2.0 (*Literature Review*).

1.3 MOTIVATION FOR THE STUDY

Outdoor insulators play an important role in high-voltage power networks. The polymer insulators have displayed some better features in comparison with the glass insulators, particularly due to (i) better pollution performance (ii) light weight (iii) hydrophobicity recovery etc. RTV-SR coating can improve the leakage current performance of glass insulators in cases where pollution problems are experienced. This study will evaluate the leakage current performance of RTV-SR coated borosilicate glass rod samples compared to HTV-SR coated fiber glass rod samples energised under AC, DC+, and DC- in a controlled laboratory using the Rotating Wheel Dip Test (RWDT) method.

The emphasis is on high-voltage direct current (HVDC) applications, given the fact that studies (Elombo, 2012; Mouton, 2012; Limbo, 2009) performed on commonly used insulator materials involved the use of alternating current (AC) voltages. Since high-voltage direct current (HVDC) lines are a relatively recent development, a testing procedure for multi-stress ageing with DC application was necessary. In terms of exploring mechanisms to reduce leakage current, minimise maintenance costs, and increase the lifespan of insulators, this study was an essential preliminary step.

The failure of an outdoor insulator or insulator string, being an essential component of an electrical power network, can result in an overhead line fault and power outage in

that particular section of the network. If overhead line insulators are contaminated with acid rain, sulphuric acid, nitric oxide, and industrial pollution such as dust and sea salt, this can lead to high leakage currents and insulator failure in both AC and DC networks. The financial consequences of such failures are considerable, and so are the maintenance costs.

1.4 PROBLEM STATEMENT

Glass insulators experience higher leakage currents in moist polluted environments due to sand particles, seawater, and fly ash pollutants together with water, forming a thin conductive layer (through ionization of the contaminants inside the water), which result in high leakage currents. In such a polluted environment, alternative options such as different coating methods must be sought to reduce leakage currents in the surface of glass insulators. The use of grease could be one possible method. This is, however, a labour-intensive and expensive process. An alternative to regular greasing is to coat glass insulators with room temperature vulcanised (RTV) silicone rubber (SR). As a result, it is necessary to determine whether RTV-SR coated borosilicate glass or HTV-SR extruded over fiber glass insulators perform better under HVAC and HVDC of either polarity when tested on an RWDT apparatus.

1.5 RESEARCH OBJECTIVES

The main objectives of this study are as follows:

- To evaluate the leakage current performance of RTV-SR coated borosilicate glass rod test samples, compared to HTV-SR extruded onto glass fibre test samples, energised under HVAC, HVDC+, and HVDC- in a controlled local laboratory simulated by a rotating wheel dip test (RWDT); and
- To determine the suitability of RTV-SR coated glass borosilicate rod test samples and HTV-SR extruded onto glass fibre test samples in a coastal environment simulated in a controlled local laboratory setting.

1.6 RESEARCH QUESTIONS

To achieve the above objectives, the following research questions are formulated:

- Do RTV-SR coated borosilicate glass rod samples have the same leakage current performance as HTV-SR extruded onto glass fibre test samples under HVAC, HVDC+, and HVDC- in a simulated coastal pollution environment?

- What is the value of the leakage current of RTV-SR coated borosilicate glass rod test samples in relation to HTV-SR extruded onto glass fibre test samples under HVAC, HVDC+, and HVDC- energization during a rotating wheel dip test (RWDT)?

1.7 IMPORTANCE OF THE STUDY

Eskom operates and maintains the South African section of the Cahora Bassa scheme. The Cahora Bassa scheme is responsible for importing hydroelectric power from Mozambique to South Africa. South Africa's total power output is around 5% (1 500 MW). In this scheme, 533 kV HVDC operates at 1 800 A (Mahatho *et al.* 2016). These power lines are insulated with glass (cap and pin) insulators, which are known to perform poorly in polluted conditions. High levels of pollution are exacerbated by the local weather and atmospheric conditions, and this is a problem that glass insulators cannot withstand. Glass insulators are inherently hydrophilic, which means that they have an affinity for water and they easily get wet. If the surface is dirty, the surface of the glass insulator will form a continuous conductive layer, thereby generating high leakage currents and eventual flash-over.

Glass insulators and porcelain insulators were the first to appear on the market and have been used for many years (Han *et al.* 2009). These insulators exhibited some advantages, albeit overtaken by polymeric insulators (Al-Gheilani *et al.* 2017; El-Shahat & Anis, 2014). Despite ceramic and glass insulators' excellent insulation abilities and weather resistance, they have several drawbacks, including their weight, fragility, and performance under contaminated conditions (Kobayashi *et al.* 2001). Outdoors, the high-voltage insulators are exposed to harsh environmental conditions such as high temperature, moisture, and pollution due to coastal, industrial, agricultural, and desert environments. These factors result in high leakage current over the surface of ceramic and glass insulators that may lead to flashover. In the event of contamination, flashover may result due to leakage current, which may subsequently lead to electrical system failures (Ibrahim *et al.* 2014).

Taking advantage of the strength of ceramic and polymer insulators is extremely important, but the long-term benefits of ceramic insulators coated with silicone rubber need to be determined. Undoubtedly, one of the most important properties of a coating is its ability to restore hydrophobicity even after the contamination layer has built up. It is this characteristic that allows the coating of ceramic insulators with RTV rubber

(Cherney, 1995). However, the problems of material tracking or erosion remains are significant problems that polymer materials must overcome; they are accentuated in DC applications due to the more effective build-up of contamination by electrostatic forces.

1.8 SCOPE AND LIMITATIONS OF THE STUDY

This research will be conducted at an existing rotating wheel dip test facility located at the Eskom Stikland 400 kV substation. The facility is owned by Eskom Research Testing and Development (RT&D), and all testing will be done under the guidance of RT&D staff. A tracking wheel test will be undertaken in accordance with IEC / TR 62730-HV polymeric insulators for indoor and outdoor use. The tests will be modified for DC application. Twelve test insulator rods will be used for this experiment: six RTV-SR coated glass rod samples and six HTV-SR rod samples. Moreover, all test insulators are expected to be exposed to the same environmental conditions and electrical stresses. A voltage of up to 10 kV could be used for AC and DC operation.

1.9 STRUCTURE OF THE THESIS

This thesis consists of six chapters as follows:

- In **Chapter 1**, an introduction to the study and a brief description of the importance of ceramic and non-ceramic insulators is given, as well as the motivation for the study, the problem, and the significance of the study.
- In **Chapter 2**, the reviewed literature focuses on the history of ceramic and non-ceramic insulators and the approach to insulator design over the years. It also compares the performance of ceramic, polymeric, and ceramic-coated insulators, and their behaviour in a polluted environment
- In **Chapter 3**, the test samples, methodology, and procedures are described.
- In **Chapter 4**, an overview is presented of the test equipment and test samples to implement the test method.
- In **Chapter 5**, the results of various RWDT AC, DC+, and DC- excitation tests are presented and discussed.
- In **Chapter 6**, a summary of the findings and recommendations for future work concludes the thesis.

CHAPTER 2.0

LITERATURE REVIEW

This chapter provides an overview of outdoor insulators. It describes various types of outdoor insulators with their advantages and disadvantages. This chapter also discusses the evolution of high-voltage insulators, the various materials used in insulators, the performance of glass and polymeric insulators, leakage current, and the RTV-SR and HTV-SR test samples. The literature on the leakage current behaviour of RTV-SR coated borosilicate glass rod test samples and HTV-SR extruded onto glass fibre test samples energised under AC, DC+, and DC- excitation voltages are examined. Various tests are analysed to assess the leakage current performance of the RTV-SR and HTV-SR.

2.1 PROGRESSION OF THE DESIGN OF HIGH-VOLTAGE INSULATORS

The insulation of power lines is pivotal to transferring quality and reliable electrical energy from generation to distribution (Ghosh *et al.* 2015; Mouton, 2012; Nekeb, 2014; Vosloo, 2002). It is important to discuss how insulators came into existence, how they evolved and why new insulators are developed. For instance, the telegraph and telephone industry needed to insulate the wire for magnet coils and the overhead lines were strung across the countryside (Mathes, 1991). The first insulators made of annealed glass or 'dry-pressed' porcelain (refer to Figure 2-1) were developed around 1820 and were used for telegraph lines (Mouton, 2012).



Figure 2-1: Porcelain insulators for aerial lines (1820-1877)

With the introduction of power transmission lines in 1882, telegraph insulators were scaled up to meet the industry's high voltage and mechanical stress levels. It is this

characteristic that allows ceramic insulators to be coated with RTV rubber (Cherney, 1995). Porcelain insulators made in the dry press, for example, suffered from punctures because of the material's porosity. Wet-process porcelain was developed in 1896, followed by a vacuum extrusion process to remove air from the porcelain insulating body, which functions similarly to the material we use today (Mouton, 2012).

In the 1800s, the development of electrical apparatus made a variety of insulating materials available to meet increasing demand. Until about 1925, only naturally occurring products such as asphalt, rubber, mica and cotton thread or fabric were generally used (Mathes, 1991). Engineers experimented with a variety of materials to create an ultimate insulator. They used wood, rubber, cement, beeswax-coated cloths, and porcelain. At first, insulator products were made of glass and porcelain (ceramic materials). These materials dominated the market for insulators for many years (Vosloo, 2002). Historically, ceramic materials (e.g. porcelain and glass) were the materials of choice for outdoor insulation (Nekeb, 2014; Bojovschi *et al.* 2019). According to Elombo (2012), an insulator has two important functions. Besides providing electrical isolation between high-voltage and ground potentials, it also provides mechanical support to the high-voltage apparatus (and any conductors). As mechanical support for overhead line conductors and electrical isolation of the conductor from the tower, outdoor insulators are widely used in power transmission and distribution networks (Krzma, 2016; Al-Gheilani *et al.* 2017). Glass has been used as material in overhead transmission and distribution line insulators as these materials offer good insulation characteristics and excellent weather resistance. Despite these benefits, they also have several drawbacks; they are hydrophilic and perform poorly in contaminated environments. They have low seismic performance, are susceptible to punctures, cement growth, pin erosion, and vandalism, and have relatively high installation costs (Kobayashi *et al.* 2001).

Initially, glass insulators were used but are now being replaced by polymeric insulators due to certain specific advantages of polymeric insulators over conventional glass insulators. Compared with traditional glass insulators, their major advantage is their low surface energy, which maintains a good hydrophobic surface property under wet conditions such as fog, dew, and rain. Polymeric insulators exhibit good hydrophobicity under wet conditions and surface contamination and, as a result, provide improved performance in environmentally polluted areas and are more resistant to vandalism. Insulator weaknesses and failures can lead to system failures that lead to an

interruption of the power supply. In the event of a failed insulator, a phase (or line) to ground flash-over fault can occur (Elombo, 2012), resulting in a loss of continuity in the supply of power to customers.

It is evident from many researchers, including Elombo (2012), that environmental and electrical stress during service causes insulator surface degradation. Electrical factors include tracking, erosion, puncture, and cracking, while mechanical factors include long-term deterioration in tensile strength and deterioration in strength from repeated bending and twisting (Kobayashi *et al.* 2001). Ageing is a critical problem for the insulation system (Frącz *et al.* 2016). As an insulator ages, it degrades due to different environmental factors and electrical stresses. UV, moisture, heat, light, atmospheric pressure, and biological degradation caused by microorganisms in the air are all environmental influences. Corona, dry bands, arcing, roughness, and erosion of the insulator surface are examples of electrical stress (Amin & Salman, 2006).

The problem of insulator pollution is critical as it is a multifaceted phenomenon. In operational practice, major ageing factors include UV radiation, ozone, nitrogen oxides, temperature fluctuations, rainfall (including acid rain), rime deposition, dirt, and partial discharges (PD) (Frącz *et al.* 2016). Insulator pollution performance has dominated research in power line insulator design, which has led to the conception of silicone rubber (SR) insulators as having superior performance. It is worth noting that the performance of most types of insulators has been adequately researched for AC applications in recent years (Elombo, 2012).

2.1.1 Outdoor Insulators

Outdoor insulators have different properties due to the different types of material used in their design and the purpose for which the insulators are designed. The long-term stability of outdoor insulators determines their selection in high-voltage equipment (Gubanski *et al.* 2007).

Different types of polymeric materials have been used for the housing of outdoor insulators. These insulators have two functions: to support the high-voltage parts mechanically and to insulate them from ground (Larsson *et al.* 2002; Al-Gheilani *et al.* 2017; Sanyal *et al.* 2020; Wallström, 2005). The polymeric material polydimethylsiloxane (PDMS), commonly known as silicone rubber (SIR), is one kind of polymeric material. Silicone rubber has a higher resistance to ultraviolet degradation

and retains its hydrophobic (water-repellent) properties even when heavily contaminated (Macey *et al.* 2004).

In distribution and transmission overhead lines, there are three main types of outdoor insulators: porcelain, glass, and polymeric insulators (Lan & Gorur, 2008). Figure 2-2 illustrates the different types of insulators.

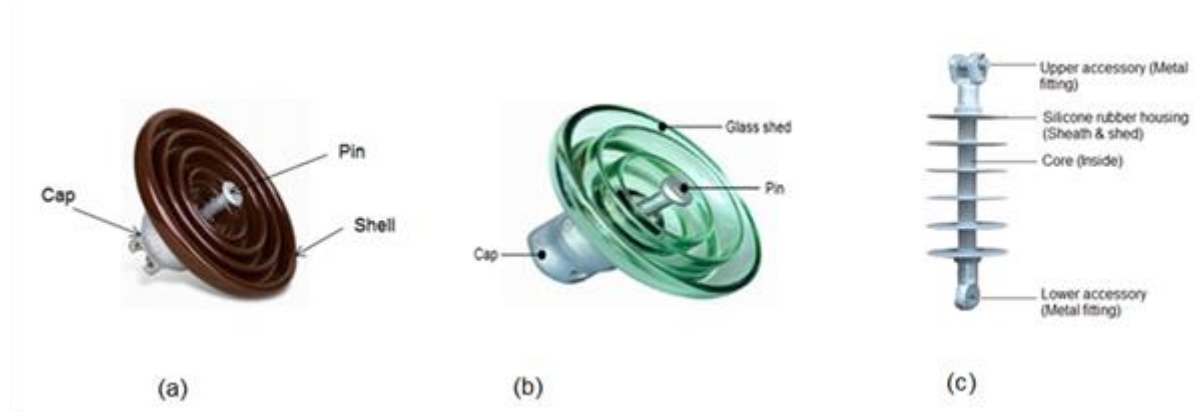


Figure 2-2: High-voltage insulators (a) porcelain (b) glass (c) polymeric

Porcelain and glass insulators are commonly referred to as ceramic insulators, while polymer insulators are commonly referred to as composite or non-ceramic insulators (Vosloo *et al.* 1996; Burnham & Waidelich, 1997; Zhao & Bernstorf, 1998; Saldivar-Guerrero *et al.* 2014). The first insulators available in service since 1800, ceramic insulators (Gubanski, 2005), have a strong ability to withstand mechanical and electrical loads. However, many disadvantages render them somewhat unpopular in certain applications (Mackevich & Shah, 1997; Gubanski *et al.* 2007). Some of the disadvantages of ceramic insulators are as follows:

- Moisture can easily condense on the surface of the glass, and therefore dust in the air settles on the surface of the wet glass and forms a path for the leakage current to flow;
- Under higher voltage, glass cannot be formed into irregular shapes because irregular cooling will generate internal strains;
- High electric stressing of the insulating material;
- Risk of electric puncture;
- Susceptibility to corrosion of the numerous fittings;
- Higher weight of insulator sets;

- Higher maintenance cost; and
- Can bear large compressive force but less tensional force (Khedkar & Dhole, 2010).

In the past, insulators were only made of ceramic (porcelain and glass); however, the accumulation of debris on the surface during long-term operation reduces their dielectric strength, resulting in poor insulation breakdown performance (Khatoon *et al.* 2017). According to studies conducted on high-voltage porcelain or glass, a continuous film of water forms easily on their surface, resulting in flash-overs and power outages (Ibrahim *et al.* 2014; Bojovschi *et al.* 2019).

Therefore, there was a clear necessity to improve insulator performance in polluted conditions, which led insulator developers to invent non-ceramic insulators, which first appeared in the industry in 1970 (Hall, 1993; Venkataraman & Gorur, 2006; Gençoğlu, 2007; Amin & Salman, 2006; Gubanski *et al.* 2000). Composite insulators have replaced glass and porcelain insulators and are widely used in power transmission and distribution lines (Gençoğlu, 2007). These insulators have shown superior performance against pollution conditions due to their water film repellent nature.

NCI performance is primarily influenced by the loss of hydrophobicity and ageing of the material under naturally occurring electrical and environmental stresses (Fernando & Gubanski, 1999; Gençoğlu, 2007). During the design process, care must be taken to ensure that the correct material and dimensions minimise the susceptibility to leakage current (Elombo, 2012). The limitations of composite materials are:

- Possible leakage current when using the wrong materials or dimensions, possible low electrical power in the mould line;
- Special care is required during design and manufacture to ensure that no moisture penetrates at the interfaces; and
- Deflection under load in certain applications (Macey *et al.* 2004).

2.1.2 Insulator Material

Insulating material can be divided into two main groups:

- Inorganic materials (ceramic insulators)
- Organic materials (non-ceramic insulators)

2.1.2.1 Inorganic materials (ceramic insulators)

Inorganic materials include two main subgroups: glass and ceramics (Heger, 2009). By definition, glass is not ceramic because it is an amorphous (non-crystalline) solid. However, glass involves several steps in a ceramic process, and its mechanical properties work similarly to ceramic materials. Ceramic insulators have been used for many years (Madhavan, 2015; Kubai, 2007; Limbo, 2009; Chudnovsky, 2012). The main focus of this research project is glass insulators.

Ceramic materials can be crystalline or partially crystalline. Once heated, they must then be cooled. Clay was used to make the first ceramics, such as pottery, but today, many different ceramic materials are used in various products (Subedi, 2013; Sudha *et al.* 2018; Repalle & Kumar, 2015).

2.1.2.2 Organic materials (non-ceramic insulators)

A non-ceramic insulator for high-voltage electrical conductors was developed using a combination of materials to form the outermost surface of the insulator. The polymers used as insulators usually are silicon rubber, epoxy, ethylene propylene diene monomer (EPDM) and polyester (Amin & Salman 2006; Ersoy *et al.* 2007; Nasrat *et al.* 2013). As these polymers differ in their properties, their properties must be carefully examined and controlled for best results, especially in high-voltage insulated applications (Sundhar *et al.* 1992). Non-ceramic insulators consist of a fibreglass core and one or more weather sheds, as shown in Figure 2-2 (a) above.

Polymer insulators are used in overhead transmission and distribution lines with 69 to 735 kV line voltages. According to Kumosa *et al.* (2005), although non-ceramic insulators have many advantages over glass insulators, they can be mechanically damaged if the rod breaks due to stress corrosion cracking (SCC).

2.2 COMPARING GLASS AND POLYMERIC INSULATORS

There are several differences between glass and polymeric insulators. Glass refers to inorganic, non-metallic materials that provide tough and strong mechanical properties (Subedi, 2013; Mishra, 2017). The polymeric insulator has three components, namely housing material (insulation), core (mechanical strength), and metal end fittings (Natarajan *et al.* 2015). Housing materials have water-repellent properties, commonly known as hydrophobicity, and are primarily responsible for improved performance in polluted conditions (Venkataraman & Gorur, 2006).

Commonly used housing materials for polymeric insulators include SR, EPDM, ethylene-propylene rubber (EPR), polytetrafluoroethylene (PTFE) and polyurethane (PUR) polyolefin elastomers (Natarajan *et al.* 2015). Silicone rubber (SR) has been a widely used composite insulation in outdoor applications. It offers greater resistance to ultraviolet (UV) radiation and less heat build-up during dry-band arc than EPDM. The SR protects the core, i.e. the housing material, from environmental influences. A rod made of glass fibre reinforced polymer (GRP) is used as the core material in the centre of the insulation system (Natarajan *et al.* 2015).

As indicated earlier in § 2.1.1, porcelain and glass are examples of ceramic insulators (Limbo, 2009; Vosloo, 2002). Among the most widely used insulators in the power industry, glass is known for its long history. According to Costea and Baran (2012), this inorganic material has a relatively high thermal resistance and strength. The following table presents a comparative study of glass insulators and polymer-based insulators, considering a variety of parameters, including general, technical, and other factors. The comparative study is presented in Table 2-1.

Table 2-1: Comparison of glass and polymeric insulators
(Mackevich & Shah, 1997; Gubanski *et al.* 2007)

Factors	Glass	Polymer
General Comparison		
Weight	Heavy and the approx. weight of 400 kV string is 135 kg	Lighter and offers equal or better strength. The approximate weight of the 400 kV string is about 20 kg
Fragility	Fragile	Fragile
Packing and transport	Risky and expensive	Easy and economical
Installation	Risky, expensive, more labour intensive	Easy and economical
Handling	Difficult and needs to be handled with care	Easy to handle
Maintenance cost	Being fragile, the maintenance cost is moderately high	Low when compared to porcelain
Vandalism (stone-pelting, gunshots)	More susceptible	Highly resistant
Breakages and secondary damage	Highly fragile, about 10-15% of breakages are reported during transportation, storage, and installation	Flexible, highly resistant to breakage, yet susceptible to cuts and scratches
Technical Comparison		
Mechanical failure	Life span reduces with time because separation due to pins gets eroded	Single piece; hence no such problems occurred

Factors	Glass	Polymer
Resistance to flash-overs and punctures	Resistance is lower but can sustain a maximum of 2 to 3 flash-overs and then require replacement	High resistive, yet should flash-overs occur, immediate replacement of the insulator is necessary
Anti-tracking and erosion resistance	Low tracking resistance	Excellent tracking resistance and also avoids erosion or tracking of the housing material
Contamination and pollution	Affected	Less affected
Hydrophobicity	Non-hydrophobic (i.e. hydrophilic), as porcelain forms water films on the surface, making an easy path leading to flash-overs	Hydrophobicity properties of silicon rubber provide better performance and resist wetting by forming water beads without washing or greasing even in humid or polluted climates; hence, low failure rate combined with low overall operating and maintenance costs
Self-cleaning quality	No. Dirt, sand, salt, and snow are easily attracted but get cleaned by rain	Yes. This is due to hydrophobicity recovery characteristics
Tensile strength	Good	Excellent due to crimping technology
Maintenance	Requires regular maintenance by cleaning, washing, and greasing	No maintenance is required
Performance in snow	Better	Comparatively poor, develops cracks with time
Manufacturing process	Long delivery schedule, manufacturing process causes pollution and health risk	Pollution-free, safe and with less process time; hence short delivery period.
Safety	Susceptible to explosion and breakages due to poor fragility properties, stone-throwing etc.	Provide a high level of safety, superior flexibility, and strength; not susceptible to an explosion—no breakages due to stone-throwing etc.
Design	Design flexibility is limited. Requires larger and heavier towers for installation and more space	Insulator design allows for adaptations to suit specific needs such as creep distance, subsequently resulting in space-saving and lower cost
Other factors		
Part replacement	Possible	Not possible
Shelf life	Excellent	Develops fungus/algae when kept for long and in a wet area
Susceptible to reptiles, rats in storage	Nil	Yes
Life expectancy	> 25 years in non-polluted environments	Yet to be established in extended applications

As much as the table above shows the strength and viability of polymer insulators, they present several problems, namely, (i) poor bond between rod and shell material; (ii) poor bond between weather barrier and rod insulation; (iii) improper attachment of the bar to metal fittings; and (iv) incorrect selection of the insulating material itself, which can be susceptible to electrical degradation. However, the market for glass and porcelain insulators is still actively growing today, even with all the disadvantages associated with their mass, assembly and installation costs, and brittleness due to mechanical stress or breakage (Costea & Baran, 2012).

Experience has shown that in most cases, the degradation of polymeric housing materials is due to electrical activity, which reduces the lifespan of the insulator, a process known as ageing (Lopes, 2001; Que, 2002). As the surface of the insulator housing ages, it allows the leakage current to flow, which manifests itself as tracking and erosion. After that, if conditions are favourable for developing high leakage current, this will result in a complete insulator failure (Al-Hamoudi, 1995; Pylarinos *et al.* 2015).

2.3 LITERATURE RELATING TO THE RESEARCH QUESTION

2.3.1 Leakage current on glass insulators

Flash-over under contaminated conditions is a well-known weakness of glass insulators. Insulators made of glass are cemented between an iron cap and steel pin end fittings. It is advantageous to use glass insulators because they have high mechanical strength and a long service life exceeding 50 years. However, glass insulators are vulnerable to vandalism. Power network efficiency is affected by the failure of insulators caused by lightning, pollution, and contamination. Another form of pollution on insulators is surface tracking, where the formation of carbon tracks lead to increased leakage current. A high leakage current level on an insulator could indicate contamination, which in turn could cause a fault such as a flash-over. Such issues are particularly relevant in coastal areas. Internationally, leakage current is recognised as an indicator of insulator performance. Contamination of insulators leads to leakage current flow and increased electrical losses (Rudolf, 2009). Peak leakage current magnitude provides a measure of the probability of insulator flash-over when it reaches a certain threshold value, usually termed maximum current (Elombo, 2012; Vosloo, 2002). However, the magnitude of peak leakage currents is the major parameter in this study. Elombo (2012) performed an investigation on insulator pollution performance under natural pollution.

Mouton, 2009 evaluated different line insulators in a marine environment. The insulators used for investigation were glass and polymeric insulators. Observed was that the highest occurring leakage current was recorded for the glass disc insulator installed on DC- and two flash-over events were recorded on the same insulator. The test observed that the AC test had the highest peak leakage current performance for glass insulators, which may be attributed to the electrostatic pull forces of the DC-voltage electric fields, which pulled the charged pollution particles to the bottom surface of the glass insulator. Roman *et al.* 2019 monitored a leakage current on Cahora Bassa HVDC transmission line glass insulators. From the study, high humidity and the onset of rain raised the nominal leakage current levels on the glass insulator. The authors measured the leakage current, especially in a polluted environment. It was found that the influence of temperature, humidity, dew, rain, sea salt levels increased the leakage current activity. Figure 2-2a below shows a typical standard profile of a cap-and-pin glass insulator with equivalent circuit.

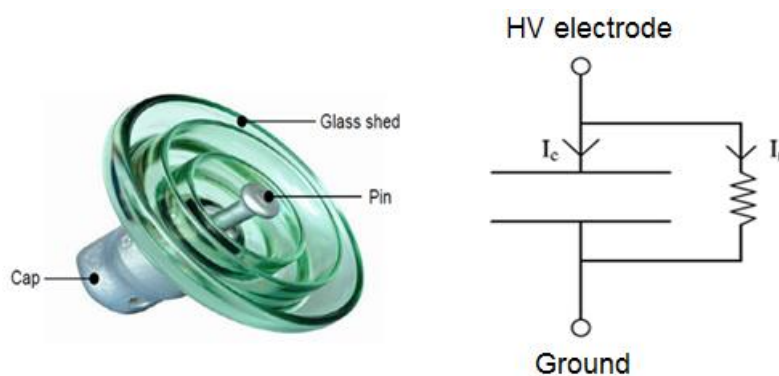


Figure 2-2a: Cap and pin glass insulator with equivalent circuit

2.3.2 Leakage current on polymeric insulators

Darwison *et al.* (2019) argue that with low pollution levels on the insulators, the leakage current is very low, and the power transmission functions normally. However, in the case of higher leakage currents, the power transmission and distribution continue to function normally. Still, they are under severe constraint due to the high-level temperatures on the surface of the insulator that ultimately leads to a power failure. Most of the highest contaminated insulators can be found in coastal, industrial and cement industrial areas (Darwison *et al.* 2019).

Polymeric insulators have recently gained popularity due to their superior insulation performance compared to glass insulators in contamination resistance. When placed near industrial, agricultural, or coastal areas, the pollution builds up slowly on these

insulators, resulting in leakage current flow during wet weather conditions such as dew, fog, or drizzle. There is a non-uniform LC density on the surface of the insulator, and in some areas, sufficient heat is developed, causing dry bands to form. A voltage redistribution along the insulator leads to high electric field intensity across dry bands, which results in partial arcing. The partial arcs will cause erosion and chemical degradation of polymeric insulators. The partial discharges will elongate along the insulator profile if the surface resistance is sufficiently low and may eventually cause insulator flash-over. Mouton (2012) explains the advantages and disadvantages of polymeric insulators. The main advantages of polymer composites are:

- High tensile strength-to-weight ratio;
- Improved performance in highly polluted areas by silicone rubber types; and
- They are an unattractive target for vandals and resistant to projectile damage.

On the contrary, polymeric insulators have the following disadvantages:

- Erosion on polymer housing due to leakage currents with incorrect material or dimensioning;
- Possible electrical weakness at the mould line for moulded constructed insulators;
- Deflection under load in certain applications; and
- Special care is needed in design and manufacturing to eliminate the ingress of moisture at the interface between core, polymer housing and the metal end fittings (Mouton, 2012).

The leakage current of polymeric insulators does not always increase with pollution deposits as time passes. An insulator's leakage current is dependent on its surface resistance, which is dependent on its hydrophobicity. Polymeric insulators have shown a cyclic decrease followed by the recovery of hydrophobicity with time. Hydrophobic surfaces of polymeric insulators are widely desired since they prevent the formation of water paths for electric current, thereby minimising flash-over and discharge on the insulation (Thomazini *et al.* 2012). In times of hydrophobicity loss, the insulator behaves as hydrophilic, and similar surface activity steps may lead to flash-over if the conditions are favourable and hydrophobicity is not recovered in time (Pylarinos *et al.* 2011). Polymeric insulators age more quickly when exposed to environmental factors (such as outdoor conditions). As a result of outdoor conditions like ultraviolet radiation,

snow and salt, polymers can age faster and lose their hydrophobicity (Thomazini *et al.* 2012). Polymeric insulators have surface tracking as an important component for detecting several conditions associated with them, such as leakage of current, discharges, initiation of tracking, dry state, and severe damage. According to (Elombo, 2012; Madi *et al.* 2016), surface tracking is the formation of carbon tracks on the surface of polymeric insulators that makes the insulators lose their dielectric property.

Leakage current provides information on contamination on a polluted insulator (Joneidi *et al.* 2013). The authors confirm that two types of discharges can determine insulation performance: (i) partial corona discharge between water droplets; and (ii) dry band arc discharge between dry bands on the surface of polymeric materials. The latter is believed to cause much larger cumulative charges than the former, which is why it may lead to tracking and erosion phenomena.

Mouton, 2009 evaluated different line insulators in a marine environment. From the test, it was observed that HTV-SR and RTV-SR performed best under all excitation voltages. Vosloo, 2002, compares the relative performance of different insulator materials used in South Africa when subjected to a severe marine pollution environment. The results showed that RTV-SR coated porcelain test insulator 4C and HTV-SR test sample 1S performed best in leakage current. The authors measured the leakage current in those test samples, especially in a polluted environment. It was observed that HTV-SR and RTV-SR insulators displayed good leakage current suppression performance in that environment. They exhibited a remarkable property to recover their characteristics under the effect of different pollution environments to which they were exposed.

Some recommendations have been made in the literature about improvements in the strength and durability of polymeric insulators:

- Exploration of degradation studies of polymeric insulators, conducted in Brazil, asserted that polymeric products would have greater durability in the field. They will be functionally more trustworthy through the stabilisation required in the formulation of the polymeric masses; that is, the supplier will have to use a specific stabilisation system thermo and photo-oxidative for the application of the final product (Nasrat *et al.* 2016).
- In Greece, several studies were conducted on polymeric insulators. Various test methods of testing have been suggested. Most importantly, the construction and operation such as that of the Talos high-voltage test station

at Iraklion in Crete and a currently running project (Polydiagno) to assess the lifespan (ageing) of polymer insulators have been recommended (Pylarinos *et al.* 2014, 2016).

- An online LC monitoring system was studied in Malaysia that analyses leakage current (LC) signals in the time domain, frequency spectrum, time-frequency representation, fundamental value, total harmonic distortion (THD), total non-harmonic distortion (TnHD) and total wave distortion (TWD). The results of this study have shown that the system is appropriate and reliable to be implemented for leakage current online monitoring system (Nordin *et al.* 2013; Ramani *et al.* 2015; Abidin *et al.* 2013).
- During a 37-year study on composite outdoor high-voltage insulators conducted in Crete (Greece), the silicone rubber composite insulators performed well and efficiently. However, there are ageing defects in this model, and that necessitates further evaluation (Siderakis *et al.* 2016).
- A study on surface tracking on polymeric insulators used in electrical transmission lines was performed in China. Polymeric insulators need proper management and maintenance. Two solutions have been proposed: (i) the use of filler technology; and (ii) the monitoring of the insulators to maintain a clear surface free from carbon deposits (Madi *et al.* 2016). Filler technology enhances the properties of polymeric insulators. It involves using other dielectric materials to fill the tracks on the surface of the damaged polymeric insulators.
- The effects of RTV-SR coating on the electrical performance of polymer insulators under lightning impulse voltage conditions were explored in China. It was determined that the RTV-SR coating could improve and protect the surface condition of a polymer insulator. This may help improve the polymer insulator's performance, increase its lifespan, and hence, power system reliability (Jamaludin *et al.* 2017).
- In a study conducted by UK and Canadian researchers, flash-over and ageing of silicone rubber insulators were investigated under different contamination and dry band conditions. Utilising FTIR spectroscopy, they investigated chemical changes on the surface of the insulator caused by high-energy partial arcs and flash-over. After flash-over, the polymeric content of the silicone

rubber surface decreases while the hydrophilic content increases. Based on the results of this study, it may be possible to improve the mathematical models currently used to predict the flash-over voltage of polluted polymeric insulators (Nekahi *et al.* 2017).

- In Malaysia, a study was conducted on a dynamic model that simulated and evaluated the flash-over of polluted insulators. An analysis was carried out to determine the characteristics of electric fields, pollution and insulator resistivity, conductivity, and leakage currents during the entire stage of pollution flash-over under uniform and non-uniform pollution. In this study, the spike in the electric field profile indicates a drop in surface conductance at the high field region, which is due to evaporation and heating effects. It is particularly useful for locating discharge by field measurement for locating dry bands on the insulator surface. A new insulator model is needed to investigate these characteristics (Salem & Abd-Rahman, 2018).
- In Indonesia, a study of two polymer insulators proved that the Adaptive Neuro Fuzzy Inference System (ANFIS) method could be used to forecast leakage currents for the polymeric insulators based on LabView pre-processed thermal images (Darwison *et al.* 2019).

It can be concluded from the above studies that it is worth investing in polymer insulators because of the number of advantages they present, particularly that this type of insulator can regain its hydrophobicity over time. Several studies are expected to be carried out to improve the insulators' leakage current performance, strength, and durability.

2.4 LITERATURE RELATING TO THE COATINGS

2.4.1 High-temperature vulcanising (HTV) silicone rubber (SR)

As an important material for the sheaths and sheds of composite insulators, high temperature vulcanised silicone rubber (HTV-SR) plays an important role in the insulation industry. With a glass fibre core and HTV-SR, housing core sheaths and sheds are widely used in high-voltage networks due to their lightweight, good hydrophobicity, pollution resistivity etc. These insulators are also used in the electrical engineering industry due to their good surface properties and ability to recover hydrophobicity. However, erosion patterns are often observed on the rubber surface,

particularly in outdoor and wet environments. The electrical conductivity within the said pattern is considerably increased due to discharge degradation. This electrically conductive path is generally called tracking. Tracking reduces the insulation strength and may lead to flash-over or dielectric breakdown.

Compared with a corona discharge, the probability of an arc discharge along composite insulators occurs intermittently only when surface leakage current increases to a critical level along the surface of severe polluted hydrophilic insulators during foggy conditions are much higher lower.

HTV-SR is the product of curing at high temperatures. Composite rubber insulators with high-temperature vulcanised (HTV) silicone rubber (SR) as the sheath and shed material have been widely applied in power systems worldwide for their many advantages. These include excellent antipollution flash-over performance, light weight, convenient installation, and especially hydrophobicity and hydrophobicity transfer properties. Compared with traditional porcelain and glass insulators, they offer better electrical and physicochemical properties (Wang *et al.* 2017).

It has been more than 30 years since high temperature vulcanised (HTV) silicone rubber (SR) was used as housing for high-voltage insulators in power transmission and distribution systems, according to Haddad *et al.* (2014). HTV-SR insulators, as shown in Figure 2-3, are widely used as outdoor insulation in power transmission and distribution systems (Chakraborty & Reddy, 2017).



Figure 2-3: HTV silicone rubber insulator

Based on linear silicone oil, silicone rubber is reinforced with silicone resin or silica to improve mechanical properties. Due to its excellent high-temperature resistance, radiation resistance, anti-U and anti-ageing properties (Zhu *et al.* 2017), it is used to package and seal precise electronic components, including chips, LEDs, solar cells, fuel cells and medicines. The production of HTV silicone rubber production “... is based

on high-molecular polydimethylsiloxanes, polymethylphenylsiloxanes, methyltrifluoropropylsiloxanes or their copolymers containing methyl vinylsiloxyl groups in the polymer chain...” (Kopylov *et al.* 2011).

By resemblance with ketones, the name *silicone* was given in 1901 by Kipping to describe new composites of the brut formula $(R_2SiO)_n$ (Andriot *et al.* 2007). The formula can be explained as follows: R_2 represents an organic group such as an alkyl (methyl, ethyl) or phenyl group, whereas SiO_2 stands for anti-tracking, anti-erosion and thermal-conductivity. According to Saei *et al.* (2015), these were rapidly identified as being polymeric and corresponding to polydialkylsiloxanes, with the following formulation in Figure 2-4 below:

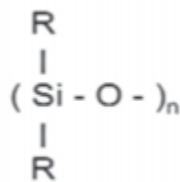


Figure 2-4: Polydialkylsiloxanes (Colas, 2005)

HTV silicone rubbers can be divided into liquid silicone rubbers (LSR) and millable silicone rubbers (MSR) (Vudayagiri *et al.* 2015; Yu & Skov, 2015). The LSR family of silicones provides fast-curing, high-precision injection moulding for high-performance parts such as transducers (Delebecq & Ganachaud, 2012; Yu & Skov, 2015). Late in 1944, Warrick’s HTV response was used to make the temperature-safe silicone elastic gaskets needed to seal the superchargers on B-29 aircraft that require high altitude operation (Brooke-Devlin, 2012).

In contrast to room temperature vulcanisation (RTV), which cures at low temperature (room temperature) through a condensation reaction, HTV cures at high temperature and high pressure through hydrosilation (Khan *et al.* 2018). Ball *et al.* (2007) and Paradisi *et al.* (1991) define hydrosilation as adding a silicon-hydrogen bond through the carbon-carbon double bond by catalysing transition metal complexes that form valid hydrogen-carbon and silicon-carbon bonds. Hydrosilation positions are among the most important mechanical applications of homogeneous catalysis, access to organofunctional silanes and silicones, typically used to manufacture adhesives (glues), cross linkers and polymers (Meister *et al.* 2016).

Table 2-2 below compares silicone rubber in high-voltage insulation applications.

Table 2-2: Comparison of silicone rubber in high-voltage insulation applications

High-Temperature Vulcanising	Room Temperature Vulcanising	Liquid Silicone Rubber
Cured at high temperature and pressure	Cured at room temperature and pressure	A mixture of two components
It is soft and easily deformable	The coating is of a thin layer	It is a fully elastic material
Surface is sticky	Condensation and reaction as one component system	Viscosity is very high
Tensile strength is good	Possibility of moisture ingress from the outer surface	Its colour is milky white
After vulcanising, the material becomes elastic and has high silicone relative permittivity	Hydrophobicity is possibility higher	No toxic or aggressive components are formed when using LSR
Temperature control in injection unit is considerably lower		Good physiological characteristics

The HTV-SR has been commonly aged under ultraviolet radiation, acid rain, ozone, and surface discharge in the high-altitude region (Qin *et al.* 2013; Moreno & Gorur, 2003). HTV-SR has mechanical properties that are considered superior to RTV-SR types. This gives HTV-SR sufficient mechanical strength to withstand long-term outdoor use. They also offer hydrophobicity that can recover quickly even if lost due to dry band activities, corona discharges and dust deposits on the insulator surface (Kumagai *et al.* 2001).

2.4.2 Room temperature vulcanised (RTV) silicone rubber (SR)

The installation of insulation in harsh environments and exposure to severe pollution can cause flash-overs and unplanned outages, which pose a significant challenge for utilities to ensure a continuous supply of electricity. To maintain the reliability of power systems, insulators' pollution performance is crucial (Elombo, 2012). In recent years, most research studies to improve the pollution performance of glass insulators have focused on using room temperature vulcanizing (RTV) silicone rubber (SR) coatings to cover the original hydrophilic surface of glass with a hydrophobic polymer.

The installation of RTV silicone coated glass insulators grew rapidly among utilities. They keep the inherent properties of toughened glass, such as mechanical reliability and ease of inspection, while upgrading their pollution performance to eliminate or, at least, sharply reduce the need for washing.

Insulator degradation and pollution performance are mostly investigated through leakage current analyses and by visual observations. Insulators made of toughened glass are widely used because of their tough and lasting surface properties and mechanical reliability.

The ability of an insulator to respond to wetting and, by extension, to pollution is greatly dependent on the surface material, with an important distinction between hydrophilic and hydrophobic materials. Surfaces that repel water are hydrophobic, while surfaces easily wetted by water are hydrophilic. Hydrophobic properties are important for improving insulators' pollution performance by inhibiting the formation of continuous and conductive water films that may bridge their surfaces, resulting in a flash-over. RTV silicone coatings consist of a base silicone polymer such as polydimethylsiloxane (PDMS), with optional extending fillers such as alumina trihydrate (ATH). The coating is dispersed in a solvent such as naphtha, or a non-flammable one, to act as a carrier medium to transfer the material to the insulator.

Vulcanisation can be divided into three categories of vulcanisation: (i) room temperature vulcanised; (ii) low temperature vulcanised; and (iii) high temperature vulcanised (Reynders *et al.* 1999; also see Kindersberger *et al.* 1995). RTV-SR coating can greatly reduce insulator maintenance costs (Hamadi *et al.* 2020). Li *et al.* (2012:3) made the following remarks about the performance and advantages of RTV-SR:

The silicone coating provides a virtually maintenance-free system that prevents excessive leakage current, tracking, and surge currents. Silicone is not affected by UV light, temperature, or corrosion and can provide a smooth surface with good tracking resistance. Silicone coatings are used to eliminate or reduce frequent cleaning of insulators, periodic re-application of greases, and replacement of parts damaged by flash-over. They have proven their effectiveness in a variety of conditions, from salt spray to fly ash. They are also useful for restoring burnt, cracked, or cracked insulators.

Silicone rubber is available in two forms: high temperature, vulcanised (HTV) elastomer for weather sheds, or room temperature spray for porcelain or glass insulators (Theodoridis *et al.* 2001). RTV-SR coatings are available in a liquid state and, when applied to the surface of the insulator, form a hard rubber-like layer (Siderakis *et al.* 2011). Their adhesion to ceramic insulators, their permeability to tracking or erosion, and their ability to prevent leakage currents are important characteristics of RTV-SR coating systems (Ilhan & Aslan, 2020). The application of RTV-SR coating is demonstrated in Figure 2-5 below.



Figure 2-5: Spray painting of high-voltage insulator with RTV-SR coating

According to Farhang *et al.* (2009), the coating can be applied to porcelain insulators by dipping, painting, or spraying a one-component liquid polymer system. When exposed to moisture in the air, the liquid polymer layer vulcanises into a flexible rubber layer. Among the polymeric matrices used commercially is rubber, primarily because of its ability to absorb energy. Under stress, rubber can undergo much more elastic deformation than other materials and still return to its original shape after the stress is released (Rubber, 2016; Irene *et al.* 2012). RTV silicone rubbers are made from basic polydimethylsiloxane (PDMS) molecules, which are mainly composed of a methyl group (CH₃), oxygen (O) and silicon (Si). For a chemical structure of PDMS, refer to Figure 2-6.

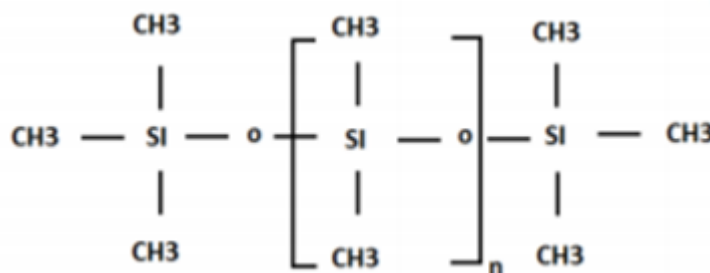


Figure 2-6: Chemical structure of PDMS (Ghosh & Khastgir, 2018; Jia *et al.* 2006)

An insulating coating may contain reinforcing fillers, such as fumed silica, alumina trihydrate filler and adhesion promoters for better bonding to insulator surfaces (Zhicheng & Zhidong, 2002). Different environments have been used with RTV-SR coatings, including coastal, desert, industrial, high humidity, and low temperatures. The use of RTV-SR coatings on both AC and DC systems has increased considerably (Jia *et al.* 2008) for preventing flash-overs caused by uneven wetting (Wu *et al.* 1998).

The ability of the coating to suppress leakage currents and thus flash-overs is by far the most important property. This property is fundamental to the concept of coating ceramic insulators with RTV-SR (Cherney, 1995). However, the problem of material tracking or erosion remains one of the greatest issues to be overcome in polymeric materials and is emphasised in DC applications due to the accumulation of contaminants by electrostatic forces when compared to AC.

It is believed that ceramic insulators have good mechanical and electrical properties and are less expensive (Pratomosiwi, 2009). Table 2-3 below shows the mechanical properties of ceramic insulators.

Table 2-3: Mechanical properties of ceramic insulators

Material	Compression strength (GPa)	Compression modulus (epoxy=100)	Apparent Shear Strength (MPa)	Flexural Modulus (epoxy=100)
CTD 101K/S-2	1.35	100	88	100
Standard Ceramic	1.15	183	64	117
High Modulus	1.36	228	73	154

As evident from Table 2-3, the strength of ceramic insulation systems is favourable compared to other organic composite insulators such as the resin systems CTD101K and CTD112P, both with S2 glass reinforcement. CTD101K is a low viscosity VPI resin system that has been widely used in the superconducting magnet industry, and CTD 112P is a TGDM ready-made epoxy system currently used by the Usiter group to insulate CS model coils (Rice *et al.* 1999). The electrical characteristics of ceramic insulators are presented in Table 2-4.

Table 2-4: Summary of properties of insulator dielectrics (Looms, 1988)

Property	Unit	Glazed porcelain	Toughened glass
Density	g/cm	2.3 – 3.9	2.5
Tensile strength	MPa	30 – 100	100 – 120
	lb/in ² ($\times 10^3$)	34 – 120	30 – 40
Tensile modulus	GPa	50 – 100	72
	lb/in ² ($\times 10^6$)	7 – 14	10.1
Thermal conductivity	W/m ⁰ K	1 -4	1.0
Expansibility (20–100°C)	($\times 10^6$)/K	3.5 – 9.1	8.0 – 9.5

Permittivity (50–60 Hz)	Air = 1	5.0 – 7.5	7.3
Loss tangent (50–60 Hz)	($\times 10^{-3}$)	20 – 40	15 – 50
Puncture strength	kV/mm	10 – 20	> 25
Volume resistivity (at 20°C)	Ωcm	$10^{11} - 10^{13}$	10^{12}

The basic raw materials used for porcelain preparation are local quartz, potassic feldspar (PF) and kaolin (Kitouni & Harabi, 2011). The clay $[\text{Al}_2\text{Si}_2\text{O}_5(\text{OH})_4]$ gives plasticity to the ceramic mixture; flint or quartz (SiO_2) maintain the shape of the formed article during firing; and feldspar $[\text{K}_x\text{Na}_{1-x}(\text{AlSi}_3)\text{O}_8]$ serves as flux (Olupot, 2006). Table 2-5 presents the chemical composition of ceramic.

Table 2-5: Chemical composition of ceramics (Kitouni & Harabi, 2011)

Oxides' content	Kaolin	Feldspar	Quartz
SiO_2	37.77	60.68	86.68
Al_2O_3	35.50	10.68	0.91
Fe_2O_3	0.34	0.66	4.57
CaO	0.80	0.17	6.48
SO_3	0.95		
K_2O	0.28	> 10.0	0.78
Cl	0.01		
MnO	0.89		0.09
TiO_2	0.06	0.11	0.12
Na_2O			0.48

Eskom (the research site) uses ceramic and non-ceramic insulators. The advantages of ceramic insulators, which often indicate their use, are superior in electrical properties, no creep or deformation under stress at room temperature, and greater resistance to environmental changes (Islam *et al.* 2004). Nonetheless, ceramic insulators still have certain disadvantages. Since the problems with both polymeric and ceramic insulators are known (refer to Table 2-1 and Table 2-2 above), it is important to study the effects of coating ceramic insulators to determine the behaviour and performance of RTV-SR coated glass insulators under AC excitation and DC excitation in a controlled laboratory.

In the United Kingdom, ceramic (porcelain) insulators with and without coatings were compared in the laboratory. In artificial pollution tests, the clean-fog method of IEC 60507 was used to compare these insulators. The coated test sample suppressed

leakage current activities significantly more than the uncoated test sample (Braini *et al.* 2011).

An experimental facility located in a heavily polluted area of France has monitored toughened glass insulators coated with a super hydrophobic nano-coating for over two years. Its pollution performance has been compared with that of RTV-SR coated glass insulators. During the monitoring, the RTV-SR insulator string showed lower leakage current levels, better performance, and more stable pollution performance (de Santos *et al.* 2021). From the above authors, it can be concluded that, to date, silicone coatings applied to glass insulators in polluted or harsh environments have been found to enhance pollution performance due to their ability to perform in the field and their durability.

2.5 LITERATURE ON METHODS USED FOR EVALUATING LEAKAGE CURRENT

2.5.1 Non-artificial test methods to evaluate leakage current performance on RTV-SR coating

The long-term exposure to environmental and operational stresses on insulating polymer surfaces (non-ceramic insulators) leads to various changes in the surface composition and morphology and reduces their water repellence (Amin & Salman, 2006). The effect of environmental and climatic conditions on insulator performance should be assessed in sites with reliable measuring equipment, such as the Koeberg Insulator Pollution Test Station (KIPTS) in the Western Cape (South Africa), generally considered a major coastal pollution test station and ageing performance of outdoor insulation (Hillborg *et al.* 2010; Vosloo *et al.* 1996).

KIPTS, located relatively close to Cape Town, is renowned for testing natural marine pollution insulators. The main types of contamination detected at KIPTS during the test period ranged from insoluble oxides, weakly soluble carbonates, fully soluble nitrates, hydroxides, sulphates, and chlorides (Vosloo *et al.* 1996). Vosloo (2002) compared the relative performance of various insulation materials used in South Africa in a highly polluted marine environment. The following insulators have been tested:

- High-temperature vulcanised (HTV) silicone rubber (SR), fumed aluminium trihydrate (ATH)-filled;

- Ethylene propylene diene monomer (EPDM), fumed aluminium trihydrate (ATH)-filled;
- Glazed, quartz-filled porcelain;
- Pre-primed (glazed, quartz-filled) porcelain surface, coated with a sprayable, two-part (catalyst added to cure), room-temperature vulcanised (RTV), fumed ATH-filled silicone rubber (SR);
- Cycloaliphatic epoxy resin with silane-treated silica filler (quartz); and
- Resistive/semi-conductive (antimony-doped tin oxide) glazed (RG), aluminium-filled porcelain (Vosloo, 2002).

Dry band and discharge were considered the predominant discharge activity in all insulators. The relative ratings show that the glazed porcelain insulator has the best leakage current performance of all insulators tested. In terms of performance, the HTV-SR test sample is the next best. Using EPDM as a test insulator and porcelain as a reference insulator performed similarly to HTV-SR. However, the cyclo-aliphatic epoxy resin test insulator showed the worst results (Vosloo, 2002).

The KIPTS includes test chambers for 11, 22, 33, 66 and 132 kV with a control room, an environmental monitoring station, a pollution monitor, and a leakage current recording system. The contamination rate in KIPTS is extremely high. The set-up was made to prevent the ingress of inferior quality polymer insulators. Many test specimens are tested in a natural environment from eight months to a maximum of five years (Amin *et al.* 2007). A climate typical to the KIPTS region is hot, dry summers and cold, wet winters, with frequent mist banks, strong winds, and high levels of marine pollution from the sea. This makes KIPTS an ideal maritime and industrial pollution area to evaluate insulation materials (Vosloo & Swinny, 2013).

Below are the main sources of pollution around KIPTS:

- To the west of the test station lies the Atlantic Ocean. An influx of moisture and salt particles occurs near the test station due to exposure to waves, sea breezes, winds and periodic banks of fog and mist. It has been noted that the air contains organic matter, such as plankton.
- The breakwater of the Koeberg nuclear power plant north of KIPTS leads to the formation of local salt fog banks.

- To the east of the test site is a predominantly agricultural area (wheat, vineyards) with periodic forest fires, ploughing, harvesting, and spraying of crops.
- Northeast of KIPTS (10-13 km) is an industrial zone (Atlantis) that emits burnt particles of diesel fuel, coal, and heavy fuel oil (HFO) into the atmosphere.
- The lime plant (Kilson) operates 10 km south of the test station.
- Southeast of the test station, heavy industries such as the Kynoch fertiliser plant and the Caltex refinery (the now so-called Astron Energy) are the main sources of emissions (Vosloo, 2002).

The KIPTS test procedure, now the official national Eskom standard and part of the Eskom Distribution insulator material specification, is globally recognised (Vosloo, 2002). The strength of KIPTS lies in the fact that testing is carried out in a natural environment over long periods. For example, ageing in KIPTS correlates with the IEC 61109, 5 000-hour ageing test. It has a ratio of at least 2:1 (KIPTS: IEC 61109), making KIPTS an ideal environment for evaluating insulator products (Vosloo & Swinny, 2013).

Elombo *et al.* (2013) evaluated at KIPTS the performance of HTV (high-temperature vulcanisation) SR (silicone rubber) power line insulators under AC and both DC polarities when exposed to natural pollution. The area is known for its heavily polluted coastline and high humidity at night. In summer, there are high levels of leakage current due to high pollution levels and high humidity. In contrast, lower leakage current levels were recorded in winter, which confirms the washing effect of winter rain. The leakage current level for silicone rubber insulators is the same for positive AC and DC but lower for negative DC. The implications of the study indicate that contamination testing of silicone rubber insulators should be considered (Elombo *et al.* 2013). The above proposal is consistent with the objective of the present study to evaluate the leakage current performance of RTV-SR coated glass test samples energised under AC, DC+, and DC- excitations in a local controlled laboratory.

2.5.2 Artificial test methods to evaluate leakage current performance on RTV-SR coating

Several tests have been carried out to evaluate the leakage current performance of SR insulators, namely salt fog tests (Fernando & Gubanski, 1999; Gorur *et al.* 1986;

Gutman *et al.* 1997; Kumagai *et al.* 2006; Lambeth *et al.* 1973; Naito & Schneider, 1995; Schwardt *et al.* 2004), inclined plane tests (Bruce *et al.* 2008, 2010; Ghunem *et al.* 2013a, 2013b, 2015; Billings *et al.* 1968; Sarkar *et al.* 2010) and rotating wheel dip test (Banhthasit *et al.* 2011; Krzma *et al.* 2014; Holtzhausen *et al.* 2010; Mackiewicz *et al.* 2017; Kumagai *et al.* 2001; Sebo & Liu, 2010). According to Fernando and Gubanski (1999), the evaluation of the leakage currents is carried out to improve the understanding of the artificial ageing processes, assess its relevance to the natural conditions of the field, and determine how individual stresses affect the performance of the insulator. Siderakis *et al.* (2004) agree that leakage current evaluation can be used to study outdoor insulation performance; nevertheless, it can provide information about the development of the surface activity from the start of the current flow to the event of a breakdown discharge or flash-over.

2.5.2.1 Salt fog test (SFT)

“The salt fog test according to IEC 1109 has given engineers a simple but effective method for evaluating the leakage current, tracking and erosion resistance of polymer insulation” (Arklove & Wheeler, 1996:299). This test method was first derived in Great Britain in 1960-1964 as a simple and straightforward method for evaluating the resistance properties of insulators in a saline atmosphere (Lambeth *et al.* 1973). For Sebo and Zhao (1999), the salt fog test evaluates materials' leakage current and ageing mechanisms in wet, dirty, contaminated, and energised conditions. In this test, insulators are energised and exposed to salt fog sprays (Fernando & Gubanski, 1999).

The salt fog test has been used in various countries such as the United States, Germany, Japan, and South Africa (Fernando & Gubanski, 1999; Kumagai *et al.* 2006; Sebo & Liu, 2010; Schwardt *et al.* 2004). In the USA, according to Sebo and Liu (2010), the two most commonly used accelerated ageing tests are the rotating wheel test and the fog chamber (the latter appears to offer more versatile testing options), medium-size medium-voltage (between 1 and 5 m) and small-size medium-voltage fog chambers (less than 1 m). A good example of a medium fog chamber is the one used in the high-voltage laboratory at Ohio State University (Sebo & Liu, 2010).

Studies of the effect on test parameters (fog intensity and conductivity) have led to proposals to change the test procedure in Germany (Fernando & Gubanski, 1999). Here the test is divided into three parts, the early ageing period (EAP), the transition period (TP) and the late ageing period (LAP). In EAP, only low capacitance (LC) was

monitored for hydrophobic samples. The level changes significantly during the TP phase, i.e. surfaces become hydrophilic, and the current becomes more resistive. In the LAP, the LC level is even higher, completely resistive, and surface erosion occurs (Fernando & Gubanski, 1999).

Kumagai *et al.* (2006) report on studies carried out in Japan by comparing silicone rubber and porcelain leakage current and ageing in the salt fog and the field. The field test site was not in heavy polluted coastal conditions but a mild suburb of the central district of Japan. The salt fog test was carried out in the laboratory. Salt fog tests highlighted the superiority of SR over porcelain compared to field-testing. The difference between the salt fog and natural rain was probably the reason for the differences (Kumagai *et al.* 2006).

In South Africa, Schwardt *et al.* (2004) compared measured leak currents and surface conductivity during the salt fog test. The insulator pollution monitoring relay (IPMR) monitors the degree of pollution of the high-voltage insulators by measuring the surface conduction on standard test insulation (two glass cap-and-pin discs). The salt fog chamber has been designed according to the technical characteristics of the IEC 60507. Differentiated salt spray tests have been carried out in different salinities representing various levels of results. Still, the results are inconclusive, and additional work is needed to investigate the effects of variations in specific creepage distances and the effects of different forms of insulation (Schwardt *et al.* 2004).

2.5.2.2 Inclined plane test (IPT)

The inclined plain tracking and erosion materials test (IPT) is the most common means of testing the relevance of polymeric materials for high-voltage applications. It is also recommended by IEC 60587 and ASTM D2303 (El-Hag *et al.* 2010:44). The IEC 60587, a standard for inclined plane tracking and erosion test, introduced in 1986 and last updated in 2007, is used to compare the resistance of each solid insulating material to surface tracking and erosion. The test is much more severe than in-service conditions, but this gives accelerated surface ageing with a high level of reproducibility (Bruce *et al.* 2008).

In 1961, Mathes and McGowan reported on tracking and erosion. Their study formed the basis of ASTM D2303, the test methods for liquid contamination materials. These tests have been used to classify materials regarding resistance to tracking and erosion. It has helped choose suitable polymeric materials for insulators and other outdoor

applications (Ghunem *et al.* 2015). Fernando and Gubanski (1999) support that IPT has been used to evaluate the monitoring and resistance to erosion of insulating materials for a long time. These researchers even claim that the stresses used in the inclined plane test (IPT) are quite harsh, even when compared to highly contaminated outdoor conditions. IPT has been widely used as a means of determining suitable materials for AC insulators, with a focus on using this test for DC insulators (Ghunem *et al.* 2013b).

The polymer material test was conducted in different countries (Japan, United States, Germany, Canada, and South Africa). In the late 1950s, studies were conducted in Japan on monitoring organic or polymeric insulating materials. Between 1959 and 1968, epoxy resin, phenolic resin and butyl rubber were evaluated to determine their resistance. It became clear that this test method did not work under all circumstances, so various modified IEC publications on tracking test methods were proposed in Japan (Yoshimura *et al.* 1997).

In Germany, a modified version of the IPT was introduced, which included recordings of the behaviour of the leakage current (LC) on the surfaces tested (current intensity and time of discharge burning) (Fernando & Gubanski, 1999). An LC monitoring system was installed to measure electrical activity during Raychem's inclined plane (IP) testing. The results showed that the silicone and EVA materials exhibited good tracking and erosion resistance. Another modification was made in the United States, and the test performed was based on the IPT test and dust fog test (AST 2123) (Fernando & Gubanski, 1999). The duration of the discharge, the size and the harmonic content of the LC provided information about the degradation. It has been suggested that the modified test procedure can adequately screen the material for high-voltage outdoor insulation (see also Gorur *et al.* 1997).

In Canada, Ghunem *et al.* (2013b) carried out an erosion test of silicone rubber composites in AC and DC inclined plane tests, comparing SIR erosion under AC and DC excitation voltages with the constant voltage method of the inclined plane test (IPT). The results showed that DC+ was the strongest voltage, followed by DC-. In South Africa, Heger *et al.* (2010) conducted a comparative study of insulating materials exposed to high-voltage AC and DC surface discharges. The inclined plane test method described in the international standard IEC 60587 (IPT) was used to determine the performance of insulation materials for power lines: room temperature vulcanised (RTV) silicone rubber (SR) coated with porcelain, high-temperature vulcanised (HTV)

silicone rubber (SR), and EPDM rubber. The results showed that the RTV-SR coating had the least erosion under AC excitation but exhibited significant erosion with negative DC excitation.

2.5.2.3 Rotating wheel dip test (RWDT)

One track and erosion testing method involves using a rotating wheel (Sebo & Liu, 2010). The rotating wheel dip test (RWDT), according to Mackiewicz *et al.* (2017) and Zago (2017), is a method for testing composites insulator housing materials for tracking and erosion. RWDT is designed in accordance with IEC / TR 62730.

In the most recent IEC / TR 62730:2012, the rotating wheel dip test (RWDT) is described as a screening test conducted to eliminate incompatible materials or designs with overhead transmission lines (Krzma *et al.* 2014). Kaltenborn *et al.* (1997) provide background information on establishing the rotating wheel dip test (RWDT) as a test method developed because material testing in the past only focused on tracking and erosion. Therefore, there was a need for a test method that would measure hydrophobicity in the advanced materials available for composite and polymer insulators. Gubanski (1990) reports on studies carried out on the merry-go-round test (MGR), the precursor of the rotating wheel dip test (RWDT). The tests were carried out by immersing the test samples in saltwater and then exposing them to HV energization. However, the data collected did not recommend a standardised method, as there were doubts and questions about its correlation with natural exposure to the outdoors.

This method involves anchoring cylindrical specimens to a rotating wheel, rotating them continuously, soaking them in seawater, and exposing them to high voltage. In addition, continuous increases in leakage current (LC) and loss of hydrophobicity are observed during the test (Fernando & Gubanski, 1999). RWDT has been tested in Germany, Canada, and South Africa. These tests were born from criticisms levelled against the rotating wheel test (RWT). According to Fernando and Gubanski (1999), the testing procedure was heavily criticised as it generated results contradicting expectations and experiences in the field. Based on the reviews, a modified version of the RWDT test was introduced in Germany by adding two resting phases to the previous procedure. Instead of the continuous rotation, the wheel has now turned 90 steps. The time that the sample remained in each step could vary but was generally 1 minute.

Another modification of the RWDT was made in Canada. By adding periods of solar UV radiation to the rotation cycle, silicone and EPDM rubber insulations were assessed for 25 kV applications. The effect of the addition of radiation was evaluated by monitoring the activity of the leakage current. Adding radiation did not increase the severity of the test (Fernando & Gubanski, 1999). In South Africa, Holtzhausen *et al.* (2010) published a similar test called the tracking wheel tester, designed in accordance with IEC 61302. The Holtzhausen TWT was used to compare the ageing behaviour of different insulators under AC and DC excitation. The device was developed to hold up to six test samples, recording AC and DC voltages. The results obtained confirmed the extreme severity of the test, especially for silicone rubber insulators. The DC tests were more severe than the AC tests, and the formation of brown deposits on the insulation was observed.

According to the latest version of the IEC / TR 62730:2012 standard, the test samples are mounted on the rotating wheel and pass through four positions in a cycle, with each sample remaining stationary in each of the four positions for approximately 40 seconds. The 90° turning of the rotating wheel from one position to the next takes approximately eight seconds. In the first part of the cycle, the insulator is submerged in the saline solution. The second part of the test cycle allows excess saline to drip from the test sample, ensuring that slight wetting of the surface causes sparks through dry bands that will form during the third part of the cycle. In this part, the sample is subjected to excitation voltage. In the last part of the cycle, the surface of the test sample heated by the dry band sparking is allowed to cool.

The current study concerns the evaluation of the leakage current performance of high temperature vulcanised (HTV) silicone rubber (SR) and room temperature vulcanised (RTV) silicone rubber (SR) coated glass insulator rods energised under AC, DC+, and DC- in a controlled laboratory environment. Initially, the study was to be conducted at the Koeberg Insulation Pollution Testing Station (KIPTS) due to its international recognition and suitability for long-term testing under non-artificial environmental conditions (see also § 2.5.1). However, due to a risky situation that developed at KIPTS owing to the development of dunes outside the station, a decision was made to opt for another test method. Concerning the KIPTS testing issue, the facility management sent the e-mail below on 24 January 2017.

Hi Siya,

My big concern is the large amount of sand that has built up inside the test station over the windy summer period. At the moment even if we had the line energized, we would not be able to energize the test station as the sand dune outside the site are so large that one can simply walk into the site. This is a huge safety risk and as such we would not be able to energize until the sand build-up subsides. We have been trying to remove the sand from within the test station but we cannot keep up with the amount of build-up on a daily basis. Due to environmental regulations, we are not allowed to remove any sand outside of the test station.

Three important issues arise from the above e-mail: (i) '*...the large amount of sand that has built up inside the test station over the windy summer...*'; (ii) '*[T]his is a huge safety risk...*' due to personnel and animals that can walk into the site'; and (iii) '*[D]ue to environmental regulations, we are not allowed to remove any sand outside of the test station*'. Therefore, the researcher had to explore alternative tests, and the rotating wheel dip test (RWDT) was deemed suitable for this study based for the following reasons:

- It is done in accordance with the IEC / TR 62730:2012 (also see Mackiewicz *et al.* 2017).
- Although the inclined plane test (IPT) has been used for a long time, the application of this test in the material ranking of non-ceramic insulators has been abandoned for some time (Fernando & Gubanski, 1999). Further, the AC tracking and erosion test IEC 60587 permits the comparison of different materials under controlled electrical stress, thereby proving which materials are suitable for dielectric surfaces of insulators. In contrast to the rotating wheel dip test (Bruce *et al.* 2010), this is not an accelerated ageing test.
- Holtzhausen *et al.* (2010) has used a tracking wheel tester (TWT) to accommodate up to six test samples to perform ageing on different insulators under AC and DC. Results obtained confirmed the extreme severity of the test. The DC test turned out to be more severe than the AC (contrary to IPT, as indicated by Ghunem, 2013b). Effectively, the formation of brown deposits may point to the direction of deterioration of the insulator. Holtzhausen *et al.* (2010:448) suggest that further work be undertaken to eliminate the uncertainties caused by the corrosion and arcing by-products.

- It can improve the evaluation of surface characteristics and chemical changes more realistically than tracking wheels because salt fog testing can reproduce water droplet formation, salt accumulation on the surface and water droplet formation (Sebo & Liu, 2010). Some test parameters and specifications have been questioned, and improvements to the test procedures have been proposed (Fernando & Gubanski, 1999).
- In addition, the rotating wheel test method has several advantages: (i) the RWDT is very good in estimating tracking and erosion of insulating materials surfaces, as well as corrosion of metal components; (ii) the erosion and surface damage simulation works well; (iii) a good simulation of a dry-band arc on a stressed insulation surface is obtained through the cycling of wet and dry periods; and (iv) voltage and water conductivity changes are displayed much more rapidly than in fog chamber experiments (Sebo & Liu, 2010).

2.6 RTV AND HTV SILICONE RUBBER TEST RESULTS ACCORDING TO IEC / TR 62730

In § 2.5.2.3, the literature described the strength or advantages of performing the rotating wheel dip test (RWDT) on insulators. The wheel test is important for determining the quality of industrial designs and materials, as shown by Verma and Subba (2018). Additionally, they suggest that the wheel test might be the most severe test regarding tracking and erosion. The inclined plane test, salt fog test, tracking wheel and voltage breakdown are common test methods to evaluate the old polymeric insulators and coatings (Jahromi *et al.* 2005).

Verma and Subba (2018) concede that there is minimal rotating wheel dip test information for long-term ageing studies, especially under DC application under different environmental conditions. Nonetheless, there have been several studies on the rotating wheel dip test in the recent past. The following studies overview the experimental research since the publication of the IEC / TR 62730:2012 standard:

- Krzma *et al.* (2014) conducted an experimental study of silicone rubber polymer insulators for 11 kV systems with a rotating wheel dip test (RWDT) based on IEC / TR 62730:2012. The main aim was to compare the ageing properties of polymer insulators under AC voltages. A conventional polymer insulator design was adopted and compared to insulators with a textured surface. The two polymer insulators were tested continuously at

190 revolutions for 10 hours. Each rotation lasts 192 seconds with four test positions: energization, cooling, dipping, and dripping positions in that sequence. The stationary time for the individual positions is 40 seconds, and the test sample took eight seconds to move from one position to another. A conventional polymer insulator design (insulator A) was adopted and compared to insulators with a textured surface (insulator B). The leakage current was more severe at the surface of insulator A, while in insulator B, the discharge activity was much lower.

- Krzma *et al.* (2015) investigated the ageing performance of polymeric insulators under positive DC and AC excitations. Tested continuously for 10 hours under positive DC and AC excitations, the SR insulators covered 190 wheel revolutions. With four test positions, energization, de-energization, dipping and dripping, each revolution takes 192 seconds. It takes approximately eight seconds for the test sample to rotate from one position to another after remaining stationary for about 40 seconds for each position. AC test results showed discharge activities on both conventional and textured surfaces. However, discharge activities were more severe on conventional surfaces. During initial energization, the high leakage current observed causes surface drying and the formation of a dry band on the surface. As far as the DC test results of the conventional insulator are concerned, leakage current is frequently observed to be completely interrupted. During AC testing, there was no evidence of a significant partial arc. Contrary to this, the textured insulator showed no current interruptions and very limited discharge activity. Apparently, no dry bands formed on the textured insulator.
- Mackiewicz *et al.* (2017) used the wheel test to study composite insulator sheds. Samples made from HTV-SR came from the sheds of two different composite medium voltage insulators manufacturers. Both types of insulation passed the 1 000-hour salt fog test without a hitch. The sheds were covered with a dark coating of varying thickness. The study determined that electrical and temperature factors significantly affected sheds during the wheel test than the 1 000-hour salt fog test. The authors concluded that the wheel test allows better differentiation between material properties.
- A recent study by Verma and Subba (2018) investigated the ageing effects on polymeric insulators subjected to multi-stress under DC voltage application.

The study was done using IEC 62730 standard, with experiments conducted for 1 000 hours with electrical and environmental stresses applied cyclically. The results showed degradation of material properties. FTIR analysis indicated the loss of main chain bonds corresponding to a peak at 1 008 cm, representing the phenomenon of depolymerisation. The loss of ATH further accelerates thermal degradation. Therefore, Verma and Subba (2018) believe that their study provides a better understanding of the degradation behaviour of polymeric insulators under multi-stress with DC voltage application.

There were limited or no studies conducted at the time of the current study on RTV-SR under IEC / TR 62730:2012. Considering that the methods for assessing the long-term reliability of RTV-SR have not been standardised, it is imperative to investigate how environmental factors and operating conditions affect the properties of these rubbers (Wen *et al.* 2017). IEC / TR 62730 points out that tracking and erosion tests are not considered “ageing tests” as the tests do not replicate real-life degradation conditions nor accelerate conditions to provide a life-equivalent test quickly. Tracking and erosion tests are better described as “screening tests” for detecting inadequate materials and designs (Klüss & Hamilton, 2017). Due to shortcomings associated with both ceramic and non-ceramic insulators, RTV silicone rubber coating became a popular form of insulation owing to its hydrophobicity (Jamaludin *et al.* 2017), resistance to ultraviolet radiation, chemicals, thermal degradation, and corona discharge (Hamadi *et al.* 2020), as well as prevention of flash-overs caused by uneven wetting (Wu *et al.* 1998). According to Pylarinos *et al.* (2015), the above claims are in accordance with their study, which concluded that RTV-SR coated ceramic insulators are a viable alternative to HTV-SR composite insulators for use in overhead power networks in polluted areas.

2.7 HIGHLIGHTS OF THE LITERATURE REVIEW CHAPTER

The important conclusions drawn from this chapter are as follows: Based on the research done in this study, it was found that glass insulators have been used for a very long time in electrical power networks. According to the literature, the lifetime expectancy of glass insulators is approximately 30 years or more (Mouton, 2012).

According to the literature, insulators should possess excellent electrical ageing properties to prevent insulation failure or deterioration. Since some of these insulators are experiencing high-voltage electrical stresses in highly polluted environments, they

face the risk of failure. Moreover, the formation of a contamination layer on the insulator surface results in an electrolytic film growing which may induce dry band arcing, surface deterioration and corona discharge when exposed to moisture (Elombo, 2012; Mouton, 2012).

Power utilities have adopted various remedial measures worldwide to mitigate this problem. Among the common methods are increasing insulator creepage (leakage) distance, reducing supply voltage, insulator washing (cleaning), oiling or greasing (silicone) the insulator surface, and insulator replacement (Kumara & Fernando, 2020). However, the use of glass material continued to have challenges, especially to meet the needs of the electrical power network worldwide, and that created an opportunity for the exploration of products classified as non-ceramic insulators (NCIs), which includes polymeric insulators.

Polymeric insulators, also called non-ceramic, have been used during the last six decades as an alternative to ceramic insulators (glass and porcelain) (Kumara & Fernando, 2020). The material used for these insulators is silicone rubber (SR) because it has water repellent (hydrophobic) properties, is lightweight, and is resistant to vandalism. Numerous studies have substantiated these characteristics in the field (Elombo, 2012; Vosloo; 2002; Mouton, 2009).

Polymeric insulators are relatively new. The first generation of polymeric transmission line insulators was introduced commercially in the 1970s and widespread use on transmission lines in the 1980s (Limbo, 2009). A typical NCI such as HTV-SR consists of a glass fibre core covered by a polymer sheet with sheds. The glass fibre core provides the NCI with the required mechanical strength to support the line conductors (Heger, 2009). The NCI housing protects the core from natural elements like moisture and contamination. A polymer insulator consists of three parts: FRP (Fibre Reinforced Plastic) rod, silicon rubber housing with sheds, and galvanised fittings (Vosloo, 2002).

Predicting the life expectancy of NCIs and forecasting their performance is always of big concern to power utilities such as Eskom since they are relatively new technology. Most experiments conducted on NCIs have accelerated life tests mainly performed in laboratories or outdoor test sites (Elombo, 2012). The most relevant test results of outdoor insulators are obtained from field station tests and actual performance on power networks (Elombo, 2012). These tests are primarily useful to both utilities and manufacturers. From the utilities' point of view, the results obtained can be used to rank the polymeric insulators, determine the ability of NCIs to meet their design

requirements, and investigate the NCIs end life modes, i.e. flash-over, tracking erosion, punctures, etc. Manufacturers can utilise the tests to develop better insulating materials and optimise NCI design (Limbo, 2009). Various scenarios of the ageing process of NCIs have been established, and several factors that contribute to the ageing process have been identified. Those factors include ultraviolet radiation, moisture, mechanical breach of the housing, thermal stresses, dry band arcing, pollution level, pollution type, and corona. Up to now, most researchers agree that these parameters affect the ageing of NCIs. Several studies have been conducted to assess the insulator performance under the stresses applied and predict their performance in different environmental conditions (Elombo, 2012). Most tests are conducted in laboratories and the field using different test methods such as IPT, salt fog test, TWT, RWDT etc.

Nowadays, composite insulators are increasingly used to replace porcelain and glass insulators due to the advantages obtained from the good performance against pollution, lower weight, and reduced installation and maintenance costs. Although the use of silicone rubber composite insulators has been increased significantly in recent years, porcelain and glass insulators are still manufactured and remain predominant in distribution and transmission lines. Except for their hydrophilic property, porcelain and glass insulators are widely used because they offer many advantages such as low cost, flexible maintenance, and high strength. When energised in polluted areas such as coal industry zones and coastal areas, the insulators are easily contaminated, forming dry bands and leading to flash-over (Vosloo, 2002).

Outdoor environmental conditions vary widely. Temperature and moisture can greatly affect the performance of insulators. For example, moisture such as rain, dew, fog, and melting ice can significantly lower the surface resistance of insulators. With pollution, the insulator surface resistance is reduced even more. The reduction of surface resistance might cause an increase in leakage current to flow on the surface and dry band arching to occur. In addition, large magnitudes of leakage currents flowing on the surface for an extended period might cause degradation of the insulator surface. With these factors, flash-over might be initiated, which leads to the failure of a section of the power line. NCIs perform well under polluted conditions, especially due to their hydrophobicity provided by their silicone rubber (SR) coating. SR helps to prevent the formation of a water film on the insulator surface, even when that surface is polluted.

However, as the insulation ages, dry band arcing may cause erosion and tracking on the surface of these insulators (Vosloo, 2002).

Silicone rubber is a polymeric material with poor ability to resist electrical tracking and erosion. According to Elombo (2012), tracking is an irreversible deterioration by forming paths starting and developing on the surface of insulating material. These paths seem to be conductive even under dry conditions.

In the literature review, various tests (artificial and non-artificial) were found to measure the performance and evaluate tracking and erosion of insulating material surfaces. Among them, the RWDT method is an example of an artificial test method designed according to the IEC / TR 62730:2012 standard, which was deemed suitable for this study.

A summary of the results for each test is supplied in § 2.6 and Table 2-6. The literature reviewed indicates the superiority of the rotating wheel dip test (RWDT). It also suggests that a gap exists in terms of comparison between RTV-SR and HTV-SR. Another important observation is that the tests performed in terms of the IEC / TR 62730:2012 standard vary. The mechanical design of the tests and the rotational cycles, which fall between 190 seconds and 200 seconds, are consistent throughout the tests performed, as indicated in the literature. Thus, researchers have the liberty to determine the duration of the test.

For the general overview of high-voltage insulators and the coating of insulator materials, refer to Table 2-6 below.

Table 2-6: General overview of the high-voltage insulators plus the coating of insulators

Item	Description
Evolution of Insulators	
<i>Ceramic</i>	<i>Non-ceramic</i>
<ul style="list-style-type: none"> • In 1820, ceramic insulators were used for telegraph lines made of annealed glass or “dry-pressed” porcelain • In 1882, these insulators were used for power transmission lines • Since the ceramic insulators suffered from punctures because of the material porosity, this led to the development of wet-process porcelain in 1896 (Mouton, 2012) 	<ul style="list-style-type: none"> • Conventional ceramic insulators were dominant in the market for many years (Vosloo, 2002) until they were replaced by polymeric composite insulators (Elombo, 2012; Krzma, 2016) • The non-ceramic insulators show many advantages over the conventional insulators (Al-Gheilani <i>et al.</i> 2017) • Composite insulators are now widely used worldwide because of their lower weight, higher mechanical strength, higher design flexibility and reduced maintenance (El-Shahat & Anis, 2014)

Item	Description
Advantages of Ceramic and Non-ceramic Insulators	
<i>Ceramic</i>	<i>Non-ceramic</i>
<ul style="list-style-type: none"> • Ceramic materials (e.g. porcelain and glass) have been used for a long time and were chosen for outdoor insulation (Nekeb, 2014; Kuffel, 2000) • They demonstrated great capability of withstanding mechanical and electrical stresses (Mackevich & Shah, 1997; Gubanski <i>et al.</i> 2007) • Both ceramics and glass offer good insulation characteristics and excellent weather resistance (Kobayashi <i>et al.</i> 2001) • Some of the advantages of ceramic insulators are immunity to degradation by environmental factors, i.e. ultraviolet radiation and aggressive pollutants because of its inert inorganic nature; resistance to damage caused by partial surface discharges and leakage current activity; ability to be easily formed into a variety of shapes for different applications; and high compressive strength (Mouton 2012; Macey <i>et al.</i> 2004) 	<ul style="list-style-type: none"> • The main advantages of polymeric insulators over conventional ceramic insulators are their lighter weight, ease of transportation (unbreakable) and installation in the electrical transmission lines (Ghosh <i>et al.</i> 2015) • Non-ceramic insulators have shown a superior performance against contamination conditions due to their water filming repellent property (Mackevich & Shah, 1997; Gubanski <i>et al.</i> 2007) • Some of the advantages of polymeric insulators are high tensile strength-to-weight ratio and improved performance in highly polluted areas by the silicone rubber types. They are an unattractive target for vandals as they are very resistant to projectile damage (Mouton, 2012; Macey <i>et al.</i> 2004)
Advantages of Ceramic and Non-ceramic Insulators	
<i>Ceramic</i>	<i>Non-ceramic</i>
<ul style="list-style-type: none"> • Ceramic insulators are heavy, have poor resistance to impact and suffer major deterioration in terms of the voltage withstand characteristics under contamination (Kobayashi <i>et al.</i> 2001) • With porcelain and glass insulators, it has been observed that water readily forms a continuous film on their surfaces, which may lead to the development of flash-overs and which could result in power outages (Deng & Hackam, 1997) • The accumulation of deposits of the surface during the long-term operation reduces their dielectric strength, resulting in poor flash-over performance of the insulator (Khatoun <i>et al.</i> 2017) • With ceramic insulators, there is a possibility of severe leakage current erosion; electrical weakness at mould line may result in material degradation; and their use is limited to medium voltages on overhead lines (Mouton, 2012; Macey <i>et al.</i> 2004) 	<ul style="list-style-type: none"> • Non-ceramic insulators experience electrical, mechanical, and environmental deterioration • Electrical factors include tracking, erosion, puncture of sheds and cracking, while mechanical factors include long-term degradation of tensile strength and degradation of strength due to repetitive bending and twisting (Kobayashi <i>et al.</i> 2001) • The environmental effects include ultraviolet, moisture, heat, light, atmospheric pressure, and biological degradation caused by microorganisms in the air • While electrical stress includes corona, formation of dry bands, arcing over the surface of insulators, roughness, and erosion of surface (Amin & Salman, 2006) • Other disadvantages are as follows: erosion on polymer housing due to leakage currents if incorrect material or incorrect dimensions are used; possible electrical weakness at the mould line for moulded constructed insulators; deflection under load in certain applications; and special care needed in design and manufacturing to eliminate entrance of moisture at the interface between core, polymer housing and metal end fittings (Mouton, 2012; Macey <i>et al.</i> 2004)

Item	Description
Insulator Material	
<i>Ceramic</i>	<i>Non-ceramic</i>
<ul style="list-style-type: none"> • Ceramic materials are inorganic, non-metallic materials made from compounds of metal and non-metal • Ceramic materials may be crystalline or partly crystalline. They are formed by the action of heat and subsequent cooling • Clay was one of the earliest materials used to produce ceramics, like pottery, but many different ceramic materials are now used in domestic, industrial, and building products (Shukla, 2011; Subedi, 2013) • Table 2-3, Table 2-4 and Table 2-5 contain mechanical and electrical properties and the chemical composition of ceramic insulators 	<ul style="list-style-type: none"> • Composite or polymeric materials are based on polydimethylsiloxanes (PDMS), commonly named silicone rubber (SR). Other materials used are ethylene-propylene-diene monomer rubber (EPDM), ethylene-vinyl-acetate (EVA) and so-called alloy rubbers. The latter is a blend of EPDM and silicone (Gubanski <i>et al.</i> 2007) • Polymeric materials such as silicon rubber, epoxy, ethylene propylene diene monomer (EPDM) and polyesters are used as insulators for transmission, distribution, termination of underground cables, bushings, and surge arrester housings (Amin & Salman, 2006; Ersoy <i>et al.</i> 2007; Nasrat <i>et al.</i> 2013) • Table 2-1, Table 2-2 and Table 2-3 describe the mechanical and electrical properties and the chemical composition of non-ceramic insulators
Leakage Current	
<i>Ceramic</i>	<i>Non-ceramic</i>
<ul style="list-style-type: none"> • The measurement of leakage current is used for monitoring the performance of insulators to minimise system outages attributable to pollution (Ramirez <i>et al.</i> 2012; Li <i>et al.</i> 2009) • The leakage current on ceramic insulators is often greater than the leakage current on non-ceramic insulators (Chrzan, 2010) • Leakage current may lead to flash-over that could be followed by an outage of the power system (Ibrahim <i>et al.</i> 2014) • Ceramic materials (porcelain and glass) are hydrophilic because they have a high affinity with water – possess enticing surface properties that render them susceptible to the formation of a continuous electrolytic film (Elombo, 2012; Heger, 2009) 	<ul style="list-style-type: none"> • Most of the highest contaminated insulators can be found in coastal, industrial estates and cement industrial areas (Darwison <i>et al.</i> 2019) • Hydrophobic materials (non-ceramic) possess water repellent characteristics (Elombo, 2012; Venkataraman & Gorur, 2006) • Polymer materials have better dielectric properties, low weight, easy handling, and vandal resistance (Sarathi <i>et al.</i> 2004) • Polymeric insulators have shown a cyclic decrease and then the recovery of hydrophobicity with time (Amin <i>et al.</i> 2009) • During hydrophobicity loss periods, the insulator behaves as hydrophilic, and surface activity follows the same basic steps towards flash-over, which may occur if favourable conditions exist and hydrophobicity is not recovered in time (Pylarinos <i>et al.</i> 2011)
Coating	
<i>Room temperature vulcanised (RTV)</i>	<i>High temperature vulcanised (HTV)</i>
<ul style="list-style-type: none"> • The original RTV-SR coating was developed in the early 1970s and was commercialised about 15 years later (Goudie & Collins, 2004) • RTV-SR silicone coating can retain water repellence under outdoor weathering and high-voltage conditions (Jamaludin <i>et al.</i> 2017) • All RTV-SR coating systems are made from basic polydimethylsiloxane (PDMS) polymer 	<ul style="list-style-type: none"> • HTV-SR is a type of silicone rubber in a solid-state before curing under high temperatures • It is used for the manufacturing of composite insulators (Wang <i>et al.</i> 2017) • Not only does HTV-SR has excellent properties for weathering, tracking and arc resistance, and it is lighter and easier to handle compared to porcelain

Item	Description
<p>system that may contain a fumed silica reinforcer, a polymerisation catalyst and ATH filler</p> <ul style="list-style-type: none"> • PDMS molecules are mainly composed of the methyl group (CH₃), oxygen (O) and silicon (Si). For a chemical structure of PDMS, refer to Figure 2-6. • The environmental requirements for RTV silicone rubber are under 25°C ± 2°C and the relative humidity of 40% ~ 70% (Jia <i>et al.</i> 2006; Wu <i>et al.</i> 2017). • RTV silicone rubber coatings are available in a liquid state, and after being applied on the insulator surface, they form a solid, rubber-like coat (Cherney & Gorur, 1999). • See Figure 2-5 for the application of RTV-SR coating. • RTV-SR coatings have been used in various environments, such as coastal, desert, industrial, high humidity, and low temperature. Today, RTV-SR coatings are being used on both AC systems and DC systems (Jia <i>et al.</i> 2008) to prevent flash-overs caused by uneven wetting (Wu <i>et al.</i> 1998) • Artificial test methods to evaluate leakage current performance on RTV-SR coating were conducted in the following countries: the United States, Germany, Japan, South Africa, Canada, and Great Britain. See § 2.5.2 for further details. 	<ul style="list-style-type: none"> • The electrical properties of HTV are characterised by being constant against strong winds, high-temperature heat, rain, snow, and high humidity • The HTV -SR has been commonly aged under ultraviolet radiation, acid rain, ozone, and surface discharge in the high-altitude region (Qin <i>et al.</i> 2013; Moreno & Gorur, 2003) • HTV-SR possesses mechanical properties that are deemed superior to those of room temperature vulcanised (RTV) types. This provides HTV-SR with sufficient mechanical strength to endure long-term outdoor service • Such mechanical properties also provide hydrophobicity, which can be quickly recovered even it is lost as a result of dry-band arcing, corona discharges, and deposits of dust on the insulator surface (Kumagai & Yoshimura, 2001). HTV-SR is cured at a high temperature at 180°C (Tong <i>et al.</i> 2018). • HTV-SR tests were performed in various countries such as South Africa, Thailand, Iran, the United States, and the United Kingdom. For more details, refer to § 2.4.1

From all the above, it can be seen that the performance of RTV-SR and HTV-SR, in particular, are not extensively studied. This is particularly so in an environment with coastal pollution. An alternative indoor testing method has been specified because of the unavailability of outdoor testing stations such as KIPTS. It will be used to determine whether HTV-SR and RTV-SR coated test samples have the same leakage current performance under AC, DC+, and DC- in a simulated coastal pollution environment and determine the leakage current value of these test samples using a rotating wheel dip test (RWDT). Researchers such as Elombo, Limbo, and Vosloo have performed studies on different test samples. However, failures on them were experienced. Therefore, it was necessary to explore and verify the performance of those insulators using a different method (RWDT), which will be cost-effective and quick to find results quicker than having insulators out in the field for a long time. Results will be used to compare with and verify the findings of other researchers. It was also noted that it is important to determine which of the two insulators (coated with RTV-SR and HTV-SR) is more suitable for DC applications. This is because there does not seem to be a comprehensive practical study on RTV-SR and HTV-SR insulator leakage current

performance for DC networks. Therefore, it is pertinent to determine the performance of power line insulators under HV DC applications when subjected to natural pollution environments.

2.8 CHAPTER SUMMARY

This chapter explored and reviewed the literature on ceramic (glass and porcelain), ceramic coated and polymeric high-voltage insulators. The following aspects were explored:

- An overview of the effect of environmental and climatic conditions on RTV-SR glass-coated insulators and HTV-SR insulator performance;
- A review on the common ageing modes that may serve as indicators on the ageing performance of insulators;
- A brief review on the insulator pollution flash-over;
- Various tests were analysed to assess the leakage current performance of RTV-SR coating and HTV-SR. To test the RTV-SR and HTV-SR coatings' leakage current performance on borosilicate and fibreglass rod insulators, the rotating wheel dip test (RWDT) was chosen as the most appropriate compared to other tests.

The tests will be performed in accordance with the IEC / TR 62730:2012 standard (refer to § 3.3).

CHAPTER 3.0

TEST SAMPLES, METHODOLOGY, AND PROCEDURE

This chapter describes the test procedures and methodology of this present study. This includes measuring the hydrophobicity of insulator surfaces to determine the extent to which water forms films on the insulator surface or is repelled by the insulators. Regarding the research objectives as outlined in § 1.5, the choice of approach for insulator monitoring needed to be carefully considered to ensure the objectives are adequately addressed. The research work reported in this thesis was conducted at Eskom's 400 / 132 / 66 kV Stikland substation. A set of two RTV-SR coated glass test samples and two HTV-SR test samples (a total of four) were installed on the rotating wheel dip test (RWDT) under three voltage types, namely AC, DC+, and DC-. All insulators have been supplied from a common manufacturer, GlassChem Cc.

The performance of polymeric insulators in outdoor and laboratory test facilities was reported as better than porcelain and glass. The main reason for better performance seems to be that energy providers such as Eskom value their substantial advantages over inorganic insulators, porcelain, and glass insulators (Ehsani *et al.* 2005). Outdoor high-voltage insulators such as polymeric insulators should maintain a high dielectric strength under all environmental conditions.

To achieve the objectives of this study, as stated in § 1.5, a set of two RTV-SR coated borosilicate glass test samples and two HTV-SR extruded onto glass fibre test samples were chosen accordingly (see Figure 3-1 and Figure 3-2).



Figure 3-1: HTV-SR extruded onto glass fibre test samples (6x)



Figure 3-2: RTV-SR coated borosilicate glass test samples (6x)

The test samples displayed were manufactured by GlassChem in Stellenbosch. The important insulator dimensions of the HTV-SR and RTV-SR test samples are summarised in Table 3-1 below.

Table 3-1: HTV-SR and RTV-SR test sample dimensions and parameters

Dimensions	Parameters
Measured creepage distance	275 mm
Average diameter	20.5 mm
Form factor	4.27

3.1 FORM FACTOR

In a uniformly distributed electrolytic pollution layer on an insulator, the form factor F_f of an insulator is directly related to the surface layer resistance. Among other factors, form factor value has a significant impact on pollution flash-over performance. In electrical insulators, the form factor is defined as the integral of the incremental leakage distance dl divided by the circumference $2\pi r$ at each measurement point. By ensuring that the desired conditions for pre-contamination and wetting have been met, the form factor is used, and it can also be used to compare insulators of the same length, diameter, and leakage distance, but with different profiles (Vosloo, 2002; Farzaneh & Chisholm, 2009; Mouton, 2012).

The above authors concur that the value of the form factor of an insulator is determined by the following equation:

$$F_f = \int_0^L \frac{dl}{2\pi \times r(l)}$$

Where F_f is the form factor value; L is the total creepage distance of the insulator measured in mm, and $r(l)$ is the radius of the insulator at a position along the insulator in mm. Figure 3-3 provides a graphical representation of the form factor equation.

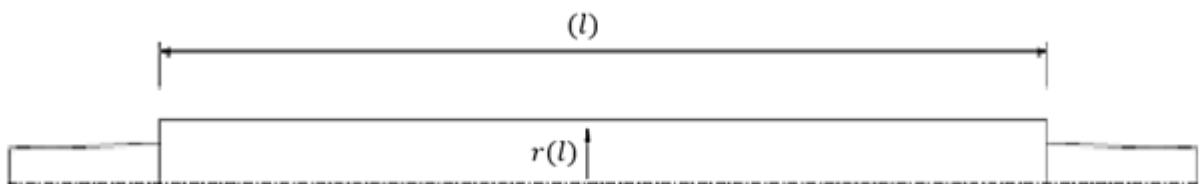


Figure 3-3: Graphical representation of the form factor equation

3.2 PROPERTIES OF HTV-SR AND RTV-SR TEST SAMPLES

Compared with other materials, HTV-SR and RTV-SR have higher tensile strengths because the test samples will not break unless under the condition of tensile elongation and a high elongation percentage of 422% to 445% (Mitra *et al.* 2014). Due to the nonlinearity of the deformation characteristics of these materials, the dynamic modulus is an important characteristic, and they behave differently under high and low loading rates. High dynamic modulus elastomers are very tough materials. However, RTV-SR has the lowest dynamic modulus of 2.12 MPa (Mitra *et al.* 2014). The manufacturer did not provide the actual specifications of the test samples. Table 3-2 shows typical values for the RTV-SR and HTV-SR insulator rods used in the test.

Table 3-2: Typical properties of HTV-SR and RTV-SR test samples

Properties		Silicone Rubber Type	
		HTV-SR	RTV-SR
Viscosity (mPa.s)		2×10^7	$5 \times 10^3 \approx 1 \times 10^5$
Curing condition	Temperature (°C)	150 \approx 170	80 \approx 100
	Pressure (MPa)	10 \approx 15	5 \approx 10
	Time (min)	60 \approx 30	30 \approx 60
Molar mass ($\times 10^5$ g/mol)		30 \approx 80	1 \approx 10
Polymerisation degree ($\times 10^3$)		0.1 \approx 1	5.0 \approx 10
Volume resistivity (Ω .cm)		$10^{13} \approx 10^{15}$	$10^{13} \approx 10^{15}$
Dielectric strength (kV/mm)		20.0 \approx 26.0	20.0 \approx 24.0
Dielectric constant, E_r		2.0 \approx 5.0	2.0 \approx 5.0
Ultimate tensile strength (MPa)		5.87	4.20
Maximum elongation (%)		200 – 441	200 – 445
Tensile strength (MPa)		11	7
Maximum service temperature (°C)		200	200
Dynamic modulus (MPa)		4.66	2.12

The RTV-SR coated glass test sample used in this study is made of borosilicate glass manufactured by GlassChem in Stellenbosch. Borosilicate glass, also known as Pyrex, is widely used in the chemical, electrical and mechanical engineering industries. This glass is chemically resistant, has a low coefficient of thermal expansion, and can be used at relatively high temperatures. Moreover, it offers a variety of shapes and sizes to choose from, such as a rod or tube.

Several researchers have provided data on mechanical, thermal and electrical properties of borosilicate glass such as density (Sinev & Petrov, 2016), Young Modulus

(Bouras *et al.* 2009; Schott, 2007), maximum temperature and coefficient of linear thermal expansion (Lima *et al.* 2012; Park & Lee, 1995), resistance (Hiremath & Hemanth, 2017; Lima *et al.* 2012), dielectric constant (El-Kheshen & Zawrah, 2003; Lima *et al.* 2012), and dielectric strength (Hiremath & Hemanth, 2017; Lima *et al.* 2012). Table 3-3 below summarises the borosilicate glass properties.

Table 3-3: Borosilicate glass properties

	Properties	Units	Value
General	Density	g/cm ³	2.23
Mechanical	Young's Modulus	GPa	64
Thermal	Max use temperature	°C	500
	Thermal conductivity	W/mK	1.14
	Coefficient of linear thermal expansion	10 ⁻⁶ /°C	500
Electrical	Volume resistance	Ωcm	10 ¹⁵
	Dielectric constant	1 MHz	4.8
	Dielectric strength	kV/mm	30

3.3 TESTING METHODOLOGY

A testing methodology evaluates a device, system, or component to determine if it meets specific requirements. It assists in identifying any types of gaps, errors, or missing requirements. The testing methodology utilised in this study complied with IEC / TR 6273:2012 standard (Figure 3-4 below). According to Li *et al.* (2017), IEC / TR 62730:2012 has an existing internationally recognised test procedure to evaluate the resistance of composite insulators to tracking and erosion for rejecting inadequate materials or designs. This standard specifies the test parameters and criteria for AC excitation. As a utility company in South Africa, Eskom bases most of the specifications for high-voltage insulators on IEC specifications and guidelines. Therefore, the IEC 62730:2012 standard applied to AC excitation and was adapted for DC+ and DC- for this study.

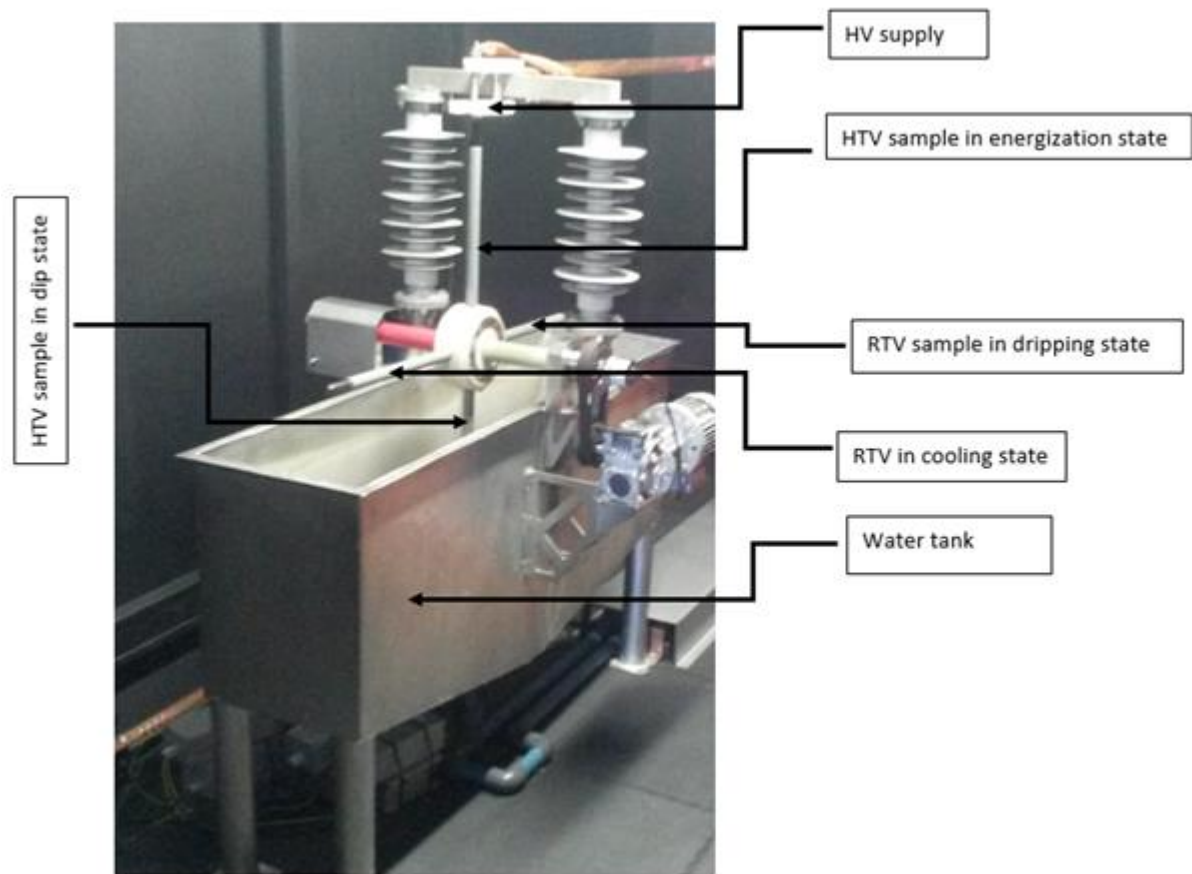


Figure 3-4: Schematic diagram of the RWDT (IEC / TR 6273:2012; Krzma, 2020)

Figure 3-4 above shows that the test specimens are mounted on the wheel. They go through four positions in one cycle. Each test specimen remains stationary for about 40 seconds in each of the four positions. The 90° rotation takes about eight seconds from one position to the next. In the first part of the cycle, which is vertical (upside down), the insulator is dipped into a saline solution (NaCl content). The second part of the test cycle, which is horizontal (flat), permits the excess saline solution to drip off the specimen, ensuring that the light wetting of the surface gives rise to sparking across dry bands that will form during the third part of the cycle. In that part, the specimen is submitted to a power frequency voltage, and the leakage current is recorded with the OLCA. In the last part of the cycle, which is horizontal (flat), the surface of the specimen heated by the dry band sparking is allowed to cool (IEC / TR 62730:2012; Krzma *et al.* 2020).

3.4 TEST CONDITIONS

In accordance with the standard (IEC / TR 62730:2012), the actual creepage distance in mm is divided by 28.6 to determine the power frequency test voltage in kV. The actual creepage distance of the test samples was measured as 275 mm, which yielded

a power frequency test voltage of 9.616 kV (≈ 10 kV). The salt content of the solution in the water tank composed of NaCl and deionised water was 1.4 g/L, and the salt solution was changed weekly.

There must be four test positions per revolution of rotation during the test, including the energization position, de-energization position, the dipping or immersion position, and the dripping position. To ensure that the acceptance criteria are met and the tracking wheel test passed, (i) the test samples of the same design shall be evaluated together; (ii) the pairs of test samples of different designs shall be assessed separately; and (iii) the surface tracking and erosion should not reach the glass fibre core.

3.5 PRELIMINARY TESTS

Preliminary tests were performed before the commencement of the investigation, i.e. the main test. Table 3-4 below indicates that all the samples passed the preliminary insulation resistance test.

Table 3-4: Insulation resistance test on RTV-SR and HTV-SR test samples

Test voltage	Test samples	Acceptance criteria	Test results	Comments
5 kV	6 × RTV-SR	$\geq 2 \text{ M}\Omega$	$\geq 5 \text{ M}\Omega$	Acceptable
	6 × HTV-SR	$\geq 2 \text{ M}\Omega$	$\geq 5 \text{ M}\Omega$	Acceptable

Before energizing the test apparatus, the following aspects were ensured:

- The end of each test specimen was covered with a glassy carbon end piece which was glued on the tip using silicone glue/paste. The paste on the test sample was left on the test sample for 24 hours to cure.
- Electrodes were cleaned in an ultrasonic bath and wiped with distilled water;
- The test specimens were mounted on the wheel (see Figure 3-4), and each test sample was marked with an identification number;
- The test samples were tested for continuity with a multi-meter after installation;
- The water tank was filled and the salt-solution was prepared by adding sodium chloride (NaCl) to distilled water to achieve a concentration of 1.4 g/L;
- Hall effect sensor is connected;
- The multimeter was switched on;

- The probe was mounted on an HV terminal;
- The camera was set up and switched on; and
- The OLCA and the PC were switched on.

3.6 DURING THE TEST

The temperature inside the high-voltage room is maintained at 16°C using the air-conditioning unit. Switch on the RWDT drive motor.

1. Remove the earth stick attached to the transformer.
2. Lock the door to the test chamber
3. Reset the emergency stop button.
4. Switch on the main circuit breaker CB1 (see Figure 3-5). The green “MAINS ON” lamp will illuminate.
5. Set the variac to zero.
6. Switch on the transformer supply circuit breaker CB2 (see Figure 3-5).
7. Adjust the variac located on the control panel until a required voltage of 10 kV is reached. This 10 kV was measured using a digital multi-meter attached to a voltage probe connected to the HV supply.
8. Press the start button; the red “CONTROL ON” lamp will illuminate.
9. Record the start time of the test.

Note: To make sure that repeatable results are obtained and that the test conforms to the IEC / TR 62730:2012 standard, close supervision and the following monitoring interventions are required at all times:

- Continuous monitoring of the water level in the water tank.
- Monitoring of the conductivity.
- Visual monitoring of the rotating wheel every 24 hours ensures that the hardware is working properly.

In case of fault, the following steps must be adhered to:

1. Press the emergency stop so that the LV supply can be disconnected.
2. Switch off RWDT drive motor.

3. Open the chamber door and apply the earth stick to the HV supply.
4. Investigate the fault.

To stop the machine, do the following:

1. Set the variac to zero.
2. Switch off the control circuit supply.
3. Switch off the transformer supply circuit breaker CB2.
4. Switch off the main circuit breaker CB1.
5. Record the stop time of the test.
6. Unlock the door and apply the earth stick to the HV supply.

3.7 MEASUREMENT OF LEAKAGE CURRENT ON INSULATOR TEST SAMPLE

According to the following researchers – Li *et al.* (2010), Castillo-Sierra *et al.* (2018), Elombo (2012) and Amirbandeh *et al.* (2014) – when a certain threshold value is reached, the magnitude of peak leakage current indicates the probability of an insulator flash-over. Therefore, the peak leakage current magnitude was the major parameter considered in this study. Further, the cumulative electrical charge for each test sample was recorded to evaluate the test sample in relation to the continuous charge accumulation on its surface.

For each test sample, a Hall effect current sensor (see Figure 4-10 and Figure 4-11 below) was installed and connected to the OLCA for data logging purposes. A diagram in Figure 3-5 represents the circuit used for the leakage current measurements in the study.

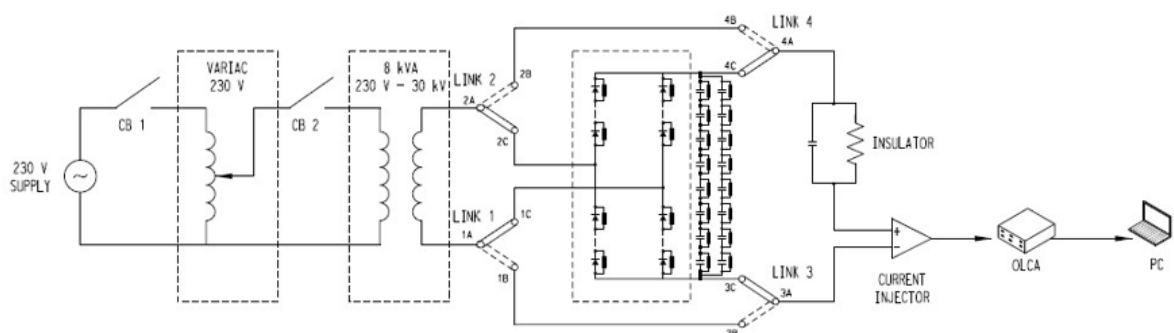


Figure 3-5: 230 V/30 kV transformer and DC rectifier circuit diagram

3.8 CUMULATIVE ELECTRIC CHARGE

Maximum values of the leakage current measured are stored in a register until the end of the 1-minute interval on the OLCA instrument. The maximum leakage current values taken are then multiplied by the sampling interval to calculate the cumulative charge flowing over the surface of the insulator through the pollution layer (Vosloo, 2002).

A charge can be calculated according to the following equation:

$$Q = \int_0^N i(n) \times dt = \sum_{n=0}^N (i(n)) \times \Delta t$$

Where:

Q : is the 1-minute interval positive electric charge in coulomb (C);

$(i(n))$: is the n^{th} value of the leakage current (i) at a time (t) in ampere (A);

Δt : Sampling interval, $\frac{1}{f} = \frac{1}{2 \text{ kHz}} = 0,5 \text{ ms}$;

$N = f \times t = 120\,000$;

$f = 2 \text{ kHz}$; and

$t = 60 \text{ seconds}$.

The formula above is applicable for the positive and negative electrical charges. This recording approach makes the insulator leakage current performance clearer to observe.

3.9 HYDROPHOBICITY CLASSIFICATION

Several researchers have provided definitions of hydrophobicity and explained how it is measured (Al-Ammar & Arafa, 2012; Amin *et al.* 2007; Dong *et al.* 2015; Elombo, 2012; Jarrar *et al.* 2014; Khan, 2010; Limbo, 2009; Mavrikakis *et al.* 2015; Mouton, 2012; Thomazini *et al.* 2012; Yang *et al.* 2018). According to Mouton (2012), hydrophobicity refers to the manner water interacts with the surface of insulators. If the surface repels water, it is considered hydrophobic. When an insulator is hydrophobic, it causes water droplets to form on the surface of the insulator. However, when the insulator attracts water, it is considered hydrophilic. This means that a continuous water film is observed on the surface of the insulator.

Jarrar *et al.* (2014) characterise hydrophobicity of the material in terms of its ability to repel and resist water flow on its surface. Khan (2010) mentions resistance to the formation of a continuous film of water as a defining characteristic of hydrophobicity of a material. Amin *et al.* (2007) describe hydrophobicity as the resistance to the formation

of conducting water tracks that increase leakage current, chances of flash-over and other deterioration effects. Elombo (2012:73) cites hydrophobicity as a superior electrical property of most polymeric insulators, but it can wear out over time when insulator surfaces are exposed to harsh weather conditions and electrical discharge activities.

Amin *et al.* (2007) suggest that the loss of hydrophobicity is due to the loss of low molecular weight components from the surface of the insulator. These components are either removed by excessive wetting conditions and applying an electrical field, by dry band arcing due to carbon tracking on the surface, or by acidic rain. The above researchers tested the ageing of polymeric insulators in Pakistan by measuring hydrophobicity using STRI classification and leakage current measurement techniques. One of the techniques used to determine hydrophobicity or the hydrophobicity class (HC) of non-ceramic insulators (NCIs) is by measuring the contact angle (Jarrar *et al.* 2014).

In line with Jarrar *et al.* (2014), Yang *et al.* (2018) suggest that the contact angle method, surface tension method and spray method are the most common methods for detecting the hydrophobicity of insulators. As Amin *et al.* (2007) assert, surface wettability can be measured by calculating the contact angle (θ_c) between a liquid drop and a solid surface when the drop touches the surface. The result is that a wet material has a large surface area and a contact angle below 90° . By contrast, hydrophobic materials have a smaller surface area and thus a greater contact angle (see Figure 3-6 for details).

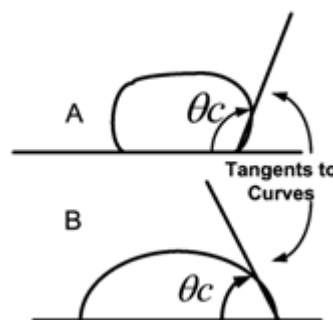


Figure 3-6: A: hydrophobic surface; B: a less hydrophobic surface

When the contact angle is less than 35° , surfaces are assumed to be hydrophilic. Amin *et al.* (2007) assume that surfaces with contact angles greater than 90° are hydrophobic. When the surface of the insulator is hydrophobic, water drops will form as independent droplets with contact angles $> 90^\circ$ (Jarrar *et al.* 2014). Mavrikakis *et*

al. (2015) posit that polluted SIR insulators, when sprayed with water, only show distinct water droplets on the contaminated layer and that water will not be absorbed by the pollutants. As shown in Figure 3-7, the wetness of the insulator surface can be determined using reference materials obtained from different classes of hydrophobicity (Kokalis *et al.* 2020). These classes are based on Hydrophobicity Classes – STRI Guide (de Jesus *et al.* 2013; Kokalis *et al.* 2020). Different hydrophobicity classes (HC) from class 1 to class 6 were obtained (see Figure 3-7).

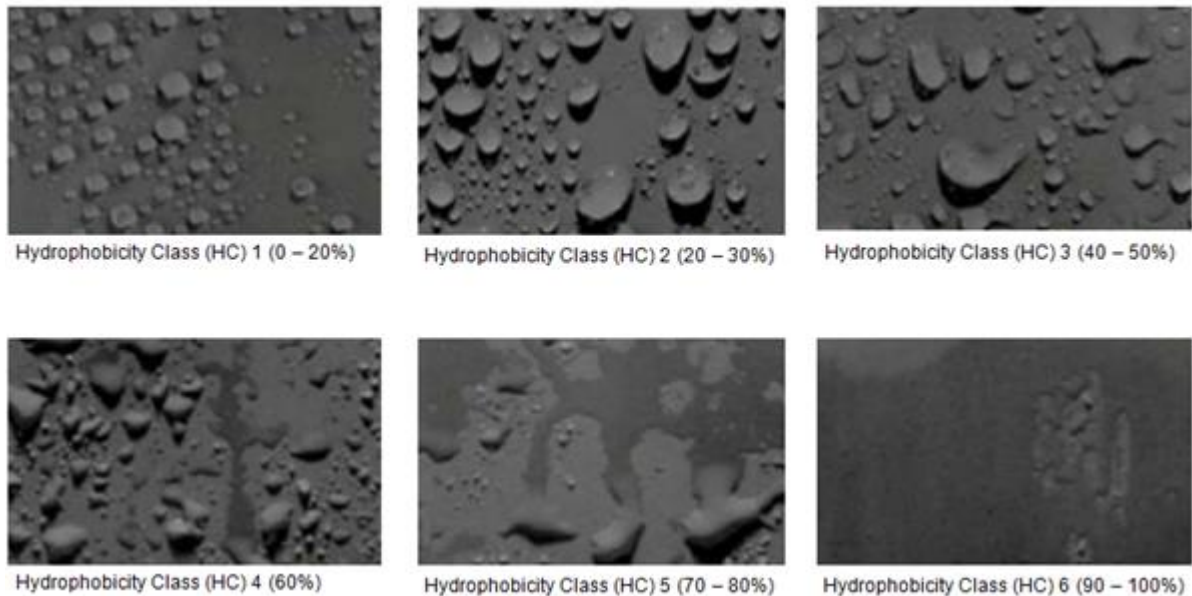


Figure 3-7: Hydrophobicity classes with percentages - HC1 to HC6

This study employed the hydrophobicity classification by Jarrar *et al.* (2014) for several reasons:

- It is consistent with STRI guide 1992.
- It attaches percentages that are pivotal in providing more accurate analysis and interpretation of hydrophobicity on the surface of the insulator.
- It is easy to administer given the strip-round shape of the insulators, whereas the contact angle method would have been extremely difficult to perform.

3.10 JUSTIFICATION OF THE DURATION OF THE TEST

The tests were conducted using a modified version of the IEC 62730 standard. The IEC / TR 62730:2012 standard for wheel test specifies the total test duration of 30 000 cycles. In the current study, 2 700 cycles were used for each of the three tests (AC, DC+, and DC-), for a total of 8 100 cycles. This means that instead of 30 000 cycles for each test, only 2 700 cycles were completed. Each subtest was conducted over six days or 144 hours. Thus, the total hours for the entire test (AC, DC+, and DC-) were 432 hours or 18 days.

The Eskom-authorized Responsible Person was only available for a limited time due to commitments at the workplace. Therefore, I was not allowed to work alone in the HV yard without supervision at all times. Even though the standard stipulates 30 000 cycles, other researchers have performed tests using a lesser number of cycles (refer to Table 3-5 below). Nevertheless, the information gathered at the Master's level is acceptable as the goal is not to create new knowledge but to ensure that the research can be conducted.

Table 3-5: Rotating wheel dip tests according to IEC / TR 62730:2012

Source	Aim	Test Duration
Krzma <i>et al.</i> (2014)	An experimental study of silicone rubber polymeric insulators for 11 kV systems using a rotating wheel dip test (RWDT) based on IEC 62730:2012 whose aim is to compare the ageing performance of polymeric insulators under AC voltages.	Two polymeric insulators were tested continuously for 190 revolutions with a total duration of 10 hours. Each revolution takes 192 seconds with four test positions in sequence: energization, cooling, dipping, and dripping. The stationary time for individual positions is 40 seconds, and the test sample takes eight seconds to move from one position to another.
Krzma <i>et al.</i> (2015)	The main purpose of this study is to compare the ageing performance of polymeric insulators under AC and positive DC excitations.	Two silicone rubber insulators were tested continuously under AC and positive DC excitations for 190 wheel revolutions for a total of 10 hours. Each revolution takes 192 seconds with four test positions: energization, de-energization, and dipping and dripping positions. For each position, the test sample remains stationary for about 40 seconds and takes eight seconds to rotate from one position to another.

Source	Aim	Test Duration
Klüss and Hamilton (2017)	The paper presented the components, configurations, and alternatives for constructing a cost-effective standalone RWDT system for tracking and erosion testing of NCIs.	The insulator sample was dipped into a NaCl solution of 1.40 g/L of water and allowed to drip. This process was repeated 30 000 cycles without interruptions. Considering the required 30 000 cycles with an approximate duration of 200 seconds and the mandatory 24-hour rest every four days, the approximate duration for the tracking and erosion test is 2083 hours (86.6 days, not including maintenance interruptions).
Mackiewicz <i>et al.</i> (2017)	The study presented the results of testing – surface parameters and stiffness-vulnerability of a batch of samples of composite insulator sheds, which were previously subjected to the wheel test.	The test comprised two series of the samples of medium voltage (MV) composite insulators sheds of various manufacturers – designated as Pf and Lt. All samples were cut out of the sheds and were made of high-temperature vulcanised (HTV) silicone rubber (SR) at present also called high consistency rubber (HCR). The test duration is 30 000 cycles. No hours are specified.
Verma and Reddy (2018)	The study explored surface degradation on polymeric insulators using the rotating wheel dip test under DC stress.	In one tank, standard contaminant NH ₄ Cl according to IEC 62217 / IEC TR 62730 is used, and in another tank, the acidic contaminant is used to simulate normal and acidic rain conditions. A complete rotation cycle of four positions was of 192 seconds. The total experimental duration was kept for 1 000 hours.

The Eskom technical supervisor approved the shortened test duration for this study. The test duration was deemed sufficient given the scope of the research.

3.11 CHAPTER SUMMARY

The chapter explains the testing procedure followed, and the form factor is explained. Testing procedures used in this study adhered to the IEC / TR 6273:2012 standard, an internationally recognised test procedure for evaluating the resistance of composite insulators to tracking and erosion as a means of rejecting materials or designs that did not meet the required specification. In this case, this procedure was used to measure leakage current, hydrophobicity, and surface degradation. Test samples were installed on the rotating wheel dip test (RWDT), designed according to the standard. Hydrophobicity was measured using STRI classification and leakage current measurement techniques as an important test variable. HC (hydrophobicity

classification) is a method proposed by STRI (the Swedish Transmission Research Institute). Different hydrophobicity classes (HC) range from class 1 to class 6. The results of the HC and RWDT are summarised in Chapter 5.0.

Table 3-5 above provides a summary of the test duration justification. The mechanical design of the tests and the rotational cycles, which fall between 2 700 cycles were used for each of the three tests (AC, DC+, and DC-), for a total of 8 100 cycles, are consistent throughout the tests performed, as indicated in the methodology. Thus, researchers have the liberty to determine the duration of the test (refer to Table 3-5 above).

CHAPTER 4.0

TEST DESIGN AND IDENTIFICATION OF APPARATUS

The chapter discusses the design of the test apparatus. It sheds light on the types of apparatus used to determine the test results for this study. It provides an overview of the test facility, devices used for testing, data logging measuring, and the design of the test samples. The rationale for the test programme is explained in terms of choice of test location, the insulator samples, test instruments and the high-voltage test for a water resistor.

4.1 LOCATION OF TESTING FACILITY

The test site, located in Brackenfell South in the Western Cape, is reached via the Bottelary Rd / M23 from Cape Town. The Stikland substation is approximately 32.4 km from the City of Cape Town, with approximate coordinates of -33.8049792, 18.5106989. The test facility at the Stikland 400 / 132 / 66 kV substation was provided by Research, Testing and Development for testing purposes. The test facility was built according to IEC / TR 6273:2012 to study the effect of pollution on insulators in a variety of polluted conditions. Refer to Figure 4-1 below for the RWDT test facility.

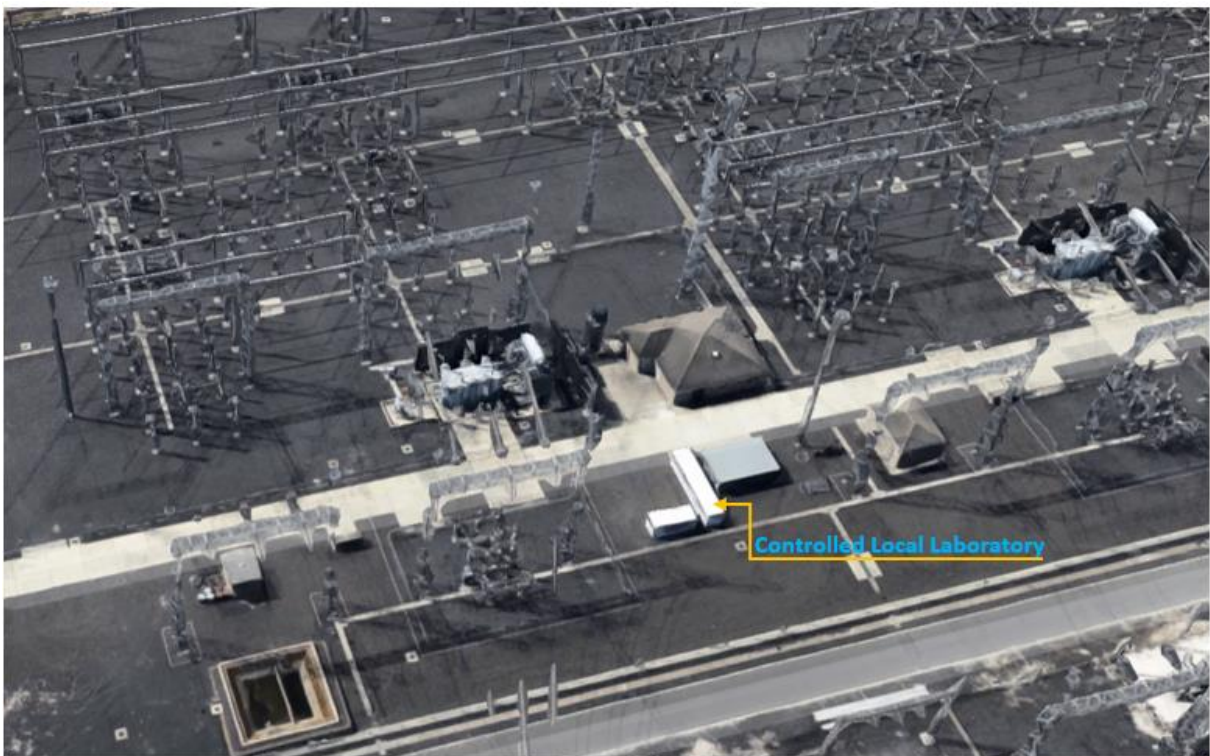


Figure 4-1: Stikland substation (RWDT test facility)

Figure 4-2 below shows the test devices secured in a white insulated shipping container of approximately 5 m in length in the test facility. According to the Research, Testing and Development technical staff, this container was procured to address the pollution performance of high-voltage insulators in various pollution conditions and other related insulator issues in the industry.



Figure 4-2: Overview of the test apparatus inside insulated shipping container:
(a) control panels (b) 30 kV transformer and DC rectifier (c) RWDT and (d) HV earth stick

Figure 4-2 illustrates the control panels, the transformer and DC rectifier, the rotating wheel dip test and the high-voltage earth stick. These devices are instrumental for the performance of the tests (AC, DC+, and DC-) in this study.

4.2 IDENTIFICATION OF TESTING DEVICES

The continuity and integrity of the tests (AC, DC+, and DC-) depend on the electrical equipment's reliability, particularly the high-voltage transformer and the rectifier. The testing apparatus in use for the study is a single-phase transformer and DC rectifier. A Single-phase transformer and DC rectifier were among the most important (and most expensive) pieces of equipment required to perform the test at hand.

4.2.1 Single-phase transformer and DC rectifier

In accordance with the IEC 62730:12 standard, RWDT requires a 50 Hz power supply. The test voltage and maximum test current will be determined as shown below (in section 4.4.1). Figure 4-3 below shows the transformer and DC rectifier.

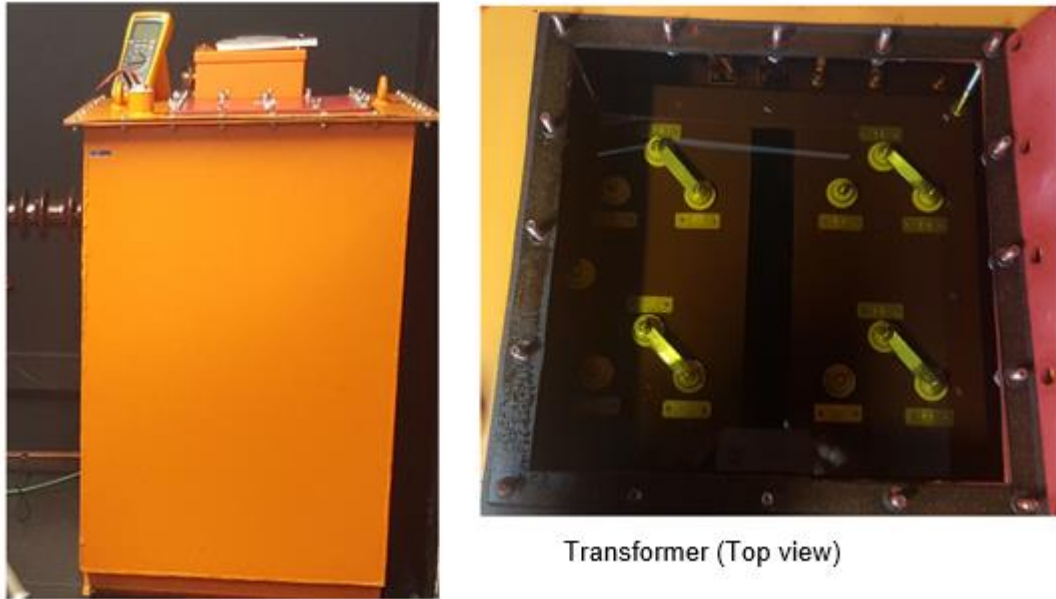


Figure 4-3: 230 V / 30 kV transformer and DC rectifier

The transformer and DC rectifier contains a bridge rectifier circuit that may be engaged or activated by selecting several combinations of connections or links to provide DC voltage. An 8 kVA source feeds the RWDT test circuit, 230 V / 30 kV single-phase transformer and DC rectifier fed from the variac connected to a wall socket. For the test in this study, 10 kV was used. The transformer can supply a maximum current of 250 mA on the secondary side. This enables the testing of 4 × insulator test samples. The output can be regulated up to 30 kV using the variac situated on the primary side of the transformer. The frequency of the test voltage is 50 kHz.

4.2.2 Diode rectifier

For DC testing purposes, the rectifier consisted of four high-voltage diode modules connected in a full-wave bridge configuration. Each diode module consists of six diodes connected in series, with their balancing resistors connected, as shown in Figure 4-4. It efficiently converts AC voltage into DC voltage. After that, the output of the rectifier is pulsed DC and filtered by a filter circuit, which is usually composed of capacitors (see capacitor bank in Figure 4-5 below).

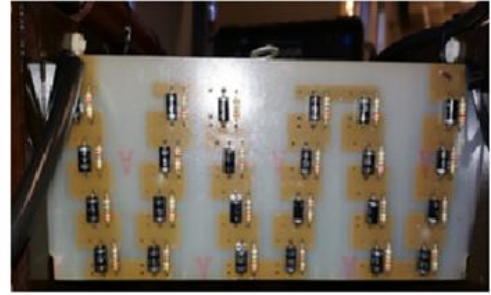
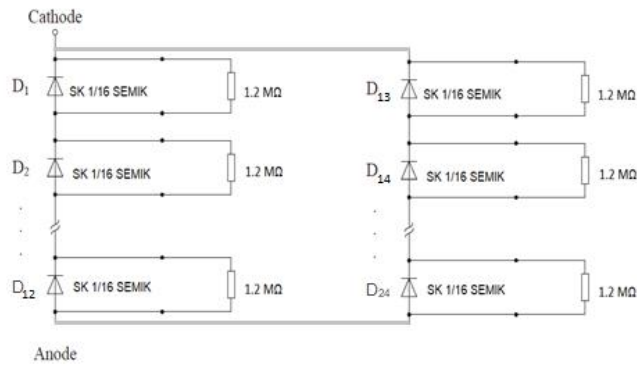


Figure 4-4: Diode rectifier

Table 4-1 below shows the technical specification of the diode rectifier.

Table 4-1: Semikron SK1/16 rectifier diode technical specification

Manufacturer	Semikron
Serial no	SK1/16
Diode type	Rectifier diode
Reverse repetitive voltage max. (RRVM)	1.6 kV
Forward current (I_F)	1.45 A
Forward voltage (V_F)	1.5 V
Peak non-repetitive surge current	60 A
Reverse current	400 mA
Operating temperature minimum	- 40°C
Operating temperature maximum	150°C
Length	7 mm

Figure 4-5 below displays a capacitor bank.

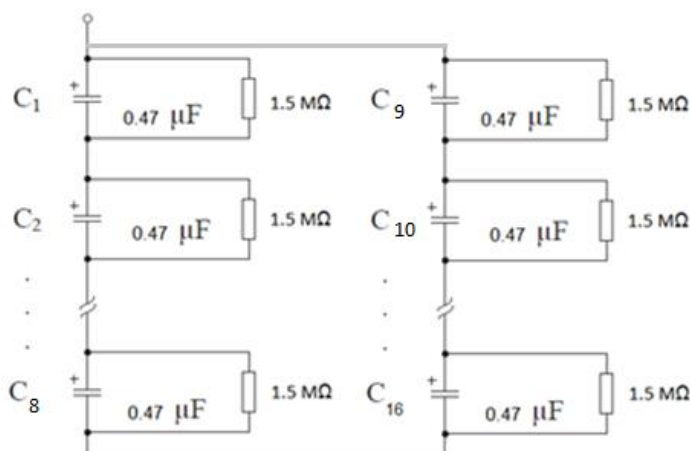


Figure 4-5: Capacitor bank

The technical specification of the capacitor is provided in Table 4-2 below.

Table 4-2: Electronicon capacitor technical specification

Manufacturer	Electronicon
Serial no	E62.F62-471B20
MKP	0.47μF +/- 10%
V _N	4200 VDC
V _N	2500 VAC
Operating temperature minimum	-25°C
Operating temperature maximum	85°C
Oil filled	Castor oil
IEC standard	61071

The capacitor consisted of sixteen smaller 0.47 μF electrolytic capacitors, 4200 VDC / 2500 VAC, stacked in series (see Figure 4-5 above). To ensure that the voltage across the capacitors remains balanced, 1.5 MΩ resistors have been shunted with each capacitor.

4.3 VOLTAGE RIPPLE CALCULATION

The maximum ripple component is calculated when a voltage of 10 kV DC is applied with a maximum test current of 200 mA. The voltage ripple on the DC bus, dependent on the load current (load current between 6 and 13 mA), is obtained from the following equation:

$$V_{pp} \approx \frac{I_{load}}{2fC}$$

$$V_{pp} \approx \frac{13 \text{ mA}}{2 \times 50 \times 0.12 \mu\text{F}}$$

$$= 1083 \text{ V}$$

The ripple factor is:

$$V_r = \frac{V_{pp}}{V_{dc}}$$

$$= \frac{1083}{10\,000} \times 100$$

$$= 11\%$$

Therefore, the HV DC voltage may contain a ripple voltage component between 6 and 11%.

The ripple reduces the device's efficiency and often leads to noise. If you have a high ripple voltage on the DC, the breakdown is more likely to occur at the peak of the ripple. However, it was assumed that because of the test's short duration, the effects of the DC ripple would not be significant to the test performed. The system functioned well, and there were no faults such as trips and alarms. The ripple voltage component must be eliminated in future tests of longer duration by using more smoothing capacitors.

4.4 BASIC DESIGN OF SODIUM CHLORIDE (NaCl) WATER RESISTOR FOR LOAD TEST

The load test on 230 V / 30 kV transformer and DC rectifier was instrumental in determining the amount of voltage and current suitable for the test (AC, DC+, and DC-). Before presenting the load test results of the sodium chloride (NaCl) water resistor, it was important to design and construct the water resistor. The basic electrical design and the required specifications are covered first, followed by the choice of resistor type and its construction. Finally, thermal calculations are dealt with.

The basic electrical design required (i) the voltage, (ii) the resistance and (iii) the power to be calculated.

4.4.1 Calculation of the test voltage

From the standard (IEC / TR 62730), the power frequency test voltage in kV is determined by dividing the actual creepage distance in mm by 28.6. The following formula was used to calculate the test voltage:

$$V = \frac{CD}{USCD} \text{ mm} / \text{kV}$$

where creepage distance (CD) is a measured test sample's length = 275 mm, and unified specific creepage distance (USCD) from the IEC standard = 28.6. Based on the above calculations, the test voltage is 10 kV.

To check that the source (test voltage) from the transformer is 10 kV, a resistive load had to be used to allow a current of 250 mA to flow, in accordance with the standard (IEC / TR 62730).

After calculating the test voltage, it was necessary to determine the resistance and the electric power using Ohm's Law and Joule's Law.

4.4.2 Calculation of the resistance

The resistance was calculated using the following formula:

$$R = \frac{V}{I}$$

where:

R = Resistance in ohms (Ω);

V = Voltage in (V); and

I = Current in amps (A).

The calculated resistance was 38.46 k Ω .

4.4.3 Calculation of the electric power

The power was calculated using the following formula:

$$P = I^2R$$

where:

P = Power in watt (W);

I = Current in amps (A); and

R = Resistance in ohms (k Ω).

The calculated power was 2.404 kW. However, since there was no 38.46 k Ω resistor available with a rated power of 2.404 kW, the author had to design the sodium chloride (NaCl) water resistor described in § 4.5.

4.5 CONSTRUCTION OF SODIUM CHLORIDE (NaCl) WATER RESISTOR

Finding a suitable resistor type (38.46 k Ω , a nominal power of 2.404 kW) was challenging. Due to the lack of availability of the type of resistor, the author decided to construct a sodium chloride (NaCl) water resistor that is easy to move, portable and effective for test purposes.

4.5.1 Material

The following materials were used to construct the water resistor:

- 1.5 m long PVC gutter pipe;
- 10 cm in diameter PVC end cap × 2;
- Strap-on fitting with an aperture for filling and emptying resistor, with lid;
- PVC weld glue for joining the various parts;
- Silicon sealer and a rubber seal;
- Various nuts, bolts, and washers; and
- Distilled water (obtained from Eskom laboratory) and Cerebos table salt.

Thermal calculations were also performed. It was necessary to calculate the volume of the resistor, its thermal capacity, and therefore the thermal resistance of the plastic. In this respect, it was calculated whether or not the resistor would adequately be subjected to the specified power of 2.404 kW from a thermal (temperature rise) point of view. The applicable outputs of the electrical calculations were used where necessary.

Thermal calculations include dimensions, area and volume of PVC pipe, water mass, resistance, and temperature rise.

4.5.2 Dimensions

- Diameter

$$\text{Diameter} = \varnothing = 10\text{cm} = 0.1\text{m}.$$

- Radius

$$r = \frac{D}{2}$$

The calculated radius is 0.05 m.

- Length

The length used is 1.5 m.

- Constants

Specific heat capacity of water = $C = 4\,180 \text{ J/kg}^\circ\text{C}$ (Blake *et al.* 2000);

The resistivity of distilled water = $1.8 \times 10^5 \Omega\text{m}$ at 20°C

(https://en.wikipedia.org/wiki/Electrical_resistivity_and_conductivity). (This value was assumed for distilled water without other information.)

The resistivity of seawater = $2 \times 10^{-1} \Omega\text{m}$ at 20°C

(https://en.wikipedia.org/wiki/Electrical_resistivity_and_conductivity). (This was used to estimate distilled water with salt dissolved.)

1 litre (ℓ) = 0.001m^3 (for water);

1 ℓ = 1 kg (for water) (<https://en.wikipedia.org/wiki/Litre>).

4.5.3 Area, volume, and mass

- Area

$$A = \pi r^2$$

$$A = 0.0079 \text{ mm}^2$$

- Volume

$$V = \pi r^2 h$$

$$V = 11.78 \text{ l}$$

Therefore, the mass of the water is 11.78 kg.

4.5.4 Resistance of the water

$$R = \frac{\rho \times l}{A}$$

$$R = 34.177 \text{ M}\Omega \text{ for distilled water}$$

$$R = \frac{\rho \times l}{A}$$

$$R = 37.975 \text{ k}\Omega \text{ for seawater}$$

The calculations show that the resistor can theoretically be used for a large portion of the range of resistances required. However, the power rating needed to be checked carefully for lower resistances (larger currents). Resistor performance for all resistances (high and low) was experimentally verified.

4.5.5 A rise in the temperature of the water

Heat energy = $Q = E = 2880 \text{ kJ}$ under fault conditions (worst case as in where there is an overvoltage)

$$Q = m \times C \times \Delta T$$

$$\therefore \Delta T = \frac{Q}{m \times c} \text{ where } \Delta T = \text{temperature rise}$$

Under normal conditions:

$$\Delta T = 0.508 \text{ } ^\circ\text{C}$$

Under fault conditions:

$$\Delta T = 0.573 \text{ } ^\circ\text{C}$$

The water resistor was expected to perform acceptably under normal and fault conditions (as might happen in those conditions). This was verified by means of numerous high-voltage tests. Figure 4-6 shows a basic design drawing of a water resistor, and Figure 4-7 shows a fully constructed water resistor using a PVC pipe.

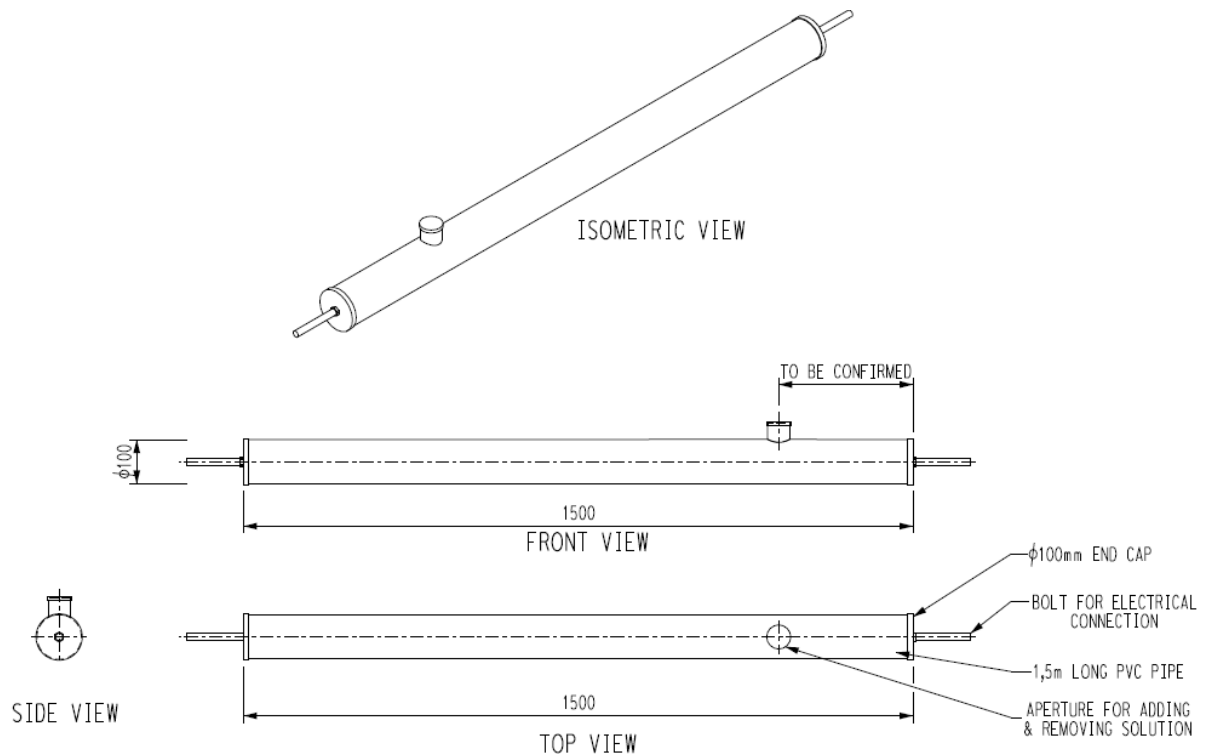


Figure 4-6: Basic design drawing of a sodium chloride (NaCl) water resistor



Figure 4-7: Fully constructed sodium chloride (NaCl) water resistor

4.6 LOAD TEST SETUP

For the setup, the following components were required: a sodium chloride (NaCl) water resistor with two copper electrodes fixed at the ends (see Figure 4-7), distilled water, a supply of 10 kV, a digital multimeter and a current clamp. Figure 4-8 depicts the load test schematic diagram.

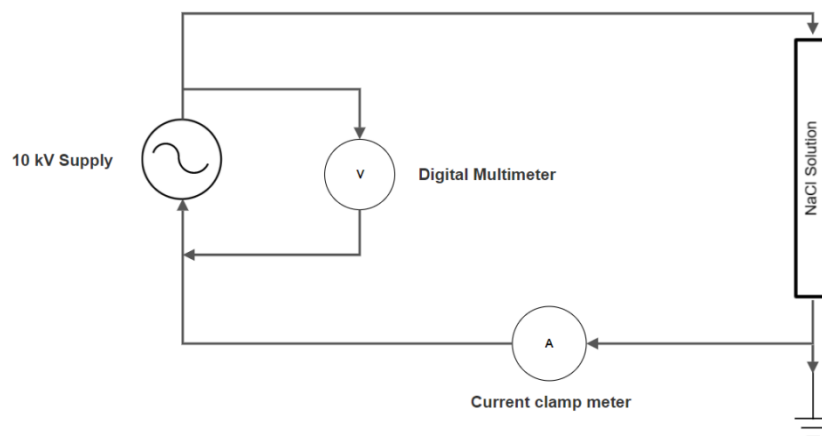


Figure 4-8: Load test schematic diagram

The load test was performed using the sodium chloride (NaCl) water resistor. The test was performed by applying a voltage of approximately 10 kV AC between the anode and cathode of the liquid resistor for about 10 seconds. The water resistor was tested first without adding salt to the distilled water. Salt was added incrementally to reduce water resistance. The salt content of the solution was varied to draw various currents. At the higher resistance, with no salt content, resistance was measured at 424 k Ω , and

the current was measured as approximately 23.585 mA. After adding salt, the resistance decreased to 264.583 kΩ, and the current was 38.4 mA.

Adding more salt to the deionised water decreased the resistance further and increased the current. It was observed that the resistor's surface temperature increased over time when left energised for several minutes, but it was not too hot to the touch. At 208 mA, the resistance measured was 45.673 kΩ, which is close to the target of 40 kΩ, according to the calculations. Nonetheless, the main circuit tripped. Another test was performed with a lower current of 200 mA, and the resistance measured was 50 kΩ.

Since it was not possible to change the transformer, it was decided to use a 200 mA current instead of 250 mA, according to the standard (IEC / TR 62730). Effectively, the intention is not to test the standard but to use the procedure specified in the standard to test the samples. The test results are listed in Table 4-3 below.

Table 4-3: Sodium chloride (NaCl) water resistor load test results

No	Voltage (multi-meter)	Current (current clamp)	Resistance (calculated)	Test condition	Temperature
1	10.16 kV	38.4 mA	264.583 kΩ	1 teaspoon of salt added	19°C
2	10.08 kV	58.7 mA	171.721 kΩ	1 teaspoon of salt added	19°C
3	10.04 kV	170.6 mA	58.851 kΩ	1 teaspoon of salt added	19°C
4	9.5 kV	208 mA (tripped)	45.673 kΩ	4 teaspoons of salt added	20°C
5	10 kV	200 mA	50 kΩ	No salt added	20°C

From the values (voltage and current) reflected in Table 4-3, it is clear that resistance was calculated using readings from the Fluke 233 digital multi-meter and clamp meter. The resistor was monitored for excessive heating and other danger signs throughout the test period. The required pass criterion was a successful withstand of the applied voltage over the test period. No signs of excessive heating or other danger signs were detected. Therefore, the load test with a water resistor was deemed successful. The trip of the supply and flash-over was noticed when the current reached 208 mA at 9.5 kV. However, the author reset the panel and varied the voltage up to 10 kV, and the measured current was approximately 200 mA. At this stage, no tripping was noticed.

4.7 IDENTIFICATION OF DATA LOGGING AND MEASURING DEVICES

The literature review describes the various tests (artificial and non-artificial methods) used to measure performance and evaluate tracking and erosion of insulating material surfaces (refer to § 2.5.1 and § 2.5.2). RWDT, an example of an artificial test method designed according to the IEC / TR 62730:2012 standard, was deemed suitable for this study (refer to § 2.6). The following devices were used to collect the test conditions and data during the various tests. After that, individual measuring and data logging devices are discussed further.

- Online leakage current analyser (OLCA) for leakage current measurements;
- Leakage current sensor;
- Rotating wheel dip test (RWDT);
- Conductivity meter GMH 3410;
- Citizen scale CG 4102; and
- Hikvision IR network camera.

4.7.1 Data logger device: Online Leakage Current Analyser (OLCA)

A data logger is an electronic device that records data over a given period. It can be installed in almost any location and left to operate unattended. According to Htay (2011), a data logger is an electronic instrument that records measurements (temperature, relative humidity, light intensity, on/off, open/closed, voltage, pressure, and events) over time. Typically, data loggers are small, battery-powered devices equipped with sensors, a microprocessor, and data storage. Most data loggers utilise turnkey software on a personal computer to initiate the logger and view the collected data, which can easily be exported to a PC via a serial port (Perez *et al.* 1997).



Figure 4-9: Front view of the OLCA used as a leakage current data logging device

The data logging device (see Figure 4-9) was used to record data in the current study. It is called an online leakage current analyser (OLCA). OLCA is a microprocessor-based data acquisition system developed by a South African company, CT Lab (Pty) Ltd, to record leakage current data and specific weather data. Nine channels are available for leakage current measurements, three for voltage measurements, and four more to record weather data (Bogias, 2012; Mouton, 2012; Heger, 2009; Vosloo, 2002; Elombo, 2012; Swinny, 2021).

For this study, only the leakage current sensor was used. Data stored on the OLCA hard drive can be retrieved through the RS232 port and downloaded for further analysis using Microsoft Office application software (Mouton, 2012; Heger, 2009; Elombo, 2012; Swinny, 2021). The OLCA data logger device records the leakage current parameters measured directly by the sensors or derived from the measured values (Elombo, 2012). The device has a sampling accuracy of 0.5% of the full-scale value at a sampling rate of 2 kHz and a resolution of 12 bits. All desired parameters (A min and a max leakage current value) are saved in registers at 1-minute intervals.

Retrievable leakage current parameters include:

- In mA – positive and negative peak leakage current values;
- In mA – absolute peak leakage current;
- In mA – positive and negative average leakage current;
- In mA – RMS leakage current;
- In Coulomb – positive and negative cumulative charge; and
- Daily maximum leakage current waveforms (Mouton, 2012; Heger, 2009; Vosloo, 2002; Elombo, 2012; Swinny, 2021).

To ensure the reliability of the data logger, it was taken for calibration at CompuCell situated in Shop No 5, Nobelpark Shopping Centre, Bellville, 7530. This study obtained only the root mean square (rms) leakage current values for the RTV-SR and HTV-SR test samples, as evaluated in Chapter 5.0.

4.7.2 Data measuring device: Leakage Current Sensor

According to Crescentini *et al.* (2017), current sensors are key elements in designing a large family of power systems, such as motor drivers and power converters. As used in this study, current sensors play an important role in detecting electric current and

converting current to an easily measured output voltage proportional to that current. The sensor in Figure 4-10 is based on Hall effect technology to measure current.

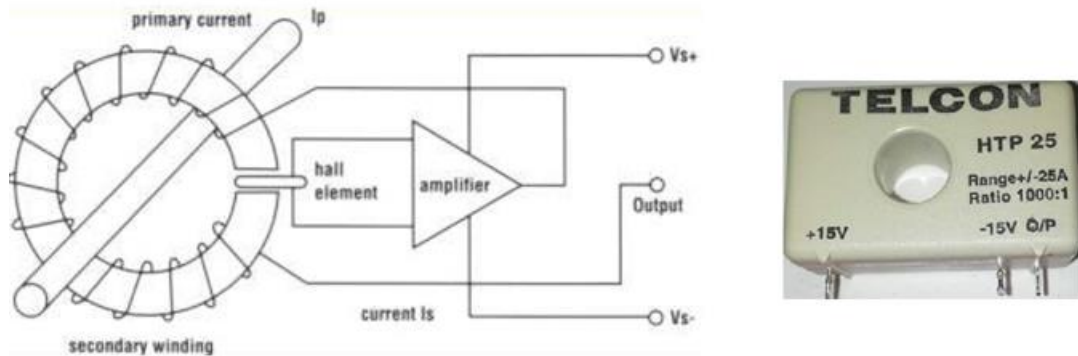


Figure 4-10: Current sensor with Hall probe

According to Petruk *et al.* (2014), a Hall effect current sensor is a transducer that varies its output voltage in response to a magnetic field generated by the current flow. Hall effect sensors are common in industrial applications for a series of low power applications, including current sensing, position detection and contactless switching (Paun *et al.* 2013). Volokhin and Diahovchenko (2017) maintain that current sensors based on the Hall effect have high linearity, low power consumption (for supplying the internal source) and high measurement accuracy. These authors claim that such sensors can be used in AC and DC meters (e.g. railway networks). AC and DC Hall effect current sensors were preferred for measuring the leakage current for the test at hand because they have three main advantages: remarkably low input resistance, large bandwidth (up to 200 kHz) and galvanic isolation of the electrical system for measuring the high-voltage side.

Figure 4-11 depicts the Hall sensor with and without its exterior housing. The inner circuit consists of a Hall coil and many integrated circuits, capacitors, and resistors to amplify and transfer the signal from the input (current) to the analogue output (voltage).



Figure 4-11: Photo of the Hall sensor

The sensor was designed by CT Lab to be placed outdoors; it is properly shielded with an aluminium die-cast box for housing electronic components and to guard those components against severe weather conditions (Elombo, 2012). The sensor can measure peak currents up to +/- 500 mA (rms). The current sensor is installed in series with the test samples on the ground potential side.

The Hall effect current sensor in this study is the Telcon HTP 25, a closed-loop type that provides an output voltage through an external load resistor. The nominal primary current of the Hall sensor is rated at ± 25 A, and the output voltage is rated +/- 15 V. The ratio of the transformer has a 1 000:1 winding ratio with a linearity of $\pm 0.1\%$ of the nominal primary current. The output of HTP25 has to be connected to a minimum load resistance of 100 Ω . It is accurate, is galvanically isolated until 3 kV and has a bandwidth of (-1 dB) dc to 200 kHz. Table 4-4 shows the specifications of the sensor.

Table 4-4: Technical specification of an integrated sensor with closed-loop

Type	I_{PN} [A]	I_{PR} [A]	f_{max} [kHz]	Ratio	Scale resources [mV/A]	Output [V]	Min load resistance [Ω]
HTP25NP	25	+/-36	200	1000:1	-	+/-15 +/-5%	150

Each test sample is equipped with a specific current sensor and connected to the OLCA for data logging purposes.

4.7.3 Calibration of the Hall effect current sensor

To obtain reliable test results for the study, the author, with the assistance of the Eskom Stikland substation personnel, ensured that the measuring devices (Hall effect current sensors) for AC and DC were precisely calibrated. The pictorial diagram in Figure 4-12

shows the circuit configuration used to calibrate the 4 X AC / DC Hall effect current sensors.

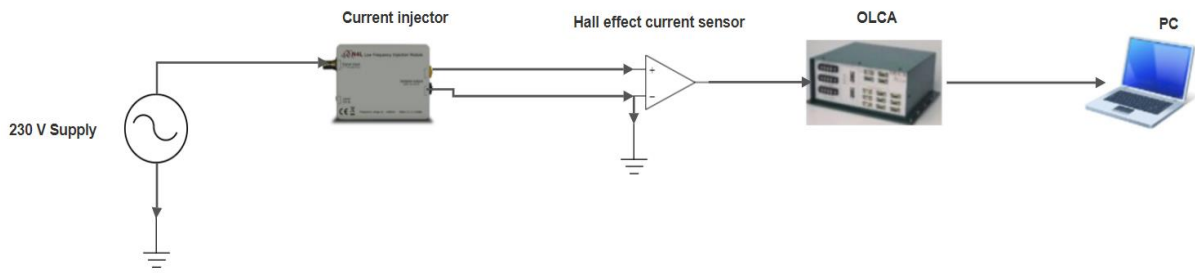


Figure 4-12: Calibration of the Hall effect current sensors (AC and DC)

The following devices (i) current injector, (ii) OLCA, and (iii) PC were used for calibration of the Hall effect current sensors. The analogue output voltage from the Hall sensor was measured from the OLCA, and the waveforms indicated that AC has an offset of +/- 5%, and DC has no offset observed; refer to Figure 4-13 and Figure 4-14. The current injector input to the Hall sensor is approximately 90 mA peak to peak for AC voltage (see Figure 4-13) and 100 mA peak for DC voltage (see Figure 4-14).

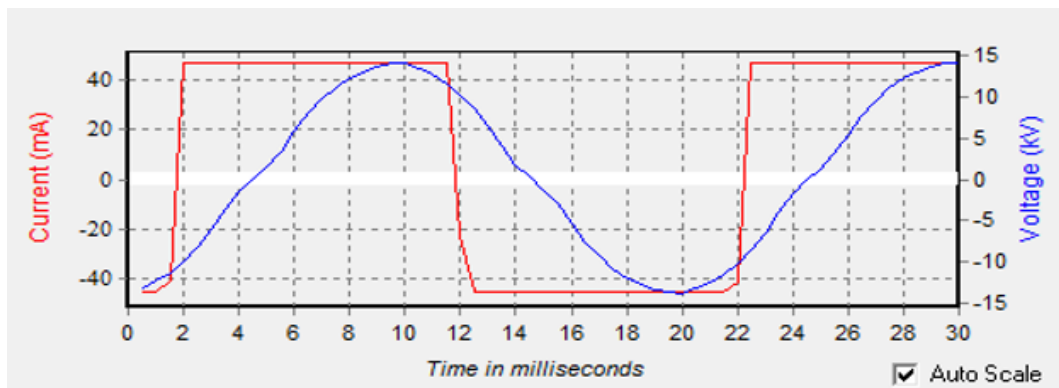


Figure 4-13: AC waveform

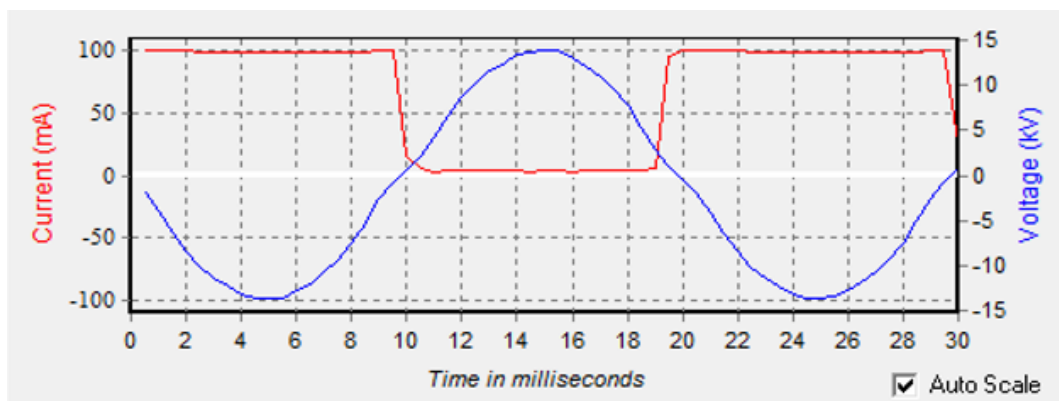


Figure 4-14: DC waveform

4.7.4 Rotating wheel dip test (RWDT)

The rotating wheel dip test (RWDT) assesses composite insulators for electrical insulation, tracking and erosion (Mackiewicz *et al.* 2017). According to Krzma *et al.* (2020), RWDT was designed and constructed according to IEC 62730 and ANSI C29.13 – 2000 standards and can accept AC and DC voltages. See Figure 4-15 below for an overview of RWDT at the local laboratory.

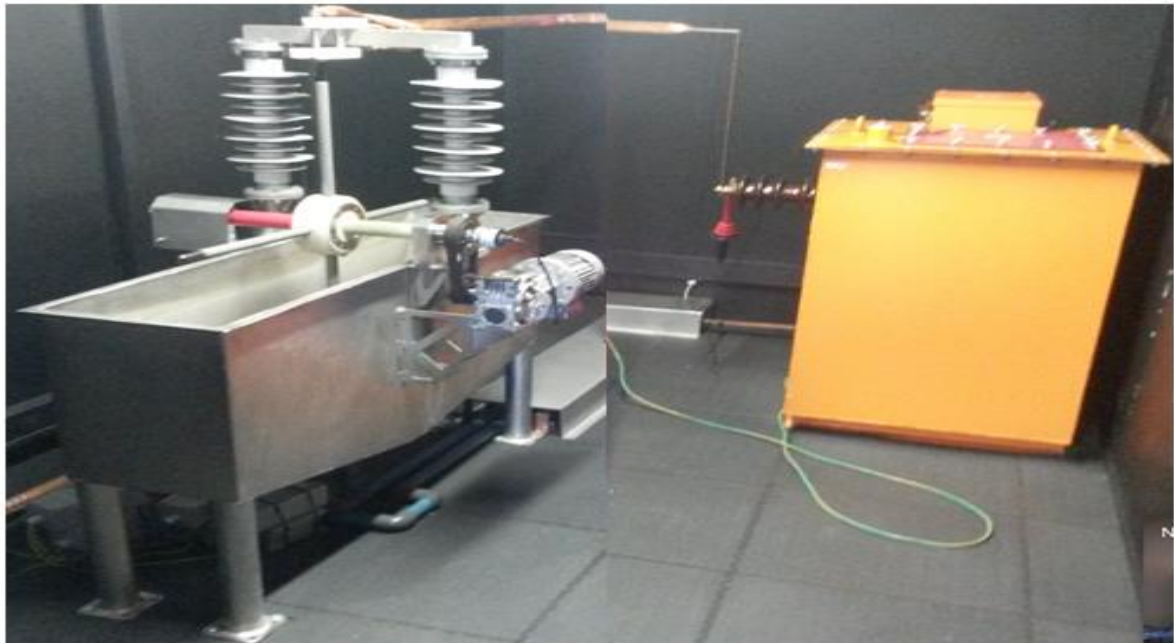


Figure 4-15: Overview of RWDT

The RWDT consist of the following main components:

- Wheel hub

The wheel hub is designed to house the test samples and rotate them, maintaining their contact with a ground connection (see Figure 4-16).

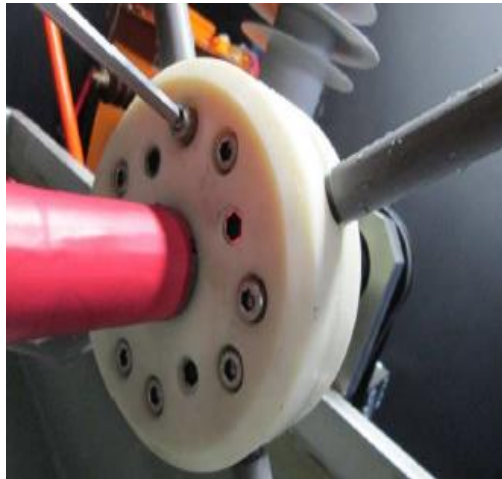


Figure 4-16: Wheel hub

- Worm-gearred drive motor

The motor provides simple speed control and responds fast to starting and stopping the wheel (see Figure 4-17).



Figure 4-17: Worm-gearred drive motor

- Measurement output points

Measuring output points measure the leakage current of each test sample (see Figure 4-18).

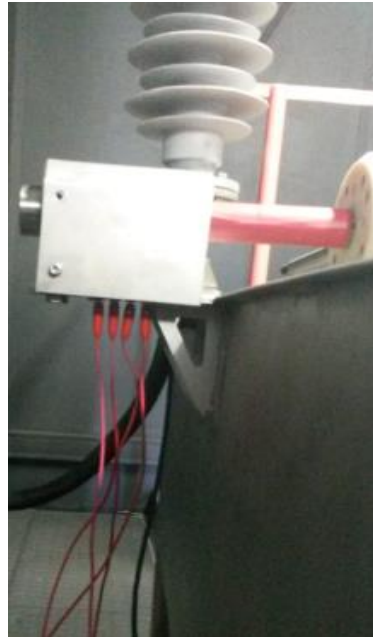


Figure 4-18: *Measurement output points*

- High-voltage electrode

The spring ensures contact between the HV source and the test sample under energization by applying slight pressure on the test sample. The connection between the spring and the test sample is not ideal because the spring does not produce firm contact; it is of high resistance and may corrode (see Figure 4-19).

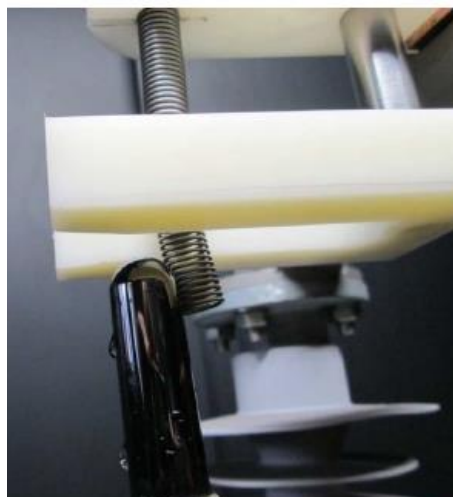


Figure 4-19: *High-voltage electrode*

- Aluminium water tank

The solution tank must be filled before energizing the test apparatus (see Figure 4-20).

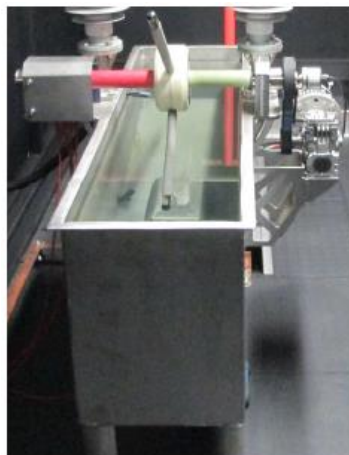


Figure 4-20: Aluminium water tank

4.7.5 Glassy carbon electrode

Glassy carbon is a form of carbon that cannot be graphitised, meaning that even at extreme temperatures, it cannot become crystalline graphite. Glassy carbon possesses both ceramic and glassy properties. As a result of its unique properties, glassy carbon is suitable for many applications. The most popular application is electrochemistry in glassy carbon electrodes (GCEs), used as sensors. Glassy carbon has a wider electrochemical activity window than gold when immersed in water. According to Dekanski *et al.* (2001) and Abdel-Aziz *et al.* (2020), glassy carbon has become an interesting and widely used electrode due to its physical and chemical properties. It exhibits a rather low oxidation rate and a very high chemical inertness. Glassy carbon is a convenient inert electrode with very small pores and low gas and liquid permeability (see Figure 4-21 below).



Figure 4-21: Overview of the glassy carbon electrode

Its most important properties are high-temperature resistance, extreme chemical resistance, and impermeability to gases and liquids. Glassy carbon electrodes were used on the test sample's end tips. The manufacturer did not provide the actual specifications of the glassy carbon electrode. Table 4-5 shows typical values for the glassy carbon electrode use on HTV-SR and RTV-SR test samples used in the test.

Table 4-5: Typical values for the glassy carbon electrode used on HTV-SR and RTV-SR test samples as end tips

Attribute	Film	Other than film
Density	1.54 g/cm ³	1.42 g/cm ³
Ash content	< 100ppm	< 100ppm
Upper temperature limit in vacuum	1 000°C	3 000°C
Porosity	0%	0%
Gas transmission rate	10 ⁻¹¹ cm ² /s	10 ⁻⁹ cm ² /s
Hardness	340 HV1	230 HV1
Bending strength	210 N/mm ²	260 N/mm ²
Compressive strength	580 N/mm ²	480 N/mm ²
Young's Modulus	35 kN/mm ²	35 kN/mm ²
Thermal expansion coefficient (20-200°C)	3.5 × 10 ⁻⁶ /K	3.5 × 10 ⁻⁶ /K
Heat conducting (@ 30°C)	4.3 W/(m • K)	6.3 W/(m • K)
Electrical resistivity	50 μΩ	45 μΩ

4.7.6 Conductivity meter GMH 3410

The conductivity of the water ionised with salt is one of the measurements undertaken. A GMH 3410 conductivity meter (Figure 4-22) measured the conductivity. Besides measuring the conductivity, it also measures resistivity, salinity, and TDS in fluids through permanently connected electrodes (measuring cells). Before each test (AC, DC+, and DC-), the conductivity of water and the temperature were measured to ensure that the study's conductivity results were within the IEC / TR 62730 standard temperature requirements.



Figure 4-22: Conductivity meter GMH 3410

The conductivity meter is owned by Eskom RT & D and was used throughout the test period. Table 4-6 below shows the technical data of the device.

Table 4-6: Conductivity meter GMH 3410 technical data

Automatic temperature compensation	Yes
Operating temperature	-5 to +80°C
Dim	(L x W x H) 26 x 71 x 142 mm
Height	142 mm
Length	26 mm
Width	71 mm
Conductivity reading range	0.0 µS - 400.0 mS
TDS reading range	0 – 1999 mg/l
Temperature reading range	-5 up to +100°C
Display	Digital
Interfaces	Serial
Reading type	TDS, conductivity, salinity, temperature
Conductivity reading range (max.)	400.0 mS
Conductivity reading range (min.)	0.0 µS
TDS reading range (max.)	1999 mg/l
TDS reading range (min.)	0 mg/l
Temperature reading range (max.)	+100°C
Temperature reading range (min.)	-5°C
Product type	Multi-tester
Spec. resistance	0.005 - 100.0 kΩ/cm
For salinity	0.0 - 70.0 g/kg

4.7.7 Citizen scale CG 4102

An accurate scale with sufficient resolution was necessary to measure the weight of salt content. The CG 4102 is an electronic scale suitable for accurate weight measurement under laboratory conditions, with zero adjustments in all measurement ranges. When deionised water is filled in the water tank, it was measured using the Citizen scale (refer to Figure 4-23).

This scale is a high-precision weighing instrument for measuring mass ranging from 0.01 mg to 100 kg. The technical specification of the scale is given in Table 4-7.



Figure 4-23: Citizen scale CG 4102 for weighing of salt content

Table 4-7: Technical specifications of Citizen scale CG 4102

Model	CG 4102	
Capacity	4100 g	
Readability	0.01 g	
Repeatability (+/-)	0.02 g	
Linearity (+/-)	0.03 g	
Pan size (mm/inch)	198 × 205 / 7.8" × 8.0	
Response time	2-3 sec.	
Display	Back light LCD	
Calibration	Automatic external	Motorised internal
Units of measure	g,mg, ct, GN, mo, oz, dwt, T1T, t1H, t1S t1S, mom, Bat, MS	
Tare range	Full	
Operating temp.	15°C to 40°C	
Power supply	AC adapter 230 V-115 V+/-20% 50-60 Hz	

4.7.8 Hikvision IR network camera

It was crucial that comprehensive visual observations regarding changes, damage and degradation on test samples be accurately documented and recorded. To achieve this, a Hikvision IR Network Camera was used. Hikvision is a data acquisition system that captures motion picture data from live environments, encoding the data into statistics that may be decoded or transcoded into digital video media. Video recordings were made for all the tests (AC, DC+, and DC-) using high-quality video cameras with infrared capability – Hikvision IR network camera, Model DS-2CD2042WD-I (Figure 4-24).



Figure 4-24: Hikvision IR network camera

The observed leakage current and the electrical discharge activities were captured and stored in an external hard drive. A personal computer is used to store, access, and

view data from the video camera footage. Hikvision has a 3 MP resolution which yields a sharp image. Technical specifications of the camera are in Table 4-8 below.

Table 4-8: Technical specification of Hikvision camera

Make	Hikvision
Manufacturer	Hikvision
Model code	DS-2CD2020-I
Chip Inch Size	1/3 inch
Colour Type	Colour/Monochrome
Resolution	3 MP resolution
Digital (DSP)	Yes
Specialist Type	Infrared
Sensitivity Lux	0 lux
Electrical Specifications	Voltage: 12 VDC; Power Consumption: 7 W
Motion Activated	Yes
Wide Dynamic Range	Yes
Picture Elements HxV	1920 × 1080
Network Properties	Image Frame Rate: 25 fps Interface: 1 RJ45 10M/100M Ethernet interface Network Protocols: TCP/IP, ICMP, HTTP, HTTPS, FTP, DHCP, DNS, DDNS, RTP, RTSP, RTCP
Back Light Compensation	Yes
Auto Gain Control	Yes
Electronic Shutter Range	1/25 ~ 1/100 000 s
Compression Type	H.264, MJPEG
Physical Specifications	Weight g: 500
Environmental Specifications	Protection: IP66 Operating Temperature °C: -30 ~ +60 C (-22 ~ +140 °F)

4.8 CHAPTER SUMMARY

The chapter described the test facility and different types of equipment used to perform the test. The test facility in Stikland, a substation located at Brackenfell South in the Western Cape, was provided by Eskom’s Research, Testing and Development for testing purposes. The test facility was built according to IEC / TR 6273:2012 to study the pollution performance of insulators in different polluted conditions. The transformer and DC rectifier, the rotating wheel dip test and the high-voltage earth stick were instrumental for the performance of the tests (AC, DC+, and DC-).

CHAPTER 5.0

TEST RESULTS AND INTERPRETATION

This chapter describes the AC, DC + and DC RWDT results performed at Stikland in accordance with IEC 62730:2012. A test voltage of 10 kV was used for the AC and DC tests. The obtained test results are presented in the following order:

- *leakage current performance of HTV-SR and RTV-SR (AC, DC+, and DC- excitation voltage);*
- *visual observations of ageing on individual test samples (AC, DC+, and DC- excitation voltage);*
- *overview of hydrophobicity classification (AC, DC+, and DC- excitation voltage); and*
- *overall cumulative electrical charge between HTV-SR and RTV-SR (AC, DC+, and DC- excitation voltage).*

The test results are evaluated according to the acceptance criteria defined in IEC 62730:2012, as below:

- *Erosion shall not reach the core, and erosion depth shall be less than 3 mm.*
- *There should not be a test specimen puncture due to excessive erosion.*

The logic of the discussion and analysis from § 5.1 applies to § 5.2, § 5.3, and § 5.4.

5.1 OVERVIEW OF LEAKAGE CURRENT TESTS

The OLCA device samples continuously at 2 kHz and captures peak currents in a 60-second period. During this study, however, the test rods were only energised for 40 seconds, and during the energization period, the OLCA captured the minimum and maximum peak currents. The online leakage current analyser (OLCA) is designed to capture and record the Maximum and minimum peak currents in a 60-second period. Figure 5-1 shows the maximum and minimum peak currents captured by the OLCA.

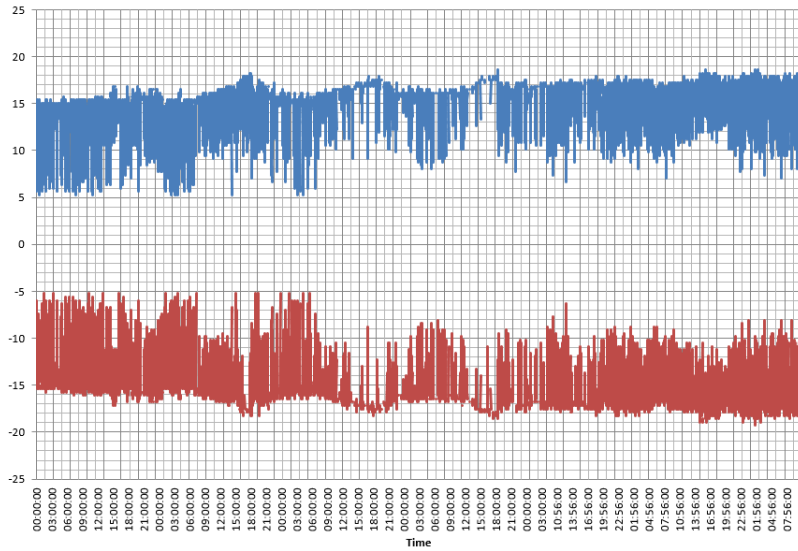


Figure 5-1: Maximum or highest leakage current captured by OLCA

Figure 5-1 displays the readings of the OLCA as it shows the positive and negative maximum or highest leakage current value captured at every 1-minute interval throughout the 6-day test period. Figure 5-2 and Figure 5-3 display, as stated above, positive and negative values on an expanded time scale. The dots represent the maximum leakage current value captured at every 1-minute interval throughout the 6-day test period.

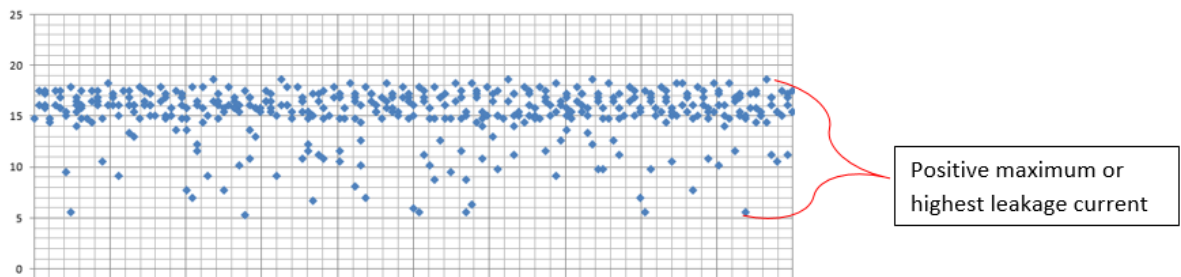


Figure 5-2: Dots representing positive maximum or highest leakage current

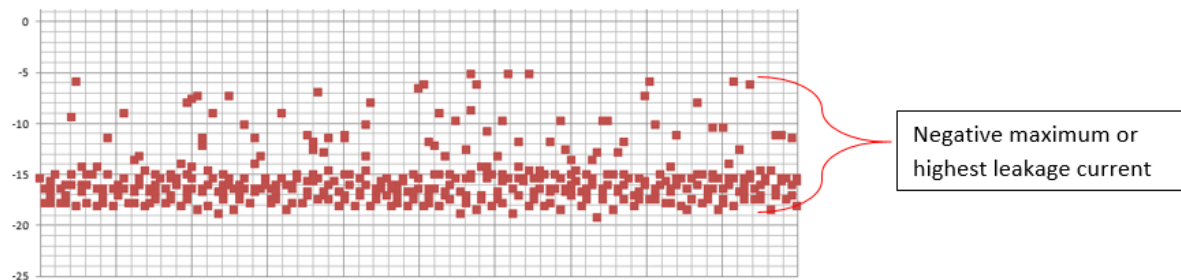


Figure 5-3: Dots representing negative maximum or highest leakage current

The tests were carried out according to the procedure specified in the IEC / TR 62730:2012 standard, as mentioned in Chapter 3.0. In the standard, the test specimens are mounted on the wheel (refer to Figure 5-4) and move through four positions in one cycle. Each test sample remains stationary for about 40 seconds in each of the four positions. The 90°-rotation from one position to the next takes about eight seconds. In the first part of the cycle, which is vertical (upside down), the insulator is dipped into a saline solution (NaCl content).

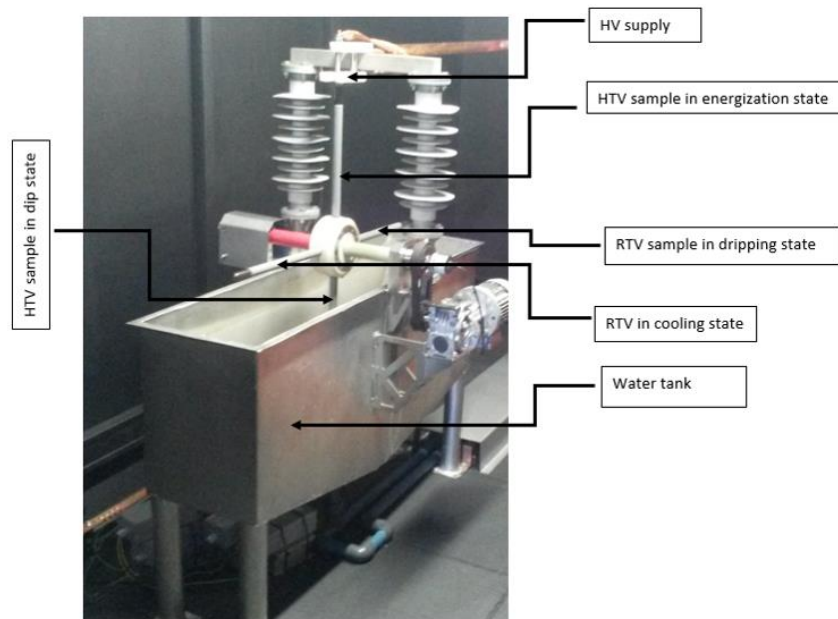
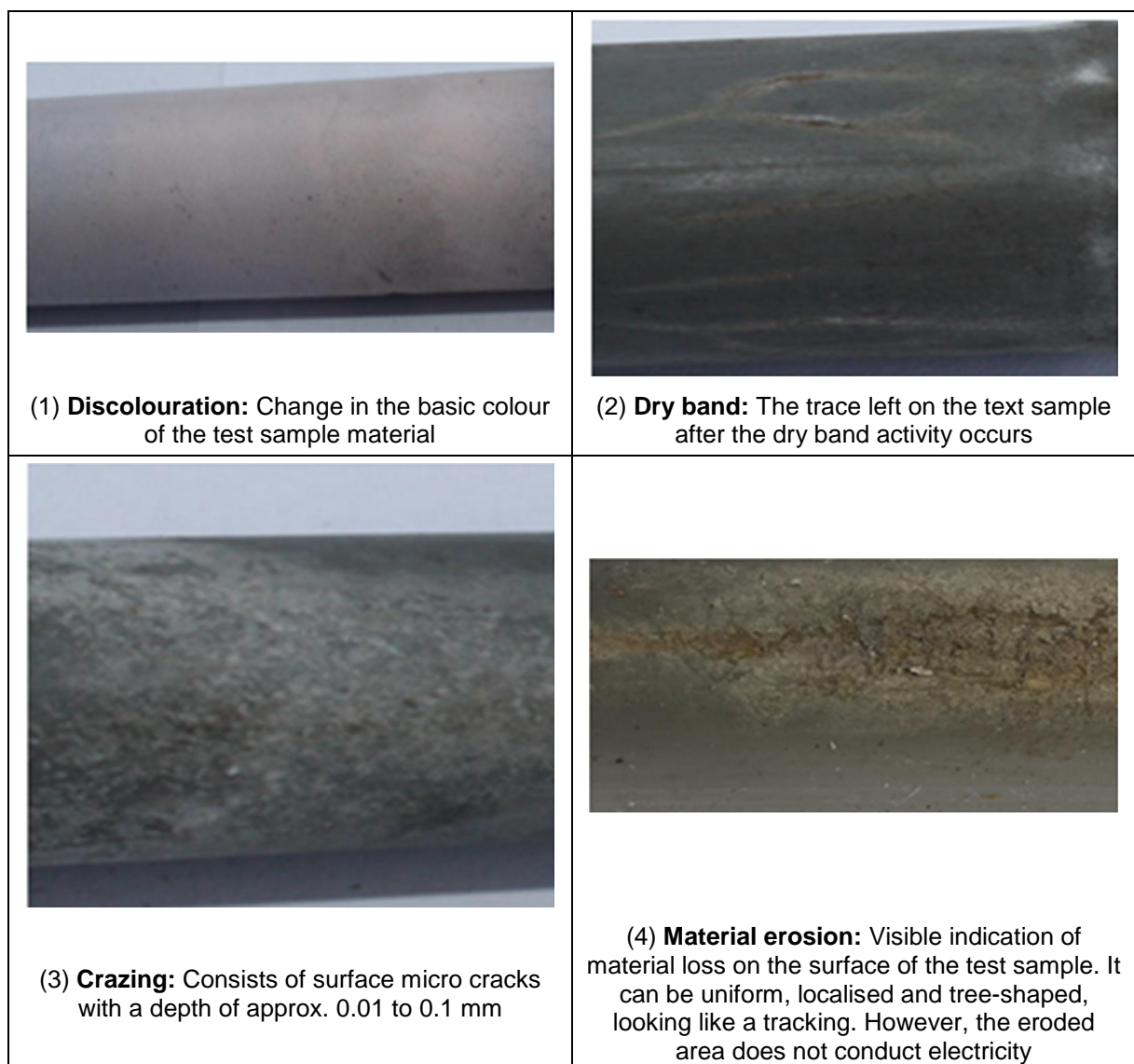


Figure 5-4: Schematic diagram of the RWDT (IEC / TR 62730:2012)

The second part of the test cycle, which is horizontal (flat), permits the excess saline solution to drip off the specimen. This ensures the light wetting, which remains on the surface, and that gives rise to leakage current, which forms dry bands during the third part of the cycle. In the third part, the specimen is submitted to a power frequency voltage for AC and DC. The maximum leakage current over one minute is captured and recorded with the OLCA. In the last (fourth) part of the cycle, the test sample is horizontal (flat) so that the surface that the leakage current had heated in phase 3 is allowed to cool (IEC / TR 62730:2012). The leakage current is continuously sampled at a frequency of 2 kHz, and the maximum and minimum leakage current over a 1-minute interval is captured (actually during the 40-second interval where the test sample is energised).

5.2 FAILURE INDICATORS IN TEST SAMPLES

Ageing modes, discolouration, crazing (which is a form of deformation that occurs on the surface of a material as a precursor to cracking), dry-bands, tracking and erosion (Ferreira *et al.* 2010; Fraçz *et al.* 2016; Madi *et al.* 2016; Roman *et al.* 2014; Zhu *et al.* 2017) are some of the key failure indicators on the surface of the insulators which this study sought to identify and analyse. Figure 5-5 below shows indications of the surfaces of the test samples. The photographs illustrate the failure indicators in test samples from the least severe to the most severe. Photos 1 to 3 of Figure 5-5 show the least severe modes, whereas, in photos 4 and 5, this effect can be interpreted as the most severe mode and as a warning sign of insulator surface deterioration.



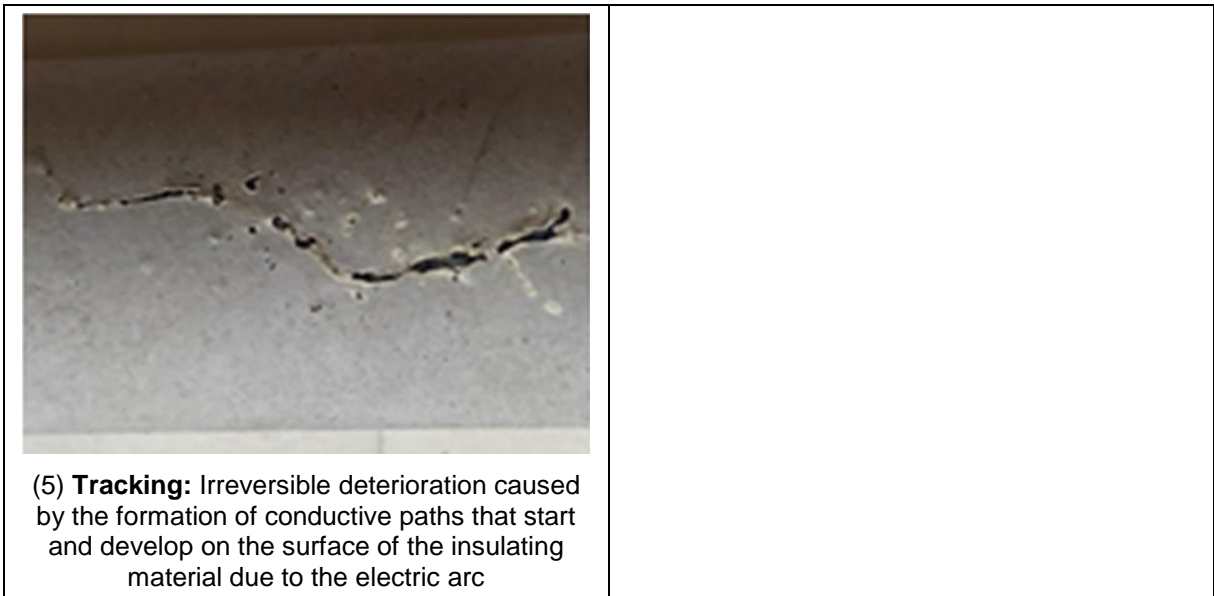


Figure 5-5: Test sample material ageing modes

The photos in Figure 5-6 below summarise the observations made with the Hikvision IR network camera for each set of test samples in different excitation voltages (AC, DC+, and DC-) with the same creepage length. Each test was observed for a total of six days. In Chapter 3.0, the observations are discussed in more detail.



Figure 5-6: Overview of visual observations made (on RTV-SR and HTV-SR test samples) under AC, DC+, and DC- excitation voltages after the 6-day testing period

5.3 WETTABILITY / HYDROPHOBICITY CLASSIFICATION

Hydrophobic and hydrophilic surface descriptors are often used for high-voltage insulators. If the surface of the insulator does not absorb water or is not wetted by water, the surface is considered hydrophobic (Amin *et al.* 2009; Fernando & Gubanski, 1999; Qin *et al.* 2013; Pratomosiwi, 2009; Thomazini *et al.* 2012; Wang *et al.* 2017). The surface of a high-voltage insulator is considered hydrophilic if it tends to absorb or be wetted by water (Elombo, 2012; Heger, 2009; Nekahi *et al.* 2017; Pylarinos *et al.* 2011).

Hydrophobicity is an important parameter for characterising the electrical properties of insulating materials. The hydrophobicity classification (HC) method proposed by the STRI (Swedish Transmission Research Institute) offers a simple guide (STRI, 1998) to obtain a collective estimate of the hydrophobicity of an insulating surface under consideration in the field. This method defines six hydrophobic classes from HC1 to HC6, depending on the shape of the water droplets and the percentage of wet areas on the hydrophobic surface (Dong *et al.* 2015).

HC1 – HC3 shows the highest hydrophobic surface on which only discrete and extremely circular water droplets are formed. With an increasing HC value, the hydrophobicity gradually decreases. When approaching HC4 or HC5 – HC6, the insulator becomes hydrophilic. This effect can be interpreted in terms of time as a warning sign for insulator surface deterioration (Dong *et al.* 2015). In this study, the hydrophobicity of each test sample surface is identified by comparing the surface with one of the photos in Figure 5-7 of the hydrophobicity classes (HC), which are between HC1 and HC6.

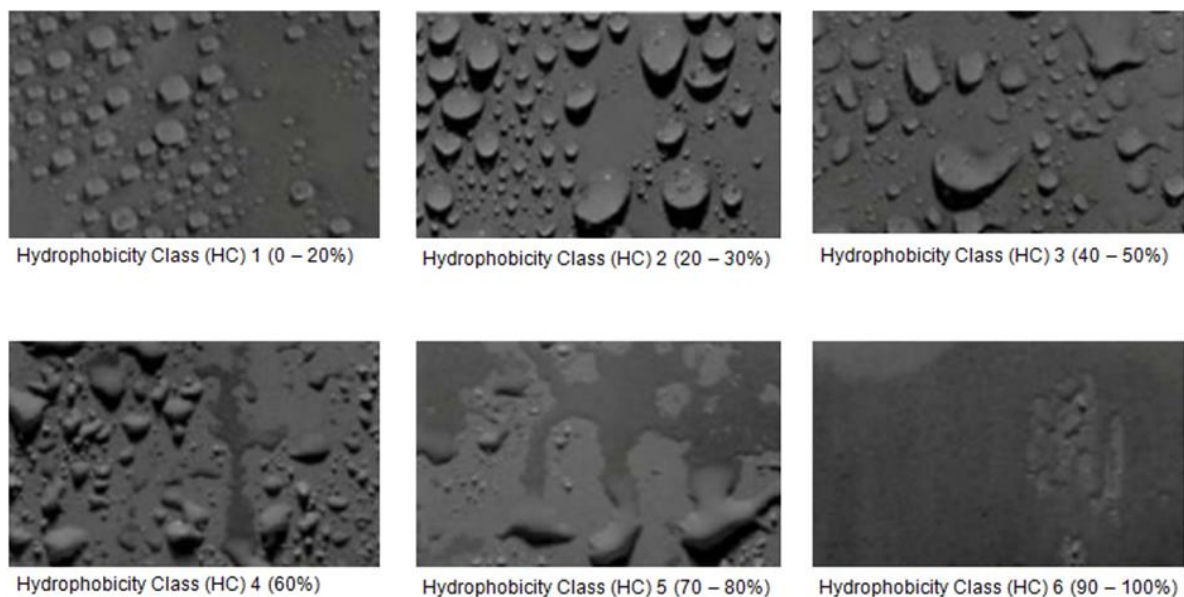


Figure 5-7: Criteria for evaluating the hydrophobicity classification (HC)

5.4 ROTATING WHEEL DIP TEST (RWDT) UNDER AC EXCITATION (CH1 – CH4)

5.4.1 Leakage current performance for HTV-SR test sample 1 in channel 1

According to Figure 5-8, during the first day of the tests, the leakage current remains uniform at 15.5 mA, and as the test progresses, the leakage current fluctuates between

16 mA and 18 mA. By the last third portion of the test, the leakage current fluctuation had decreased, and the leakage current value was stable (increases at a very low rate) at around 18 mA. The results seem consistent with those of Limbo (2009, p.122), who performed much longer tests but found similar results. Leakage current fluctuations could be due to partial discharges on the insulator's surface and arcs across dry bands on the insulator's surface. The test performed observed that it is covered with a conductive layer (saline solution) when the test sample is in the salt bath. The sample then moves to the top where it is connected to the voltage supply; at that point, due to water conductivity, the leakage current flowing on the surface of the test sample begins. Then, the rod moves to the next position, where the excess water drips off.

The energy of the leakage current may lead to some water evaporation and the creation of dry bands. Due to potential difference across the dry bands, an electrostatic field is created across the dry band, ionizing the air and allowing for a discharge across the dry band. The moment there is a spark across the dry band, the partial discharge may stop, resulting in fluctuations in leakage current. The size of the dry band may vary due to various amounts of water evaporating off the surface of the rod. In this way, the size of the dry bands may vary, contributing to further leakage current fluctuations. The leakage current will lower as the dry bands increase (in number/size). This process repeats itself depending on the prevailing conditions, including levels of the pollutants on the surface of the rod, atmospheric pressure, humidity, and temperature.

It should be noted that in the test environment, only the temperature was controlled to a limited extent using an air-conditioning unit, which was set for 16°C, but the actual temperature was not monitored. As shown, the test continued for six days until the leakage current fluctuations almost stabilised. These results are consistent with the findings of Limbo (2009, p.122).

These unstable arc discharges caused erosion at the insulator surface. According to (Heger, 2009; Elombo, 2012), leakage current (LC) leading to dry-band arcing is one of the main causes of aging in non-ceramic insulators.

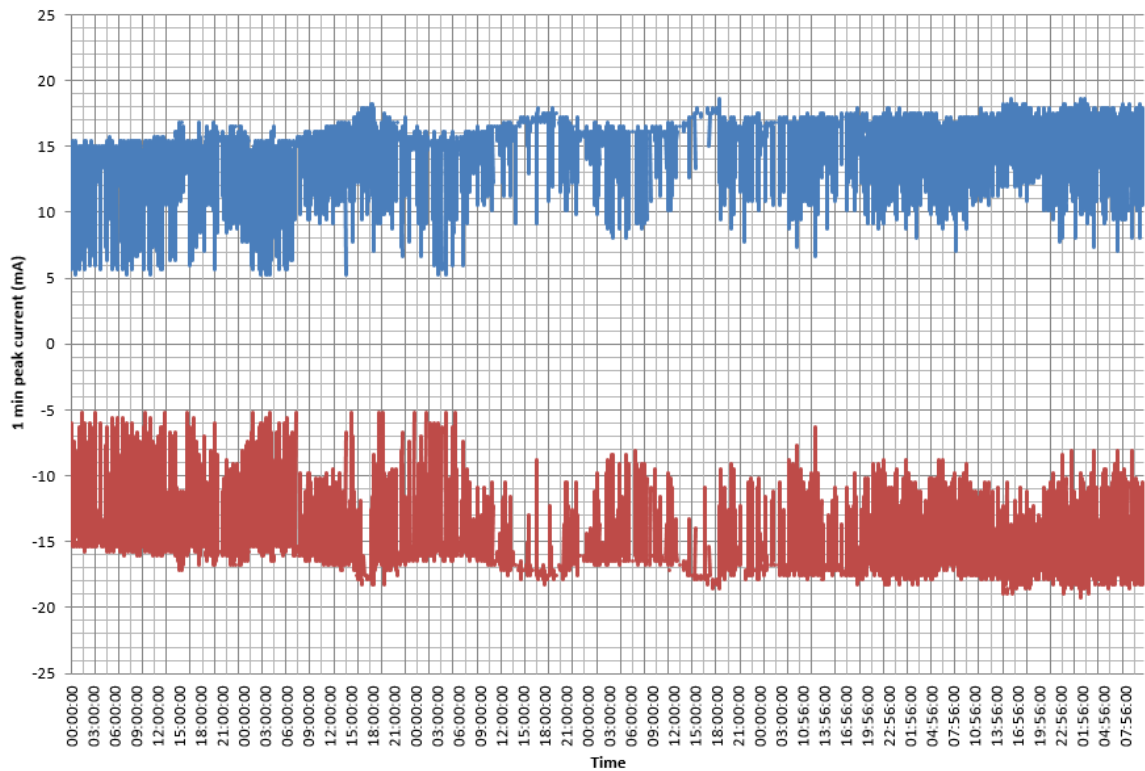


Figure 5-8: AC positive/negative 1-minute peak current

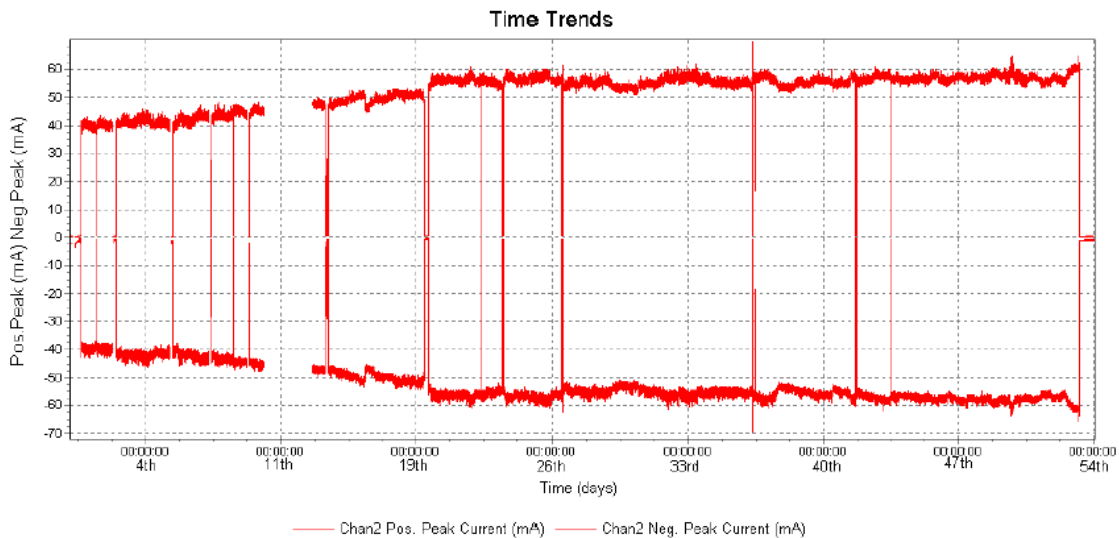


Figure 5-9: Peak leakage current over the 54-day period for the HTV-SR (Limbo, 2009)

5.4.1.1 Visual observation of ageing on HTV-SR test sample 1 in channel 1

At the end of the test, traces of dry band activity were observed on the surface of the test sample. Slight crazing and discolouration were also observed in the test sample. Erosion of the material was observed in the test sample towards the ground potential side. Dark burn marks, discolouration and dry band activities were visible around the crazed and eroded area. The above observations are depicted below in Figure 5-10,

which shows the dry bands, material erosion, crazing and dark burn marks. These were seen in the HTV-SR test sample 1. No other signs were observed in the test sample.

Electrical activity, imperfections in the HTV-SR coating, the residue of the saline solution can be the reason for crazing or cracking on HTV-SR test sample 1. When polymer materials are subjected to electrical stress, they can be deformed by shear forces and manifest or experience crazing or cracking (Yarysheva *et al.* 2012).

This study was performed in a controlled environment, and the environmental pollution is simulated in the salt bath used for the test. Discolouration around the crazed and eroded area on the ground potential of the HTV-SR test sample 1 is due to the constant operating voltage, which can ultimately degrade the test sample. Discolouration on the surface of polymer insulators can occur due to cyclisation of the intramolecular process and high electrical voltages in combination with other stresses (Ullah *et al.* 2020).

Dark pollution/contamination build-up around a discolouration area can be associated with different contaminant deposits during testing, such as dirt left over from water tank cleaning. According to Ramos *et al.* (2006), pollution is one of the main causes of insulator breakdown. Insulators start to fail when airborne pollutants settle on the surface of the insulators and combine with moisture from fog, rain, or dew. Pollution degrades insulators and seriously affects their electrical properties, one of the main causes of insulator failure.

Dry band formation on the HTV-SR test sample 1 indicates discharge activities on the ground potential side of the test sample. According to Zhou *et al.* (2010), the formation of the dry band greatly influences the distribution of the electric field along the insulator, which leads to partial arcing and flash-over. According to Roman *et al.* (2019), light rain and high humidity conditions worsen dry band arcs and possible flash-over in insulators used in the field.

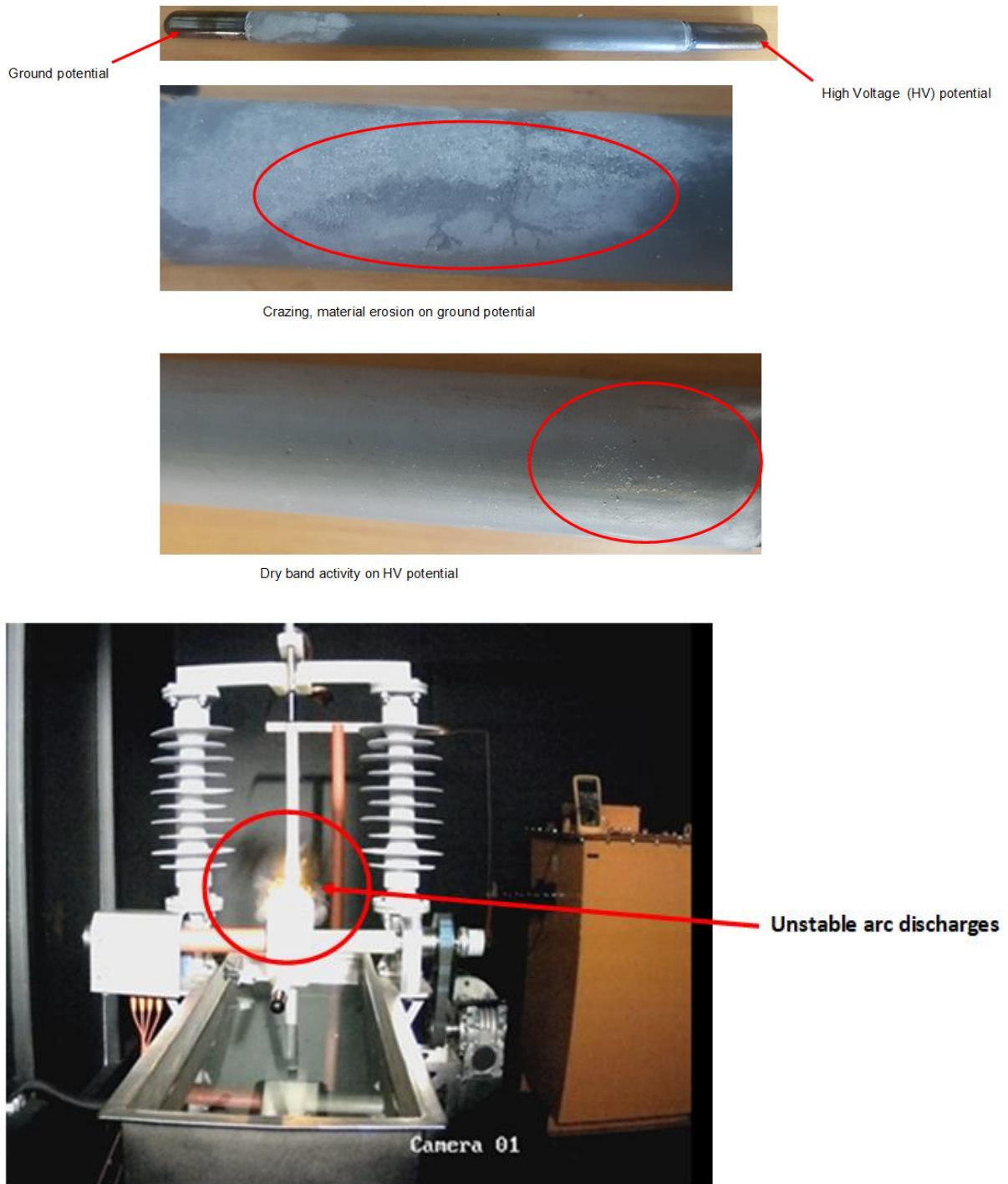


Figure 5-10: Material erosion, crazing, dry band activities, and unstable arc discharges observed on the HTV-SR test sample

5.4.1.2 Overview of hydrophobicity classification

After the 6-day test, a reduction in hydrophobicity was observed for the HTV-SR sample 1 tested under AC excitation. According to Figure 5-7 above, the hydrophobicity classification (HC) and the percentage hydrophobicity values are given for each test sample. Only discrete droplets corresponding to HC5 (70-80%) are formed, and therefore the test sample is considered highly hydrophilic. The loss of

hydrophobicity in the tested sample material may have been caused by the increased electrical stress and discharge activities on the surface during the test (see Figure 5-11).

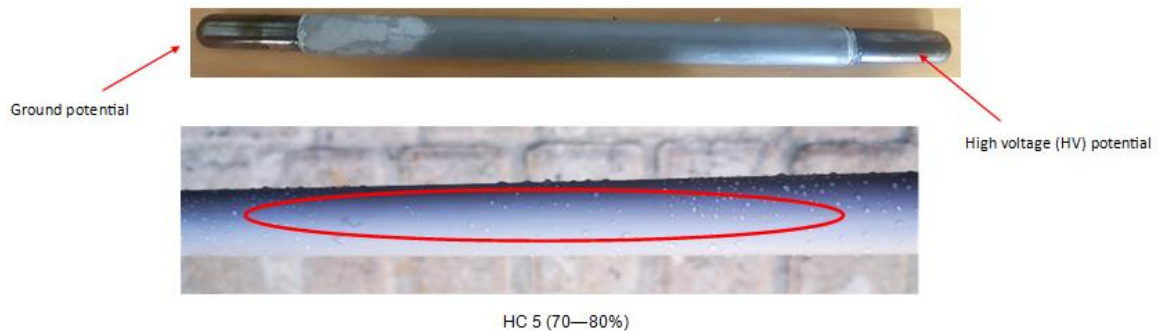


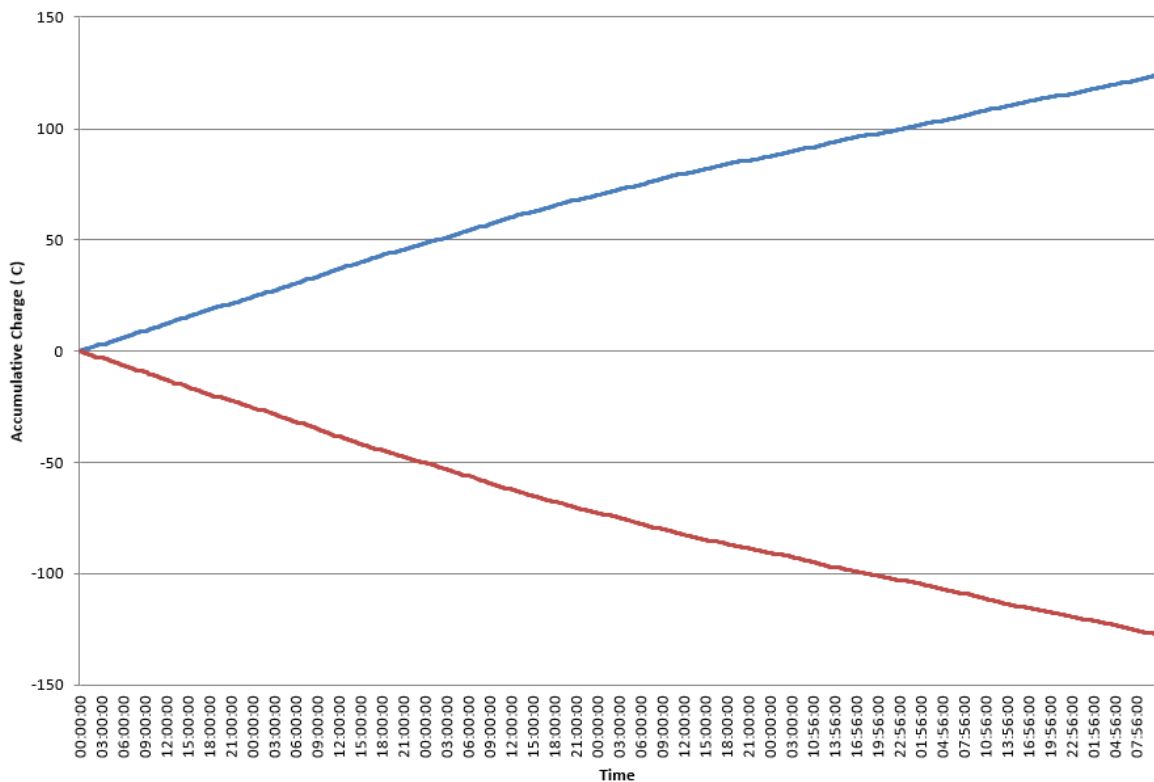
Figure 5-11: *Hydrophobicity of the HTV-SR sample 1*

5.4.1.3 Cumulative electrical charge

According to Vosloo (2002, p.147), “*The cumulative electric charge flowing over the insulator surface is used as an indicator of the continuous interaction of the insulator material surface with the deposited pollution and wetting. This study uses the amount of electrical charge flowing over the insulator as a cumulative value of current and time (charge). For the same reasons as explained before (same environment and climate and same designs and profiles), it is assumed that the differences in cumulative electrical charge measured are mainly due to the material properties*”. In other words, the difference in cumulative charge values can be used to conclude the coating used on the test samples. Figure 5-12 indicates that the rate of increase in leakage current at the beginning is slightly higher than the rate of change after the halfway mark. This is for the HTV-SR test sample 1 tested under AC excitation for six days. This can be attributed to the beginning of stabilization of dry band formation on the surface of the test sample. See § 5.4.1 above.

Comparing Figure 5-11 to Figure 5-8, it can be said that since the slope of the cumulative charge lines in Figure 5-12 corresponds nicely with the leakage current levels in Figure 5-8, it can be said that the cumulative charge graph is a reliable way to represent the trend in leakage current changes despite leakage current fluctuations. It can also be concluded that the saline solution and stresses to which the test samples were subjected were fairly constant throughout the testing period. The positive and negative cumulative electrical charge flowing over the surface of the insulator reached approximately 125 coulomb at the end of the 144-hour test; this will be used as a

comparison with RTV-SR to determine test sample performance (AC, DC+, and DC-). After each test (i.e. AC, DC+, and DC-), the overall cumulative electrical charge over the HTV-SR and RTV-SR test samples will be compared.



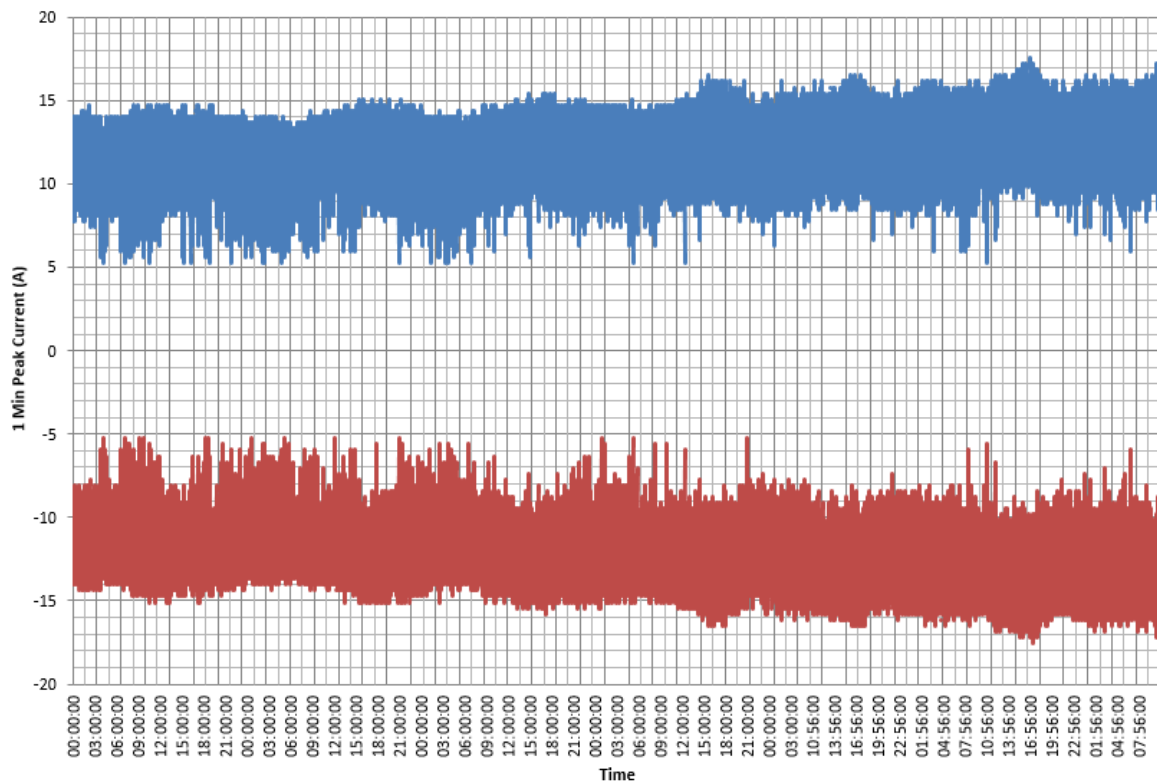


Figure 5-13: AC positive/negative 1-minute peak current

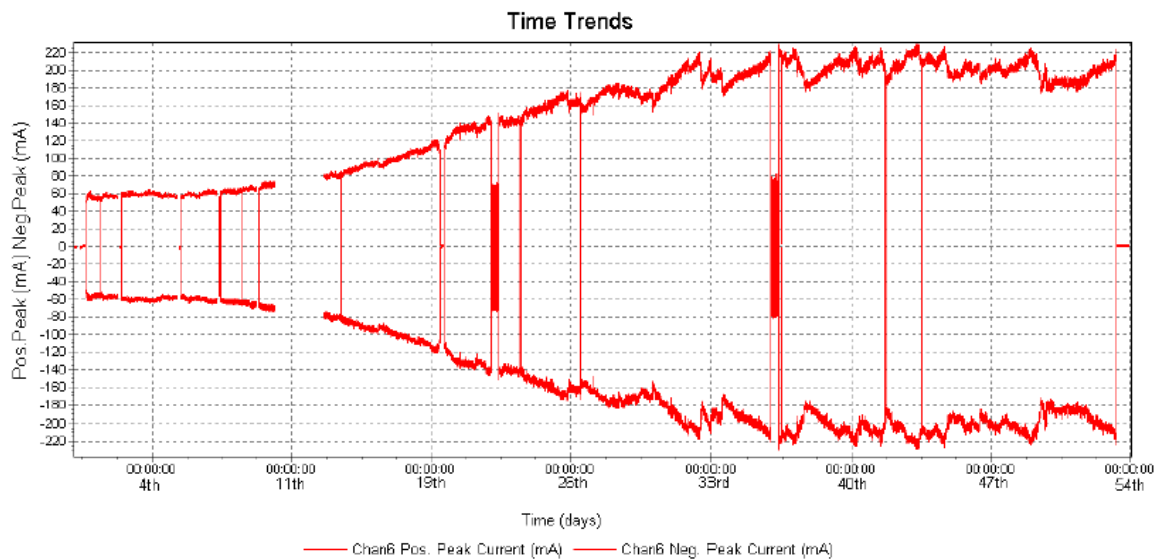


Figure 5-14: Peak current for the RTV SR coated porcelain insulator (channel 6) for HVAC excitation (Limbo, 2009)

5.4.3 Visual observation of ageing on RTV-SR test sample 2 in channel 2

At the end of the test, dark contamination and discolouration were accumulated on the surface of the test sample and towards the HV terminal. The above observations can be seen in Figure 5-15. No other indications were found on the test sample. When looking at the surface of the RTV-SR test sample, the level of deterioration is less

compared to that of the HTV-SR sample. This, therefore, can be used to conclude that at this early stage (6 days) of testing, the RTV-SR test sample is less affected by electrical stresses. This result corresponds to Limbo's (2009) findings.

Insulators start to fail when airborne pollutants settle on the surface of the insulator and combine with moisture from fog, rain, or dew. Pollution degrades insulators and seriously affects their electrical properties, one main cause of insulator failure (Elombo, 2012; Frącz *et al.* 2016; Garrard, 2008; Izadi *et al.* 2017; Ramirez *et al.* 2012). For insulators outdoor in the field, dark pollution/contamination build-up around a discolouration area can be associated with different types of contaminant deposits such as dirt, exposure to severe environmental conditions, and discharge activity, according to Ramos *et al.* (2006). However, this is not the case in this study as the test is performed in a controlled environment, and the environmental pollution is simulated in the salt bath used for the test.

Discolouration on the surface of polymer insulators can occur due to cyclisation (a process that limits the degree of polymerization of their intramolecular structure) and high electrical voltages in combination with other stresses (Ullah *et al.* 2020).



Figure 5-15: Dark pollution build-up and discolouration on RTV-SR test sample

5.4.3.1 Overview of hydrophobicity classification

After the 6-day test, a reduction in hydrophobicity was observed for the sample tested under AC excitation. Figure 5-16 below shows the hydrophobicity percentage given for each test sample. Only discrete droplets corresponding to HC1 (0-20%) are formed, and therefore the test sample is considered highly hydrophobic.



Figure 5-16: *Hydrophobicity of the RTV-SR sample 2*

5.4.3.2 Cumulative electrical charge

The cumulative electric charge represents the leakage current flowing through the pollution layer over time. The cumulative electric charge for the RTV-SR test sample 2 tested under AC excitation for six days is presented as follows: Figure 5-17 indicates that the slope of the cumulative electric charge graph is slightly changed (slight drop) after the 100-coulomb value line. Therefore, the rate of change in leakage current is slightly lower (i.e. slight increase), which might be attributed to dry band formation on the surface of the test sample. Keep in mind that the saline solution and stresses to which the test samples were subjected seemed constant throughout the testing period, given the levels of discolouration on the surface of the test sample. The positive and negative cumulative electrical charge flowing over the surface of the insulator reached approximately 120 coulomb over six days or 144 hours of testing.

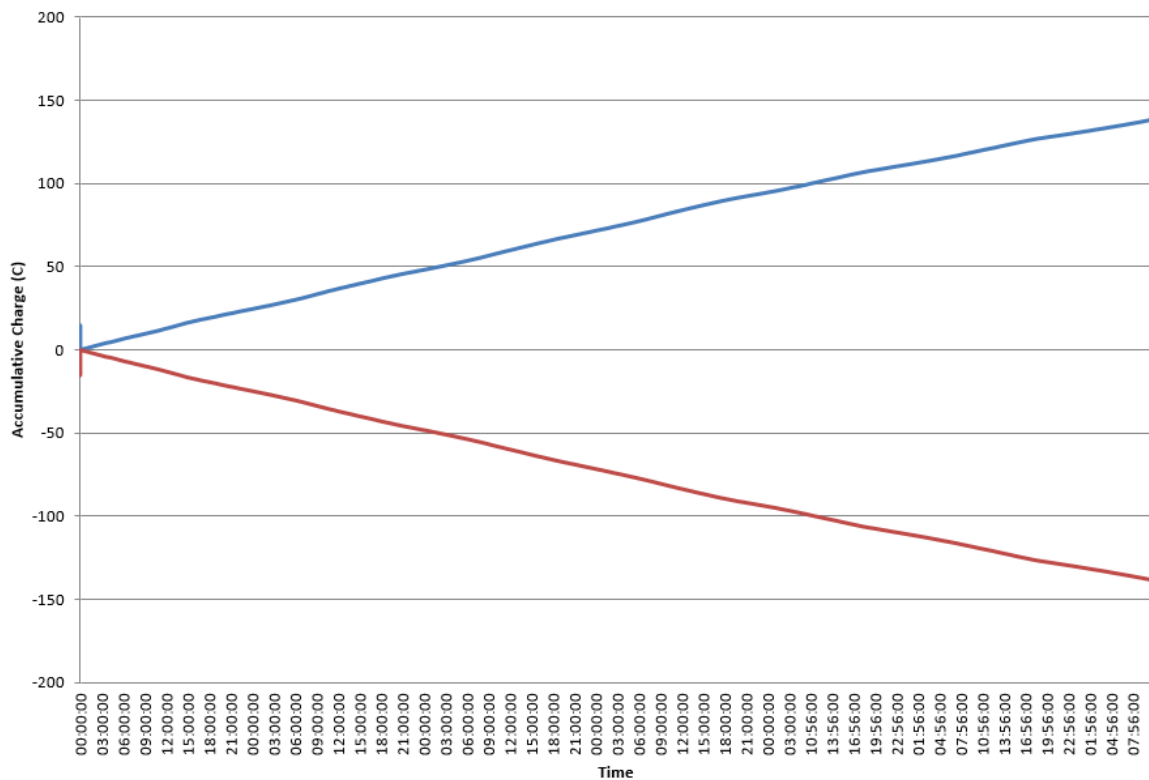


Figure 5-17: Positive/negative cumulative electric charge graph

5.4.4 Leakage current performance for HTV-SR test sample 3 in channel 3

According to Figure 5-18, during the first day of the tests, the leakage current remains uniform at 16 mA and 16.2 mA, and as the test progresses on the second day, the leakage current fluctuates between 18 mA and 20 mA. By the third portion of the test, the leakage current fluctuation had further increased between 20 mA and 22 mA, and on the last day, the leakage current value increased at around 18 mA and 24 mA. The results seem consistent with those of Limbo (2009, p.122), who performed much longer tests but found similar results (see Figure 4-19). Leakage current fluctuations could be due to partial discharges on the insulator’s surface, as well as arcs across dry bands on the insulator’s surface (see § 5.4.1 above for further explanation).

These unstable arc discharges caused erosion at the insulator surface, which according to Heger (2009) and Elombo (2012), led to dry-band arcing, which contributes to ageing in non-ceramic insulators.

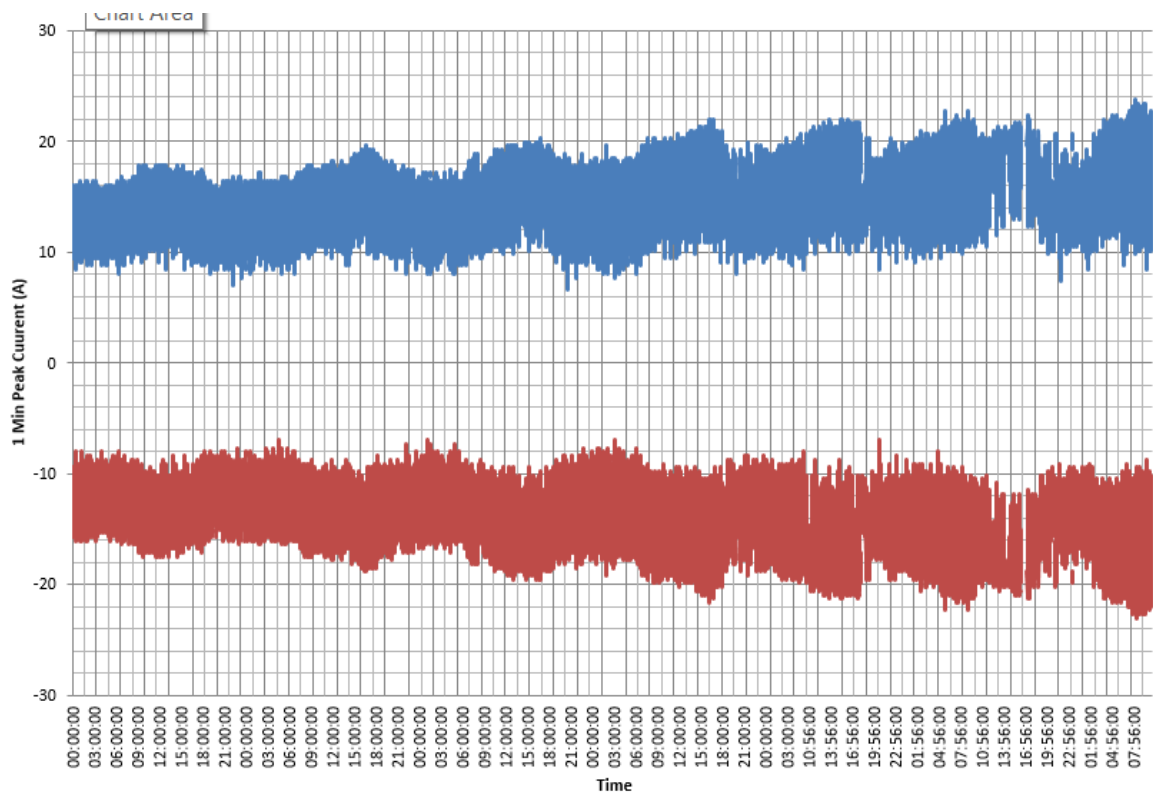


Figure 5-18: AC positive/negative 1-minute peak current

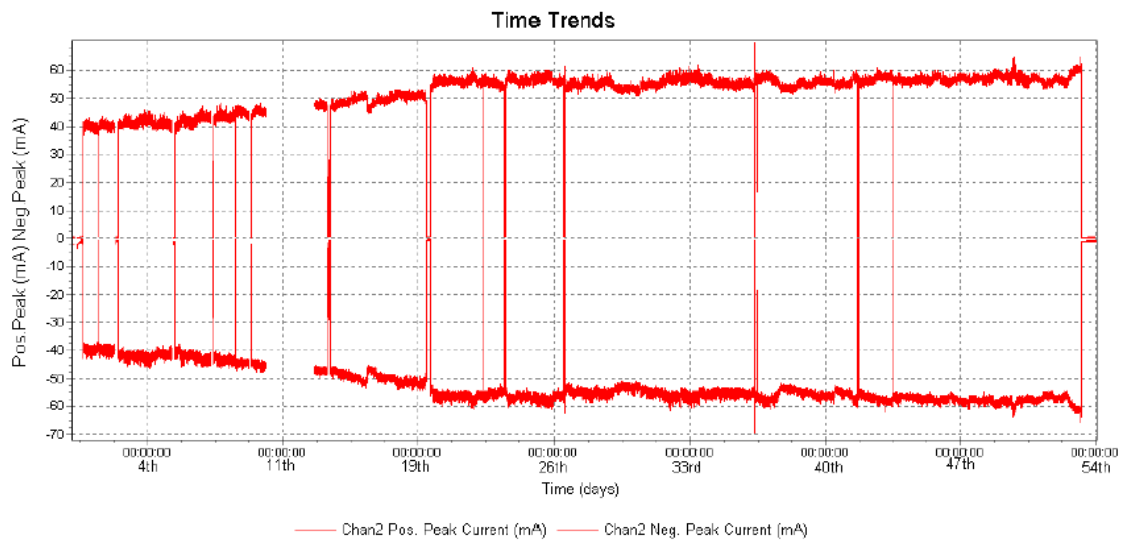


Figure 5-19: Peak leakage current over 54 days period for the HTV-SR (Limbo, 2009)

5.4.4.1 Visual observation of ageing on HTV-SR test sample 3 in channel 3

At the end of the test, traces of dry band activity, crazing, and material erosion were observed on the surface of the test sample. These observations are presented in Figure 5-20 below.

Dry band formation on the HTV-SR test sample 3 indicates discharge activity at the ground potential end. Zhou *et al.* (2010) posit that the formation of the dry bands may

influence the distribution of the electric field along the insulator, which leads to partial arcing and flash-over. Dry band arcs and possible flash-over across an insulator are exacerbated by light rain and high humidity conditions in the field (Kumagai *et al.* 2001; Krzma *et al.* 2015; Nekahi *et al.* 2017; Roman *et al.* 2019).

Electrical activity, coating imperfections on the surface of the test sample, and the saline solution under electrical excitation can be the reason for crazing or cracking on the HTV-SR test sample 3. According to Awaja *et al.* (2016), the rubber particles of the coating can also be responsible for developing multiple cracks, acting as stress concentrates during the craze initiation process. When polymer materials are subjected to stress, they can be deformed by shear yielding, crazing, or cracking (Yarysheva *et al.* 2012).

Material tracking and erosion in the HTV-SR test sample 3 are caused by localised heat generated by the discharges during the test. Material tracking and erosion can occur due to the dry-band discharges on insulating surfaces (Schmidt *et al.* 2010). Further, researchers such as Macey *et al.* (2004) and Thomazini *et al.* (2012) suggests that tracking and erosion are exacerbated if the housing material is exposed to solar ultraviolet (UV) radiation when the insulators are outdoors.



Figure 5-20: Traces of dry band activities, crazing and material erosion on HTV-SR test sample

5.4.4.2 Overview of hydrophobicity classification

After the 6-day test, a reduction in hydrophobicity was observed for the sample tested under AC excitation. Hydrophobicity classification (HC) and the percentage given for each test sample can be observed in Figure 5-21. Only discrete droplets corresponding to HC3 (40-50%) are formed, and therefore the test sample is considered hydrophobic.



Figure 5-21: Hydrophobicity of the HTV-SR sample 3

5.4.4.3 Cumulative electrical charge

The cumulative electric charge for the HTV-SR test sample 3 tested under AC excitation for six days is presented below. Figure 5-22 indicates that the slope of the cumulative electric charge graph has a slight drop in it at the 45- and 80-coulomb levels. This may be attributed to fluctuations in the leakage current and dry band formation on the surface of the test sample. This raises questions about the saline solution distribution on the surface of the insulator and the stresses to which the sample was subjected. The positive and negative cumulative electrical charge flowing over the surface of the insulator reached approximately 120 coulomb over six days or 144 hours of testing.

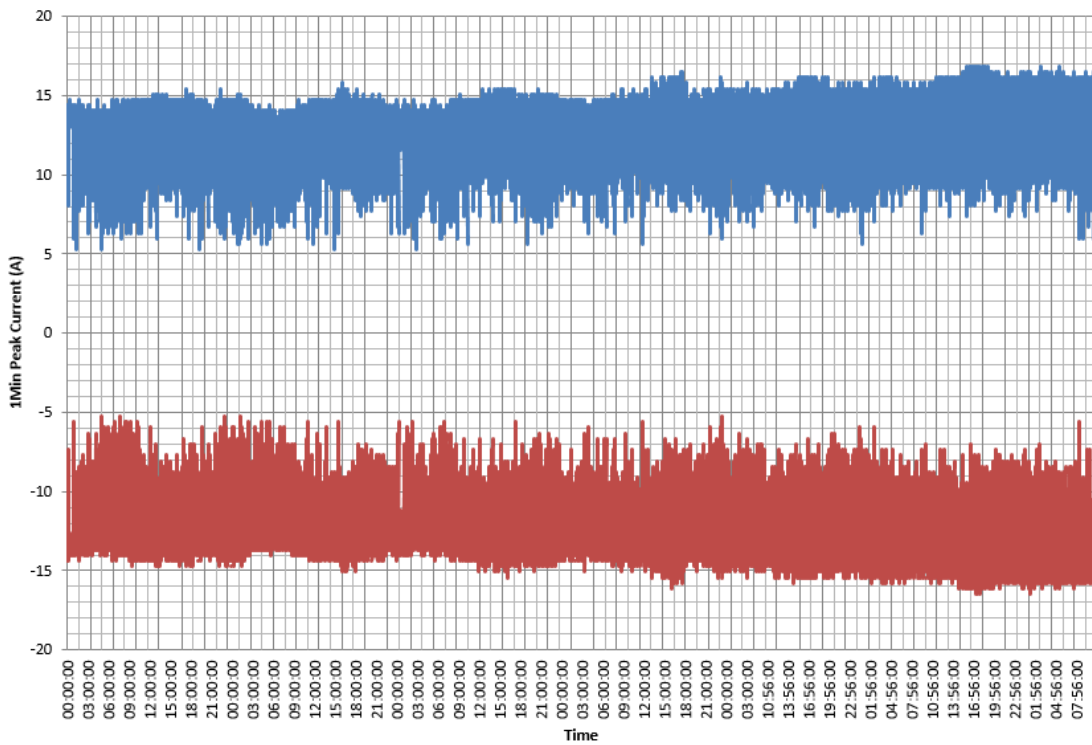


Figure 5-23: AC positive/negative 1-minute peak current

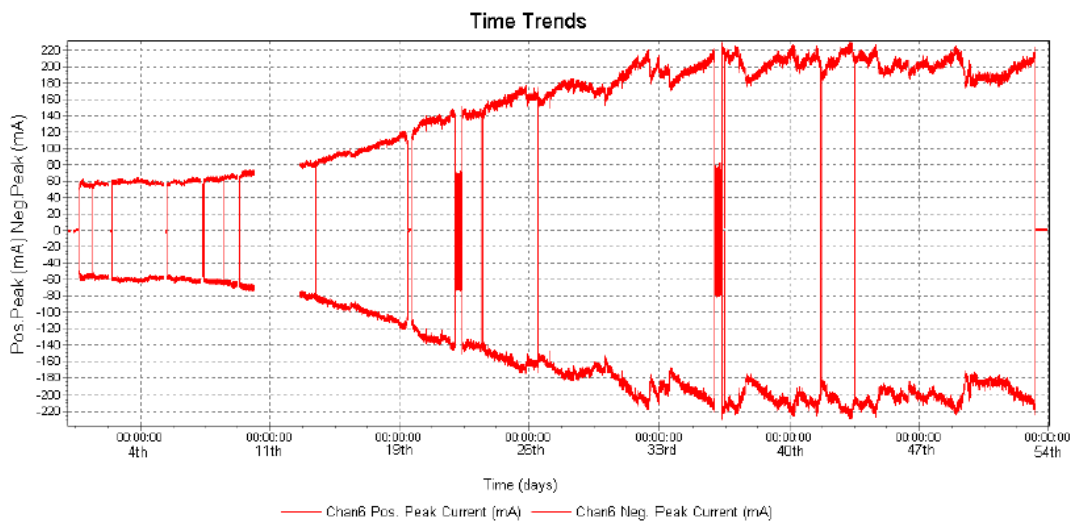


Figure 5-24: Peak current for the RTV-SR coated porcelain insulator (channel 6) for HVAC excitation (Limbo, 2009)

5.4.5.1 Visual observation of ageing on RTV-SR test sample 4 in channel 4

At the end of the test, discolouration and pollution build-up on the surface and towards the high-voltage potential side of the test sample were observed. These observations are presented in Figure 5-25 below.



Figure 5-25: Tracking and erosion, discoloration, and pollution on RTV-SR test sample

Discolouration on the surface of polymer insulators can occur due to cyclisation (a process that limits the degree of polymerization of their intramolecular structure) and high electrical voltages in combination with other stresses (Ullah *et al.* 2020).

Insulators start to fail when airborne pollutants settle on the surface of the insulator and combine with moisture from fog, rain, or dew. Pollution degrades insulators and seriously affects their electrical properties, one main cause of insulator failure (Elombo, 2012; Frącz *et al.* 2016; Garrard, 2008; Izadi *et al.* 2017; Ramirez *et al.* 2012). For insulators outdoor in the field, dark pollution/contamination build-up around a discolouration area can be associated with different types of contaminant deposits such as dirt, exposure to severe environmental conditions, and discharge activity, according to Ramos *et al.* (2006). However, this is not the case in this study as the test is performed in a controlled environment, and the environmental pollution is simulated in the salt bath used for the test.

5.4.5.2 Overview of hydrophobicity classification

After the 6-day test, a reduction in hydrophobicity was observed for the sample tested under AC excitation. Figure 5-26 shows the hydrophobicity classification (HC) and the percentage given to the test sample. Only discrete droplets corresponding to HC3 (10-20%) are formed, and therefore the test sample is considered highly hydrophobic.



Figure 5-26: Hydrophobicity of the RTV-SR sample 4

5.4.5.3 Cumulative electrical charge

The cumulative electric charge for the HTV-SR test sample 3 tested under AC excitation for six days is presented below. Figure 5-27 indicates that the slope of the cumulative electric charge graph has a slight drop in it at the 50-coulomb level. This may be attributed to fluctuations in the leakage current and dry band formation on the surface of the test sample. This raises questions about the saline solution distribution on the surface of the insulator and the stresses to which the sample was subjected. The positive and negative cumulative electrical charge flowing over the surface of the insulator reached approximately 150 coulomb over six days or 144 hours of testing.

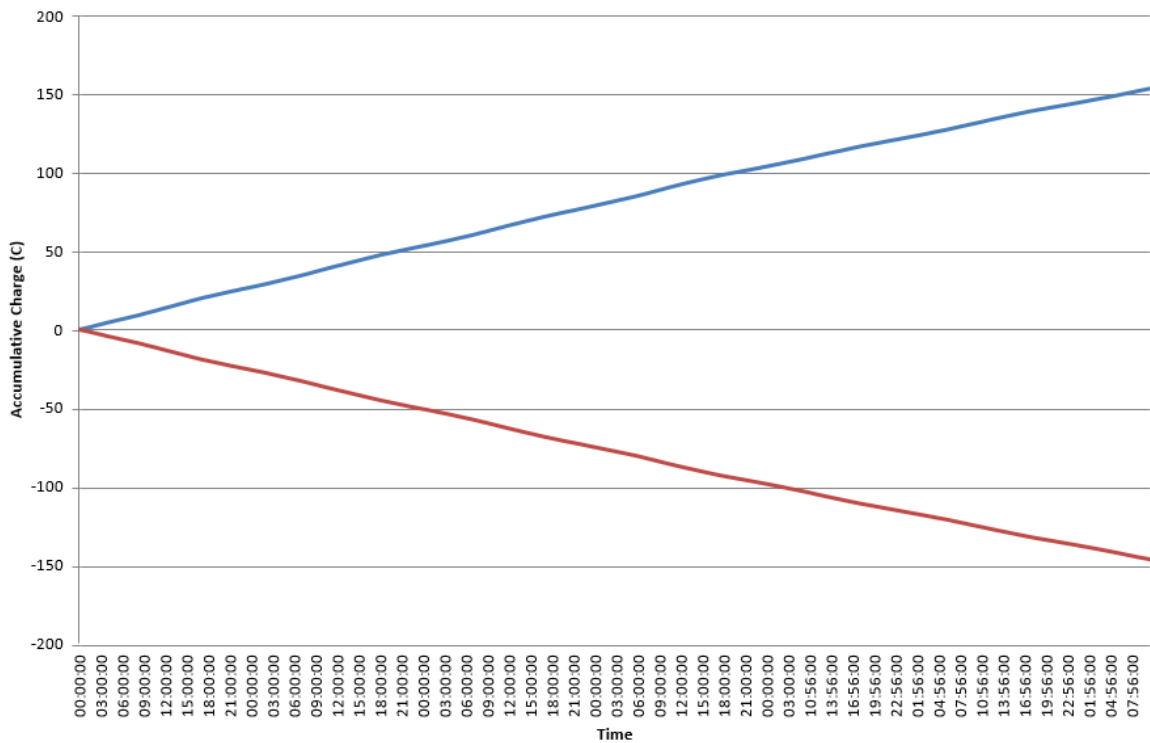


Figure 5-27: Cumulative positive/negative charge

5.4.5.4 Overall positive/negative cumulative electric charge comparison between HTV-SR and RTV-SR

The overall cumulative electric charge for the HTV-SR and RTV-SR test samples tested under AC excitation is presented below. The test samples were energised under AC excitation for six days. The overall cumulative electrical charge of the HTV-SR and RTV-SR test samples are divided into three phases as follows:

Phase 1: No distinction can be made in the lines as they appear close to each other. It is therefore difficult to distinguish which test sample performed better.

Phase 2: Lines or paths become clear as they begin to change or separate. Also, cross-over points on the graph for both the HTV-SR and RTV-SR test samples are evident.

Phase 3: Both RTV-SR test samples and HTV-SR test samples follow different paths. The trends for RTV-SR samples 2 and 4 are similar, whereas HTV-SR 1 and 3 are close, and because the slope of these lines seems to drop, one can deduce that the leakage current is trending towards stabilization and a lower rate of charge. Further, the relative average difference in leakage current between RTV-SR and HTV-SR is 14.2% = $[(162 - 139)/162] \times 100$.

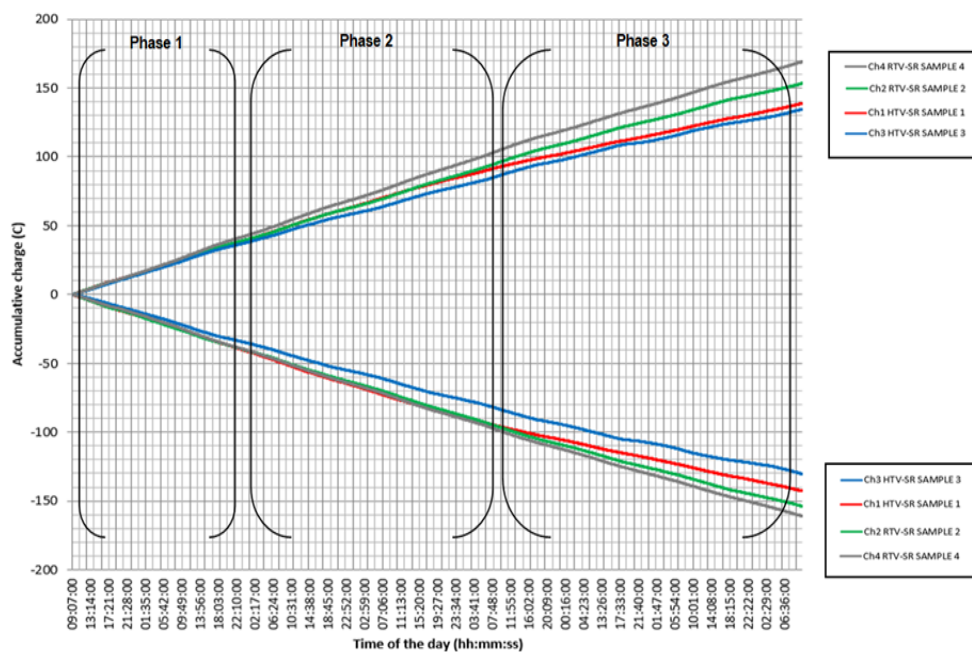


Figure 5-28: Overall cumulative positive/negative electrical charge between HTV-SR and RTV-SR

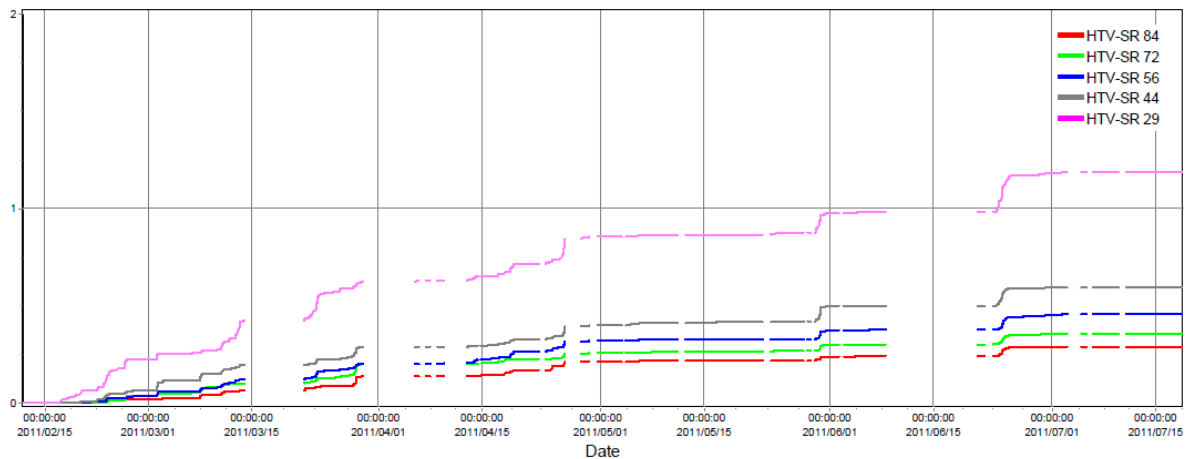


Figure 5-29: Accumulative coulomb-ampere for all the HTV-SR insulators installed on the AC excitation voltage (Elombo, 2012)

Figure 5-29 above indicates that both HTV-SR samples 1 and 3 performed slightly better compared to RTV-SR test samples 2 and 4, that had a higher cumulative electrical charge performance. The results seem consistent with those of Elombo (2012, p.120), who performed much longer tests but found similar results. At the beginning of the results on test sample HTV-SR 84, a similar trend to the tested Ch1 and HTV-SR samples 1 and 2; see Figure 5-29 above. The trend towards the leakage current stabilization can also be seen in Elombo's work.

5.5 ROTATING WHEEL DIP TEST (RWDT) UNDER DC+ EXCITATION (CH1 – CH4)

5.5.1 Leakage current performance for HTV-SR test sample 5 in channel 1

According to Figure 5-30, during the first part of the test, the leakage current fluctuated between 13.2 mA and 14 mA. Later on, the third day of the test, the leakage current fluctuated between 13.2 mA and 15 mA before it gradually increased to 16.8 mA. Then, a sudden drop in leakage current was observed from 16.8 mA until 9.5 mA. This sudden drop in leakage current could be due to the puncture marks observed on the test samples indicating a faulty connection when the rod was in position 1 (energization), resulting in a high impedance connection point that subsequently caused the leakage current to decrease. Slowly, the situation improved, the connection got better, and the leakage current increased until it reached 14 mA. By the third portion of the test, the leakage current value was stable at around 13.4 mA. The results seem consistent with those of Elombo (2012, p.115), who performed much longer tests but

found similar results (see Figure 5-31 below). Leakage current fluctuations could be due to partial discharges on the insulator's surface, as well as arcs across dry bands on the insulator's surface (see § 5.4.1 above for further explanation).

These varying arc discharges caused erosion at the insulator surface, which according to Heger (2009) and Elombo (2012), led to dry-band arcing as one of the main causes of ageing in non-ceramic insulators.

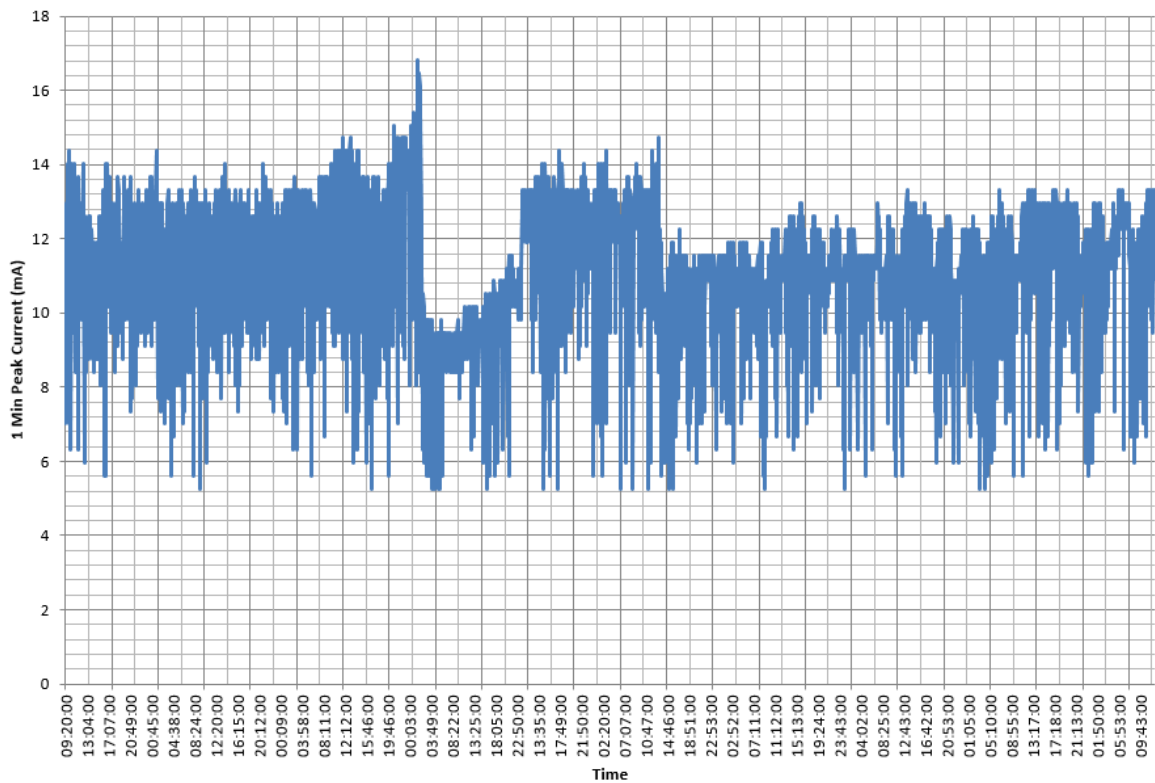


Figure 5-30: DC+ 1-minute peak current

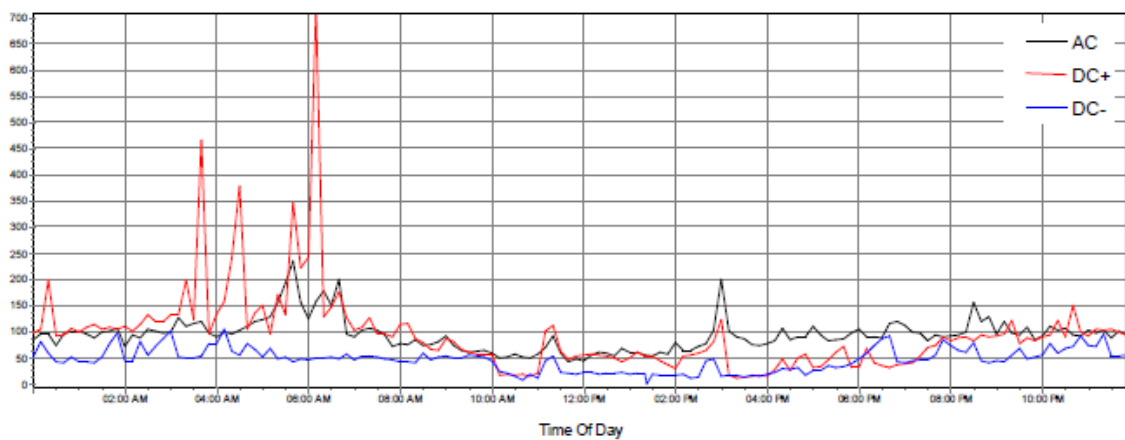


Figure 5-31: The time-of-day maximum absolute peak leakage current profile recorded for all the HTV-SR 29 insulators (Elombo, 2012)

5.5.1.1 Visual observation of ageing on HTV-SR test sample 5 in channel 1

At the end of the test, crazing was observed in the ground potential side. Pollution build-up on the surface of the test sample and burn marks over the glassy carbon electrode were noted. These observations are presented in Figure 5-32 below.

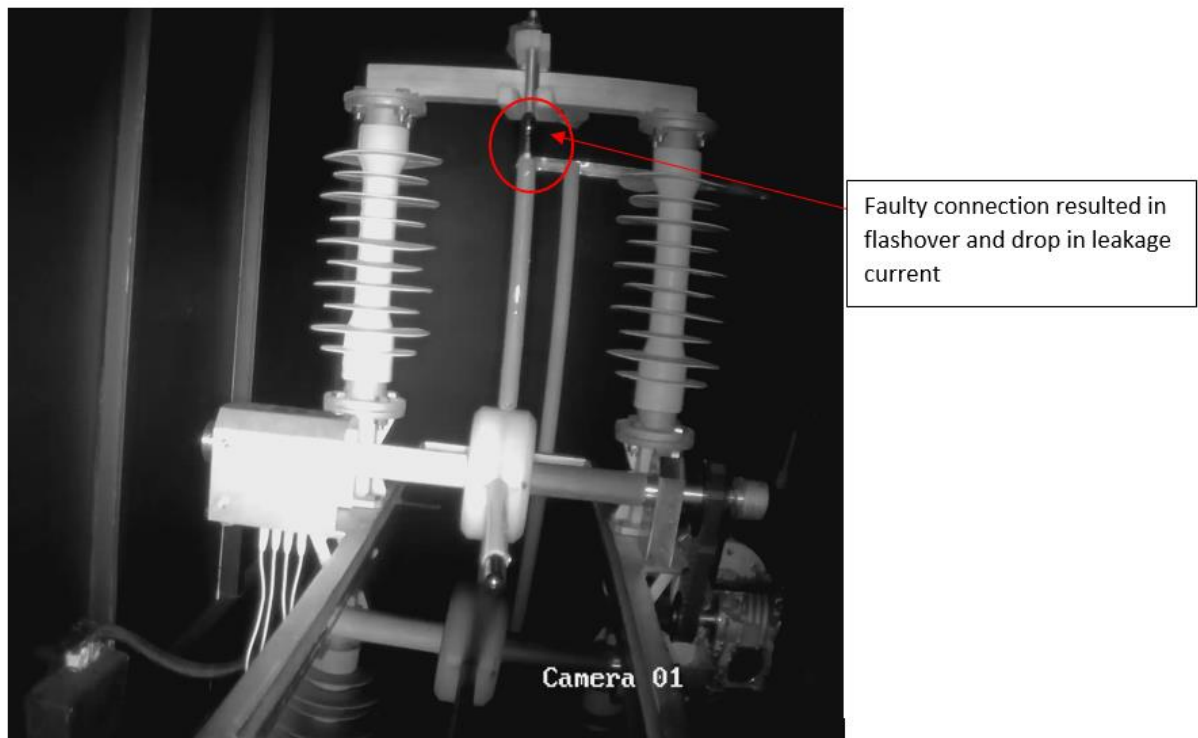


Figure 5-32: Crazing, pollution build-up, and burn marks over a glassy carbon electrode on the HTV-SR test sample

Dry band formation on the HTV-SR test sample 5 indicates discharge activity at the ground potential end. Zhou *et al.* (2010) posit that the formation of the dry bands may influence the distribution of the electric field along the insulator, which leads to partial arcing and flash-over. Dry band arcs and possible flash-over across an insulator are exacerbated by light rain and high humidity conditions in the field (Kumagai *et al.* 2001; Krzma *et al.* 2015; Nekahi *et al.* 2017; Roman *et al.* 2019).

Electrical activity, coating imperfections on the surface of the test sample, and the saline solution under electrical excitation can be the reason for crazing or cracking on the HTV-SR test sample 5. According to Awaja *et al.* (2016), the rubber particles of the coating can also be responsible for developing multiple cracks, acting as stress concentrates during the craze initiation process. When polymer materials are subjected to stress, they can be deformed by shear yielding, crazing, or cracking (Yarysheva *et al.* 2012).

Material tracking and erosion in the HTV-SR test sample 5 are caused by localised heat generated by the discharges during the test. Material tracking and erosion can occur due to the dry-band discharges on insulating surfaces (Schmidt *et al.* 2010). According to Macey *et al.* (2004), silicone rubber is a polymeric material with a poor ability to resist electrical tracking and erosion. Further, researchers such as Macey *et al.* (2004) and Thomazini *et al.* (2012) suggests that tracking and erosion are exacerbated if the housing material is exposed to solar ultraviolet (UV) radiation when the insulators are outdoors.

Burn marks and puncture marks on the glassy carbon electrode could be due to prolonged oxidation at a high-voltage potential and also by a faulty connection when the rod was in position 1 (energization).

5.5.1.2 Overview of hydrophobicity classification

After the 6-day test, a reduction in hydrophobicity was observed for the sample tested under DC+ excitation. Figure 5-33 shows the hydrophobicity classification (HC) percentage given for the test sample. Only discrete droplets corresponding to HC4 (60%) are formed, and therefore the test sample is considered highly hydrophilic. The loss of hydrophobicity in the test sample material tested may have been caused by increased electrical stress and discharge activities on the surface.

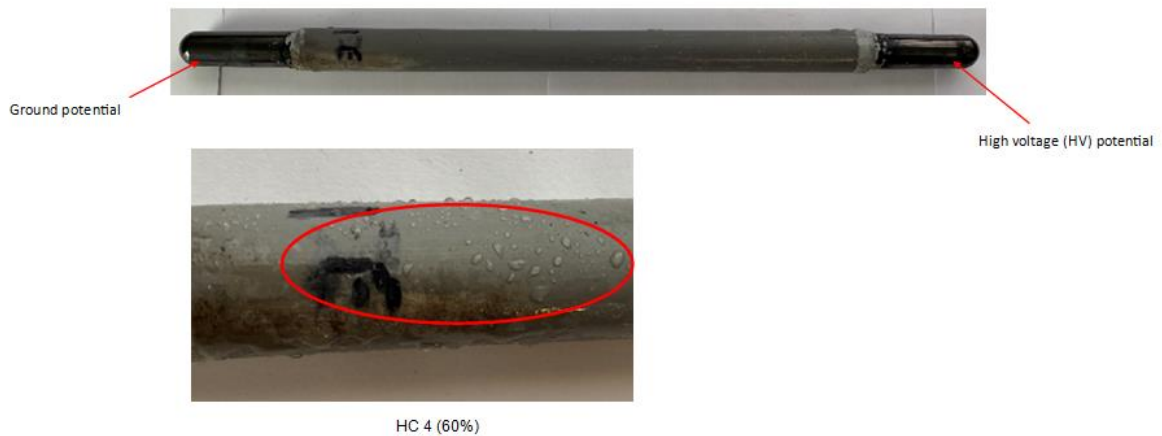


Figure 5-33: *Hydrophilicity of the HTV-SR sample 5*

5.5.1.3 Cumulative electrical charge

The cumulative electric charge for the HTV-SR test sample 5 tested under DC+ excitation for six days is presented as follows: Figure 5-34 indicates that the slope of the cumulative electric charge graph has a slight drop at the 70-coulomb level and a slight increase at the 90-coulomb level. This may be attributed to faulty connection experienced, fluctuations in the leakage current and dry band formation on the surface of the test sample. This raises questions about the saline solution distribution on the surface of the insulator and the stresses that the sample was subjected to. The positive cumulative electrical charge flowing over the surface of the insulator reached approximately 235 coulomb over six days or 144 hours of testing.

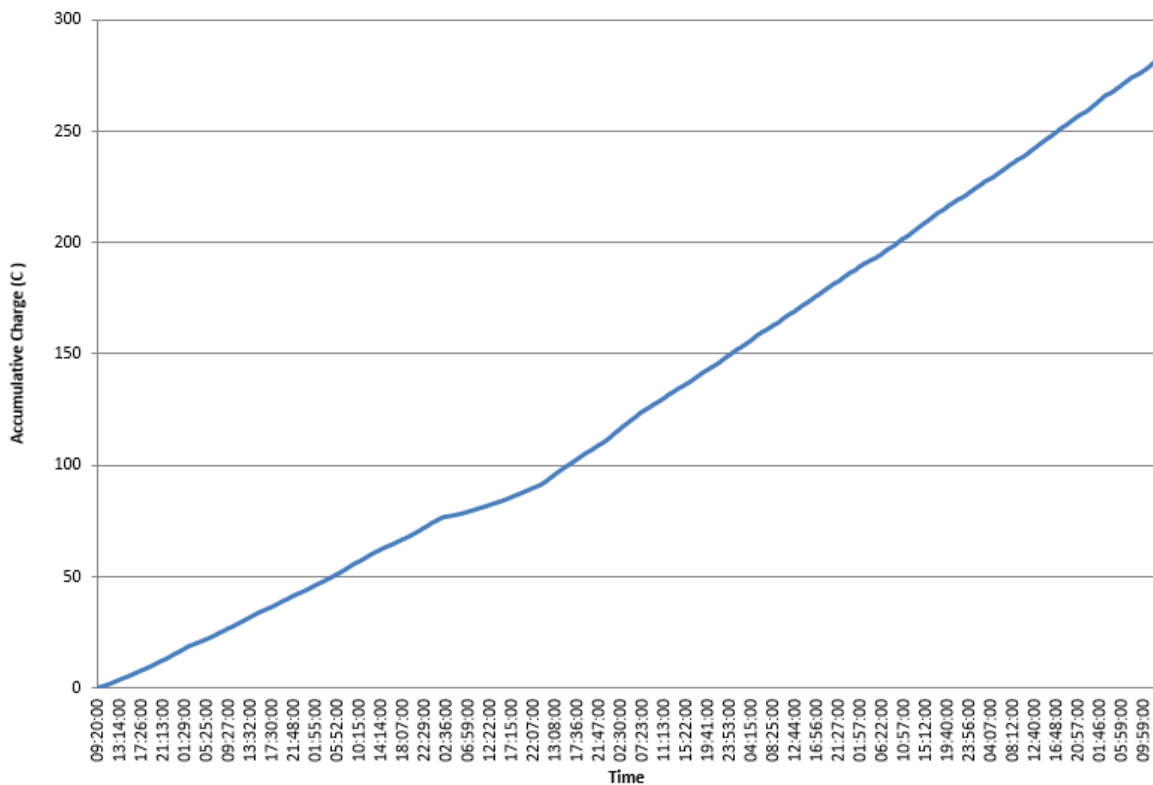


Figure 5-34: Cumulative positive charge

5.5.2 Leakage current performance for RTV-SR test sample 6 in channel 2

According to Figure 5-35, the leakage current remains uniform at 11 mA and 11.2 mA during the first day of the tests. As the test progressed, the leakage current fluctuated slightly between 10.2 mA and 10.5 mA, then increased to a stable level of 12.2 mA. The results seem consistent with those of Limbo (2009, p.138), who performed much longer tests but found similar results (see Figure 5-36). Leakage current fluctuations could be due to partial discharges on the insulator’s surface, as well as arcs across dry bands on the insulator’s surface (see § 5.4.1 above for leakage further explanation).

These unstable arc discharges caused erosion at the insulator surface. According to Heger (2009) and Elombo (2012), this led to dry-band arcing, one of the main causes of ageing in non-ceramic insulators.

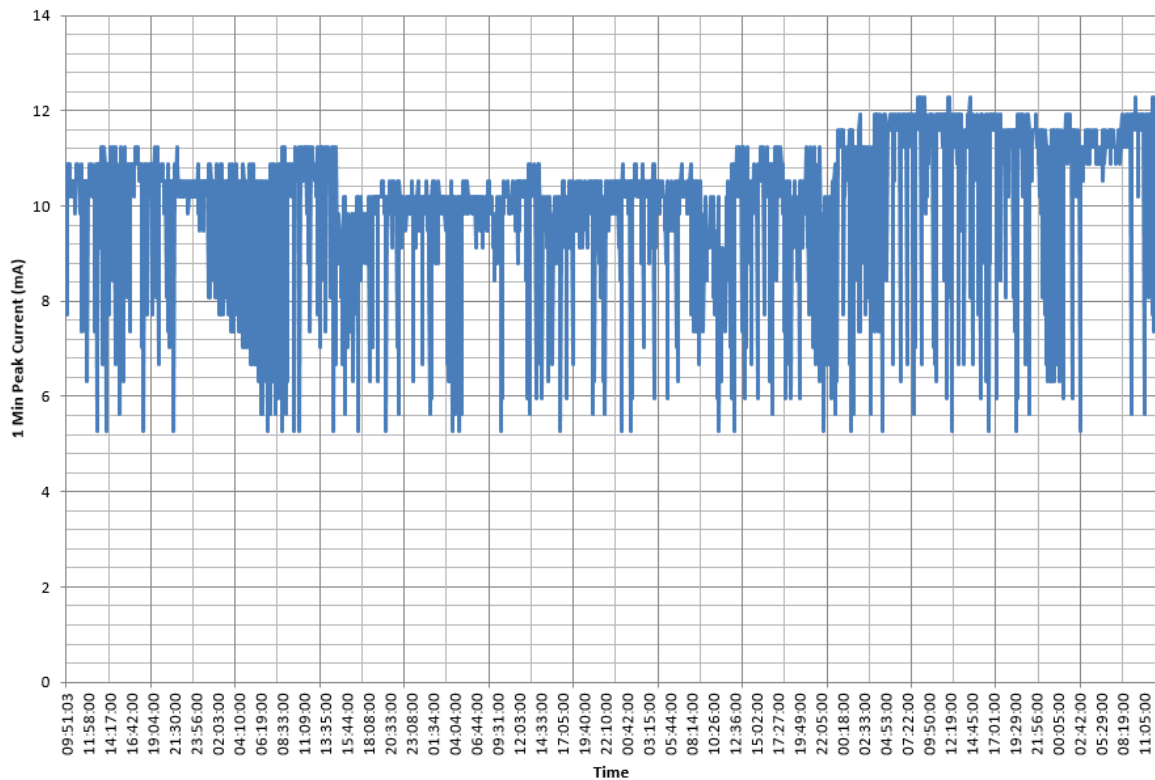


Figure 5-35: DC+ 1-minute peak current

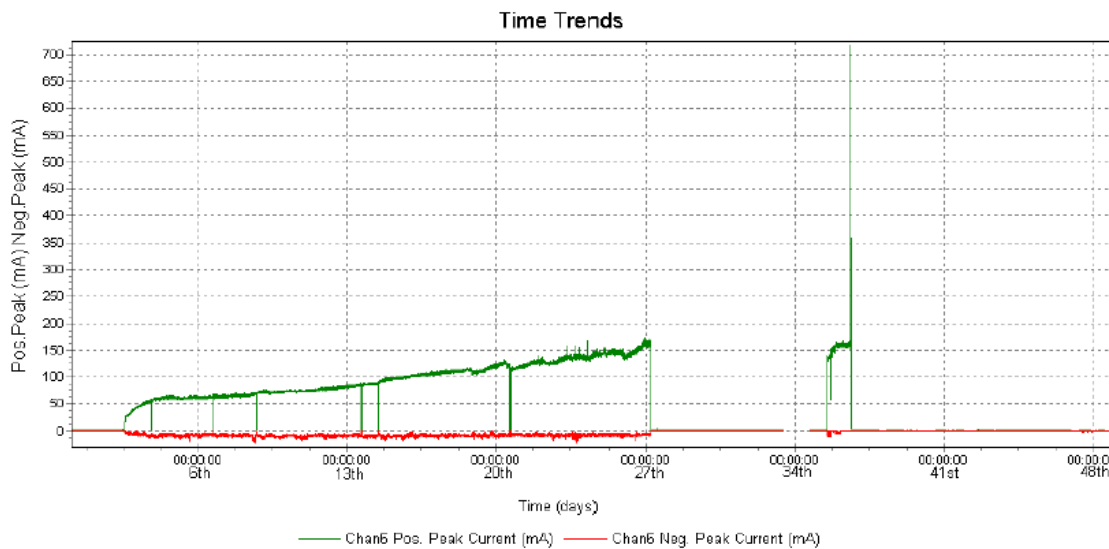


Figure 5-36: Peak current for the RTV-SR coated porcelain insulator (channel 6) for positive polarity HVDC excitation (Limbo, 2009)

5.5.2.1 Visual observation of ageing on RTV-SR test sample 6 in channel 2

At the end of the test, tracking and erosion, burn marks were observed on the surface of the test sample and towards the high-voltage side. Discolouration and pollution build-up on the surface of the test sample was on the surface. These observations are presented in Figure 5-37 below.



Figure 5-37: Black marks, burn marks on glassy carbon electrode, discoloration, and pollution on RTV-SR test sample

Material tracking and erosion in the HTV-SR test sample 6 are caused by localised heat generated by the discharges during the test. Material tracking and erosion can occur due to the dry-band discharges on insulating surfaces (Schmidt *et al.* 2010). According to Macey *et al.* (2004), silicone rubber is a polymeric material with a poor ability to resist electrical tracking and erosion. Further, researchers such as Macey *et al.* (2004) and Thomazini *et al.* (2012) suggests that tracking and erosion are exacerbated if the housing material is exposed to solar ultraviolet (UV) radiation when the insulators are outdoors.

Discolouration on the surface of polymer insulators can occur due to cyclisation (a process that limits the degree of polymerization of their intramolecular structure) and high electrical voltages in combination with other stresses (Ullah *et al.* 2020).

5.5.2.2 Overview of hydrophobicity classification

After the 6-day test, a reduction in hydrophobicity was observed for the sample tested under DC+ excitation. Figure 5-38 illustrates the hydrophobicity classification (HC) percentage given for each test sample. Most of the surface is covered by discrete droplets corresponding to HC1 (0-20%), and therefore the test sample is considered highly hydrophobic.

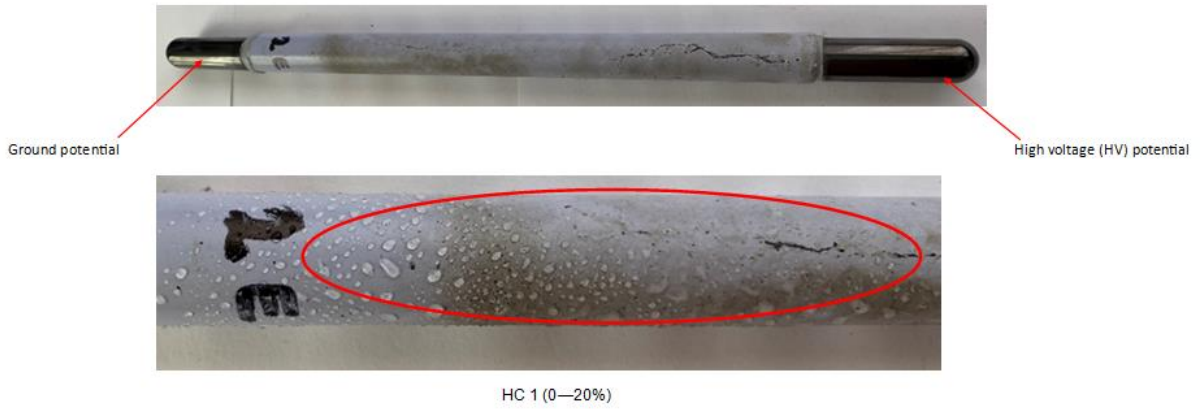


Figure 5-38: Hydrophobicity of the RTV-SR sample 6

5.5.2.3 Cumulative electrical charge

The cumulative electric charge for the HTV-SR test sample 3 tested under DC+ excitation for six days is presented below. Figure 5-39 indicates that the slope of the cumulative electric charge graph has a slight drop in it at the 35- and 110-coulomb levels. This may be attributed to fluctuations in the leakage current and dry band formation on the surface of the test sample. This raises questions about the saline solution distribution on the surface of the insulator and the stresses that the sample was subjected to. The positive cumulative electrical charge flowing over the surface of the insulator reached approximately 135 coulomb over six days or 144 hours of testing.

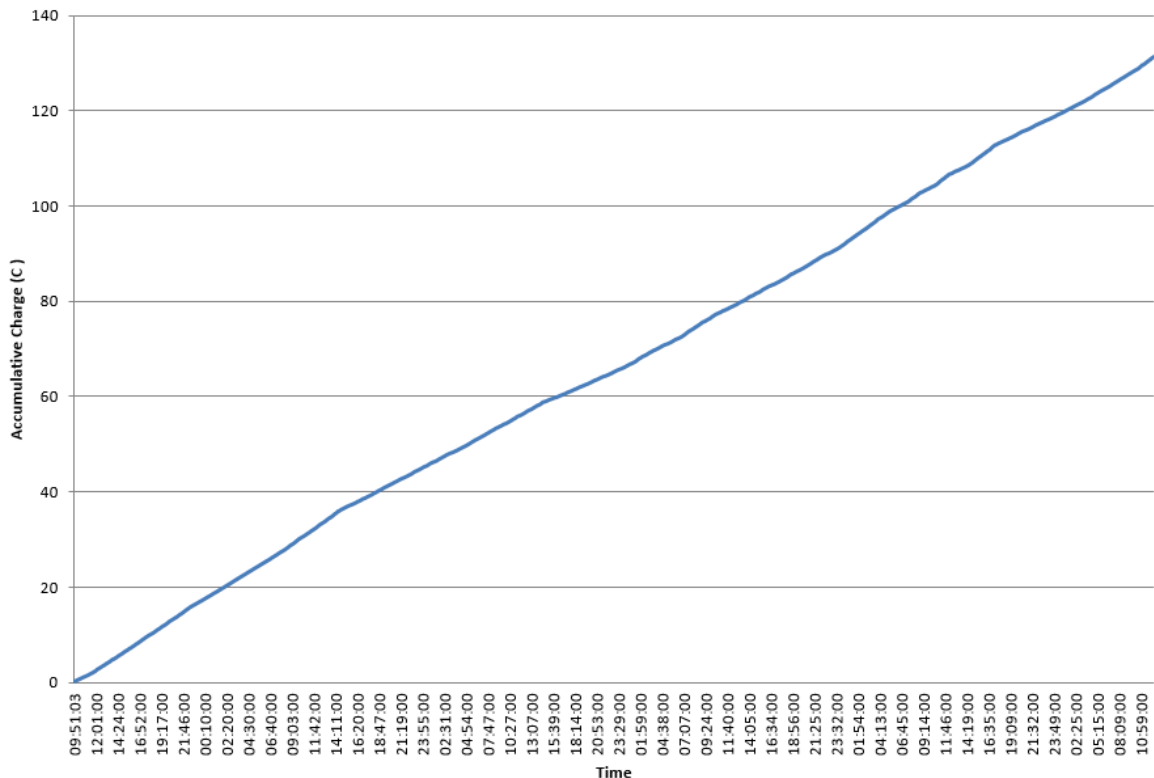


Figure 5-39: Cumulative positive charge

5.5.3 Leakage current performance for HTV-SR test sample 7 in channel 3

According to Figure 5-40, during the first part of the test, the leakage current fluctuated between 14.2 mA and 15 mA. Later on the third day of the test, the leakage current fluctuated between 15.8 mA and 16 mA before gradually increasing to 16.1 mA. Then, a sudden drop in leakage current was observed from 16.1 mA until 9.5 mA. This sudden drop in leakage current could be due to the puncture marks observed on the test samples indicating a faulty connection when the rod was in position 1 (energization), resulting in a high impedance connection point that subsequently caused the leakage current to decrease. Slowly, the situation improved, the connection improved, and the leakage current value was stable at around 13.5 mA. The results seem consistent with those of Elombo (2012, p.115), who performed much longer tests but found similar results (see Figure 5-41). Leakage current fluctuations could be due to partial discharges on the insulator's surface, as well as arcs across dry bands on the insulator's surface (see § 5.4.1 above for further explanation).

These variable arc discharges caused erosion at the insulator surface, which according to Heger (2009) and Elombo (2012), led to dry-band arcing as one of the main causes of ageing in non-ceramic insulators.

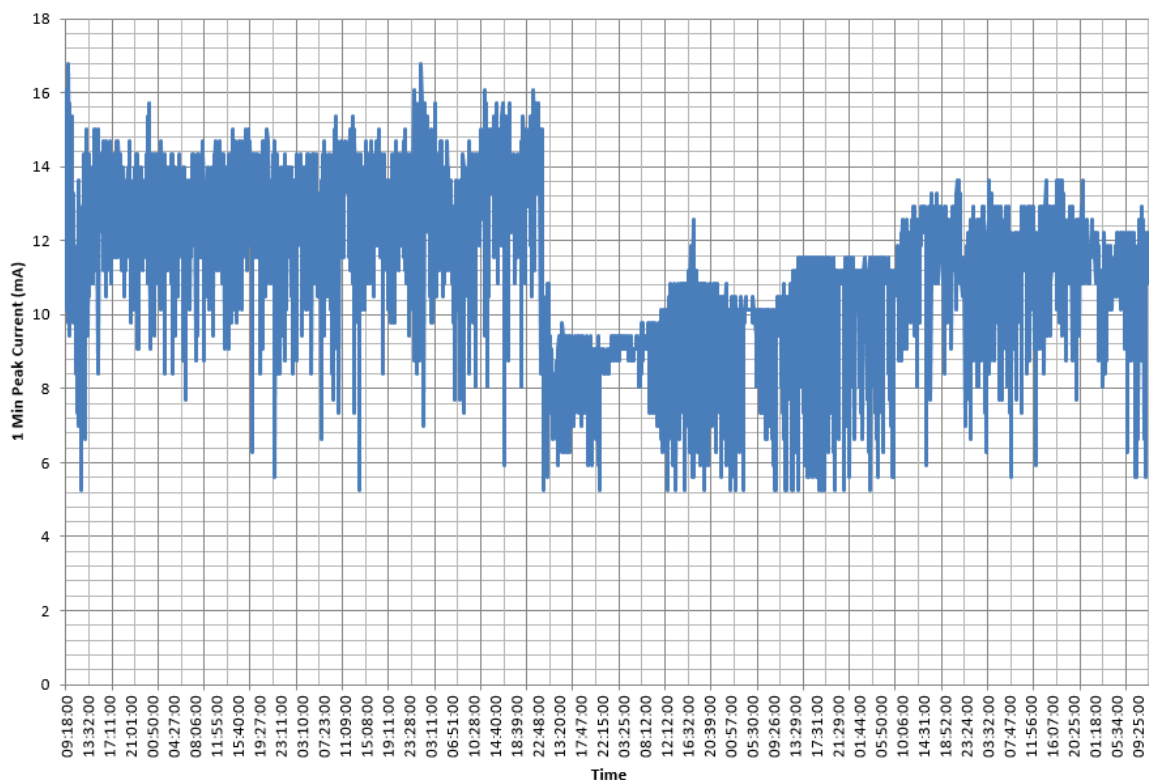


Figure 5-40: DC+ positive 1-minute peak current

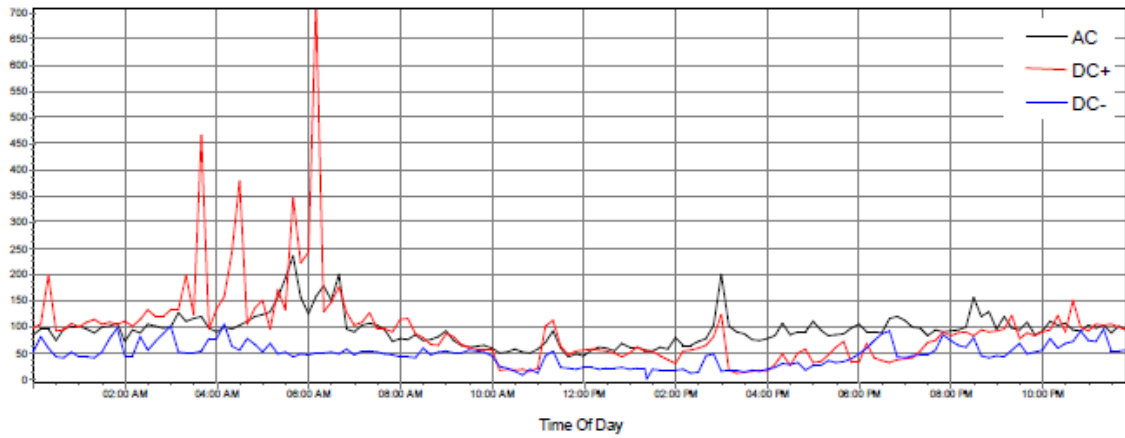


Figure 5-41: The time-of-day maximum absolute peak leakage current profile recorded for all the HTV-SR 29 insulators (Elombo, 2012)

5.5.3.1 Visual observation of ageing on HTV-SR test sample 7 in channel 3

At the end of the test, discolouration and crazing were observed in the ground potential side. Pollution build-up on the surface of the test sample and burn marks over the glassy carbon electrode tip were noted. These observations are presented in Figure 5-42 below.



Dry band activities on the surface



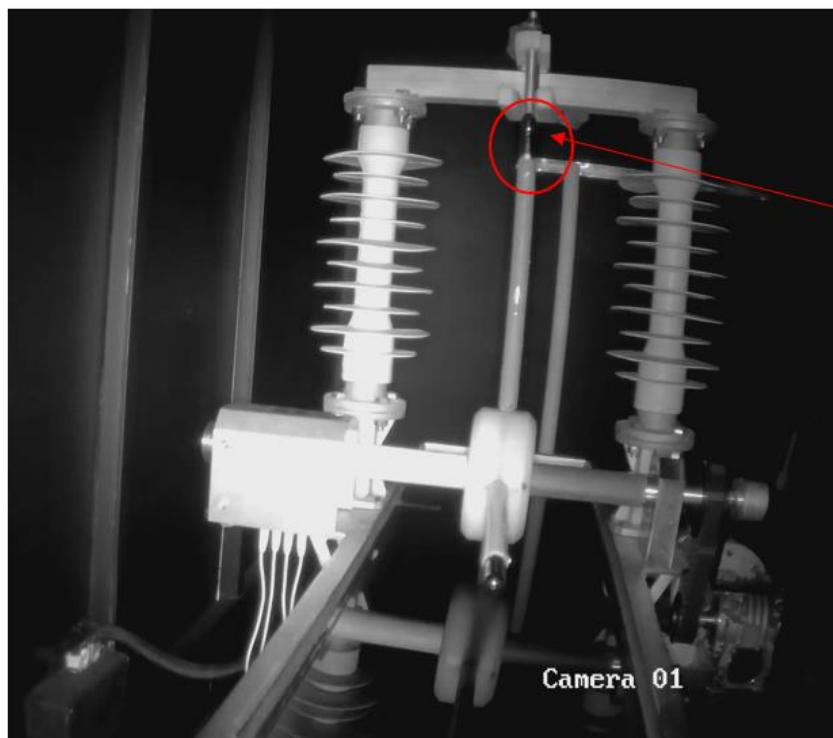
Puncture and burn marks on glassy carbon electrode (HV potential side)



Crazing, material erosion and discoloration



Crack and burn marks on glassy carbon electrode (HV potential side)



Faulty connection resulted in flashover and drop in leakage current

Figure 5-42: Discoloration, tracking, and light erosion and burn marks on a glassy carbon electrode tip observed on HTV-SR test sample

Dry band formation on the HTV-SR test sample 7 indicates discharge activity at the ground potential end. Zhou *et al.* (2010) posit that the formation of the dry bands may influence the distribution of the electric field along the insulator, which leads to partial arcing and flash-over. Dry band arcs and possible flash-over across an insulator are

exacerbated by light rain and high humidity conditions in the field (Kumagai *et al.* 2001; Krzma *et al.* 2015; Nekahi *et al.* 2017; Roman *et al.* 2019).

Electrical activity, coating imperfections on the surface of the test sample, and the saline solution under electrical excitation can be the reason for crazing or cracking on the HTV-SR test sample 5. According to Awaja *et al.* (2016), the rubber particles of the coating can also be responsible for developing multiple cracks, acting as stress concentrates during the craze initiation process. When polymer materials are subjected to stress, they can be deformed by shear yielding, crazing, or cracking (Yarysheva *et al.* 2012).

Material tracking and erosion in the HTV-SR test sample 7 are caused by localised heat generated by the discharges during the test. Material tracking and erosion can occur due to the dry-band discharges on insulating surfaces (Schmidt *et al.* 2010). According to Macey *et al.* (2004), silicone rubber is a polymeric material with a poor ability to resist electrical tracking and erosion. Further, researchers such as Macey *et al.* (2004) and Thomazini *et al.* (2012) suggests that tracking and erosion are exacerbated if the housing material is exposed to solar ultraviolet (UV) radiation when the insulators are outdoors.

Burn marks and puncture marks on the glassy carbon electrode are most likely due to prolonged arcing caused by a faulty connection and possible oxidation at the high-voltage potential side.

5.5.3.2 Overview of hydrophobicity classification

After the 5-day test, a reduction in hydrophobicity was observed for the sample tested under DC+ excitation. Figure 5-43 indicates that there are very few droplets left on the surface of the test sample, which corresponds to HC5 (70-80%). This suggests that the test sample is considered highly hydrophilic. The loss of hydrophobicity in the test sample material may have been caused by the increased electrical stress and discharge activities on the surface (Mouton, 2012).

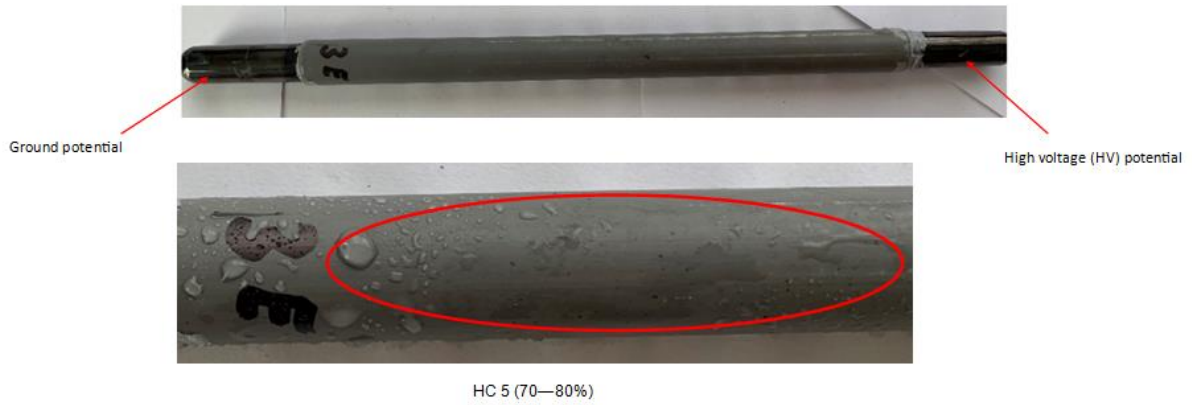


Figure 5-43: *Hydrophobicity of the HTV-SR sample 7*

5.5.3.3 Cumulative electrical charge

The positive cumulative electrical charge flowing over the surface of the insulator reached approximately 250 coulomb over six days or 144 hours of testing. The cumulative electric charge for the HTV-SR test sample 7 tested under DC+ excitation for six days is presented as follows: Figure 5-44 indicates that the initial curve section shows that the Leakage current is almost constant. Because it is known from Figure 5-42 above that at around 22:48, there was a leakage current drop and then a gradual leakage current increase, the slope of the cumulative electric charge graph also increases from that point onward. However, if there were no sudden leakage current drop, the final cumulative value would have been higher. This will have a bearing on the final sample performance assessment since the RTV-SR samples did not have such a problem at the high-voltage terminal.

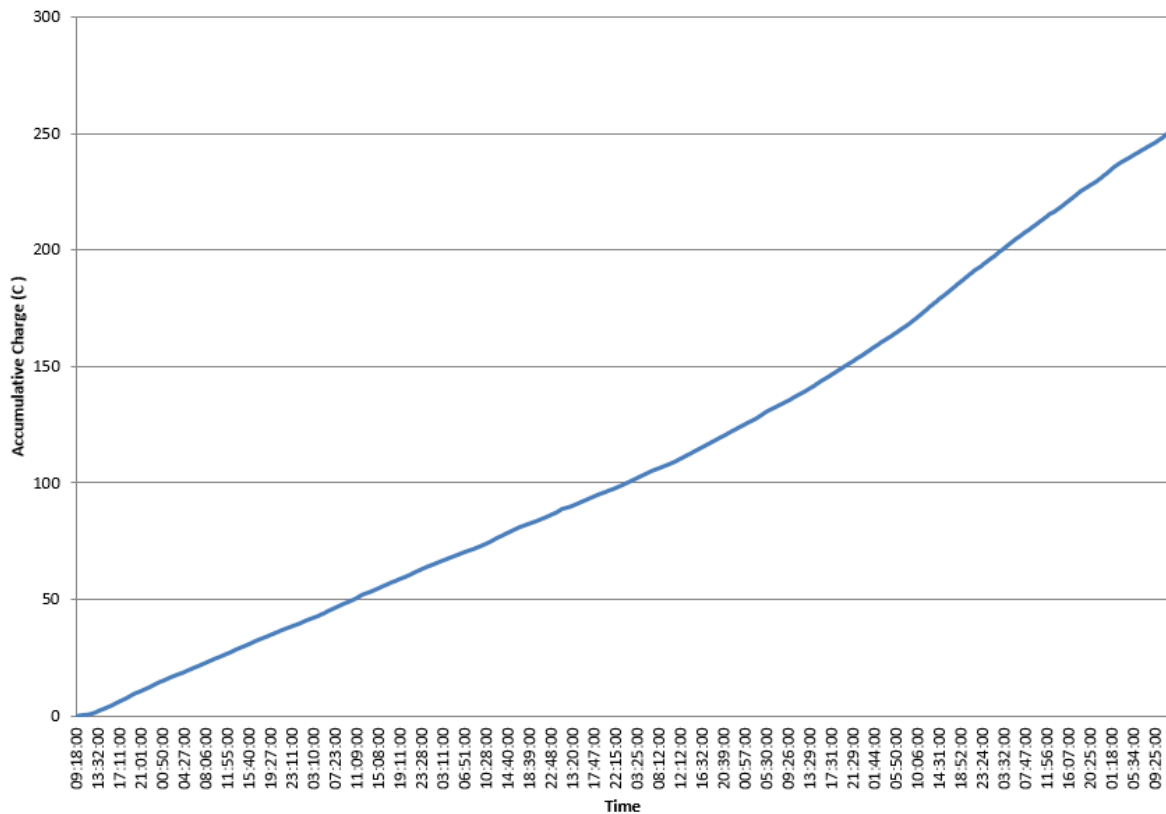


Figure 5-44: Cumulative positive charge

5.5.4 Leakage current performance for RTV-SR test sample 8 in channel 4

According to Figure 5-45, during the first hours of the first day of the DC+ test, the leakage current is high at about 13.5 mA, which means there was very little dry band formation. Then, the leakage current drops to 8.5 mA without burn marks on the HV terminal. This is probably due to dry band formation followed by a gradual increase of the leakage current up to 11.8 mA, which indicates a change in the dry band size. Further, because of the slight variation of the current, the dry band size also varies accordingly. This stable fluctuation between 11 and 11.8 mA was observed at about the 3rd half of the test. The results seem consistent with those of Elombo (2012, p.115), who performed much longer tests but found similar results (see Figure 5-46). Leakage current fluctuations could be due to partial discharges on the insulator’s surface, as well as arcs across dry bands on the insulator’s surface (see § 5.4.1 above for further explanation).

These varying arc discharges caused erosion at the insulator surface, which according to Heger (2009) and Elombo (2012), led to dry-band arcing as one of the main causes of ageing in non-ceramic insulators.

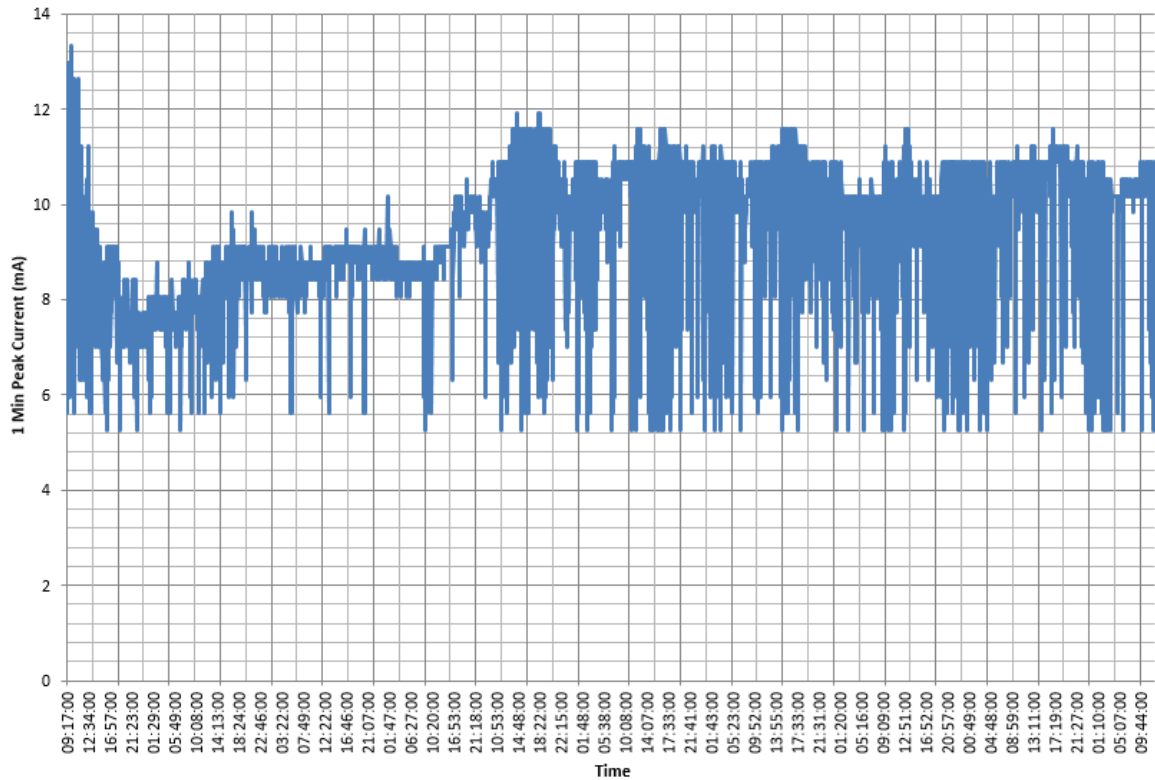


Figure 5-45: DC+ 1-minute peak current

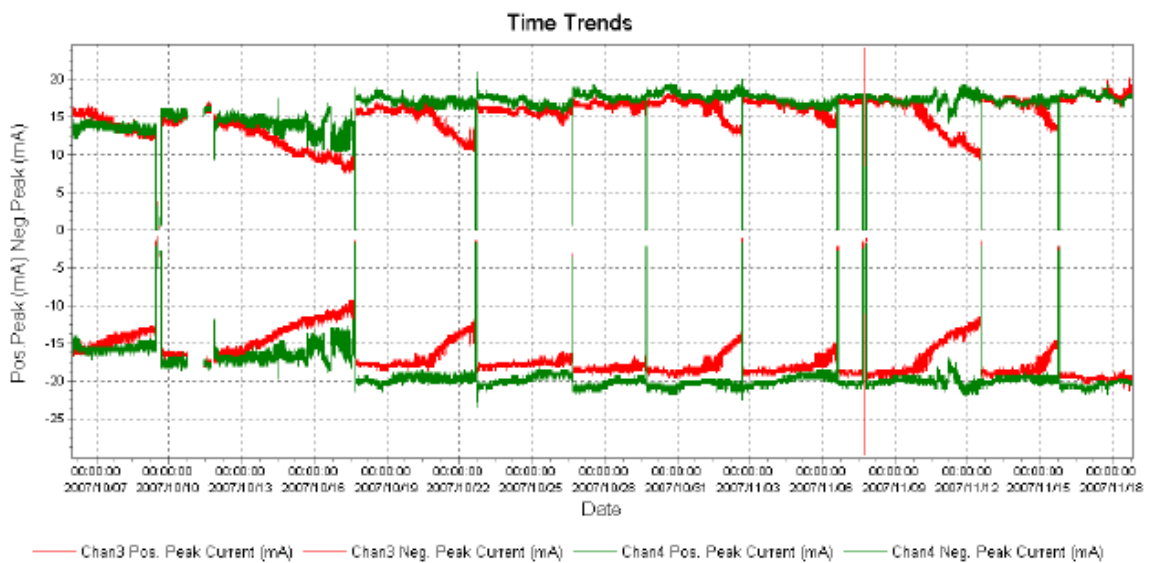


Figure 5-46: Peak leakage currents for the glass and RTV-SR coated glass rods with a creepage distance of 346 mm (Elombo, 2012)

5.5.4.1 Visual observation of ageing on RTV-SR test sample 8 in channel 4

At the end of the test, tracking, erosion and burn marks (which could explain the sudden drop of leakage current at the beginning of the test) were observed on the surface of the test sample towards the high-voltage side. Discolouration and pollution

build-up were also observed on the surface of the test sample. These observations are presented in Figure 5-47 below.



Figure 5-47: Material erosion, pollution, and discolouration on RTV-SR test sample

Material tracking and erosion in the HTV-SR test sample 6 are caused by localised heat generated by the discharges during the test. Material tracking and erosion can occur due to the dry-band discharges on insulating surfaces (Schmidt *et al.* 2010). According to Macey *et al.* (2004), silicone rubber is a polymeric material with a poor ability to resist electrical tracking and erosion. Further, researchers such as Macey *et al.* (2004) and Thomazini *et al.* (2012) suggests that tracking and erosion are exacerbated if the housing material is exposed to solar ultraviolet (UV) radiation when the insulators are outdoors.

Discolouration on the surface of polymer insulators can occur due to cyclisation (a process that limits the degree of polymerization of their intramolecular structure) and high electrical voltages in combination with other stresses (Ullah *et al.* 2020).

5.5.4.2 Overview of hydrophobicity classification

After the 6-day test, a reduction in hydrophobicity was observed for the sample tested under DC+ excitation. Figure 5-48 shows the hydrophobicity classification (HC) percentage given for the test sample. A very small surface section is covered by

discrete droplets corresponding to HC4 (60%), suggesting that the test sample is mostly hydrophilic. The loss of hydrophobicity in the test sample material may have been caused by the increased electrical stress and discharge activities on the surface.



Figure 5-48: *Hydrophilicity of the RTV-SR sample 8*

5.5.4.3 Cumulative electrical charge

The cumulative electric charge for the HTV-SR test sample 8 tested under DC+ excitation for six days is presented as follows: Figure 5-49 indicates that initially, the leakage current values are low (despite the high leakage current at the origin), gradually increasing until the leakage current reaches a higher stable value. The slight dips in the graph may be attributed to fluctuations in the leakage current and dry band formation on the surface of the test sample on those points. This raises questions about the saline solution distribution on the surface of the insulator and the stresses that the sample was subjected to. The positive cumulative electrical charge flowing over the surface of the insulator reached approximately 275 coulomb over six days or 144 hours of testing.

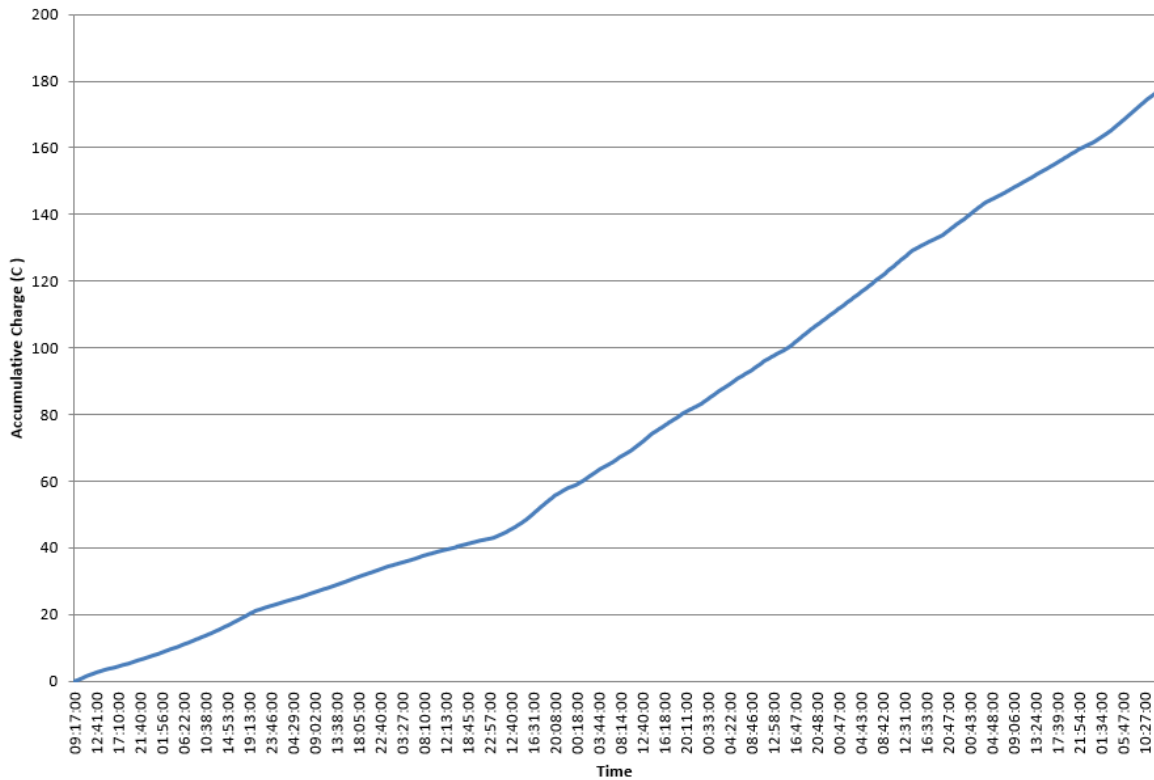


Figure 5-49: Cumulative positive charge

5.5.4.4 Overall DC+ cumulative electrical charge between HTV-SR and RTV-SR

The overall cumulative electric charge for the HTV-SR and RTV-SR test samples tested under DC+ excitation is presented below. The test samples were energised under DC+ excitation for a period of 6-days. The overall cumulative electrical charge of the HTV-SR and RTV-SR test samples are divided into three phases as follows:

Phase 1: At the beginning, there is no distinction in the lines, as they appear close to each other. At this point, it is difficult to distinguish which test sample is performing better. However, later, the lines appear to have reached crossover points. From the onset, it can be noted that RTV-SR sample 8 had a lower leakage current than the other test samples, this need to be investigated further. This is not true for the RTV-SR sample 6.

Phase 2: Lines or paths get quite clear. Crossover points are visible between the HTV-SR sample 5 and RTV-SR sample 6. RTV-SR sample 8 still showed a lower leakage current than other test samples.

Phase 3: Both RTV-SR samples and HTV-SR samples have taken different paths. The inclination or trend for HTV-SR samples 5 and 7 is similar, and because the slope of these lines seems to drop, we can deduce that the leakage current is trending towards stabilization and a lower rate of charge. Further,

the relative average difference in leakage current between RTV-SR and HTV-SR is 30% = $[(250 - 175)/250] \times 100$.

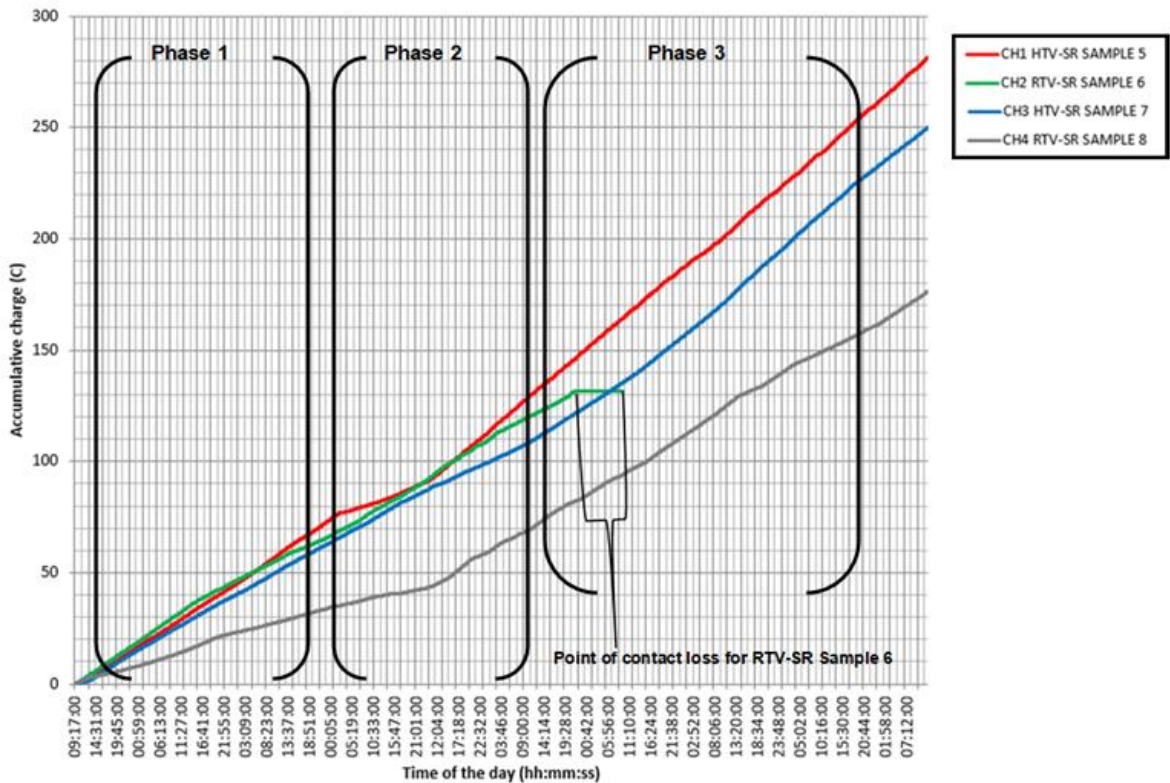


Figure 5-50: Overall cumulative positive electrical charge between HTV-SR and RTV-SR

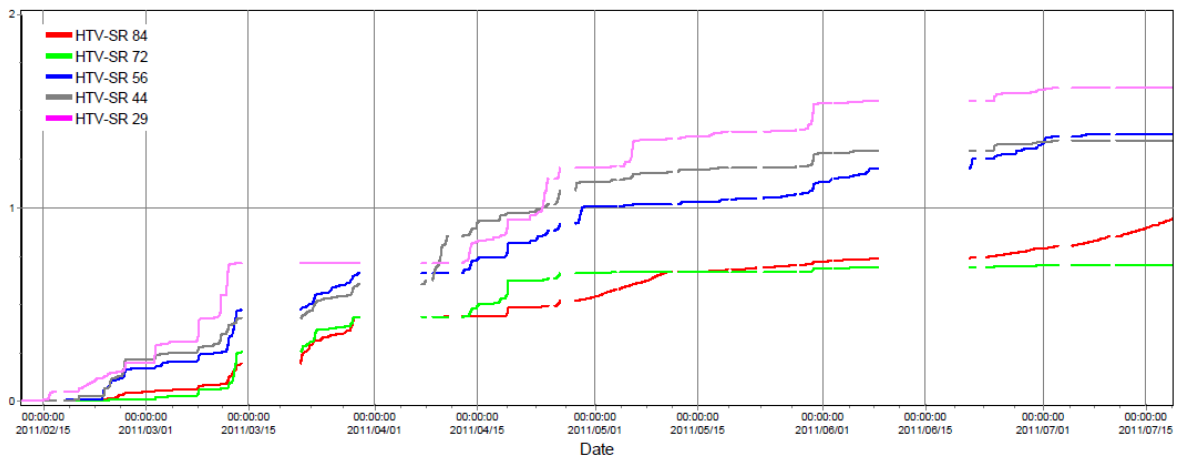


Figure 5-51: Accumulative coulomb-ampere for all the HTV-SR insulators installed on the DC+ excitation voltage (Elombo, 2012)

At 22:00 of day 5, RTV-SR test sample 6 on CH2 lost contact with the HV electrode. As a result, no further measurements were taken. However, since RTV-SR sample 6 could not complete the test, RTV-SR sample 6 was not considered as it was deemed to have failed. The best performing test sample is RTV-SR sample 8 with 175 coulomb,

followed by HTV-SR sample 7 with 250 coulomb. The worst performing test sample is RTV- SR sample 5 with 285 coulomb.

Figure 5-50 above indicates that RTV-SR sample 8 performed better compared to HTV-SR test samples 5 and 7 that had higher cumulative electrical charges. The results seem consistent with those of Elombo (2012, p.121), who performed much longer tests but found similar results (see Figure 5-51). From his results, on the following test samples (HTV-SR 72), similar trends were observed (in the initial section) to the ones tested in our tests in Ch4 RTV-SR sample 8.

5.6 ROTATING WHEEL DIP TEST (RWDT) UNDER DC- EXCITATION (CH1 – CH4)

5.6.1 Leakage current performance for HTV-SR test sample 9 in channel 1

According to Figure 5-52, during the first hours of the first day of the tests, the leakage current is low at about -6 mA. As the test progressed, it fluctuated until it reached a stable position (increasing at a very low rate), after that decreased reaching -7.5 mA, and later slightly increase until getting stable at -12.2 mA.

The results seem consistent with those of limbo (2009, p.107), who performed much longer tests but found similar results (see Figure 5-53). Leakage current fluctuations could be due to partial discharges on the insulator's surface, as well as arcs across dry bands on the insulator's surface (see § 5.4.1 above for further explanation).

These varying arc discharges caused erosion at the insulator surface. According to (Heger, 2009; Elombo, 2012), leakage current (LC) leads to dry-band arcing as one of the main causes of ageing in non-ceramic insulators.

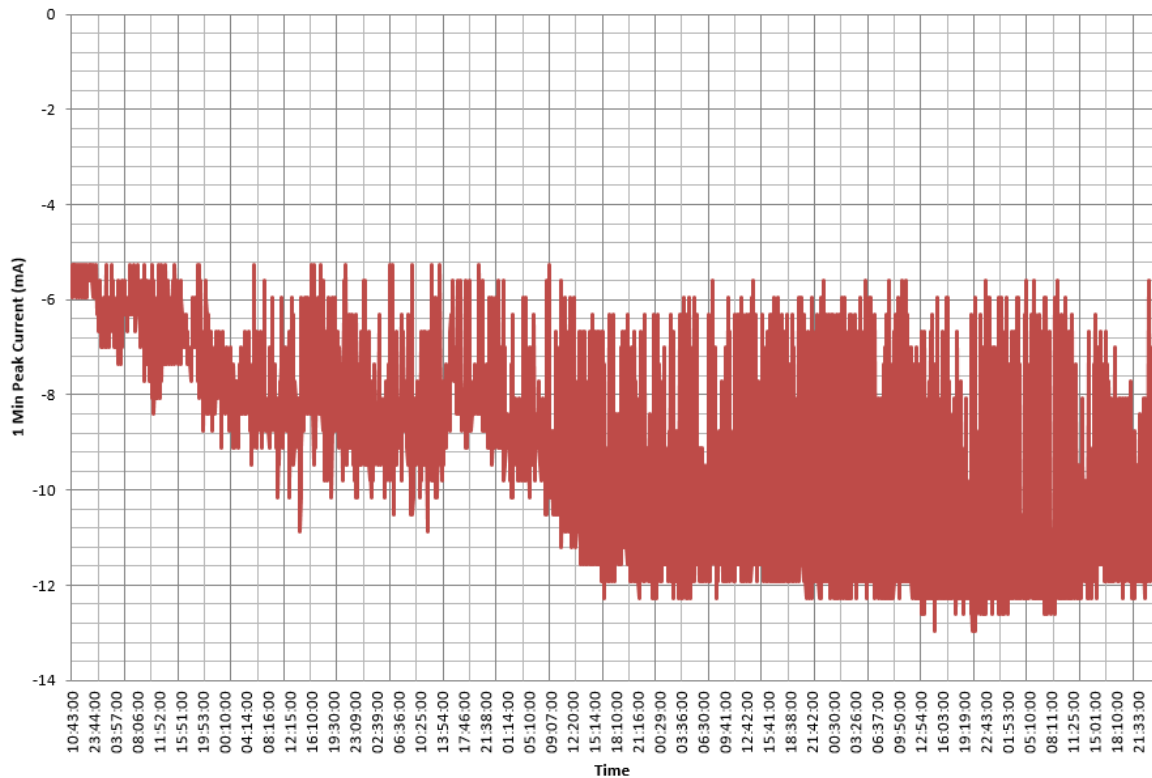


Figure 5-52: DC- 1-minute peak current

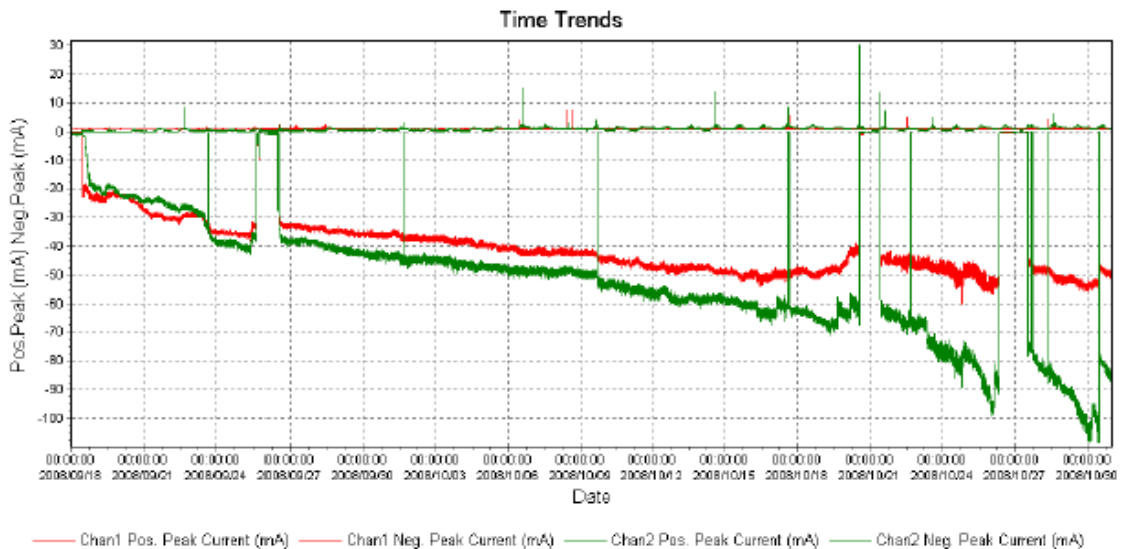


Figure 5-53: Peak leakage currents for the EPDM insulator (Channel 1) and HTV-SR insulator (Channel 2) for negative HVDC negative excitation (Limbo, 2009)

5.6.1.1 Visual observation of ageing on HTV-SR test sample 9 in channel 1

At the end of the test, tracking, erosion, crazing and burn marks (which could explain the sudden drop of leakage current at the beginning of the test) were observed on the surface of the test sample towards the high-voltage side. Discolouration and pollution

build-up were also observed on the surface of the test sample. These observations are presented in Figure 5-54 below.



Figure 5-54: Discoloration, material erosion, crazing and dark pollution/contamination build-up on the HTV-SR test sample

Material tracking and erosion in the HTV-SR test sample 9 are caused by localised heat generated by the discharges during the test. Material tracking and erosion can occur due to the dry-band discharges on insulating surfaces (Schmidt *et al.* 2010). According to Macey *et al.* (2004), silicone rubber is a polymeric material with a poor ability to resist electrical tracking and erosion. Further, researchers such as Macey *et al.* (2004) and Thomazini *et al.* (2012) suggests that tracking and erosion are exacerbated if the housing material is exposed to solar ultraviolet (UV) radiation when the insulators are outdoors.

Dark pollution/contamination build-up around a discolouration area can be associated with different contaminant deposits during testing, such as dirt left over from water tank cleaning. According to Ramos *et al.* (2006), pollution is one of the main causes of insulator breakdown. Insulators start to fail when airborne pollutants settle on the surface of the insulators and combine with moisture from fog, rain, or dew. Pollution

degrades insulators and seriously affects their electrical properties, one of the main causes of insulator failure.

Discolouration on the surface of polymer insulators can occur due to cyclisation (a process that limits the degree of polymerization of their intramolecular structure) and high electrical voltages in combination with other stresses (Ullah *et al.* 2020).

Overview of hydrophobicity classification

After the 6-day test, a reduction in hydrophobicity was observed for the sample tested under DC- excitation. The hydrophobicity classification (HC) percentage given for the test sample is shown in Figure 5-55. Most of the surface is covered by discrete droplets corresponding to HC2 (20-30%), indicating that the test sample is highly hydrophobic.

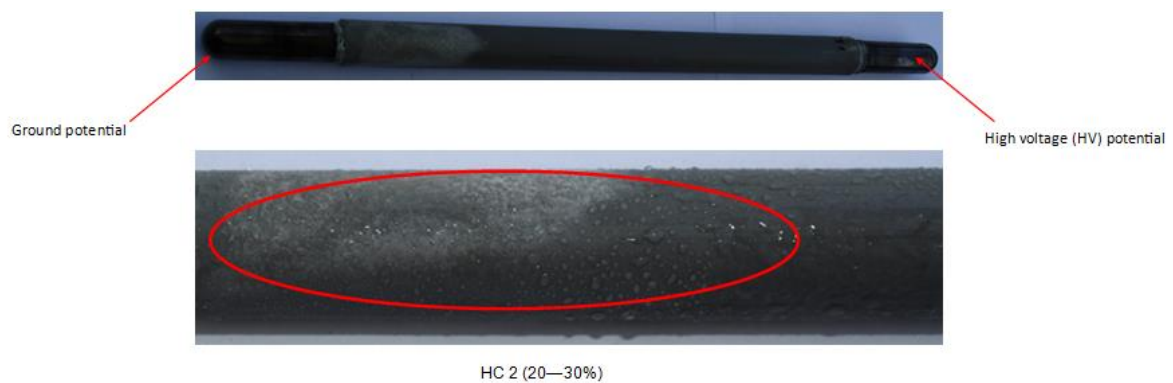


Figure 5-55: Hydrophobicity of the HTV-SR sample 9

5.6.1.2 Cumulative electrical charge

The cumulative electric charge for the HTV-SR test sample 9 tested under DC- excitation for six days is presented as follows: Figure 5-56 indicates that the slope of the cumulative electric charge graph has a slight drop at the 70- and 90-coulomb levels. This may be attributed to dry band formation on the surface of the test sample. This raises questions about the saline solution distribution on the surface of the insulator and the stresses that the sample was subjected to. The positive cumulative electrical charge flowing over the surface of the insulator reached approximately -250 coulomb over six days or 144 hours of testing.

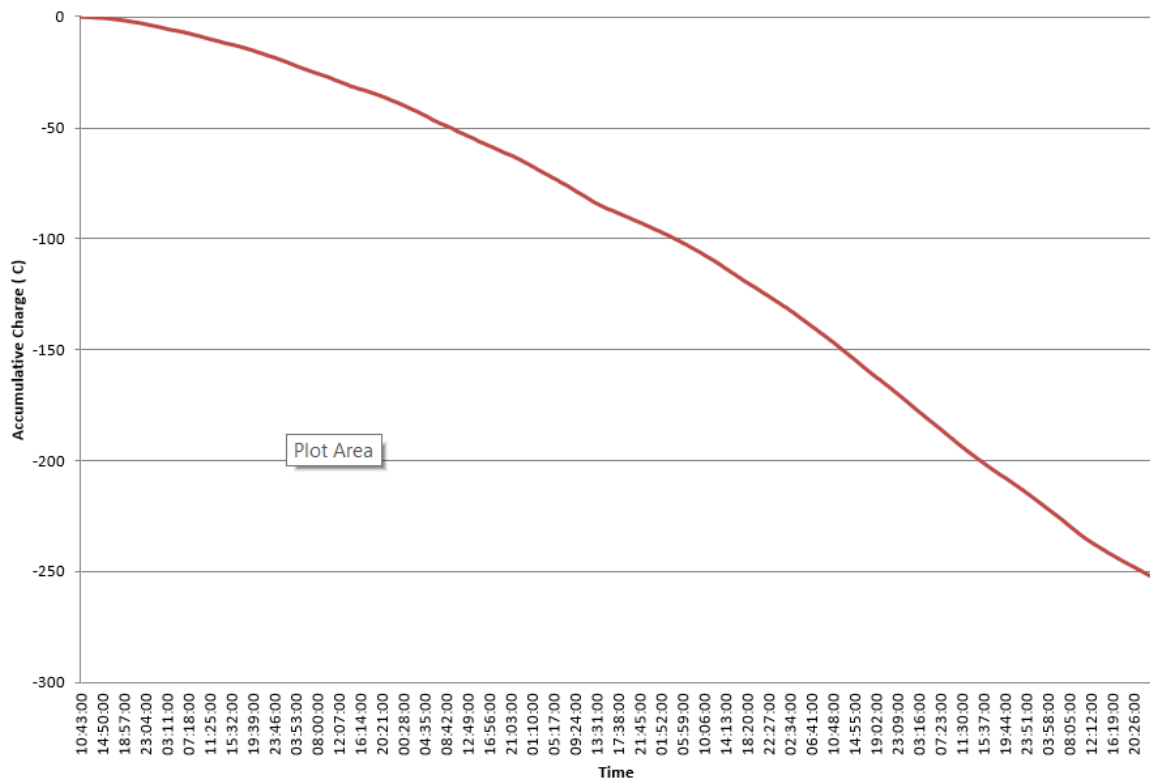


Figure 5-56: Cumulative negative charge

5.6.2 Leakage current performance for RTV-SR test sample 10 in channel 2

According to Figure 5-57, during the first hours of the first day on the tests, the leakage current is somewhat high at about -6 mA before fluctuating until it reached -10.5 mA, after that decreased reaching -6.2 mA, and later slightly increase until getting at stable position (increasing at a very low rate) at -13 mA.

The results seem consistent with those of Limbo (2009, p.123), who performed much longer tests but found similar results (see Figure 5-58). Leakage current fluctuations could be due to partial discharges on the insulator’s surface, as well as arcs across dry bands on the insulator’s surface (see § 5.4.1 above for further explanation).

These unstable arc discharges caused discolouration at the insulator surface. It was impossible to tell whether the discolouration caused UV degradation or electrical stress. Despite this, there was no evidence of electrical discharge activity in the vicinity of the discoloured areas. Therefore, it is hypothesised that chemical changes in the insulator materials could cause them.

These varying arc discharges caused discolouration at the insulator surface. Evidence from Figure 5-57 can be used to show discharge activities on the test samples.

Chemical changes in the insulator materials could also cause discolouration. For dry band formation explanation, refer to § 5.4.1.

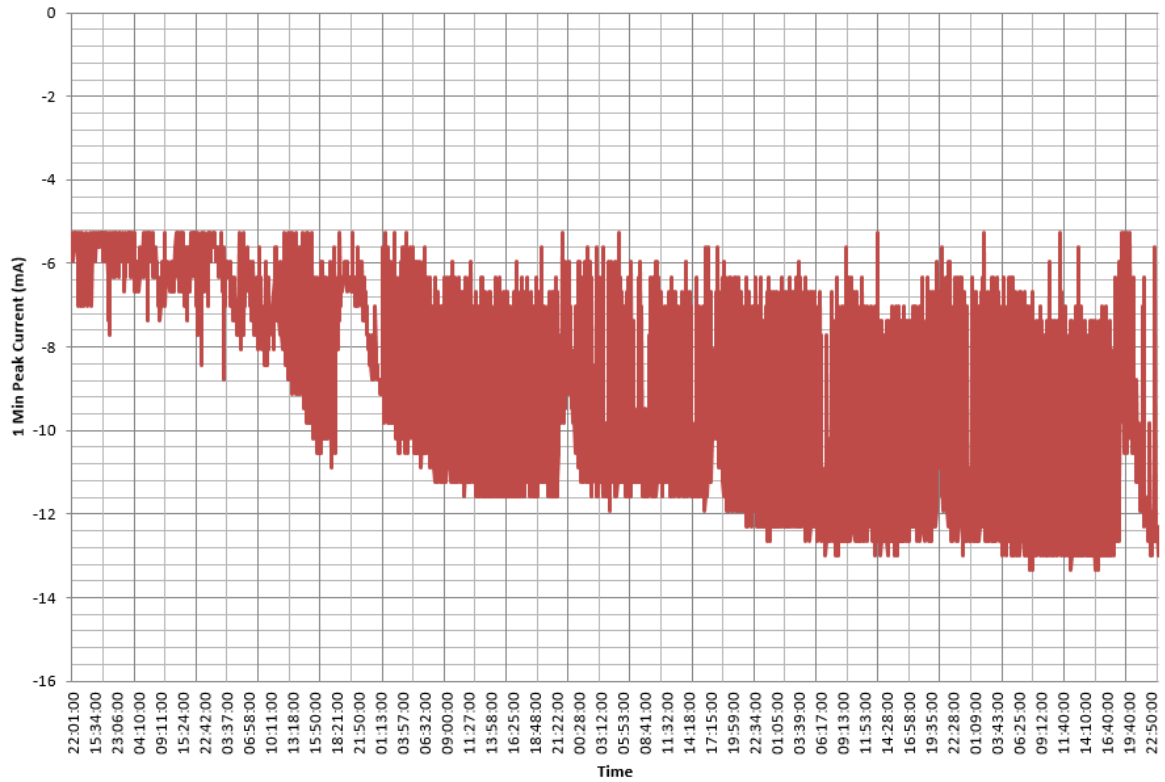


Figure 5-57: DC- 1-minute peak current

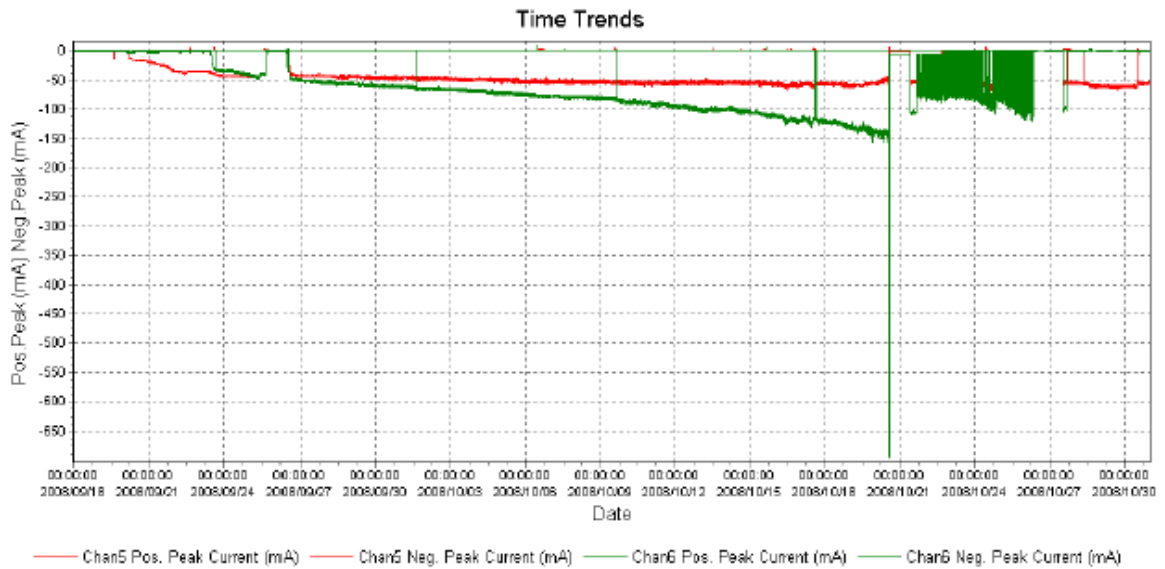


Figure 5-58: Peak leakage currents for the porcelain insulator (Channel 5) and the RTV-SR

5.6.2.1 Visual observation of ageing on RTV-SR test sample 10 in channel 2

At the end of the test, dark pollution was observed on the surface and towards the ground potential side of the test sample. Discolouration and pollution build-up were also observed on the high-voltage potential side. These observations are presented in Figure 5-59 below.

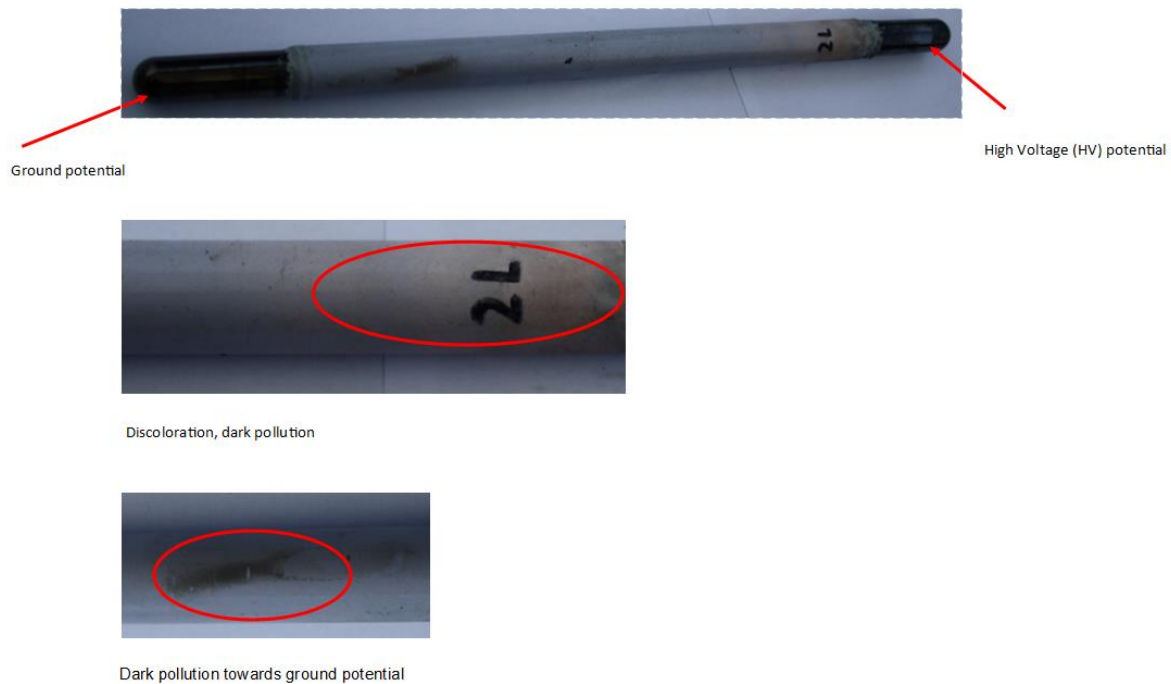


Figure 5-59: Pollution build-up and tracking on RTV-SR test sample

Discolouration on the surface of polymer insulators can occur due to cyclisation (a process that limits the degree of polymerization of their intramolecular structure) and high electrical voltages in combination with other stresses (Ullah *et al.* 2020).

Dark pollution/contamination build-up around a discolouration area can be associated with different contaminant deposits during testing, such as dirt left over from water tank cleaning. According to Ramos *et al.* (2006), pollution is one of the main causes of insulator breakdown. Insulators start to fail when airborne pollutants settle on the surface of the insulators and combine with moisture from fog, rain, or dew. Pollution degrades insulators and seriously affects their electrical properties, one of the main causes of insulator failure

5.6.2.2 Overview of hydrophobicity classification

After the 6-day test, a reduction in hydrophobicity was observed for the sample tested under DC- excitation. The loss of hydrophobicity in the test sample material may have

been caused by the increased electrical stress and discharge activities on the surface. Figure 5-60 shows the hydrophobicity classification (HC) percentage given for the test sample. A very small surface section is covered by discrete droplets corresponding to HC4 (60%), suggesting that the test sample is mostly hydrophilic.

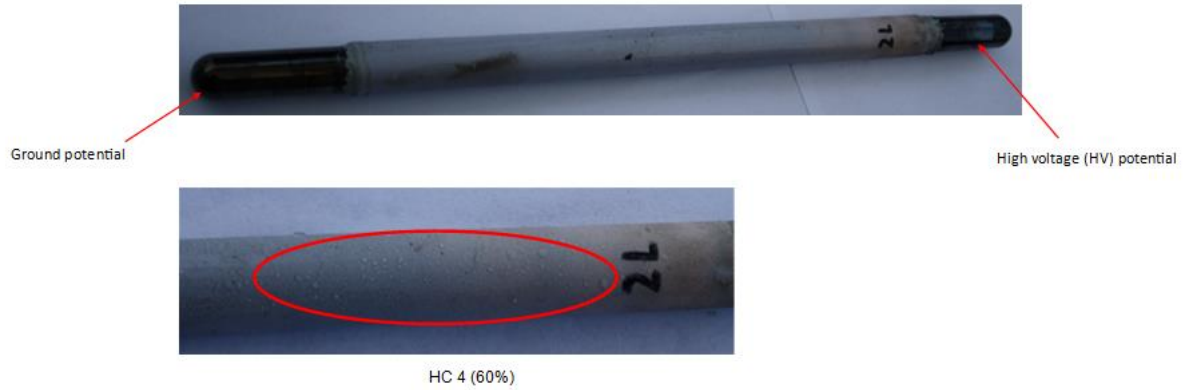


Figure 5-60: Hydrophobicity of the RTV-SR sample 10

5.6.2.3 Cumulative electrical charge

The cumulative electric charge for the HTV-SR test sample 10 tested under DC+ excitation for six days is presented as follows: Figure 5-61 indicates that the slope of the cumulative electric charge graph has a slight drop in it at the 270-coulomb level. This may be attributed to dry band formation on the surface of the test sample. This raises questions about the saline solution distribution on the surface of the insulator and the stresses that the sample was subjected to. The positive cumulative electrical charge flowing over the surface of the insulator reached approximately 275 coulomb over six days or 144 hours of testing.

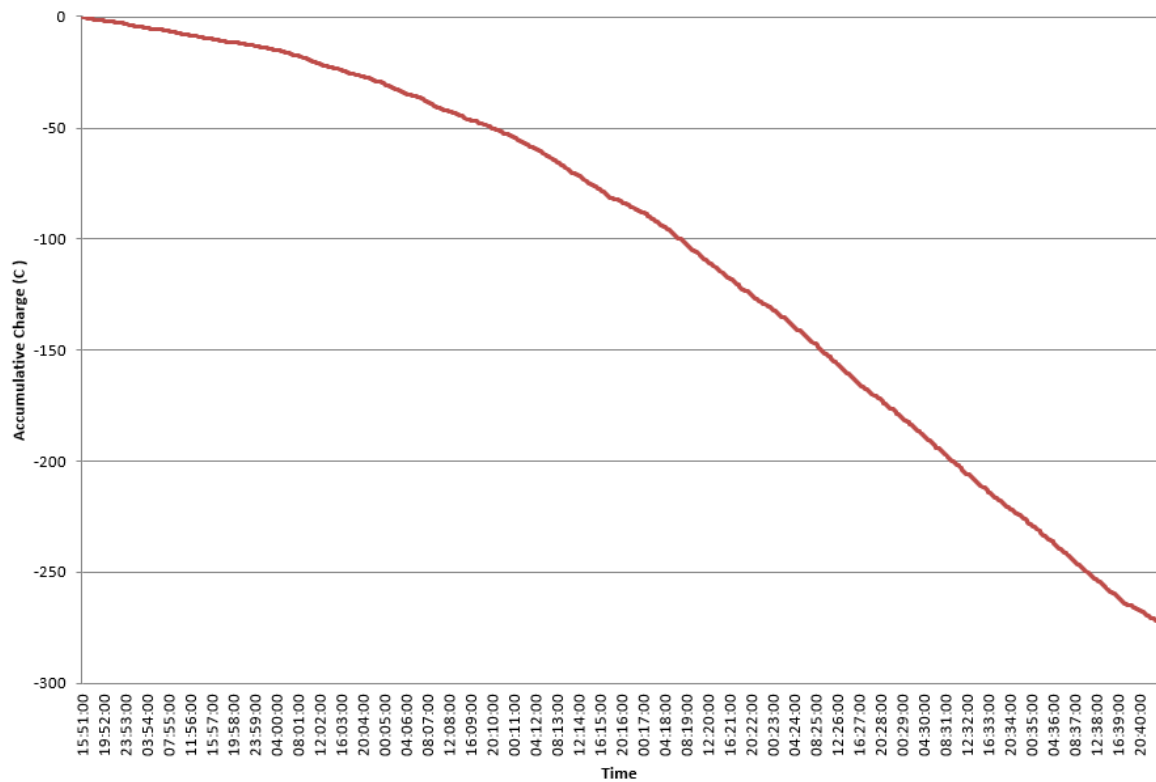


Figure 5-61: Cumulative negative charge

5.6.3 Leakage current performance for HTV-SR test sample 11 in channel 3

According to Figure 5-62, during the first hours of the first day of the tests, the leakage current fluctuated between -8.2 mA and -9.8 mA. After that, it decreased to -6.5 mA and later fluctuated until stable at -12.8 mA.

The results seem consistent with those of limbo (2009, p.123), who performed much longer tests but found similar results (see Figure 5-63). Leakage current fluctuations could be due to partial discharges on the insulator's surface, as well as arcs across dry bands on the insulator's surface (for dry band formation explanation, refer to § 5.4.1 above).

These unstable arc discharges caused erosion at the insulator surface. According to (Heger, 2009; Elombo, 2012), leakage current (LC) leading to dry-band arcing is one of the main causes of aging in non-ceramic insulators.

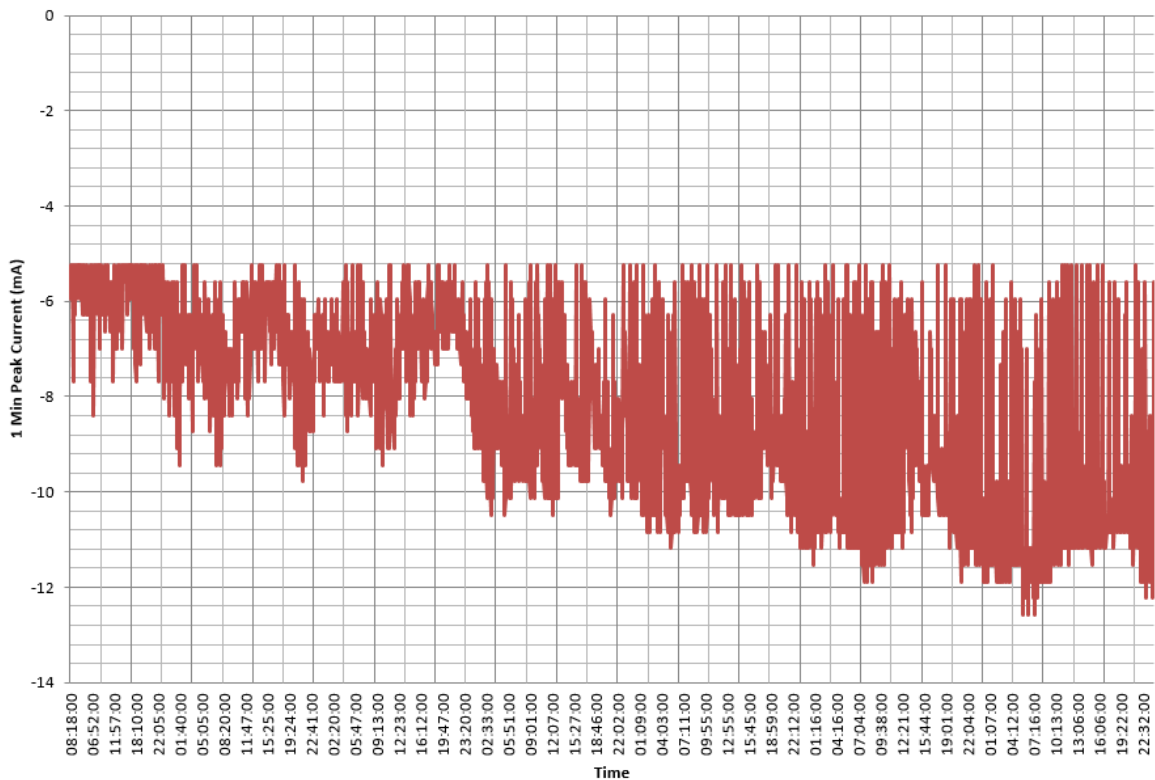


Figure 5-62: DC- 1-minute peak current

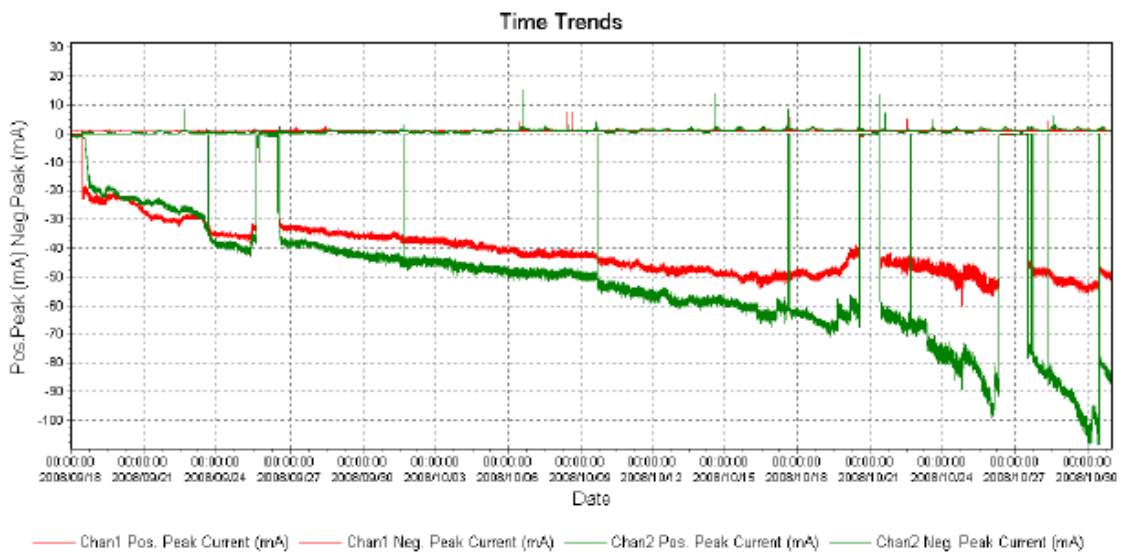


Figure 5-63: Peak leakage currents for the EPDM insulator (Channel 1) and HTV-SR insulator (Channel 2) for negative HVDC negative excitation (Limbo, 2009)

5.6.3.1 Visual observation of ageing on HTV-SR test sample 11 in channel 3

At the end of the test, dry band activities, crazing, material erosion, discolouration around the ground, and the high-voltage potential side of the test sample were observed. These observations are presented in Figure 5-64 below.



Figure 5-64: Dry band activity on HTV-SR test sample

Material tracking and erosion in the HTV-SR test sample 11 are caused by localised heat generated by the discharges during the test. Material tracking and erosion can occur due to the dry-band discharges on insulating surfaces (Schmidt *et al.* 2010). According to Macey *et al.* (2004), silicone rubber is a polymeric material with a poor ability to resist electrical tracking and erosion. Further, researchers such as Macey *et al.* (2004) and Thomazini *et al.* (2012) suggests that tracking and erosion are exacerbated if the housing material is exposed to solar ultraviolet (UV) radiation when the insulators are outdoors.

Discolouration on the surface of polymer insulators can occur due to cyclisation (a process that limits the degree of polymerization of their intramolecular structure) and high electrical voltages in combination with other stresses (Ullah *et al.* 2020).

Dry band formation on the HTV-SR test sample 11 indicates discharge activity at the ground potential end. Zhou *et al.* (2010) posit that the formation of the dry bands may influence the distribution of the electric field along the insulator, which leads to partial arcing and flash-over. Dry band arcs and possible flash-over across an insulator are exacerbated by light rain and high humidity conditions in the field (Kumagai *et al.* 2001; Krzma *et al.* 2015; Nekahi *et al.* 2017; Roman *et al.* 2019).

3.1.1.1. Overview of hydrophobicity classification

After the 65-day test, a reduction in hydrophobicity was observed for the sample tested under DC- excitation. Figure 5-65 shows the hydrophobicity classification (HC) percentage given for the test sample. A very small surface section is covered by discrete droplets corresponding to HC4 (60%), suggesting that the test sample is mostly hydrophilic. The loss of hydrophobicity in the test sample material may have been caused by the increased electrical stress and discharge activities on the surface.

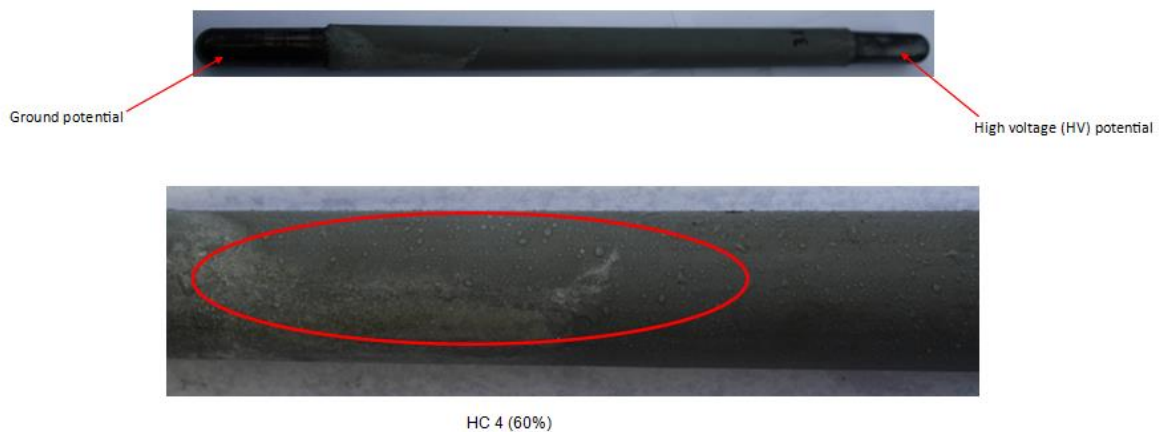


Figure 5-65: Hydrophilicity of the HTV-SR sample 11

5.6.3.2 Cumulative electrical charge

The cumulative electric charge for the HTV-SR test sample 11 tested under DC- excitation for six days is presented as follows: Figure 5-66 indicates that the slope of the cumulative electric charge graph has a slight drop 40-coulomb level. This may be attributed to fluctuations in the leakage current and dry band formation on the surface of the test sample. This raises questions about the saline solution distribution on the surface of the insulator and the stresses that the sample was subjected to. The positive cumulative electrical charge flowing over the surface of the insulator reached approximately -245 coulomb over six days or 144 hours of testing.

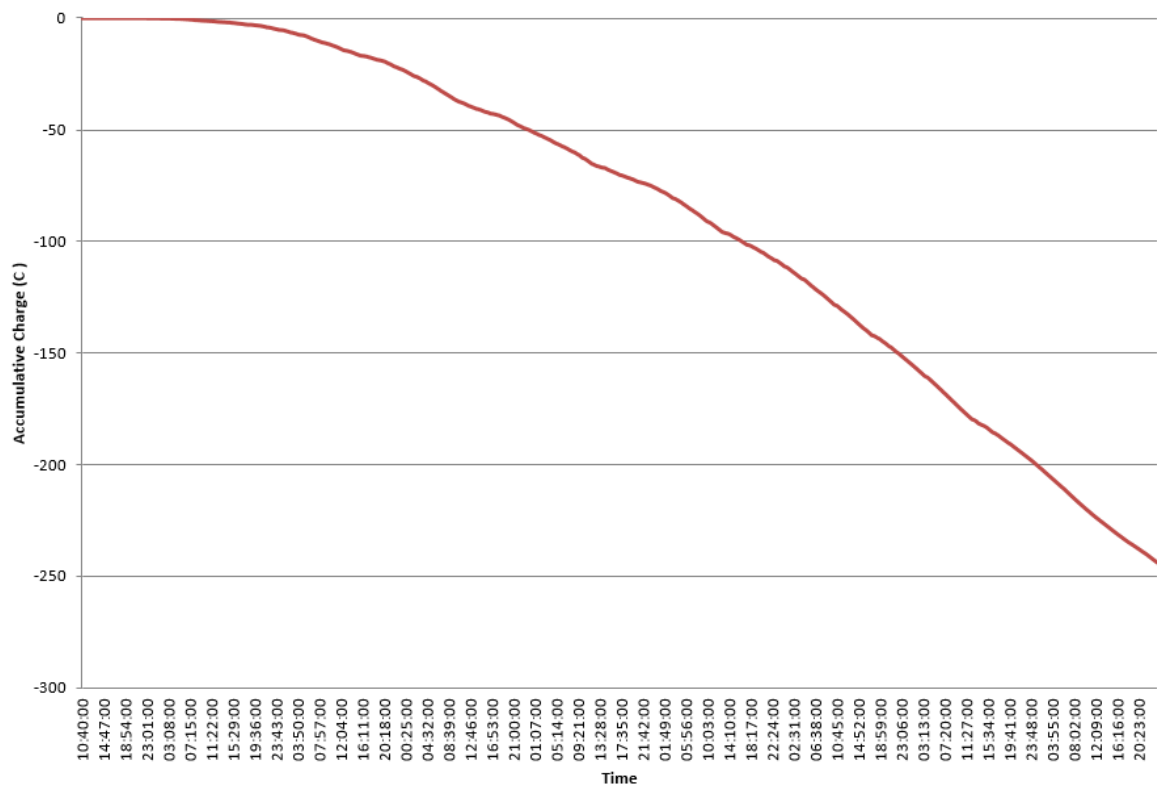


Figure 5-66: Cumulative negative charge

5.6.4 Leakage current performance for RTV-SR test sample 12 in channel 4

According to Figure 5-67, during the first hours of the day on the tests, the leakage current was somewhat high at about -6.2 mA before fluctuating until it reached -8.2 mA. After that, it decreased, reaching -6.2 mA, and later slightly fluctuating until it reached a stable position (increasing at a very low rate) at -13 mA.

The results seem consistent with those of Limbo (2009, p.123), who performed much longer tests but found similar results (see Figure 5-68). Leakage current fluctuations could be due to partial discharges on the insulator’s surface and arcs across dry bands on the insulator’s surface (for dry band formation explanation, refer to § 5.4.1).

These unstable arc discharges caused discolouration at the insulator surface. Discolouration could also be caused by chemical changes in the insulator materials. Evidence from Figure 5-69 can be used to show discharge activities on the test samples.

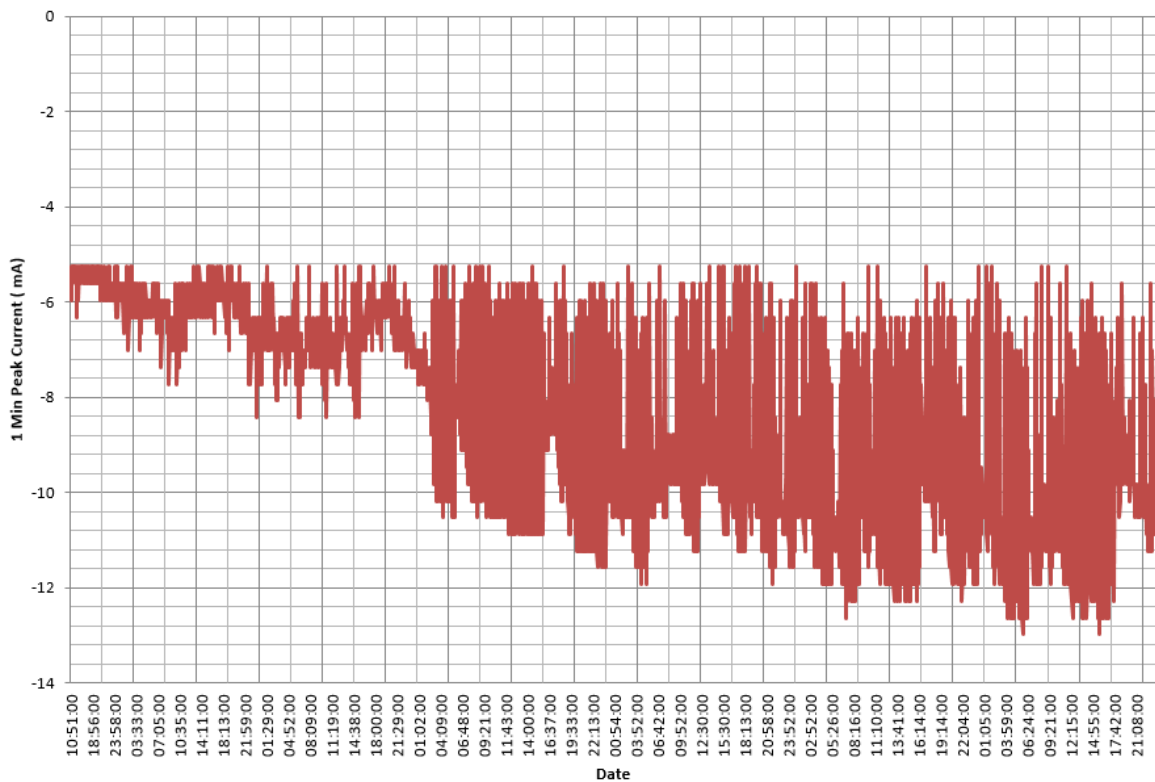


Figure 5-67: DC- negative 1-minute peak current

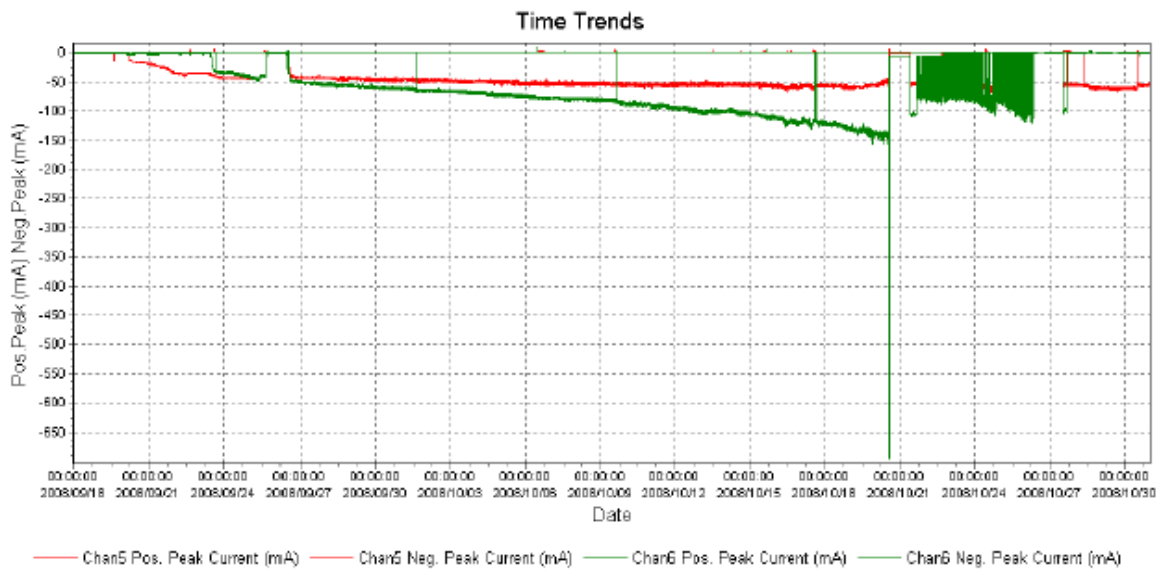


Figure 5-68: Peak leakage currents for the porcelain insulator (Channel 5) and the RTV-SR (Limbo, 2009)

5.6.4.1 Visual observation of ageing on HTV-SR test sample 12 in channel 4

At the end of the test, dark pollution and discolouration around the high-voltage potential side of the test sample were observed. These observations are presented in Figure 5-69 below.



Figure 5-69: Discolouration, burn marks and pollution observed on an RTV-SR test sample

Dark pollution/contamination build-up around a discolouration area can be associated with different contaminant deposits during testing, such as dirt left over from water tank cleaning. According to Ramos *et al.* (2006), pollution is one of the main causes of insulator breakdown. Insulators start to fail when airborne pollutants settle on the surface of the insulators and combine with moisture from fog, rain, or dew. Pollution degrades insulators and seriously affects their electrical properties, one of the main causes of insulator failure

Discolouration on the surface of polymer insulators can occur due to cyclisation (a process that limits the degree of polymerization of their intramolecular structure) and high electrical voltages in combination with other stresses (Ullah *et al.* 2020).

5.6.4.2 Overview of wettability (hydrophobicity) classification

After the 6-day test, a reduction in hydrophobicity was observed for the sample tested under DC- excitation. Figure 5-70 shows the hydrophobicity classification (HC) percentage given for the test sample. A very small surface section is covered by discrete droplets corresponding to HC4 (60%), suggesting that the test sample is mostly hydrophilic. The loss of hydrophobicity in the test sample material may have been caused by the increased electrical stress and discharge activities on the surface.

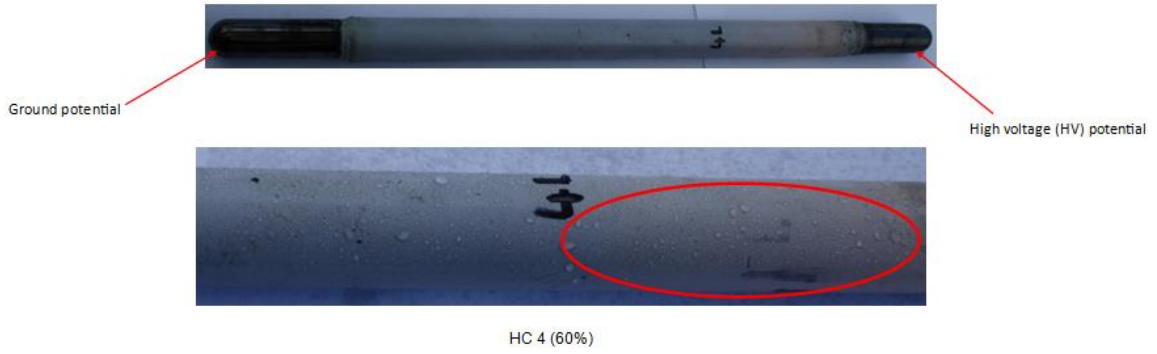


Figure 5-70: Hydrophilicity of the HTV-SR sample 12

5.6.4.3 Cumulative electrical charge

The cumulative electric charge for the RTV-SR test sample 12 tested under DC-excitation for six days is presented as follows: Figure 5-71 indicates that the slope of the cumulative electric charge graph has a slight drop in it at the -60-coulomb level. This may be attributed to fluctuations in the leakage current and dry band formation on the surface of the test sample. This raises questions about the saline solution distribution on the surface of the insulator and the stresses that the sample was subjected to. The positive cumulative electrical charge flowing over the surface of the insulator reached approximately -225 coulomb over six days or 144 hours of testing.

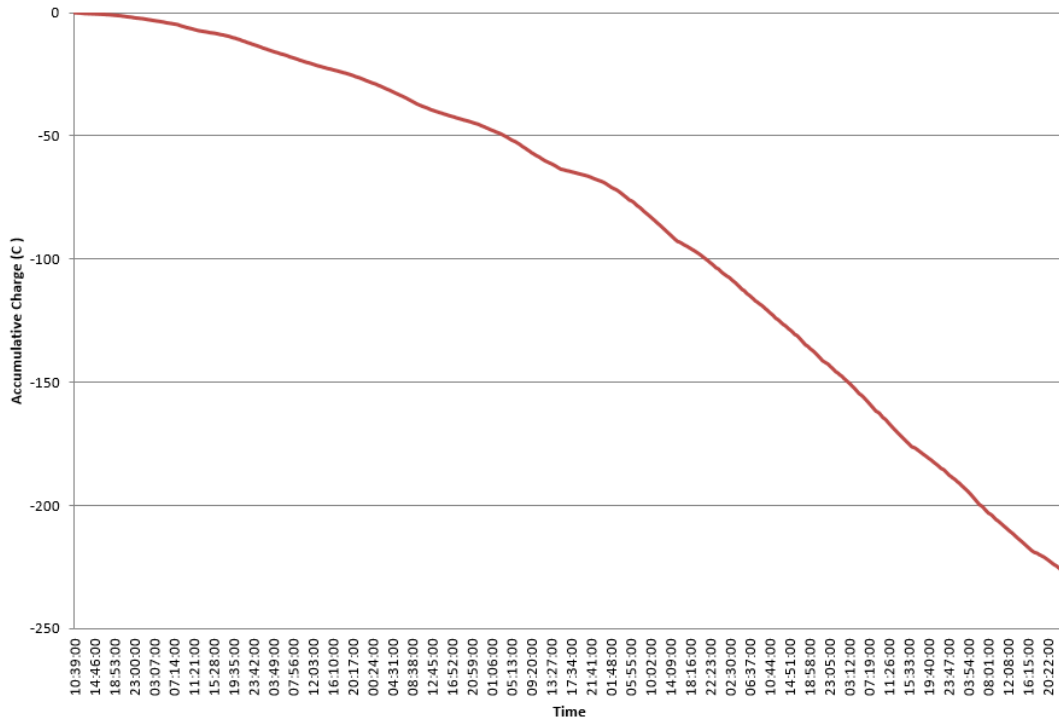


Figure 5-71: Cumulative negative charge

5.6.4.4 Overall DC- cumulative electrical charge between HTV-SR and RTV-SR

The overall cumulative electric charge for the HTV-SR and RTV-SR test samples tested under DC- excitation is presented below. The test samples were energised under DC- excitation for six days. The overall cumulative electrical charge of the HTV-SR and RTV-SR test samples are divided into three phases as follows:

Phase 1: At the beginning, there is no difference in the lines as they appear to be close to each other and at this point, it is difficult to distinguish which test sample is performing better. However, the lines later appeared to have crossover points between HTV-SR sample 9 and RTV-SR sample 10, which were later separated.

Phase 2: Initially, HTV-SR sample 9 and RTV-SR sample 10 had no crossover points but later did have crossover points. It is the other way around for HTV-SR sample 11 and RTV-SR sample 12 as there are crossover points at the beginning, and later the paths were separated.

Phase 3: Lines or paths remain quite clear, and no crossover points are visible until the end of the test. However, the slope of these lines seems to drop. One can deduce that the leakage current is trending towards stabilization and a lower charge rate. Further, the relative average difference in leakage current between RTV-SR and HTV-SR is $17.1\% = [(275 - 228)/275] \times 100$.

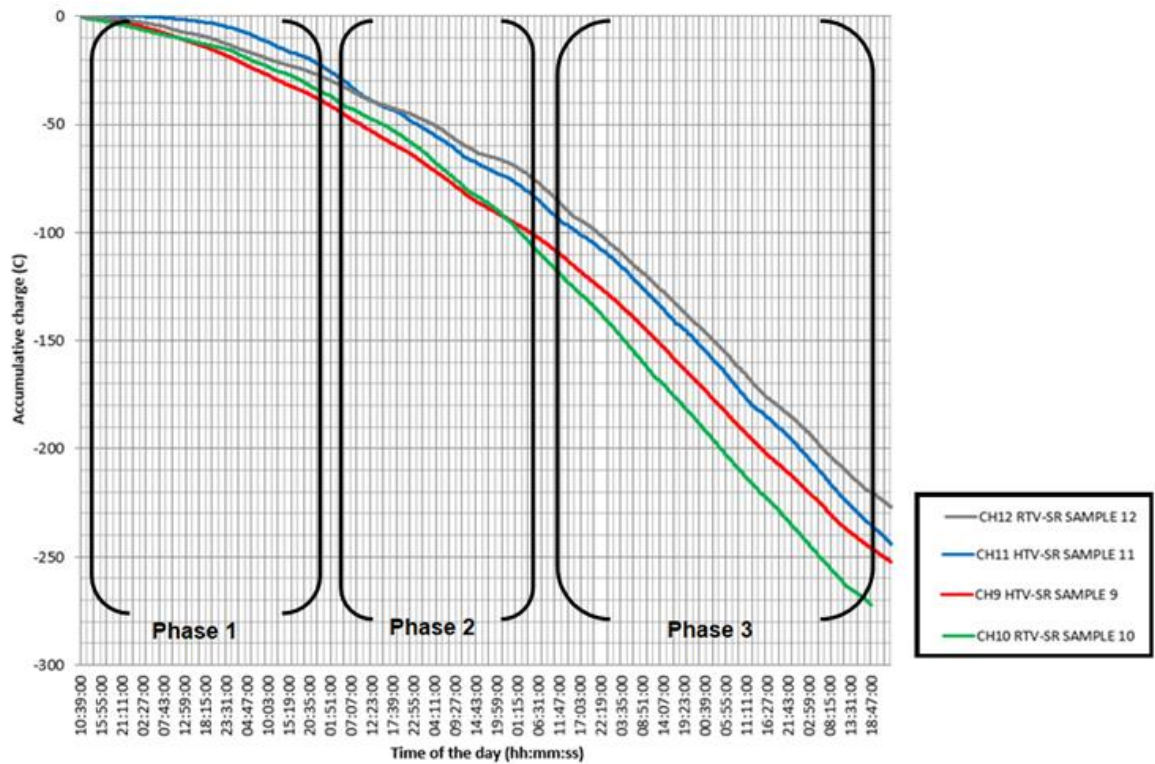


Figure 5-72: Overall cumulative negative electrical charge between HTV-SR and RTV-SR

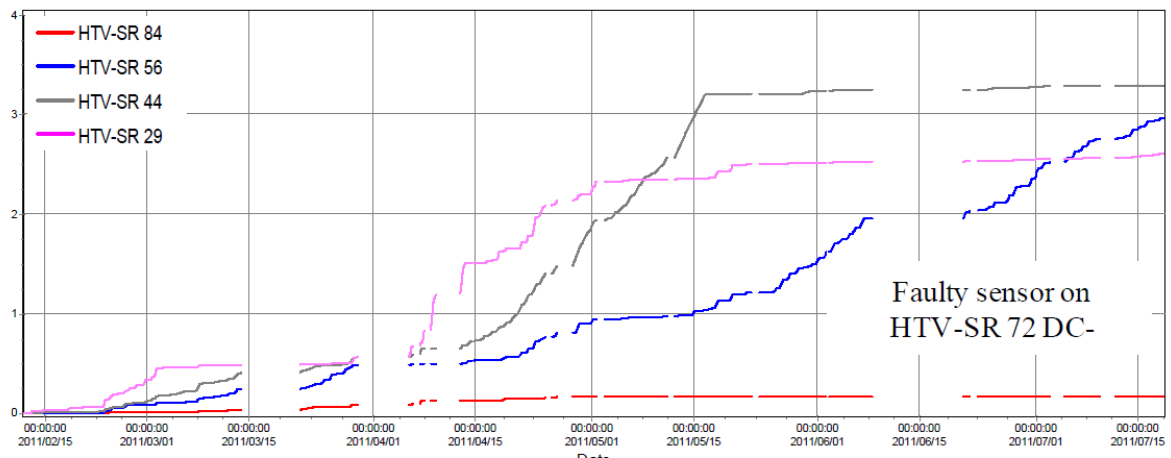


Figure 5-73: Accumulative coulomb-ampere for all the HTV-SR insulators installed on the DC- excitation voltage (Elombo, 2012)

Figure 5-72 above indicates the best performing RTV-SR sample 12 with -228 coulomb, followed by HTV-SR sample 11 with -245 coulomb. The worst performing test sample is RTV-SR sample 10 with -275 coulomb. The results seem consistent with those of Elombo (2012, p.122), who performed much longer tests but found similar results (see Figure 5-73). From the results on the following test samples (HTV-SR 82), similar trends were observed (in the initial section) to the ones tested in our tests in Ch12 RTV-SR sample 12.

5.7 OVERALL SUMMARY OF TEST RESULTS

The tests were performed using a rotating wheel dip test. The rotating wheel goes through four positions in one cycle. Each test specimen remains stationary for about 40 seconds in each of the four positions. The 90° rotation takes about eight seconds from one position to the next. In the first part of the cycle:

1. In the vertical, upside-down position, the test specimen is dipped into a saline solution (NaCl content – 1.4 kg/m³);
2. The horizontal position permits the excess saline solution to drip off the specimen;
3. In the vertical, upright position, the test specimen is subjected to alternating voltage, and the leakage current is recorded with OLCA; and
4. In the horizontal position, the test specimen rests (or cools) without electrical stress before the cycle is repeated.

The tests were conducted using a modified version of the IEC 62730 standard. The IEC / TR 62730:2012 standard for wheel test specifies the total test duration of 30 000 cycles. In the current study, 2 700 cycles were used for each of the three tests (AC, DC+, and DC-), for a total of 8 100 cycles. This means that instead of 30 000 cycles for each test, only 2 700 cycles were completed. Each subtest was conducted over six days or 144 hours. Thus, the total hours for the entire test (AC, DC+, and DC-) were 432 hours or 18 days.

Four channels were used for the test, namely CH1 (HTV-SR), CH2 (RTV-SR), CH3 (HTV-SR) and CH4 (RTV-SR). Each channel contains an insulator sample for the AC test.

Leakage current test results summary for AC, DC+, and DC-

Table 5-1 below summarises the overall leakage current test results in all test samples for HTV-SR and RTV-SR.

Table 5-1: Leakage current test results summary for AC, DC+, and DC-

Leakage Current (LC)	HTV-SR			RTV-SR		
	AC	DC+	DC-	AC	DC+	DC-
CH1	18.5 mA	16.8 mA	-12.8 mA			
CH2				17.5 mA	12.2 mA	-13.5 mA
CH3	24 mA	16.8 mA	-12.8 mA			

Leakage Current (LC)	HTV-SR			RTV-SR		
	AC	DC+	DC-	AC	DC+	DC-
CH4				17 mA	13.5 mA	-13 mA
Maximum	24 mA					

In the AC test, HTV-SR had a peak leakage current of 18.5 mA and 24 mA, RTV-SR had a peak leakage current of 17.5 mA and 17 mA. This indicates that under AC conditions, RTV-SR performed slightly better. In the DC+ test, HTV-SR had a peak leakage current of 16.8 mA and 16.8 mA, RTV-SR had a peak leakage current of 12.2 mA and 13.5 mA. This indicates that, under DC+ conditions, RTV-SR performed slightly better. In the DC- test, HTV-SR had a peak leakage current of 12.8 mA and 12.8 mA, RTV-SR had a peak leakage current of 13.5 mA and 13 mA. This indicates that under DC- conditions HTV-SR performed slightly better.

Hydrophobicity and hydrophilicity observation summary

Table 5-2 below summarises the overall hydrophobicity observations made in all test samples for HTV-SR and RTV-SR.

Table 5-2: Hydrophobicity and hydrophilicity observation summary

Hydrophobicity (%)	HTV-SR			RTV-SR		
	AC	DC+	DC –	AC	DC+	DC –
CH1	70 – 80%	60%	20 – 30%			
CH2				0 – 20%	0 – 20%	60%
CH3	40 – 50%	70 – 80%	60%			
CH4				60%	0 – 20%	60%

Under AC conditions, HTV-SR demonstrated low hydrophobicity with a 70-80% and 40-50% water droplet distribution. RTV-SR had 0-20 and 60% water droplet distribution. This indicates that RTV-SR performed better, and HTV-SR lost its hydrophobicity.

Under DC+ conditions, HTV-SR demonstrated 60% and 70-80% water droplet distribution, RTV-SR demonstrated 0-20% and 0-20% water droplet distribution. This indicates that RTV-SR performed better; it was highly hydrophobic.

Under DC- conditions, HTV-SR demonstrated 20-30% and 60% water droplet distribution, RTV-SR had 60% and 60% water droplet distribution. This hardly indicates any difference between the samples, which lost their hydrophobicity.

Cumulative electric charge test results summary

Table 5-3 below summarises the overall cumulative electric charge test results in all test samples for HTV-SR and RTV-SR.

Table 5-3: Cumulative electric charge test results summary

Cumulative electric charge (C)	HTV-SR			RTV-SR		
	AC	DC+	DC –	AC	DC+	DC –
CH1	140	280	-252			
CH2				152	N/A	-272
CH3	135	250	-242			
CH4				170	175	-228
Maximum		280				

The maximum cumulative electric charge under AC conditions is 140 coulomb and 135 coulomb for HTV-SR, 152 coulomb and 170 coulomb is for RTV-SR. This indicates that the HTV-SR performed slightly better under AC conditions.


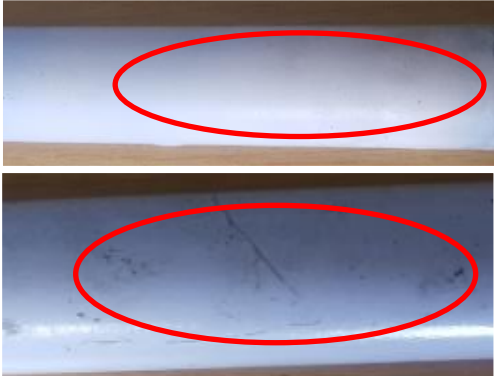



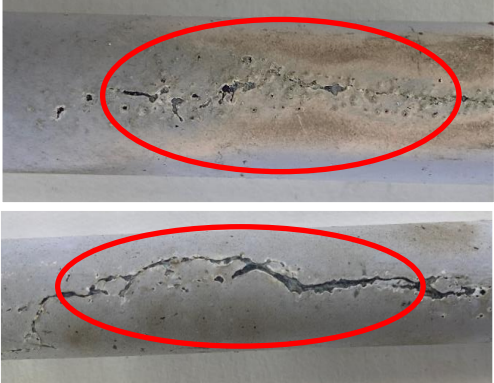


The maximum cumulative electric charge under DC+ conditions is 280 coulomb and 250 coulomb for HTV-SR, 175 coulomb is for RTV-SR. This indicates that RTV-SR performed better under DC+ conditions.


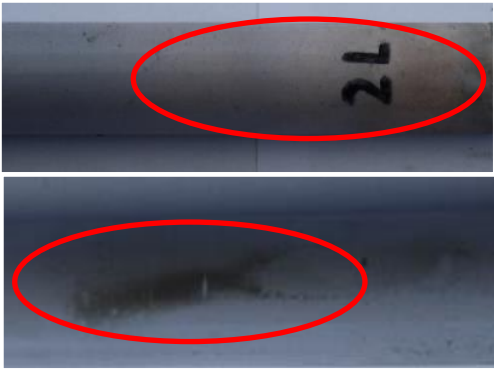

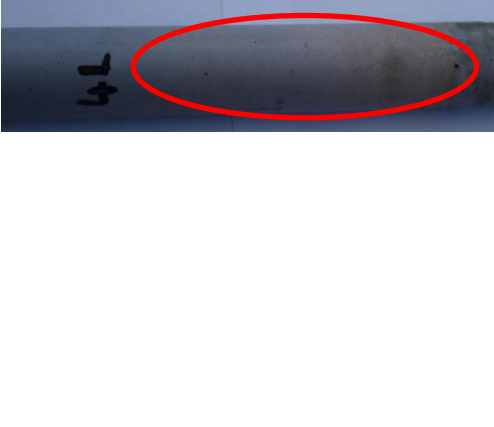
The maximum cumulative electric charge under DC- conditions is 252 coulomb and 242 coulomb for HTV-SR, 272 coulomb and 228 coulomb is for RTV-SR. These results are inconclusive as channels 1 and 3 HTV-SR are close, but channels 2 and 4 RTV-SR are at the lowest positions. Of the two, the one whose results are closest to Elombo's results is regarded as acceptable. This inconsistency can be attributed to several factors such as manufacturing flaws, connection with the HV spring, fitment of the glassy carbon end pieces etc. The author observed that the highest/maximum electric charge occurs under HTV-SR, DC+ conditions. This finding needs to be investigated further to determine whether, for a DC network, HTV-SR insulators should be used for the positive line and RTV-SR for the negative line.

Insulator ageing observation summary

Table 5-4 below summarises the overall insulator ageing observations in all test samples for HTV-SR and RTV-SR.

Table 5-4: Insulator ageing observation summary

HTV-SR Sample		RTV-SR Sample	
AC			
1		2	
3		4	
DC+			
5		6	
7		8	

HTV-SR Sample		RTV-SR Sample	
DC-			
9		10	
11		12	

Under AC test conditions, HTV-SR demonstrated the traces of dry band activity, slight crazing and discolouration, severe erosion of the material and dark burn marks on the ground side of the test samples, RTV-SR demonstrated dark contamination and discolouration in the middle of the body of the test samples. This indicates that RTV-SR performed better.

Under DC+ conditions, HTV-SR demonstrated puncture on the glassy carbon electrode and burn marks over the high-voltage side. Crazing, pollution build-up on the ground terminal side and discolouration were observed. RTV-SR demonstrated discolouration, material erosion, burn marks and pollution build-up towards the high-voltage side. From these observations, it can be seen that HTV-SR performed worse. RTV-SR performed better because there were no puncture marks (as shown in HTV-SR pictures 5 and 7), and only tracking was observed. According to the acceptance criteria defined in IEC 62730:2012, there should not be a test specimen puncture.

Under DC- conditions, HTV-SR demonstrated crazing, discolouration, tracking and light erosion on the ground side. The RTV-SR demonstrated pollution, burn marks and discolouration towards the high-voltage side. This indicates that RTV-SR performed

better. Due to this, the author concluded that the RTV-SR test samples performed better under AC and DC- conditions.

5.8 CHAPTER SUMMARY

This chapter presented the results and discussed the various tests performed on silicone-coated glass test samples. The RWDT test procedure followed the prescripts of the IEC / TR 62730:2012 standard. HTV-SR and RTV-SR tests were performed on AC, DC+, and DC-. The main variables observed and tested were leakage current, cumulative electric charge, hydrophobicity, and ageing. The overall results, including current waveforms, indicated various performances of test samples under different conditions (AC, DC+, and DC- excitations).

Under AC conditions, HTV-SR had the highest/maximum leakage current of 24 mA compared to RTV-SR, which had the highest/maximum leakage current of 17.5 mA. Therefore, RTV-SR performed slightly better than the HTV-SR.

In terms of hydrophobicity and hydrophilicity, RTV-SR performed slightly better under AC conditions, and HTV-SR lost its hydrophobicity. Under DC+ conditions, RTV-SR performed slightly better. Under DC- conditions, HTV-SR slightly lost its hydrophobicity, and RTV-SR lost its hydrophobicity. From this, the author has concluded that the test was inconclusive.

In terms of cumulative electric charge, HTV-SR performed slightly better under AC conditions. Under DC+ conditions, RTV-SR performed slightly better. Under DC- conditions, the two HTV-SR graphs are close together under DC conditions, whereas the RTV-SR graphs are in the lowest and highest position. Therefore, this finding needs to be investigated further.

In terms of insulator ageing, RTV-SR was tested under AC, DC+, and DC- conditions. The author concluded that the RTV-SR test samples performed better under AC and DC conditions from these results. RTV-SR has performed better because there were no puncture marks observed, only tracking.

CHAPTER 6.0

CONCLUSION AND RECOMMENDATIONS

This chapter presents the conclusions and recommendations based on the observations made in Chapter 5.0. As stated in § 1.4, it is important to determine which of the two insulators (RTV-SR and HTV-SR) is more suitable for DC applications. This is because there does not seem to be a comprehensive practical study on RTV-SR and HTV-SR insulator leakage current performance for DC networks. Therefore, it is pertinent to determine the performance of power line insulators under HV DC applications when subjected to natural pollution environments. The findings on AC leakage current measurements would be compared to many existing studies to determine whether they concur.

6.1 CONCLUSION

The study evaluated the performance of HTV-SR and RTV-SR coated glass rod test samples for leakage current under AC, DC+, and DC- conditions in a controlled laboratory environment. The tests were conducted using a modified version of the IEC 62730:2012 standard. In the current study, 2 700 cycles were used for each of the three tests (AC, DC+, and DC-) for a total of 8 100 cycles. Each subtest was conducted over six days or 144 hours. Thus, the total hours for the entire test (AC, DC+, and DC-) were 18 days or 432 hours. According to the standard, a value of 1.40 g/L of NaCl was added to the distilled water.

According to Madi *et al.* (2016), salt, outdoor weather conditions, and ultraviolet radiation affect the surface of the polymer insulator and therefore cause tracking, erosion, and ageing (Thomazini *et al.* 2012; Joneidi *et al.* 2013). Tracking, erosion, and ageing were used to measure the performance of HTV-SR and RTV-SR test samples. Hydrophobicity was measured as suggested by Jarrar *et al.* (2014). The hydrophobicity classification is believed to be consistent with the STRI Guide 1992. STRI is regarded as the authoritative standard (Al-Ammar & Arafa 2012; Dong *et al.* 2015; Thomazini *et al.* 2012).

The test set-up consisted of the Rotating Wheel Dip Test (RWDT), video camera, laptop, an online leakage current analyser (OLCA), a GMH 3410 conductivity meter, a Citizen Scale CG 4102, a single-phase transformer, and a full-wave DC rectifier with smoothing capacitors. Literature has affirmed that the RWDT is ideal for evaluating the

tracking and erosion of insulating material surfaces (Mackiewicz *et al.* 2017, Zago, 2017 and Krzma *et al.* 2014). This test is crucial in simulating dry-band arcing on a stressed insulation surface due to the cycling of wet and dry periods. Another advantage is that the effect of voltage and water conductivity changes occur faster in RWDT than in other tests.

The study tested glass insulators coated in silicone rubber because of the advantages of combining the two materials (Jamaludin *et al.* 2017). Many power lines across the country's network are insulated with glass (cap-and-pin) insulators because glass is compact, cost-effective, and reliable (Gençoğlu, 2007; Madi *et al.* 2016; Sarathi *et al.* 2004). Glass is preferred as it is inert, stable, and able to withstand heat (Chrzan, 2010). However, according to Elombo (2012), ceramic and glass insulators are poor under polluted conditions, as they are hydrophilic (having an affinity for water). When glass insulators are wet and their surface is severely polluted, a continuous conduction layer is formed on the surface of the glass insulator, which leads to high leakage currents and eventual flash-over (Suhaimi *et al.* 2019; Kumagai & Yoshimura 2000; Ramirez *et al.* 2012; Piah *et al.* 2003). Wet insulators tend to lose hydrophobicity (water repellence) and reduce resistivity (Elombo, 2012; Kim *et al.* 1991). Therefore, RTV-SR and HTV-SR coatings are used to bestow the insulators with hydrophobicity, anti-ageing, resistance to rough weather conditions and ultraviolet radiation (Ibrahim *et al.* 2014; Kopylov *et al.* 2011; Lopez *et al.* 2007; Schmidt *et al.* 2010; Zhu *et al.* 2017).

In this study, leakage current, charge, hydrophobicity, and ageing were the major performance determinants of insulators under excitation conditions specified above. Studying leakage current can serve as an early warning signal against line faults, which can also help classify safe and unsafe working conditions for the power utilities' live-line workers (Roman *et al.* 2019). If the leakage current is small, the insulator performs well, and power transmission operates normally (Darwison *et al.* 2019). The electric charge was used not to measure but to indicate the insulator performance as a function of the electric charge flowing over the insulator. At the same time, hydrophobicity, tracking, and erosion were observed visually. It must be noted that the overall results and observations done in Chapter 5.0 informed the conclusion and are summarised in Table 6-1 below. The following equation determined the overall best performing insulator:

$$\text{Best performing insulator} = \frac{\text{Average high value} - \text{Average low value}}{\text{Average high value}} \times 100$$

= overall best % performance for leakage current and accumulative electric charge values.

To determine the average, the two values for HTV-SR and RTV-SR were used (i.e. CH1 and CH3) for HTV-SR and (CH2 and CH4) for RTV-SR. Visual observations were used for the hydrophobicity and ageing findings. Different colour codes indicate performance, i.e. green for the best performance and red for the worst performance.

Table 6-1: Overall test results and observations for each excitation (AC, DC+, and DC-) for HTV-SR and RTV-SR

Leakage current (LC)	HTV-SR			RTV-SR		
	AC	DC+	DC-	AC	DC+	DC-
CH1	18.5 mA	16.8 mA	-12.8 mA			
CH2				17.5 mA	12.2 mA	-13.5 mA
CH3	24 mA	16.8 mA	-12.8 mA			
CH4				17 mA	13.5 mA	-13 mA
Overall best % performance			3.4%	18.82%	24.4%	
Cumulative charge (C)						
CH1	140	280	-252			
CH2				152	N/A	-272
CH3	135	250	-242			
CH4				170	175	-228
Overall best % performance	14.6%		1.2%		33.96%	
Hydrophobicity (%)						
CH1	70 – 80%	60%	20 – 30%			
CH2				0 – 20%	0 – 20%	60%
CH3	40 – 50%	70 – 80%	60%			
CH4				60%	0 – 20%	60%
Overall best performance by observations			Inconclusive but HTV-SR seems better	Inconclusive but RTV-SR seems better	Better	
Insulator ageing						
CH1	Dry band, dark burn	Puncture, burn mark, crazing, pollution, discolouration	Pollution, crazing, discolouration, light erosion			

Leakage current (LC)	HTV-SR			RTV-SR		
	AC	DC+	DC-	AC	DC+	DC-
CH2				Dark contamination, discolouration	Discolouration, material erosion, burn marks, pollution build-up	Pollution, burn marks, discolouration
CH3	Crazing, discolouration, tracking & light erosion	Crazing, puncture	Crazing, light erosion, pollution, tracking			
CH4				Discolouration	Discolouration, pollution, material erosion	Dark pollution, discolouration
Overall best performance by observations				Better	Better	Better
Green = better performing Red = worse performing						

6.1.1 Concluding remarks on the leakage current test results for AC, DC+, and DC-

1. Under AC conditions, the leakage current of the RTV-SR test sample was lower in value than HTV-SR sample by 18.82%. However, the cumulative charge graph shows the opposite; refer to § 6.1.2-1. Mouton (2012) observed that the RTV silicone rubber coated porcelain insulators performed best under all excitation voltages in his study on leakage current. According to Mouton (2012), that was due to the hydrophobicity characteristic of the RTV silicone rubber.
2. Under DC+ conditions for leakage current, RTV-SR performed better than HTV-SR by 24.4%. This aligns with what Elombo (2012) found when evaluating RTV-SR. Elombo observed lower initial peak currents than the glass insulator (channel 3). Mouton (2012) observed that the RTV silicone rubber coated porcelain insulators performed best under all excitation voltages. According to Mouton (2012), that was due to the hydrophobicity characteristic of the RTV silicone rubber.
3. Under DC-, HTV-SR performed slightly better than RTV-SR by 3.4% for leakage current.

These results are in line with Limbo, 2009 where she observed that the HTV SR insulator (channel 2) had lower initial peak currents when compared to the EPDM insulator (Channel 1).

It is shown that for leakage current, under AC and DC+ conditions, RTV-SR performed better, whereas under DC- conditions HTV-SR performed slightly better. However, due to the short duration of the test, the above results are tentative. To achieve conclusive results, they will need to be verified by longer-term studies in an outdoor environment.

6.1.2 Concluding remarks on the cumulative electric charge test results for AC, DC+, and DC-

1. The cumulative charge results show that under AC conditions, HTV-SR performed better than RTV-SR by 14.6%. This result is more significant than the leakage results, therefore, more likely to be acceptable because these results contradict the findings above in § 6.1.1, further investigations are required.
2. Under DC+ conditions, the RTV-SR performed better than the HTV-SR by 33.96%.
3. Under DC- conditions, the results are inconclusive because the percentage difference of HTV-SR and RTV-SR is very small (1.2%), and the RTV results are both the highest and lowest. Further investigation and longer duration testing are needed to determine which of the two-insulator materials should be used for DC- conditions.

6.1.3 Concluding remarks on the hydrophobicity and hydrophilicity observations for AC, DC+, and DC-

1. Under AC conditions, the test results are inconclusive, but RTV-SR indicated a slightly better performance than HTV-SR. Perhaps, the short duration of the test is the reason for such performance. It would have been expected to observe a better recovery in hydrophobicity under AC conditions since the AC voltage waveforms have zero voltage crossings, which may help provide some relief compared to the constant DC electrical stress. Therefore, the author concluded that the test was inconclusive.
2. Under DC+ conditions, RTV-SR performed better than HTV-SR.

3. Under DC- conditions, the test results are inconclusive because very similar water droplet formations were observed on both HTV-SR and RTV-SR.

6.1.4 Concluding remarks on the insulator ageing observations for AC, DC+, and DC-

1. Under AC, DC+, and DC- conditions, RTV-SR performed better than HTV-SR because there were no punctures observed: only discolouration, pollution, burn marks, and material erosion were observed on the surface of the insulator test samples. These results are consistent with what Khan *et al.* (2017) and Qin *et al.* (2013), who found that HTV-SR experiences ruptures, holes and hydrophilicity under HVDC and AC excitation conditions. As a result, its performance rapidly declines. Holtzhausen *et al.* (2010) found that using the RWT and the erosion tester (according to the IEC 61302 standard), the HTV-SR performed worse under DC than under AC.

6.1.5 Overall conclusion

1. It can be concluded that under **AC** conditions, the results seem to be inconclusive because the leakage current tests and cumulative electric charge contradict each other; however, the cumulative charge results are more significant. As a result, further testing is required to resolve this contradiction.
2. Under **DC+** conditions, RTV-SR performed better than the HTV-SR in all four categories (leakage current, cumulative electric charge, hydrophobicity, and insulator ageing).
3. Under **DC-** conditions, HTV-SR performed slightly better than RTV-SR in the categories of leakage current, cumulative electric charge, and hydrophobicity, but RTV-SR performed better in the insulator ageing category.

Due to the short duration of the test and other limitations shown below, the results above cannot be taken as conclusive but only preliminary. To achieve conclusive results, a long-term investigation will need to be performed, especially in outdoor environments.

6.1.6 Limitations of the study

1. The study was conducted at an existing rotating wheel dip test facility located at the Eskom Stikland substation in Cape Town. Since this was the simulation, a test in a natural environment should be performed to obtain more reliable data.
2. The rotating wheel test was undertaken according to IEC / TR 62730, which stipulates that the test should continue for a duration of 30 000 cycles. Since this testing was only conducted for 432 hours or 18 days, the findings can only be considered preliminary.
3. The DC voltage used (DC+ and DC-) was created using a full-wave rectifier and smoothing capacitors, providing a ripple factor between 6% and 11%. This test could be performed under DC conditions with even less ripple.
4. Only 12 test samples were used for this experiment. Six HTV-SR insulator samples and six RTV-SR glass-coated test rods were used. This number of samples could be replaced with coated glass cap and pin insulators of greater numbers to obtain more reliable results.
5. The test insulators were subjected to the same environmental conditions under AC, DC+, and DC- excitation, and the supply voltage used was only 10 kV. Therefore, more realistic voltage values should be used in future.
6. At the beginning of the study, it was necessary to move the testing from the outdoor Koeberg Insulator Pollution Test Station (KIPTS) environment to the indoor simulation environment at Stikland due to dune infringement. This is a limitation because the test was moved from a natural environment to a simulation environment.
7. Since the test was performed indoors, temperature, humidity, pollution, and other seasonal environmental variations were restricted. As a result, testing in proper outdoor environments should be conducted to obtain more realistic results.
8. Finally, the insulator samples were not subjected to voltage fluctuations, switching or lightning surges. This may be a requirement under outdoor testing conditions.

6.2 RECOMMENDATIONS

Following the information presented in Chapter 5.0 and § 6.1, the following preliminary recommendations can be made:

1. Keeping in mind that the study was of short duration and the results preliminary, the HTV-SR could be considered for AC networks given the cumulative charge results and DC- networks, while the RTV-SR could be considered for DC+ networks. In making these tentative recommendations, the hydrophobicity and ageing results also need to be considered.
2. Since the study was originally intended to be undertaken outdoors and circumstances made it impossible to be conducted at KIPTS, notwithstanding the validity and credibility of the current results, it is recommended that a study be conducted in a natural outdoor environment.
3. The test is undertaken for a longer duration.
4. Due to the initial excessive leakage current for DC+, for the HTV-SR sample in CH1 (sample 5) and CH3 (sample 7) and RTV-SR for CH4 (sample 8), the findings for those insulator types need to be verified by further testing to determine if the initial peak leakage current was due to the glassy carbon electrode being punctured.

REFERENCES

- Abidin, N.Z., Abdullah, A.R., Norddin, N. & Aman, A. 2013. Online Surface Condition Monitoring System using Time Frequency Distribution on High-voltage Insulator. *Australian Journal of Basic and Applied Sciences*, 7(11): 7-14.
- Al-Ammar, E.A. & Arafa, B.A. 2012. Experimental analysis of hydrophobic characteristics of Silicone rubber (SiR) insulators under different climatic conditions. *International Journal of Physical Sciences*, 7(47): 6162-6168.
- Al-Gheilani, A., Rowe, W., Li, Y. & Wong, K.L. 2017. Stress control methods on a high-voltage insulator: A review. *Energy Procedia*, 110: 95-100.
- Al-Hamoudi, I.Y. 1995. October. Performance of High-voltage Insulators under Heavy Natural Pollution Conditions. In *Transmission and Distribution Construction and Live Line Maintenance, 1995. ESMO-95 Proceedings.*, Seventh International Conference on (pp. 25-31). IEEE.
- Amin, M., Akbar, M. & Khan, M.N. 2007. Ageing investigations of polymeric insulators: Overview and bibliography. *IEEE Electrical Insulation Magazine*, 23(4): 44-50.
- Amin, M. & Salman, M. 2006. Ageing of polymeric insulators (an overview). *Rev. Adv. Mater. Sci*, 13(2): 93-116.
- Amin, M., Akbar, M. & Amin, S. 2007. Hydrophobicity of silicone rubber used for outdoor insulation (an overview). *Rev. Adv. Mater. Sci*, 16: 10-26.
- Amin, M., Akbar, M. & Salman, M. 2007. Composite insulators and their ageing: an overview. *Science in China Series E: Technological Sciences*, 50(6): 697-713.
- Amin, M., Amin, S. & Ali, M. 2009. Monitoring of leakage current for composite insulators and electrical devices. *Rev. Adv. Mater. Sci*, 21: 75-89.
- Amirbandeh, M., Yaghoti, A.A. and Sharifi-Tameh, G.R., 2014. The Investigation of Replacing Ceramic Bushings with Silicon Bushings in the Distribution Transformers. *Journal of Surface Engineered Materials and Advanced Technology*, 4(06), p.319.

- Andriot, M., Chao, S.H., Colas, A.R., Cray, S.E., DeBuyl, F., DeGroot, J.V., Dupont, A., Easton, T., Garaud, J.L., Gerlach, E. & Gubbels, F. 2007. Silicones in industrial applications. *Inorganic Polymers*, 61-161.
- Anjum, S. 2014. A Study of the Detection of Defects in Ceramic Insulators Based on Radio Frequency Signatures (Master's thesis, University of Waterloo). Ontario: Canada.
- ANSI, ANSI/NEMA C29.13-2012. *American National Standard for Insulators - Composite - Distribution Deadend Type*.
- Ansorge, S., Schmuck, F. & Papailiou, K.O. 2012. Improved silicone rubbers for use as housing material in composite insulators. *IEEE Transactions on Dielectrics and Electrical Insulation*, 19(1): 209-217.
- Arklove, M.C. & Wheeler, J.C.G., 1996, September. Salt-fog testing of composite insulators. In *Dielectric Materials, Measurements and Applications, Seventh International Conference on* (Conf. Publ. No. 430) (pp. 299-302). IET.
- Awaja, F., Zhang, S., Tripathi, M., Nikiforov, A. & Pugno, N., 2016. Cracks, microcracks and fracture in polymer structures: Formation, detection, autonomic repair. *Progress in Materials Science*, 83: 536-573.
- Bahrman, M.P. 2008, April. HVDC transmission overview. In *2008 IEEE/PES Transmission and Distribution Conference and Exposition*. Chicago, IL, Apr. 21–24, (pp. 1-7). IEEE.
- Ball, Z.T., Hayashi, T. & Yamasaki, K. 2007. C–E Bond Formation through Hydrosilylation of Alkynes and Related Reactions. In: Mingos, D. M. P and Crabtree, R. H. (eds.). *Comprehensive Organometallic Chemistry, (COMC-III): from fundamentals to applications*. Third Edition. Elsevier Science. pp. 815-838.
- Banhthasit, B., Tonmitra, K., Suksri, A., Kaewrawang, A. & Leeparkobboon, M. 2011. A Comparison on Leakage Current of 22 kV Porcelain Insulator Using High-voltage AC and Impulse Voltage via a Rotating Wheel Dip Test. *International Journal of Computer and Electrical Engineering*, 3(3): 409.
- Belhouchet, K., Bayadi, A., Belhouchet, H. & Romero, M. 2019. Improvement of mechanical and dielectric properties of porcelain insulators using economic

- raw materials. *Boletín de la Sociedad Española de Cerámica y Vidrio*, 58(1): 28-37.
- Bergasse, E., Paczynski, W., Dabrowski, M. & De Wulf, L. 2013. The relationship between energy and socio-economic development in the Southern and Eastern Mediterranean. *CASE Network Reports*, (412).
- Billings, M.J., Wilkins, R. & Warren, L. 1968. A Comparison of the IEC, Dust/Fog, and Inclined Plane Tests. *IEEE Transactions on Electrical Insulation*, (2): 33-39.
- Bogias, A. 2012. A wireless 802.11 condition monitoring sensor for electrical substation environments (Doctoral dissertation, Cardiff University).
- Bojovschi, A., Quoc, T.V., Trung, H.N., Quang, D.T. & Le, T.C. 2019. Environmental Effects on HV Dielectric Materials and Related Sensing Technologies. *Applied Sciences*, 9(5): 856.
- Bouras, N., Madjoubi, M.A., Kolli, M., Benterki, S. & Hamidouche, M. 2009. Thermal and mechanical characterization of borosilicate glass. *Physics Procedia*, 2(3): 1135-1140.
- Braini, S., Haddad, A. and Harid, N., 2011, September. The performance of nano-coating for high-voltage insulators. In 2011 46th International Universities' Power Engineering Conference (UPEC) (pp. 1-4). VDE.
- Brooke-Devlin, W.W., 2012. Novel Shear-Thinning of Aged PDMS/Fumed Silica Admixtures and Properties of Related Silicone Elastomers. Virginia Commonwealth University.
- Bruce, G.P., Rowland, S.M. & Krivda, A. 2008, October. DC inclined-plane testing of silicone rubber formulations. In *Electrical Insulation and Dielectric Phenomena, 2008. CEIDP 2008. Annual Report Conference on* (pp. 196-199). IEEE.
- Bruce, G.P., Rowland, S.M. & Krivda, A. 2010. Performance of silicone rubber in DC inclined plane tracking tests. *IEEE Transactions on Dielectrics and Electrical Insulation*, 17(2).
- Burnham, J.T. & Waidelich, R.J. 1997. Gunshot damage to ceramic and nonceramic insulators. *IEEE transactions on power delivery*, 12(4): 1651-1656.

- Castillo-Sierra, R., Oviedo-Trespalacios, O., Candelo, J.E. & Soto-Ortiz, J.D. 2018. Modelling leakage current of ceramic insulators subject to high pollution levels for improving maintenance activities. *Dyna*, 85(204): 364-371.
- Chakraborty, R. & Reddy, B.S. 2017. Studies on high temperature vulcanized silicone rubber insulators under arid climatic ageing. *IEEE Transactions on Dielectrics and Electrical Insulation*, 24(3): 1751-1760.
- Cherney, E.A. 1995. RTV silicone-a high tech solution for a dirty insulator problem. *IEEE Electrical Insulation Magazine*, 11(6): 8-14.
- Cherney, E.A. & Gorur, R.S. 1999. RTV silicone rubber coatings for outdoor insulators. *IEEE Transactions on Dielectrics and Electrical Insulation*, 6(5): 605-611.
- Chrzan, K.L. 2010. Leakage currents on naturally contaminated porcelain and silicone insulators. *IEEE transactions on power delivery*, 25(2): 904-910.
- Chudnovsky, B.H. 2012. *Electrical power transmission and distribution: ageing and life extension techniques*. CRC Press.
- Crescentini, M., Marchesi, M., Romani, A., Tartagni, M. and Traverso, P.A., 2017. Bandwidth limits in Hall effect-based current sensors. *Acta-Imeko*, 6(4), pp.17-24.
- Colas, A. 2005. *Silicones: preparation, properties and performance*. Dow Corning, Life Sciences.
- Conductivity ordering guide. 1999. Available at:
<https://dokumen.tips/documents/conductivity-ordering-guide-supersedes-mywebwitedusandinicresearchconductivity.html> (Accessed: 02 March 2019).
- Costea, M. & Baran, I. 2012. a Comparative Analysis of Classical and Composite Insulators Behavior. University 'Politehnica' of Bucharest Scientific Bulletin, *Series C: Electrical Engineering*, 74(1): 147-154.
- Darwison, D., Arief, S., Abrial, H., Hazmi, A., Novizon, N., Aulia, A. & Waldi, E.P. 2019. A Leakage Current Forecast of the Polymeric Insulator Using ANFIS Method Based on LabView Pre-processed Thermal Image. *International Journal of Science, Technology and Society*, 6(6): 88.
- de Jesus, R.C., Pissolato, J., de Franco, J.L., de Abreu, S.R., da Silva, D.A., Romano, A., Costa, E.C.M. & Mei, L.H.I. 2013. Hydrophobicity classification

- of distribution silicone arresters before and after solid layer contamination. 18th International Symposium on High-voltage Engineering, 23-25 August 2013, Seoul, South Korea.
- de Santos, H. and Sanz-Bobi, M.Á., 2021. Research on the pollution performance and degradation of superhydrophobic nano-coatings for toughened glass insulators. *Electric Power Systems Research*, 191, p.106863.
- Delebecq, E. & Ganachaud, F. 2012. Looking over liquid silicone rubbers:(1) network topology vs chemical formulations. *ACS Applied Materials & Interfaces*, 4(7): 3340-3352.
- Deng, H. & Hackam, R. 1997. Electrical performance of RTV silicone rubber coating of different thicknesses on porcelain. *IEEE Transactions on Power Delivery*, 12(2): 857-866.
- Dong, Z., Fang, Y., Wang, X., Zhao, Y. & Wang, Q. 2015. Hydrophobicity classification of polymeric insulators based on embedded methods. *Materials Research*, 18(1): 127-137.
- El-Hag, A., Meyer, L.H. & Naderian, A. 2010. Experience with salt-fog and inclined-plane tests for ageing polymeric insulators and materials. *IEEE Electrical Insulation Magazine*, 26(2).
- El-Kheshen, A.A. & Zawrah, M.F. 2003. Sinterability, microstructure and properties of glass/ceramic composites. *Ceramics International*, 29(3): 251-257.
- Elombo, A.I. 2012. An evaluation of HTV-SR insulators with different creepage lengths under AC and bipolar DC in marine polluted service conditions (Doctoral dissertation, Stellenbosch: Stellenbosch University).
- Elombo, A.I., Holtzhausen, J.P., Vermeulen, H.J., Pieterse, P.J. & Vosloo, W.L. 2013. Comparative evaluation of the leakage current and ageing performance of HTV-SR insulators of different creepage lengths when energized by AC, DC+ or DC–in a severe marine environment. *IEEE Transactions on Dielectrics and Electrical Insulation*, 20(2): 421-428.
- El-Shahat, M. & Anis, H. 2014. Risk assessment of desert pollution on composite high-voltage insulators. *Journal of Advanced Research*, 5(5): 569-576.
- Ersoy, A., Mukden, U.G.U.R., Güneş, İ. & Kuntman, A. 2007. A study on the insulation capacity of polymeric composite materials blended with boron

- minerals. *Istanbul University-Journal of Electrical & Electronics Engineering*, 7(1): 367-371.
- Fang, W., Lai, X., Li, H., Chen, W., Zeng, X., Zhang, L. & Yang, S. 2014. Effect of urea-containing anti-tracking additive on the tracking and erosion resistance of addition-cure liquid silicone rubber. *Polymer Testing*, 37: 19-27.
- Farzaneh, M. and Chisholm, W.A., 2009. Insulators for icing and polluted environments (Vol. 47). John Wiley & Sons.
- Farhang, F., Ehsani, M. & Jazayeri, S.H. 2009. *Effects of the filler type and quantity on the flash-over voltage and hydrophobicity of RTV silicone rubber coatings*.
- Fernando, M.A.R.M. & Gubanski, S.M. 1999. Leakage currents on non-ceramic insulators and materials. *IEEE Transactions on Dielectrics and Electrical Insulation*, 6(5): 660-667.
- Ferreira, T.V., Germano, A.D., Da Costa, E.G., Angelini, J.M.G., Nallim, F.E. & Mendonça, P. 2010, September. Naturally aged polymeric insulators: Washing and its consequences. In *2010 Modern Electric Power Systems* (pp. 1-5). IEEE.
- Frącz, P., Urbaniec, I., Turba, T. & Krzewiński, S. 2016. Diagnosis of high-voltage insulators made of ceramic using spectrophotometry. *Journal of Spectroscopy*, 2016.
- Garrard, J. 2008. Investigation into the performance of outdoor insulators under high humidity conditions (Masters in Electrical Engineering, School of Electrical, Electronic and Computer Engineering at the University of Kwa-Zulu Natal). Durban: KwaZulu Natal.
- Gençoğlu, M.T. 2007. The comparison of ceramic and non-ceramic insulators. *Engineering Sciences*, 2(4): 274-294.
- Ghosh, D. & Khastgir, D. 2018. Degradation and stability of polymeric high-voltage insulators and prediction of their service life through environmental and accelerated ageing processes. *ACS Omega*, 3(9): 11317-11330.
- Ghosh, D., Bhandari, S., Chaki, T.K. & Khastgir, D. 2015. Development of a high-performance high-voltage insulator for power transmission lines from blends of polydimethylsiloxane/ethylene vinyl acetate containing nanosilica. *RSC Advances*, 5(71): 57608-57618.

- Ghunem, R.A., Jayaram, S.H. & Cherney, E.A. 2013a. Erosion of silicone rubber composites in the AC and DC inclined plane tests. *IEEE Transactions on Dielectrics and Electrical Insulation*, 20(1): 229-236.
- Ghunem, R.A., Jayaram, S.H. & Cherney, E.A. 2013b, June. Comparative inclined plane tests on silicone and EPDM elastomers under DC. In Electrical Insulation Conference (EIC), 2013 IEEE (pp. 356-359). IEEE.
- Ghunem, R.A., Jayaram, S.H. & Cherney, E.A. 2015. The DC inclined-plane tracking and erosion test and the role of inorganic fillers in silicone rubber for DC insulation. *IEEE Electrical Insulation Magazine*, 31(1): 12-21.
- Gorur, R., Montesinos, J., Varadadesikan, L., Simmons, S. & Shah, M. 1997, January. A rapid test method for evaluating the tracking and erosion resistance of polymeric outdoor insulating materials. In Electrical Insulation and Dielectric Phenomena, 1997. IEEE 1997 Annual Report., Conference on (2): 402-405. IEEE.
- Gorur, R.S., Cherney, E.A. & Hackam, R. 1986. A comparative study of polymer insulating materials under salt-fog conditions. *IEEE transactions on electrical insulation*, (2): 175-182.
- Gorur, R.S., De La O, A., El-Kishky, H., Chowdhary, M., Mukherjee, H., Sundaram, R. & Burnham, J.T. 1997. Sudden flash-over of nonceramic insulators in artificial contamination tests. *IEEE Transactions on Dielectrics and Electrical Insulation*, 4(1): 79-87.
- Goswami, A. P. 2017. Design and Manufacturing of Porcelain Longrod Insulator for Improved Performance of National (U) HVDC Grid. *International Journal of Innovative Research in Electrical, Electronics, Instrumentation and Control Engineering*. REPSE-17. National Conference on Sustainable Development in Renewable Energy Sources and Power System Engineering Sri Venkateshwara College of Engineering, Bengaluru (5/3): 39-44.
- Goudie, J.L. & Collins, T.P. 2004, September. Development and evaluation of an improved RTV coating for outdoor insulation. In Conference Record of the 2004 IEEE International Symposium on Electrical Insulation (pp. 475-479). IEEE.
- Gubanski, S.M. 1990. Experience with the Merry-go-round Test. *IEEE Transactions on Electrical Insulation*, 25(2): 331-340.

- Gubanski, S.M. 2005. Modern outdoor insulation-concerns and challenges. *IEEE Electrical Insulation Magazine*, 21(6): 5-11.
- Gubanski, S.M., Dornfalk, A., Andersson, J. & Hillborg, H. 2007. Diagnostic methods for outdoor polymeric insulators. *IEEE Transactions on Dielectrics and Electrical Insulation*, 14(5).
- Gubanski, S.M., Fernando, M.A.R.M., Pietr, S.J., Matula, J. & Kyaruzi, A. 2000. Effects of biological contamination on insulator performance. In Properties and Applications of Dielectric Materials, 2000. Proceedings of the 6th International Conference on (2): 797-801. IEEE.
- Gutman, I., Hartings, R., Matsuoka, R. & Kondo, K. 1997. Experience with IEC 1109 1000 h salt fog ageing test for composite insulators. *IEEE Electrical Insulation Magazine*, 13(3): 36-39.
- Haddad, G., Wong, K.L. & Gupta, R.K. 2014, June. Dielectric breakdown characteristics of HTV silicone rubber under multiple stress conditions. In Proceedings of 2014 International Symposium on Electrical Insulating Materials (pp. 276-279). IEEE.
- Hall, J.F. 1993. History and bibliography of polymeric insulators for outdoor applications. *IEEE Transactions on Power Delivery*, 8(1): 376-385.
- Hamadi, S.H.K., Isa, M., Hashim, S.N.M.A. & Othman, M. 2020, June. Review on RTV Silicone Rubber Coatings Insulator for Transmission Lines. In IOP Conference Series: Materials Science and Engineering (864/1: 012188). IOP Publishing.
- Han, S., Hao, R. & Lee, J. 2009. Inspection of insulators on high-voltage power transmission lines. *IEEE Transactions on Power Delivery*, 24(4): 2319-2327.
- Heger, G. 2009. A comparative study of insulator materials exposed to high-voltage AC and DC surface discharges (Doctoral dissertation, Stellenbosch: University of Stellenbosch).
- Heger, G., Vermeulen, H.J., Holtzhausen, J.P. & Vosloo, W.L., 2010. A comparative study of insulator materials exposed to high-voltage AC and DC surface discharges. *IEEE Transactions on Dielectrics and Electrical Insulation*, 17(2).
- Hikvision IP cameras.2017. <https://www.sourcesecurity.com/hikvision-ds-2cd802p-ir1-ip-camera-technical-details.html>. (Accessed on 23 June 2017).

- Hillborg, H., Krivda, A., Schmidt, L.E. & Kornmann, X. 2010, October. Investigation of hydrophilic pollution layers on silicone rubber outdoor insulation. In 2010 Annual Report Conference on Electrical Insulation and Dielectric Phenomena (pp. 1-4). IEEE.
- Hiremath, A. & Hemanth, J. 2017. Experimental evaluation of the coefficient of thermal expansion of chilled aluminium alloy-borosilicate glass (P) composite. *J Mater Environ Sci*, 8(12): 4246-4252.
- Holtzhausen, J.P., Pieterse, P.J., Vermeulen, H.J. & Limbo, S. 2010, October. Insulator ageing tests with HVAC and HVDC excitation using the tracking wheel tester. In High-voltage Engineering and Application (ICHVE), 2010 International Conference on (pp. 445-448). IEEE.
- Htay, H.H. 2011. Design and Construction of Microcontroller Based Data Logger. *Universities Research Journal*, 271.
- Huang, J., Liu, K., Zeng, D. & Zhang, Z. 2018. An Online Measurement Method for Insulator Creepage Distance on Transmission Lines. *Energies*, 11(7): 1781.
- Ibrahim, A., Nasrat, L. & Elassal, H. 2014. Improvement of Electrical Performance for Porcelain Insulators Using Silicone Rubber Coating. *International Journal of Innovative Research in Electrical, Electronics, Instrumentation and Control Engineering*, 2(8): 1884-1888.
- IEC / TR 62730-.22012. HV Polymeric Insulators for Indoor and Outdoor Use Tracking and Erosion Testing by Wheel Test and 5000 h Test. pp. 8-41.
- Ilhan, S. & Aslan, Z. 2020. Investigation on leakage current, erosion, and hydrophobic performance of high-voltage insulator coatings of different thicknesses. *Turkish Journal of Electrical Engineering & Computer Sciences*, 28(2): 1197-1207.
- Irene, S.F., Salahh, M.E. & Hatem, E. 2012. Experimental Investigation of Natural Fiber Reinforced Polymers. *Mater Sci Appl*, 3: 59-66.
- Islam, R.A., Chan, Y.C. & Islam, M.F. 2004. Structure–property relationship in high-tension ceramic insulator fired at high temperature. *Materials Science and Engineering: B*, 106(2): 132-140.

- Izadi, M., Abd Rahman, M.S., Ab-Kadir, M.Z.A., Gomes, C., Jasni, J. & Hajikhani, M. 2017. The influence of lightning-induced voltage on the distribution power line polymer insulators. *PloS one*, 12(2): e0172118.
- Jahromi, A.N., El-Hag, A.H., Cherney, E.A., Jayaram, S.H., Sanaye-Pasand, M. & Mohseni, H. 2005, October. Prediction of leakage current of composite insulators in salt fog test using neural network. In *Electrical Insulation and Dielectric Phenomena, 2005. CEIDP'05. 2005 Annual Report Conference on* (pp. 309-312). IEEE.
- Jamaludin, F.A., Ab-Kadir, M.Z.A., Izadi, M., Azis, N., Jasni, J. & Abd-Rahman, M.S. 2017. Effects of RTV coating on the electrical performance of polymer insulator under lightning impulse voltage condition. *PloS one*, 12(11): e0187892.
- Jarrar, I., Assaleh, K. & El-Hag, A. 2014, September. Using the Gray Level Co-occurrence Matrix to Improve the Swedish Hydrophobicity Class System. In *International Conference on Condition Monitoring and Diagnosis 2014 (CMD 2014)*.
- Jia, Z., Fang, S., Gao, H., Guan, Z., Wang, L. & Xu, Z. 2008. Development of RTV silicone coatings in China: Overview and bibliography. *IEEE Electrical Insulation Magazine*, 24(2): 28-41.
- Jia, Z., Gao, H., Guan, Z., Wang, L. & Yang, J. 2006. Study on hydrophobicity transfer of RTV coatings based on a modification of absorption and cohesion theory. *IEEE Transactions on Dielectrics and Electrical Insulation*, 13(6): 1317-1324.
- Joneidi, I.A., Kamarposhti, M.A., Akmal, A.A.S. & Mohseni, H. 2013. Leakage current analysis, FFT calculation and electric field distribution under water droplet on polluted silicon rubber insulator. *Electrical Engineering*, 95(4): 315-323.
- Kaltenborn, U., Kindersberger, J., Barsch, R. & Jahn, H. 1997, January. On the electrical performance of different insulating materials in a rotating-wheel-dip-test. In *Electrical Insulation and Dielectric Phenomena, 1997. IEEE 1997 Annual Report, Conference on* (2): 398-401. IEEE.
- Karady, G., Farmer, R. & Grigsby, L. 2007. *Insulators and Accessories. In Electric Power Generation, Transmission and Distribution* (p. 6). Taylor & Francis-IEEE Press.

- Khan, H., Amin, M. & Ahmad, A. 2018. Characteristics of silicone composites for high-voltage insulations. *Reviews on Advanced Materials Science*, 56(1): 91-123.
- Khan, H., Amin, M., Ahmad, A. & Yasin, M. 2017. Impact of alumina trihydrate and silica on mechanical, thermal and electrical properties of silicone rubber composites for high-voltage insulations. *Res. Dev. Mater. Sci*, 2: 153-160.
- Khan, Y. 2010. Degradation of hydrophobic properties of composite insulators in a simulated arid desert environment. *International Journal of Engineering & Technology*, 10(1): 86-90.
- Khatoon, S., Khan, A.A. & Singh, S. 2017. A review of the flash-over performance of high-voltage insulators constructed with modern insulating materials. *Transactions on Electrical and Electronic Materials*, 18(5): 246-249.
- Kim, S.H., Cherney, E.A. & Hackam, R. 1991. Suppression mechanism of leakage current on RTV coated porcelain and silicone rubber insulators. *IEEE Transactions on Power Delivery*, 6(4): 1549-1556.
- Kindersberger, J., Kuhl, M. & Bärsch, R. 1995. Evaluation of the conditions of non-ceramic insulators after long-term operation under service conditions. In 9th International Symposium on High-voltage Engineering (ISH).
- Kitouni, S. & Harabi, A. 2011. Sintering and mechanical properties of porcelains prepared from Algerian raw materials. *Cerâmica*, 57(344): 453-460.
- Klüss, J.V. & Hamilton, J. 2017, August. Design of rotating wheel dip test system for standard tracking and erosion testing of polymeric insulators. In The 20th Int. Symp. on High-voltage Engineering (ISH), Buenos Aires, Argentina.
- Kobayashi, S., Matsuzaki, Y., Arashitani, Y. & Kimata, R. 2001. Development of composite insulators for overhead lines (Part 2). *Furukawa Electric Review*, 55-60.
- Kokalis, C.C.A., Tasakos, T., Kontargyri, V.T., Siolas, G. and Gonos, I.F., 2020. Hydrophobicity classification of composite insulators based on convolutional neural networks. *Engineering Applications of Artificial Intelligence*, 91, p.103613.

- Kopylov, V.M., Kostyleva, E.I., Kostylev, I.M. & Koviazin, A.V. 2011. Silica fillers for silicone rubber. *International Polymer Science and Technology*, 38(4): 35-47.
- Krzma, A. 2016. Comparative laboratory performance characterisation of silicone rubber textured insulators (Doctoral dissertation, Cardiff University).
- Krzma, A.S., Albano, M. & Haddad, A. 2014, September. Comparative performance of 11kV silicone rubber polymeric insulators under Rotating Wheel Dip Test. In Power Engineering Conference (UPEC), 2014 49th International Universities (pp. 1-5). IEEE.
- Krzma, A.S., Albano, M., Waters, R.T. & Haddad, A. 2015. Comparative performance of 11 kV silicone rubber polymeric insulators with HVAC and HVDC excitations using the rotating wheel dip test. In The 19th Int. Symp. on High-voltage Engineering (ISH), Pilsen, Czech Republic.
- Krzma, A., Albano, M. and Haddad, A., 2020. Comparative characterisation of conventional and textured 11 kV insulators using the rotating wheel dip test. *High Voltage*, 5(6), pp.739-746.
- Kubai, T. 2007. Computer modelling studies of the diffusion of low molecular weight cyclic PDMS oligomer in PDMS polymer (Doctoral dissertation, University of Limpopo [Turfloop Campus]).
- Kuffel, J. & Kuffel, P. 2000. *High-voltage engineering fundamentals*. Elsevier.
- Kumagai, S. & Yoshimura, N, 2000. Evaluation of leakage current on various types of polymeric materials used for HV outdoor insulation in salt-fog conditions. *IEEJ Transactions on Fundamentals and Materials*, 120(11): 1051-1055.
- Kumagai, S. & Yoshimura, N. 2001. Tracking and erosion of HTV silicone rubber and suppression mechanism of ATH. *IEEE Transactions on Dielectrics and Electrical Insulation*, 8(2): 203-211.
- Kumagai, S., Marungsri, B., Shinokubo, H., Matsuoka, R. & Yoshimura, N. 2006. Comparison of leakage current and ageing of silicone rubbers and porcelain in both field and salt-fog tests. *IEEE transactions on dielectrics and electrical insulation*, 13(6).
- Kumagai, S., Suzuki, M. & Yoshimura, N. 2001. Electrical Performances of RTV Silicone Rubber Coatings in Salt-fog and Rotating Wheel Dip Tests. *IEEJ Transactions on Fundamentals and Materials*, 121(4): 324-331.

- Kumara, S. and Fernando, M., 2020. Performance of outdoor insulators in tropical conditions of Sri Lanka. *IEEE Electrical Insulation Magazine*, 36(4), pp.26-35.
- Kumosa, M., Kumosa, L. & Armentrout, D. 2005. Failure analyses of nonceramic insulators. Part 1: Brittle fracture characteristics. *IEEE Electrical Insulation Magazine*, 21(3): 14-27.
- Lambeth, P.J., Looms, J.S.T., Sforzini, M., Cortina, R., Porcheron, Y. & Claverie, P. 1973. The salt fog test and its use in insulator selection for polluted localities. *IEEE Transactions on Power Apparatus and Systems*, (6): 1876-1887.
- Lan, L. & Gorur, R.S. 2008. Computation of ac wet flash-over voltage of ceramic and composite insulators. *IEEE Transactions on Dielectrics and Electrical Insulation*, 15(5).
- Larsson, A., Roslund, A., Kroll, S. & Dornfalk, A. 2002. In-situ diagnostics of HV outdoor insulators using laser-induced fluorescence spectroscopy. *IEEE Transactions on Dielectrics and Electrical Insulation*, 9(2): 274-281.
- Li, J., Zhao, Y., Hu, J., Shu, L. & Shi, X. 2012. Anti-icing performance of a superhydrophobic PDMS/modified nano-silica hybrid coating for insulators. *Journal of Adhesion Science and Technology*, 26(4-5): 665-679.
- Li, J.Y., Sun, C.X., Sima, W.X. & Yang, Q. 2009. Stage pre-warning based on leakage current characteristics before contamination flash-over of porcelain and glass insulators. *IET Generation, Transmission & Distribution*, 3(7): 605-615.
- Lima, M.M.R.A., Monteiro, R.C.C., Graça, M.P.F. & Da Silva, M.F. 2012. Structural, electrical, and thermal properties of borosilicate glass–alumina composites. *Journal of Alloys and Compounds*, 538: 66-72.
- Limbo, B.S. 2009. Insulator Ageing Tests with HVAC and HVDC Excitation using the Tracking Wheel Tester (Master's thesis at the University of Stellenbosch). Stellenbosch.
- Looms, J.S.T. 1988. *Insulators for high voltages* (No. 7). IET.
- Lopes, I.J.D. 2001. A Study of Surface Discharges during the early ageing of silicone rubber insulation using partial discharge analysis (Doctoral dissertation, PhD

Thesis, School of Electrical and Computer Engineering, University of Waterloo, Ontario, Canada).

- Lopez, L.M., Cosgrove, A.B., Hernandez-Ortiz, J.P. & Oswald, T.A. 2007. Modelling the vulcanization reaction of silicone rubber. *Polymer Engineering & Science*, 47(5): 675-683.
- Macey, R.E., Vosloo, W.L. & Tourreil, C. 2004. *The practical guide to outdoor high-voltage insulators*. Crown Publications.
- Mackevich, J. & Shah, M. 1997. Polymer outdoor insulating materials. Part I: Comparison of porcelain and polymer electrical insulation. *IEEE Electrical Insulation Magazine*, 13(3): 5-12.
- Mackiewicz, M., Wańkiewicz, J., Ranachowski, Z., Ranachowski, P., Mikulski, J.L. & Kucharski, S. 2017. *Study of Composite Insulator Sheds Subjected to Wheel Test*. *Archives of Metallurgy and Materials*.
- Madhavan, S. 2015. Methods of Strengthening Ceramics. *Journal of Pharmaceutical Sciences and Research*, 7(10): 873.
- Madi, A., He, Y., Jiang, L. & Yan, B. 2016. Surface Tracking on Polymeric Insulators Used in Electrical Transmission Lines. *Indonesian Journal of Electrical Engineering and Computer Science*, 3(3): 639-645.
- Mahatho, N., Parus, N., Govender, T. & Sibilant, G. 2016. An investigation into the effect of shattered glass discs on insulation strength under HVDC voltage stress. *IEEE Transactions on Dielectrics and Electrical Insulation*, 23(4): 2181-2188.
- Mathes, K.N. 1991, October. A brief history of development in electrical insulation. In [1991] Proceedings of the 20th Electrical Electronics Insulation Conference (pp. 147-150). IEEE.
- Mavrikakis, N., Siderakis, K., Kourasani, D., Pechynaki, M. & Koudoumas, E. 2015, May. Hydrophobicity transfer mechanism evaluation of field aged composite insulators. In 2015 IEEE 5th International Conference on Power Engineering, Energy and Electrical Drives (POWERENG) (pp. 215-219). IEEE.
- Meister, T.K., Riener, K., Gigler, P., Stohrer, J., Herrmann, W.A. & Kühn, F.E. 2016. Platinum Catalysis Revisited: Unraveling Principles of Catalytic Olefin Hydrosilylation. *ACS Catalysis*, 6(2): 1274-1284.

- Mishra, A.K. ed. 2017. *Sol-gel Based Nanoceramic Materials: Preparation, Properties and Applications* (pp. 253-274). Springer.
- Mitra, A., Choudhary, S., Garg, H. and HG, J., 2014. Maxillofacial prosthetic materials-an inclination towards silicones. *Journal of clinical and diagnostic research: JCDR*, 8(12), p. ZE08.
- Moreno, V.M. & Gorur, R.S. 2003. Impact of corona on the long-term performance of nonceramic insulators. *IEEE Transactions on Dielectrics and Electrical Insulation*, 10(1): 80-95.
- Mouton, G.N.J. 2012. An evaluation of different material line insulators under high-voltage AC and bipolar DC excitation in a marine polluted environment (Doctoral dissertation, Stellenbosch: Stellenbosch University).
- Naito, K. & Schneider, H.M. 1995. Round-robin artificial contamination test on high-voltage DC insulators. *IEEE Transactions on Power Delivery*, 10(3): 1438-1442.
- Nasrat, L., Ali, Z.M., Dardeer, M.M. & Tawfiq, R. 2016. Mica Filler Effect on Electrical Characteristics of Polymer Insulators. *International Journal of Engineering Innovations and Research*, 5(2): 168.
- Nasrat, L.S., Hamed, A.F., Hamid, M.A. & Mansour, S.H. 2013. Study the flash-over voltage for outdoor polymer insulators under desert climatic conditions. *Egyptian Journal of Petroleum*, 22(1): 1-8.
- Natarajan, M., Basharan, V., Pillai, K.G., Velayutham, M.R. & Silluvairaj, W.I.M. 2015. Analysis of Stress Control on 33-kV Non-ceramic Insulators Using Finite-element Method. *Electric Power Components and Systems*, 43(5): 566-577.
- National Planning Commission. 2013. *National development plan vision 2030*. Available at: <http://policyresearch.limpopo.gov.za/bitstream/handle/123456789/941/NDP%20Vision%202030.pdf?s> (Accessed: 11 July 2019).
- Nekahi, A., McMeekin, S.G. & Farzaneh, M. 2017. Effect of pollution severity and dry band location on the flash-over characteristics of silicone rubber surfaces. *Electrical Engineering*, 99(3): 1053-1063.
- Nekeb, A. 2014. Effect of some climatic conditions in the performance of outdoor HV silicone rubber insulators (Doctoral dissertation, Cardiff University).

- Nordin, N., Abdullah, A.R., Abidin, N.Q.Z. & Amin, A. 2013. High-voltage Insulation Surface Condition Analysis using Time Frequency Distribution. *Australian Journal of Basic Science*, 7(7): 833-841.
- Nzenwa, E.C. & Adebayo, A.D. 2019. Analysis of Insulators for Distribution and Transmission Network. *American Journal of Engineering Research (AJER)*, 8(12): 138-145.
- Olupot, P.W. 2006. Assessment of ceramic raw materials in Uganda for electrical porcelain (Doctoral dissertation, KTH).
- Paradisi, C., Trost, B.M. & Fleming, I. 1991. *Comprehensive Organic Synthesis. Selectivity, Strategy and Efficiency in Modern Organic Chemistry*, pp.423-450.
- Park, J.H. & Lee, S.J. 1995. Mechanism of Preventing Crystallization in Low-Firing Glass/Ceramic Composite Substrates. *Journal of the American Ceramic Society*, 78(4): 1128-1130.
- Paun, M.A., Sallese, J.M. & Kayal, M. 2013. Hall effect sensors design, integration and behaviour analysis. *Journal of Sensor and Actuator Networks*, 2(1): 85-97.
- Perez, S.J., Calva, M.A. & Castañeda, R. 1997. A Microcontroller-Based Data Logging System. *Instrumentation and Development*, 3(8).
- Petruk, O., Szewczyk, R., Ciuk, T., Strupiński, W., Salach, J., Nowicki, M., Pasternak, I., Winiarski, W. and Trzcinka, K., 2014. Sensitivity and offset voltage testing in the hall-effect sensors made of graphene. In *Recent Advances in Automation, Robotics and Measuring Techniques* (pp. 631-640). Springer, Cham.
- Piah, M.A.M. & Darus, A. 2003. Effect of electrolyte resistivity and flow rate on the leakage current for polymeric materials. In *Proc. of 13th High-voltage Engineering Symposium*.
- Pratomosiwi, F. 2009, August. Application of RTV silicone rubber coating for improving performances of ceramic outdoor insulator under polluted conditions. In *2009 International Conference on Electrical Engineering and Informatics* (2): 581-587. IEEE.

- Pylarinos, D., Siderakis, K. and Pyrgioti, E., 2011. Measuring and analyzing leakage current for outdoor insulators and specimens. *Rev. Adv. Mater. Sci*, 29(11), pp.31-53.
- Pylarinos, D., Siderakis, K. & Thalassinakis, E. 2014, October. R&D in TALOS High-voltage Test Station-Assessing ageing and performance of polymer insulators. In 13th International Conference on Circuits, Systems, Electronics, Control & Signal Processing (CSECS'14), Lisbon, Portugal.
- Pylarinos, D., Siderakis, K. & Thalassinakis, E. 2015. Comparative investigation of silicone rubber composite and room temperature vulcanized coated glass insulators installed in coastal overhead transmission lines. *IEEE Electrical Insulation Magazine*, 31(2): 23-29.
- Pylarinos, D., Siderakis, K., Thalassinakis, E., Mavrikakis, N., Koudoumas, E., Drakakis, E. & Kymakis, E. 2016. A new approach for open-air insulator test stations: experience from Talos and the Polydiagno project. *Journal of Electrical Engineering*, 16(2): 269-273.
- Qin, Y.X., Fu, J., Yu, L., Yang, Z.R. & Guo, W.Y. 2013. Comparative research on ageing properties of HTV silicone rubber via outdoor electric ageing and ultraviolet accelerated ageing. In *Advanced Materials Research* (641: 333-337. Trans Tech Publications Ltd.
- Que, W. 2002. Electric field and voltage distributions along non-ceramic insulators (Doctoral dissertation, The Ohio State University).
- Ramani, A.N., Abdullah, A.R., Norddin, N., Abidin, N.Q.Z. & Aman, A. 2015. *Automated Classification System for Polymeric Insulation Surface Condition*.
- Ramirez, I., Hernandez, R. & Montoya, G. 2012. Measurement of leakage current for monitoring the performance of outdoor insulators in polluted environments. *IEEE Electrical Insulation Magazine*, 28(4): 29-34.
- Ramos Hernanz, J.A., Martín, C., José, J., Motrico Gogeoascoechea, J. & Zamora Belver, I. 2006. *Insulator pollution in transmission lines*. Escuela Universitaria de Ingeniería, Spain.
- Repalle, J.K. and Kumar, P.R., 2015. Evaluation of various properties of ceramic materials used in ceramic industries. *J. Mater. Sci. Mech Eng*, 2, pp.345-349.

- Reynders, J.P., Jandrell, I.R. & Reynders, S.M. 1999. Review of ageing and recovery of silicone rubber insulation for outdoor use. *IEEE Transactions on Dielectrics and Electrical Insulation*, 6(5): 620-631.
- Rezaei, M., Ahmadi-Joneidi, I., Parhizgar, A., Kahuri, H. & Sayani, A. 2013. Evaluation of actual field ageing on silicone rubber insulator under coastal environment. *Life Science Journal*, 10(5s): 199-205.
- Rice, J.A., Fabian, P.E. & Hazelton, C.S. 1999. Mechanical and electrical properties of wrappable ceramic insulation. *IEEE Transactions on Applied Superconductivity*, 9(2): 220-223.
- Roman, M., Van Zyl, R.R., Parus, N. & Mahatho, N. 2014, August. Insulator leakage current monitoring: Challenges for high-voltage direct current transmission lines. In 2014 International Conference on the Eleventh industrial and Commercial Use of Energy (pp. 1-7). IEEE.
- Roman, M., van Zyl, R.R., Parus, N. & Mahatho, N. 2019. In-situ monitoring of leakage current on composite and glass insulators of the Cahora Bassa HVDC transmission line. *SAIEE Africa Research Journal*, 110(1): 4-10.
- Rubber, S.N. 2016. Natural rubber and reclaimed Rubber composites—A Systematic Review. *Polymer*, 2(1): 7.
- Rudolf, L. 2009. Leakage currents and power losses on outdoor insulators under artificial rains. *Journal of Technology and Information Education*, 1(2): 100.
- Saei, A.M., Mohebby, B. & Abdeh, M.R. 2015. Effects of oleothermal treatment and polydimethylsiloxane (PDMS) coating on natural weathering of beech and fir woods. *Maderas. Ciencia y tecnología*, 17(4): 905-918.
- Saldivar-Guerrero, R., Hernández-Corona, R., Lopez-Gonzalez, F.A., Rejón-García, L. & Romero-Baizabal, V. 2014. Application of unusual techniques for characterizing ageing on polymeric electrical insulation. *Electric Power Systems Research*, 117: 202-209.
- Salem, A.A. and Abd-Rahman, R., 2018, July. A review of the dynamic modelling of pollution flash-over on high-voltage outdoor insulators. In *Journal of Physics: Conference Series* (Vol. 1049, No. 1, p. 012019). IOP Publishing.
- Samimi, M.H. Mostajabi, A. H., Ahmadi-Joneidi, I., Shayegani-Akmal, A. A. & Mohseni, H. 2013. Performance evaluation of insulators using flash-over

- voltage and leakage current. *Electric Power Components and Systems*, 41(2): 221-233.
- Sanyal, S., Kim, T., Seok, C.S., Yi, J., Koo, J.B., Son, J.A. & Choi, I.H. 2020. Replacement Strategy of Insulators Established by Probability of Failure. *Energies*, 13(8): 2043.
- Sarathi, R. & Chandrasekar, S. 2004. Investigations of tracking phenomena in silicone rubber using moving average current technique. *Plasma Science and Technology*, 6(5): 2514.
- Sarkar, P., Haddad, A., Waters, R.T., Griffiths, H., Harid, N. & Charalampidis, P. 2010, October. Inclined-plane tests of textured silicone rubber Samples. In High-voltage Engineering and Application (ICHVE), 2010 International Conference on (pp. 532-535). IEEE.
- Schmidt, L.E., Kornmann, X., Krivda, A. & Hillborg, H. 2010. Tracking and erosion resistance of high temperature vulcanizing ATH-free silicone rubber. *IEEE Transactions on Dielectrics and Electrical Insulation*, 17(2): 533-540.
- Schott, A. 2007. *SCHOTT Technical Glasses (Physical and Technical Properties)*. Firmenschrift, Oct.
- Schwardt, W.H., Holtzhausen, J.P. & Vosloo, W.L. 2004, September. A comparison between measured leakage current and surface conductivity during salt fog tests [power line insulator applications]. In Africon, 2004. 7th Africon Conference in Africa (1): 597-600. IEEE.
- Sebo, S.A. & Liu, X. 2010, October. Accelerated ageing methods for outdoor insulation-Rotating wheel and salt fog chamber tests. In Electrical Insulation and Dielectric Phenomena (CEIDP), 2010 Annual Report Conference on (pp. 1-4). IEEE.
- Sebo, S.A. & Zhao, T. 1999. Utilization of fog chambers for non-ceramic outdoor insulator evaluation. *IEEE Transactions on Dielectrics and Electrical Insulation*, 6(5): 676-687.
- Shukla, S.P. 2011. Investigation into tribo potential of rice husk (RH) char reinforced epoxy composite (Doctoral dissertation).

- Siderakis, K., Agoris, D., Eleftheria, P. & Thalassinakis, E. 2004. Investigation of leakage current on high-voltage insulators field measurements. *WSEAS Transaction on Circuits and System*. pp. 1188-1191.
- Siderakis, K., Pylarinos, D., Mavrikakis, N., Pellas, I. & Thalassinakis, E. 2016. Composite outdoor high-voltage insulators in Crete—37 years of experience. In *Proc. 2016 Int'l. Conf. on Deregulated Electricity Market issues in South-Eastern Europe* (pp. 374-382).
- Siderakis, K., Pylarinos, D., Thalassinakis, E. & Drakakis, E. 2011. Performance investigation of composite and RTV SIR coated insulators at a coastal test station. In *UPEC 46th International Universities' Power Engineering Conference*.
- Siderakis, K., Pylarinos, D., Thalassinakis, E., Vitellas, I. & Pyrgioti, E. 2011. Pollution maintenance techniques in coastal high-voltage installations. *Engineering, Technology & Applied Science Research*, 1(1): 1-6.
- Sinev, L.S. & Petrov, I.D. 2016. Linear thermal expansion coefficient (at temperatures from 130 to 800 k) of borosilicate glasses suitable for silicon compounds in microelectronics. *Glass and Ceramics*, 73(1): 32-35.
- Swinny, R., 2021. Investigation into the influence of electrode material on the IEC Inclined Plane test procedure (IEC 60587) when applied for Direct Current (DC) voltages (Doctoral dissertation, Stellenbosch: Stellenbosch University).
- Subedi, M.M. 2013. Ceramics and its Importance. *Himalayan Physics*, 4: 80-82.
- Sudha, P.N., Sangeetha, K., Jisha Kumari, A.V., Vanisri, N. & Rani, K. 2018. *Corrosion of ceramic materials*. Fundamental Biomaterials: Ceramics, Woodhead Publishing, Boston, pp. 223-250.
- Suhaimi, S.M.I., Bashir, N., Muhamad, N.A., Rahim, N.N.A., Ahmad, N.A. & Rahman, M.N.A. 2019. Surface Discharge Analysis of High-voltage Glass Insulators Using Ultraviolet Pulse Voltage. *Energies*, 12(2): 204-229.
- Sundhar, S., Bernstorff, A., Goch, W., Linson, D. & Huntsman, L. 1992, June. Polymer insulating materials and insulators for high-voltage outdoor applications. In *Conference Record of the 1992 IEEE International Symposium on Electrical Insulation* (pp. 222-228). IEEE.

- Swedish Transmission Research Institute (STRI). 1992. *Guide 92/1 Hydrophobicity Classification Guide*.
- Taulo, J.L., Gondwe, K.J. & Sebitosi, A.B. 2015. Energy supply in Malawi: Options and issues. *Journal of Energy in Southern Africa*, 26(2): 19-32.
- Tong, Y., Liu, H., Chen, A., Guan, H., Kong, J., Liu, S. and He, C., 2018. Effect of surface chemistry and morphology of silica on the thermal and mechanical properties of silicone elastomers. *Journal of Applied Polymer Science*, 135(35).
- Theodoridis, A., Danikas, M.G. & Soulis, J. 2001. Room temperature vulcanized (RTV) silicone rubber coatings on glass and porcelain insulators: an effort to model their behaviour under contaminated conditions. *Journal of Electrical Engineering-Bratislava-*, 52(3/4): 63-67.
- Thomazini, D., Gelfuso, M.V. & Altafim, R.A.C. 2012. Classification of polymers insulators hydrophobicity based on digital image processing. *Materials Research*, 15(3): 365-371.
- Ullah, I., Amin, M., Nazir, M.T. & Hussain, H. 2020. Impact of accelerated ultraviolet weathering on polymeric composite insulators under high-voltage DC stress. *CSEE Journal of Power and Energy Systems*.
- Venkataraman, S. & Gorur, R.S. 2006. Prediction of flash-over voltage of non-ceramic insulators under contaminated conditions *IEEE Transactions on Dielectrics and Electrical Insulation*, 13(4): 862-869.
- Verma, A.R. & Reddy, B.S. 2018. Ageing studies on polymeric insulators under DC stress with controlled climatic conditions. *Polymer Testing*, 68: 185-192.
- Verma, A.R. & Subba, R.B. 2018. Understanding surface degradation on polymeric insulators using rotating wheel and dip test under DC stress. *IEEE Transactions on Dielectrics and Electrical Insulation*, 25(5): 2029-2037
- Volokhin, V. & Diahovchenko, I. 2017. Peculiarities of current sensors used in contemporary electric energy metering devices. *Energetika*, 63(1).
- Vosloo & Swinny. 2013. *Koeberg Insulator Pollution Test Station*. Available at: <http://az817975.vo.msecnd.net/wm-418498-cmsimages/May2013wn.pdf>. (Accessed: 17 August 2018).

- Vosloo, W.L. 2002. A comparison of the performance of high-voltage insulator materials in a severely polluted coastal environment (Doctoral dissertation, Stellenbosch: Stellenbosch University).
- Vosloo, W.L., Holtzhausen, J.P. & Roediger, A.H.A. 1996, September. Leakage current performance of naturally aged non-ceramic insulators under a severe marine environment. In Africon, 1996, IEEE Africon 4th (1): 489-495. IEEE.
- Vudayagiri, S., Yu, L. & Skov, A.L. 2015. Techniques for hot embossing microstructures on liquid silicone rubbers with fillers. *Journal of Elastomers & Plastics*, 47(7): 585-597.
- Wallström, S., 2005. Biofilms on silicone rubber for outdoor high-voltage insulation (Doctoral dissertation).
- Wang, X., Hong, X., Chen, C., Wang, H., Jia, Z., Zou, L. & Li, R. 2017, June. Elemental analysis of RTV and HTV silicone rubber with laser-induced breakdown spectroscopy. In 2017 IEEE Electrical Insulation Conference (EIC) (pp. 9-12). IEEE.
- Wen, X., Yuan, X., Lan, L., Hao, L., Wang, Y., Li, S., Lu, H. & Bao, Z. 2017. RTV silicone rubber degradation induced by temperature cycling. *Energies*, 10(7): 1054.
- Wijayatilake, A.C.S. 2014. Reviewing of Insulator Selection Criteria for Overhead Power Lines in Coastal Areas of Sri Lanka. *Journal of the Institute of Engineers*, 47(1): 57-73.
- Wu, D., Astrom, U., Almgren, B. & Soderholm, S. 1998, August. Investigation into alternative solutions for HVDC station post insulators. In POWERCON'98. 1998 International Conference on Power System Technology. Proceedings (Cat. No. 98EX151) (1): 512-515. IEEE.
- Wu, X., Li, X., Hao, L., Wen, X., Lan, L., Yuan, X. & Zhang, Q. 2017, June. Effect of vulcanization temperature and humidity on the properties of RTV silicone rubber. In IOP Conference Series: Materials Science and Engineering (207/1): 012011. IOP Publishing.
- Yang, L., Bi, J., Hao, Y., Nian, L., Zhou, Z., Li, L., Liao, Y. & Zhang, F. 2018. A recognition method of the hydrophobicity class of composite insulators based on features optimization and experimental verification. *Energies*, 11(4): 765.

- Yarysheva, L.M., Rukhlya, E.G., Yarysheva, A. Yu, Volynskii, A.L. & Bakeev, N.F. 2012. Crazing as a method for preparation of polymer blends. *Review Journal of Chemistry*, 2(1): 1-19.
- Yoshimura, N., Kumagai, S. & Du, B. 1997. Research in Japan on the tracking phenomenon of electrical insulating materials. *IEEE Electrical Insulation Magazine*, 13(5): 8-19.
- Yu, L. & Skov, A.L. 2015. Silicone rubbers for dielectric elastomers with improved dielectric and mechanical properties as a result of substituting silica with titanium dioxide. *International Journal of Smart and Nano Materials*, 6(4): 268-289.
- Zago, T. 2017. *Performance of textured insulators for overhead lines and substations under polluted conditions*.
- Zhao, T. & Bernstorf, R.A. 1998. Ageing tests of polymeric housing materials for non-ceramic insulators. *IEEE Electrical Insulation Magazine*, 14(2): 26-33.
- Zhicheng, G. & Zhidong, H. 2002, October. The developments of room temperature vulcanized silicone rubber coating and its application in China. In *IEEE/PES Transmission and Distribution Conference and Exhibition (3)*: 2203-2206. IEEE.
- Zhou, J.B., Gao, B. Y. & Zhang, Q.G. 2010, March. Dry band formation and its influence on electric field distribution along polluted insulator. In *2010 Asia-Pacific Power and Energy Engineering Conference* (pp. 1-5). IEEE.
- Zhu, H., Dai, Z. & Tu, W. 2017. Study on the preparation and performance of low gas permeability trifluoropropyl phenyl silicone rubber. *RSC Advances*, 7(63): 39739-39747.